

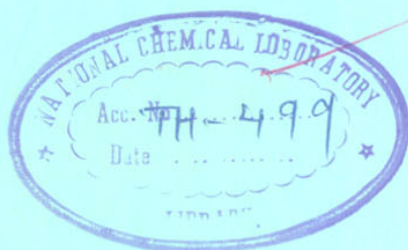
# STUDIES ON POLYPHENYLENE SULFIDE

A THESIS SUBMITTED TO THE  
UNIVERSITY OF POONA  
FOR THE DEGREE OF  
DOCTOR OF PHILOSOPHY  
IN CHEMISTRY

COMPUTERISED

BY

RAJAN C. R.  
M. Sc.



678.6'364(043)  
RAJ

POLYMER SCIENCE AND ENGINEERING GROUP  
CHEMICAL ENGINEERING DIVISION  
NATIONAL CHEMICAL LABORATORY  
PUNE 411 008 (INDIA)

JUNE 1986

2002  
11/24/02

COMPUTERISED

FORM - A

Certified that the work incorporated in the thesis 'STUDIES IN POLYPHENYLENE SULFIDE' submitted by Shri C.R. Rajan was carried out by the candidate under my supervision. Such material as has been obtained from other sources has been duly acknowledged in the thesis.



[DR. V.M. NADKARNI]

**Research Guide**

## ACKNOWLEDGEMENTS

I would like to express my gratitude to Dr.V.M. Nadkarni for his professional guidance and encouragement throughout this investigation.

The fruitful completion of a doctoral thesis is indeed due to the efforts of a number of individuals. The following individuals contributed significantly towards the fulfilment of this effort.

I would like to record my appreciation to Dr.S. Ponrathnam for his constant professional and personal help rendered during the course of the investigation.

I am grateful to Dr.S. Radhakrishnan for his assistance in the morphological studies. I would like to thank Dr. Gunjekar, Mr. Gujral and Mrs. A.P. Mitra, the division of microanalysis and my colleagues in the polymer science and engineering group for the assistance rendered.

I would like to thank Kumar Joshi for typing this manuscript that enabled me to meet the deadline comfortably.

My sincere thanks are due to Dr.R.A. Mashelkar for his active interest and encouragement during the course of the work and to the Director, NCL for permission to submit this work in the form of a thesis.



[C.R. RAJAN]

## CONTENTS

	Page No.
SCOPE OF THE RESEARCH WORK	1
CHAPTER 1 : INTRODUCTION	4
CHAPTER 2 : EXPERIMENTAL	39
CHAPTER 3 : KINETICS	60
CHAPTER 4 : THERMAL CHARACTERIZATION	144
CHAPTER 5 : MORPHOLOGICAL STUDIES	181
CHAPTER 6 : MECHANISTIC STUDIES	221
SUMMARY AND RECOMMENDATIONS	238
REFERENCES	247

\*\*\*\*\*



---

SCOPE OF THE RESEARCH WORK

---

## SCOPE OF THE RESEARCH WORK

Poly(p-phenylene sulfide) (PPS) is a versatile engineering plastic with excellent thermal/chemical resistance and mechanical performance. It is used for moulding of engineering components and also as a corrosion resistant coating on various substrates. The polymer was first commercialized in late 1972. The combination of properties offered by the material has made it an important engineering thermoplastic for metal replacement.

The polymer has great commercial significance. However, there is little published literature on the kinetics and structural development during the polymerization. A study of the polymerization to generate PPS is also of fundamental interest. This precipitation polycondensation reaction is a novel heterogeneous process. The commercially significant polycondensation reactions which are homogeneous systems are the production of unsaturated polyesters, nylons, phenolic resins, polyurethanes etc. Thus, the study of PPS synthesis would also elucidate aspects of the effect of solubility of reactants in the reaction medium on kinetics, the growth/propagation of the polymer chain in the solid phase after precipitation and the interrelation of the chemical reaction kinetics and physical processes such as precipitation and crystallization. It is this line of thinking that prompted the present investigation of the kinetics and structure development during the synthesis of PPS.

The polymerization to PPS involves the reaction of 1,4-dichloro benzene (PDCB) with sodium sulfide in N-methyl pyrrolidone (NMP),



a highly polar solvent. The reaction may be represented as:



The reaction is usually carried out in a polar solvent at high temperature (265°C) and pressure ( $\approx$  160 psi). In the present work, the reaction was studied at 195°C and at a pressure of  $\approx$  35 psi. The system involved the use of PDCB in a slight excess.

The scope of the doctoral research touched on the following aspects concerning the polymerization to generate PPS.

- i) Polymerization kinetics
- ii) Mechanistic studies by varying the reactants and catalyst.
- iii) The effect of physical reaction parameters such as stirring speed and dilution, on the yield and degree of polymerization.
- iv) Characterization of the degree of polymerization with reaction time by microanalysis and dilute solution viscosity measurements.
- v) Characterization by differential scanning calorimetry, the physical structure of the polymer generated at different conversions.
- vi) Morphological characterization by x-ray diffractometry and scanning electron microscopy.

The kinetics and structure development during the polycondensation to PPS were investigated by collecting and analysing polymer samples generated at different reaction times. The conversions were evaluated by volumetric analysis, the amount of sodium chloride formed

and the unreacted sodium sulfide present. The polymer yields were determined gravimetrically. The polymer formed at different reaction times were characterized by chlorine end group analysis, dilute solution viscosity, thermal evaluation, x-ray diffractometry studies and particle size determination by scanning electron microscopy. In this manner, the interrelationships between kinetics and structure development were studied.

The following experiments were carried out to elucidate the polycondensation mechanism and to propose a probable reaction scheme. These involved the use of:

- (a) Sodium para chloro thiophenoxide as initiating species
- (b) Excess PDCB to accelerate the initial reaction steps
- (c) Sodium hydroxide as probable catalyst
- (d) 1,4-dibromo benzene instead of 1,4-dichloro benzene

In most precipitation polymerization reactions, the polymer precipitates out after a critical degree of polymerization is attained. In such heterogeneous systems, the transport of reactants exerts considerable influence on the reaction rate. In order to study the diffusional limitations on the polycondensation to PPS, the yield data at fixed reaction time were obtained at different stirring speeds and different dilutions. The results of the study were analyzed to interrelate kinetics with structure development.





**CHAPTER 1**  
**INTRODUCTION**

## INTRODUCTION

### 1.1 Polymeric Materials

Polymeric materials are used in a wide range of applications ranging from general purpose large volume commodity household articles to low volume, speciality, load bearing components. The prime considerations for materials selection in any application are the performance requirements versus the material properties and the cost effectiveness of the material. The performance specifications may include mechanical properties such as strength, rigidity, toughness, abrasion and wear resistance, thermal characteristics, chemical resistance and electrical properties. A few typical consumer and industrial applications of polymeric materials include packaging films, luggage, toys, textile fibres, paints, lighting fixtures, electrical connectors, auto tyres and gears, bearings.

The materials are generally classified in terms of their applications as plastics, elastomers, synthetic fibers, protective coatings and adhesives. Polymers are also used as matrix material for reinforcing fillers/fibres in high performance composites for defence, aerospace and industrial applications.

Engineering thermoplastics are increasingly replacing conventional materials primarily because of their greater ease of processing into products of complicated shapes and the economics of the high productivity conversion processes such as injection moulding. The other advantages offered by thermoplastics include light weight, corrosion resistance/long life expectancy, versatility of product design

and the ease of maintenance of the product. The property requirements for a specific new application can be met through modification of the base polymer with fillers, reinforcing fibres, grafting, blending etc.

The thermoplastic materials may be categorized into three groups based on their volume of production, cost and thermal performance.

(a) **Bulk or commodity plastics:** Low priced, high volume polymers such as polyethylene, polyvinyl chloride, polypropylene and polystyrene. The maximum use temperature of these materials is  $\approx 100^{\circ}\text{C}$ .

(b) **Engineering plastics:** These are polymers exhibiting higher thermal and mechanical performance. In this class, polymers such as polyamides (Nylons), polycarbonates, polyacetals, polyphenylene oxide, thermoplastic polyesters, polyurethanes and polyphenylene sulfide may be included. On a production / cost basis, these materials are medium volume and medium priced plastics. The consumption of these materials is significantly lower than that of the commodity plastics. The use temperature of these materials is in the range  $150\text{-}200^{\circ}\text{C}$ . They display better thermomechanical properties such as high HDT and modulus, wider end use temperatures, chemical resistance and excellent load bearing characteristics. These are used in metal replacement applications. Some of the major applications for engineering plastics include pump impellers and housings, low friction components, heat and chemical resistant units, electrical parts and materials for construction industry.

TABLE 1  
CONSUMPTION FIGURES OF ENGINEERING PLASTICS

Polymer	Consumption x1000 tons	Market share %
Total polyamides including		
Nylon-6, nylon-66, speciality nylon	436	39.71
Polycarbonates	250	22.77
Polyacetals	186	16.94
Modified PPO	140	12.75
Thermoplastic polyesters (PBT, PET)	75	6.83
Polysulfones	6	0.55
Polyphenylene sulfide	5	0.45
Total -	1098	100

(c) Speciality polymers: Polymers that can be grouped in this category are low volume/high priced speciality materials and would include polymers such as fluoropolymers, polysulfones, polyether ketones, polyimides etc. which cater to specific property combinations defined to meet product performance. The polymer can be used at temperatures upto 270°C.

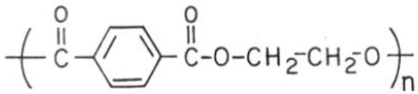
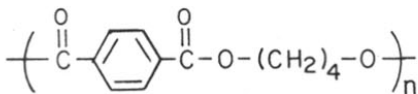
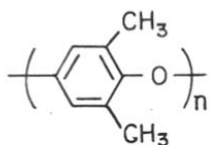
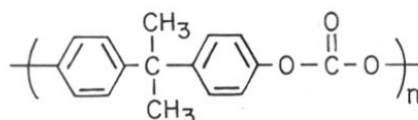
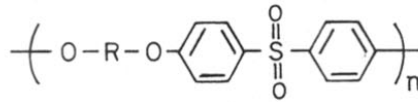
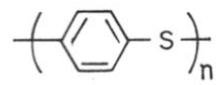
The conventional processing methods such as extrusion and injection moulding can be used for processing of engineering plastics with modification of the equipment.

The increasing use and acceptance of engineering plastics can be gauged from the reported sales of engineering plastics. This has crossed the one million 'ton mark.' The contribution of various polymers with their market share is shown in Table 1. The table excludes commodity polymers modified to meet property requirements for engineering applications. Polymers such as polypropylene and acrylonitrile-butadiene-styrene (ABS) copolymers could be used for specific engineering applications.

A number of high performance engineering plastics, with the exception of nylon 6, nylon 66 and polyacetals, are based on aromatic monomer units. The advantages of incorporating para phenylene moieties in the polymer backbone are well documented.<sup>2</sup> The physical properties of a large number of such condensation polymers can be correlated to their chemical structure. These polymers are often used with glass fibres for engineering applications.

Some of the outstanding and commercially useful aromatic polymers include the thermoplastic polyesters (PET and PBT), poly-

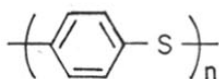
TABLE 2  
STRUCTURE AND TYPICAL PROPERTIES OF AROMATIC POLYMERS<sup>3</sup>

Polymer	Structure	Test method ASTM No.			
		D 638		D 648	
		Tensile strength psi	Modulus 10 <sup>3</sup> psi	Impact strength ft. 15/in	Deflection temperature °F
Polyethylene terephthalate PET		8500 -10,500	400 -600	0.25 -0.65	100 -106 (annealed)
Polybutylene terephthalate PBT		8200	280	0.8-1.0	122 -185
Polyphenylene oxide PPO		7800 -9600	380 -355	5	212 -265
Polycarbonate PC		9500	345	10-14	270
Polysulfone			360	1.2	345
Polyphenylene sulfide PPS		9500	480	0.5	275

sulfones, polycarbonates, polyphenylene sulfide, polyphenylene oxide (Noryl). The polymer backbone consists of one or more atoms interposed between the paraphenylene units. The structure and typical properties of a few aromatic polymers are summarized in Table 2.<sup>3</sup>

## 1.2 Poly(p-phenylene sulfide)

Poly(p-phenylene sulfide) (PPS) has gained considerable importance as a versatile engineering plastic since 1973 and is predicted to become one of the six major engineering plastics by 1990.<sup>4</sup> The polymer structure consists of para-substituted aromatic rings interconnected by sulfur linkages. Linear PPS has one sulfur atom between the paraphenylene units. The chemical structure of the polymer is represented as indicated below.



Although the polymer was first reported in 1897,<sup>5</sup> it was not till the mid seventies that PPS could be marketed. The first commercial plant was put up in late 1972 by Phillips Petroleum in USA. PPS has been a monopoly product of Phillips Petroleum and is marketed under the trade name Ryton. Though broadly available in coating and moulding grades, 72 different grades<sup>6</sup> are marketed by various companies using the base resin produced by Phillips Petroleum. The consumption figure during the year 1984 is 5000 tons. Several reviews<sup>7-42</sup> highlighting the salient features of PPS and its application potential are available.

The repeating paraphenylene unit imparts rigidity to the polymer chain and the symmetry due to paraphenylene linkages imparts

a high degree of crystallinity and excellent thermal resistance. PPS is a versatile engineering plastic with a unique combination of properties like high corrosion and solvent resistance, thermal resistance, good mechanical properties, good processability, flame retardance and ability to be compounded with various fillers. PPS has combination properties of thermoplastic and thermosetting classes of materials.)

PPS is used in coating and injection molding applications. Coatings based on PPS exhibit better adhesion to metal substrates and better filler acceptability in comparison with fluoro polymer coatings. The coating process is also simpler since the polymer melts during the curing process. The coating applications of PPS include corrosion resistant lining for chemical equipment, pump impellers, flame-proof casing for electrical equipment, non-stick coatings for cookware, low friction rollers for calendaring machines etc. For applications involving injection moulding grades, PPS is compounded with glass fibres and fillers (40% glass fibres). Typical applications include ball valves, pump impellers, electrical sockets, gears and housings, microwave oven shelves, telephone components etc.

(Sodium sulfide and paradichlorobenzene, the major raw materials used for the synthesis of PPS, are relatively inexpensive.)

The early studies on the formation of PPS resins are well reviewed. In these investigations, the polymer was observed as a side product in reactions directed at the synthesis of simple organic compounds.

The first published report on PPS dates back to 1897.<sup>5</sup> The formation of the polymer as a resinous material was observed in the reaction of benzene and sulfur. The polymer generation was also observed

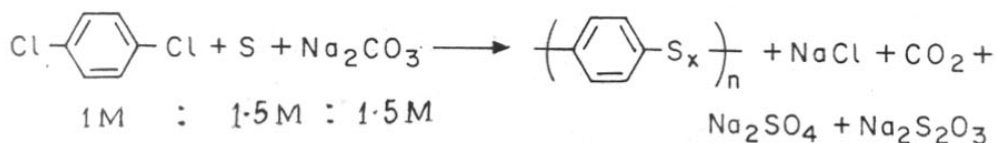


in the Friedel-Crafts reaction ( $\text{AlCl}_3$ ) involving phenol with sulfur<sup>43</sup>, of thiophenol<sup>44</sup>, of thiophenol with thionyl chloride<sup>45</sup>, self condensation of thiophenol in concentrated sulfuric acid<sup>46</sup>, reaction of benzene with sulfur,<sup>47</sup> oxidation of paraphenylene dimercaptan<sup>48</sup> and reaction of phenol with sulfur dichloride.<sup>48</sup>

These studies resulted in polymer yields only in the 50 to 80 percent range. Elemental analyses of the polymer formed in the above investigations corresponded to the empirical formula  $\text{C}_6\text{H}_4\text{S}$ . The reported physical characteristics of the formed polymer are conflicting. It was either described as amorphous or as a crystalline material. However, the high softening range of the polymer was uniformly noted. The polymers were perhaps either oligomers or with cyclic structures. The polymers were not extensively characterized.

Reinvestigation of the self polycondensation of thiophenol<sup>49</sup> in the presence of sulfuric acid gave high melting ( $310^\circ\text{C}$ ) branched polymer (80.8%) along with toluene soluble low melting ( $125\text{-}130^\circ\text{C}$ ) oligomer (11.4%).

Macallum revived the dormant field of PPS synthesis. The Macallum polymerization<sup>50-52</sup> involved the melt reaction of para dichloro benzene, sulfur and anhydrous sodium carbonate in varying proportions in a sealed vessel at temperatures in excess of  $300^\circ\text{C}$ . The reaction may be represented as,



The sulfur rank "x" in the above equation (which denotes the average number of sulfur atoms between repeat units) varied from 1 to 5. The chemical composition and the physical properties of the polymer formed were found to be dependant on the relative ratios of the reactants used. Polymers with 'x' close to unity were obtained when the molar ratios of sulfur and sodium carbonate to para dichloro benzene were maintained at 1.5:1.5:1. The number-average molecular weight of these polymers, as determined by chlorine end group analysis was found to be in the range of 35000 to 70000.

Macallum polymerization process was not a commercial success since the polymer properties could not be reproduced. The products obtained ranged in properties from hard polymers softening at high temperatures to rubbery polysulfides, depending on the ratio of the reactants. However, the work prompted further investigation towards an extensive study of the chemistry and structure of the polymers.

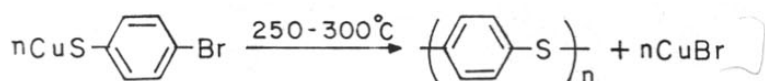
At Dow Chemical Co., USA, the research team headed by Lenz reinvestigated the Macallum polymerization process.<sup>53</sup> They observed that the polymer properties and yields were not reproducible. Polymer characterization showed these were either branched or crosslinked. They proposed a probable mechanism for the course of Macallum polymerization.

The Lenz team switched to an alternate synthetic route involving self polycondensation of metal salts of para halo thiophenols.<sup>54,55</sup> The reaction may be represented as,



where M is an alkali or alkaline earth cation, while X is a halide, fluorine, chlorine, bromine or iodine.)

(The polycondensations were carried out either in bulk or in solvent pyridine in ampules sealed under inert atmosphere, at temperatures lower than the melting point of the salt. Among the systems investigated, the commercially attractive one was found to be the system based on cuprous p-bromo thiophenoxide. This reaction could be represented as,



It was found that the rate of solution polycondensation was faster than the solid state polycondensation. The influence of the halogen on the rate was in the order I > Br > Cl > F. An overall second order rate was observed for the solution polycondensation in pyridine.

(The polycondensations resulted in linear poly(p-phenylene sulfide)<sup>55</sup> with better thermal stability than the polymers produced by the Macallum process.) However, the process could not be exploited commercially due to the expensive raw material and inherent difficulty in the complete removal of the side product, cuprous bromide.

Phillips process for PPS:

Phillips Petroleum Co. USA reinvestigated the synthesis of PPS, aiming at a viable commercial process.<sup>56,57</sup> The work culminated in the successful development of a commercial plant in 1972. The Phillips process<sup>58</sup> involves the reaction of aromatic dihalides with alkali metal sulfides in a polar organic solvent at high temperatures and pressures. The preferred route involves the reaction between para dichloro benzene and sodium sulfide in N-methyl pyrrolidone at elevated temperatures (265°C) and pressure (~ 160 psi). Linear PPS is obtained almost quantitatively. The reaction can be represented as;



Sodium sulfide, a reactant in the synthesis, was obtained in an anhydrous form by reaction between sodium hydroxide and sodium hydrosulfide, followed by the dehydration step to remove water by distillation. The polymer isolation steps include recovery of the polymer from the reaction mixture, extensive washing to remove the side product sodium chloride, and drying.]

A number of methods for the synthesis of PPS have been patented by Phillips Petroleum.<sup>59-94</sup> [The common feature in these methods is the reaction of para dichloro benzene in N-methyl pyrrolidone. The methods vary in the nature of sulfide, the co-reactant.] Other reported variations of the reaction include incremental addition of one reactant or addition of compounds like thiourea, alkali metal carbonates, mixed dichlorobenzene, lithium halides or carboxylates, etc.

[PPS obtained by the Phillips process is a low molecular weight polymer, not suitable for moulding applications. The molecular weight of

PPS was enhanced by the following methods.<sup>95-113</sup>

- (a) recycling of low molecular weight PPS from earlier batches.
- (b) use of lithium salts such as chloride, carbonate, metaborate, acetate as catalysts.
- ✓(c) using pressurized carbon dioxide atmosphere.
- ✓(d) using sodium benzene sulfonate or sodium butane sulfonate.
- ✓(e) use of sodium acetate
- ✓(f) addition of bifunctional chloride
- (g) addition of alkali-metal carboxylate with varying amounts of alkali metal hydroxide, and
- (h) co-polycondensation with a comonomer.

✓The molecular weight of PPS was also enhanced by controlled post polymerization heat treatment.<sup>114</sup> The dry polymer was subjected to a programmed thermal heating cycle below its melting point, till the desired molecular weight was attained. The heat treatments could either be at atmospheric pressure or under pressure with additives<sup>115-123</sup> such as sulfur, tetramethyl thiuram disulfide or organic peroxide, quinones, sulfuric acid, peroxide - sulfuric/nitric acid, hexamethoxy methyl melamine, alkali metal carboxylate. The increase in molecular weight was evaluated by measuring the melt flow index and the increase in inherent viscosity of the polymer. The melt flow index decreased with increase in molecular weight. ]

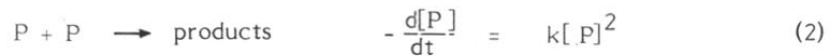
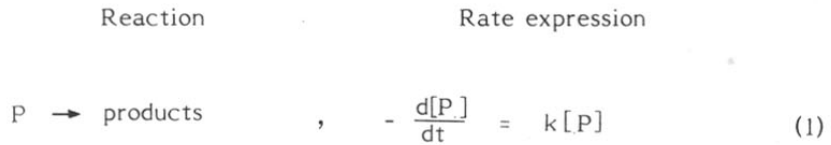
PPS is normally produced by a batch process. Phillips Petroleum Co. USA, have recently filed process patents for a continuous production of PPS.<sup>124-127</sup>

Thus Phillips Petroleum Co. USA have carried out extensive work in the synthesis of PPS. Open literature on the synthesis of PPS is rather limited.<sup>128-137</sup> Reported work by others is exclusively covered by patents.<sup>138-190</sup>

### 1.3 Kinetics of polycondensation reactions

The kinetic analysis of a reaction involves monitoring the rate and order of disappearance of the reactants as measured by the change in their concentration. This is evaluated by analysing samples drawn intermittently during the course of the reaction.

The first objective in any kinetic study is to determine the rate of the reaction. Simple reaction schemes and their corresponding rate expressions are represented as:



where P and Q are the reactants.

The constant k, the rate constant, is also known as the specific reaction rate constant. Its dimensions depend on the order of the reaction. The generalized expression between P and Q may be represented in the form,

$$-\frac{d[P]}{dt} = -\frac{d[Q]}{dt} = k[P]^x [Q]^y \quad (4)$$

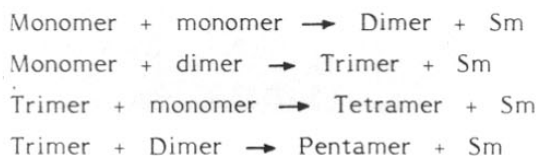
The indices x and y are defined as the order of the reaction with respect to the individual reactants and the overall rate of the reaction is represented as [x + y].

### Polycondensation reactions

Polycondensation reactions occur between difunctional reactants through a series of stepwise reactions to form dimer, trimer, tetramer, pentamer and so on, with or without the elimination of side products such as water, hydrochloric acid or sodium chloride. The molecular weight of the polymer builds up gradually. Certain polycondensation reactions such as polyesterifications are reversible. In such cases, the side product formed during the reaction has to be removed from the system to shift the equilibrium towards product formation to obtain high molecular weight polymer. In addition, reactants should be pure to prevent side reactions and the molar ratios of the reactants must be maintained in stoichiometric proportions.

Polycondensation reactions are not generally classified into different groups. The commercially important polycondensation reactions include esterification to form polyesters, amidation reactions to produce polyamides, the reaction between diols and diisocyanates to synthesise polyurethanes and nucleophilic substitution reactions resulting in the formation of polymers like polysulfones and polyphenylene sulfide. Polycondensation reactions of industrial importance are generally homogeneous systems while polymer formation to PPS is a heterogeneous one.

The various stages that occur during a polycondensation reaction can be represented as,



678.6'364(043)  
RAJ

TH-499

where  $S_m$  denotes the small molecule (side product) that is formed during the reaction.

At any given reaction time 't', molecules of different degrees of polymerization are present and any two species can react for the growth of the polymer chain. The overall rate expression would be the summation of the individual rates of formation of the various species. The kinetic analysis of such a system poses a very difficult task. This uncertainty is overcome by assuming that the reaction rate between two functional groups is independent of the chain length of the reacting species and that the effect of a similar functional group present elsewhere in the molecule on the rate is negligible. The validity of these assumptions have been experimentally confirmed. Investigations on esterification reactions as a function of chain length have shown that the rates of disappearance of  $-COOH$  groups in dibasic acids become independent of chain length  $n$ , for  $n \leq 4$ .<sup>191-193</sup> Thus, the kinetic analysis is simplified to that observed in simple organic esterification reactions and the rate of reaction can be related to the rate of disappearance of a reactant or a functional group. The degree of polymerization or the chain length increases gradually as the reaction proceeds. In a heterogeneous system such as PPS synthesis, the general features of the process and the operating parameters have not been investigated systematically.

Polyesterifications are the most extensively studied of all polycondensation reactions. The different rate expressions that emerge can be classified as under:

- (i) Internal or self catalysed reactions.
- (ii) Externally catalysed reactions.
- (iii) Non-**stoi**chiometric ratio of reactants.



The kinetic expressions differ and are discussed separately.

In the internal or self catalysed polyesterification reactions, the rate expression can be represented as,

$$- \frac{d[\text{COOH}]}{dt} = k[\text{COOH}]^2[\text{OH}] \quad (5)$$

Since stoichiometric concentrations of functional groups is taken for the reaction, the rate equation becomes,

$$- \frac{d[\text{COOH}]}{dt} = k a^3 \quad (6)$$

where, 'a' denotes the concentration of the functional groups.

Equation 6 on integration and use of initial conditions such as at  $t=t_0$   $a = a_0$  becomes,

$$2 kt = \frac{1}{a^2} - \frac{1}{a_0^2} \quad (7)$$

The fractional conversions of the reaction could be expressed as a function of the fraction of the hydroxyl or carboxyl groups reacted at time 't'. If p denotes the fractional conversions, the concentration 'a' of carboxyl or hydroxyl group, at time 't' can be expressed as,

$$a = a_0 (1 - p) \quad (8)$$

Substituting the value of a from the above equation in equation 7, results in

$$2 a_0^2 kt = \frac{1}{(1-p)^2} - 1 \quad (9)$$

The reaction follows third order kinetics and a plot of  $\frac{1}{(1-p)^2}$  against reaction time should be linear. However, the uncatalysed polycondensation reaction has been found to follow third order kinetics only after 80 per cent conversion. The deviation from third order in the early stages has been described to be due to large polarity changes in the medium as a result of the disappearance of the hydroxyl and carboxyl groups.

In externally catalysed polyesterification reactions the concentration of the strong acid, added as the catalyst, remains constant during the reaction. The rate expression in this case is represented as,

$$-\frac{da}{dt} = k a^2 \quad (10)$$

In forms of fractional conversion 'p', the rate expression is given as,

$$C_o kt = \frac{1}{(1-p)} - 1 \quad (11)$$

The reaction follows second order kinetics for most polyesterifications and a plot of  $\frac{1}{(1-p)}$  against reaction time is linear over a wide range of conversions. The form (11) represents the average number of structural units per chain and is defined as the number-average degree of polymerization ( $\overline{DP}_n$  or  $\bar{x}_n$ ). Equation 11 therefore becomes,

$$\bar{X}_n = 1 + k C_o t \quad (12)$$

The number-average molecular weight in catalysed polyesterification increases linearly with reaction time.

In catalysed reactions with non-stoichiometric ratio of reactants

used, the rate expression is expressed in the form,

$$-\frac{d[P]}{d[Q]} = k[P][Q] \quad (13)$$

where P and Q are the reactants.

Although one of the reactants is in excess, for the reacting functional groups, the stoichiometric relation is given by,

$$[P_0] - [P] = [Q_0] - [Q] \quad (14)$$

where  $[P_0]$  and  $[Q_0]$  represent the initial concentrations and  $[P]$ ,  $[Q]$ , the concentrations at time 't'.

Combining the equations 13 and 14 and integrating equation 13, the following expression is obtained,

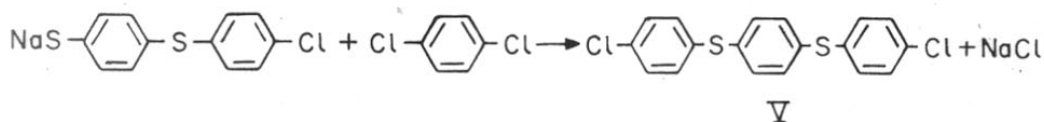
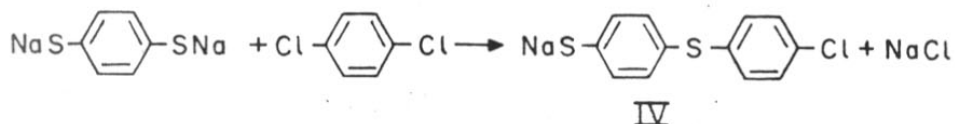
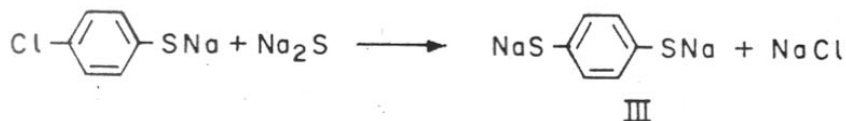
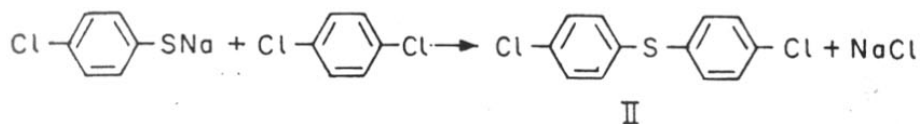
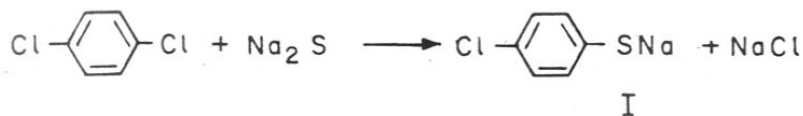
$$\ln \frac{[Q]}{[P]} = -\ln r + Q_0 [1 - r] kt \quad (15)$$

where  $r = \frac{[P_0]}{[Q_0]} < 1$  is the molar ratio of the reactants.

A plot of  $\ln \frac{[Q]}{[P]}$  against reaction time is linear and the reaction follows second order kinetics.

Published information on heterogeneous polycondensation is rather limited. The only published work on the kinetics of polycondensation to generate PPS is that of Lenz and coworkers.<sup>55</sup>

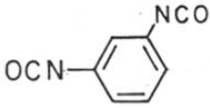

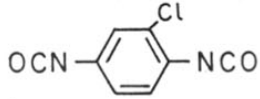
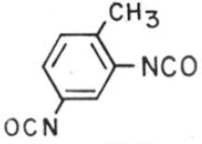
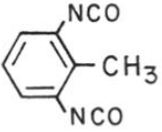
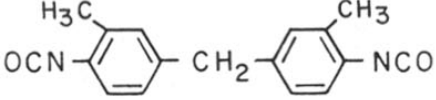
Due to a sequence of reactions in the early stages of the PPS polycondensation the following species could be formed.



The reactivities of the different species I,II,III,IV and V would be expected to be different. Thus the rates of formation of the mono-substituted moiety and its rate of growth would be different. No published information exists on elaborate kinetic evaluation of this system.

In reactions involving diisocyanates, the reactivity of the isocyanate group is affected by the structure of the organic moiety to which it is attached. In aromatic diisocyanates reactivity is influenced by the position of attachment of the second isocyanate group to the benzene ring. The reactivity of the two isocyanate groups are not equivalent and the disappearance of one isocyanate group through urethane formation reduces the reactivity of the other. The reaction follows an overall second order kinetics and the rate expression can be represented as,

TABLE 3  
REACTIVITY OF DIISOCYANATES

Diisocyanate	Structure	Rate constant $k \times 10^{-4} \text{ s}^{-1}$	
		Initial	Final
m-phenylene diisocyanate		6.0	2.5
p-phenylene diisocyanate		5.7	1.6
1-chloro, 2,4-phenylene diisocyanate		13.0	4.3
2,4-toluene diisocyanate		2.0	0.22
2,6-toluene diisocyanate		0.8	0.12
4,4'-bis(2-methyl isocyanato phenyl) methane		0.11	0.1



SUMMARY AND RECOMMENDATIONS

$$-\frac{d[\text{NCO}]}{dt} = \frac{d[\text{urethane}]}{dt} = k[\text{NCO}][\text{OH}] \quad (16)$$

The reactions of aromatic diisocyanates and diols leading to the formation of polyurethanes have been published.

In the case of the most widely used aromatic diisocyanate, namely, 2,4-toluene diisocyanate (TDI), the inductive effect of the isocyanate group is moderated by the steric effect of the methyl group. It was observed that in the early stages of the reaction, the isocyanate moiety para to methyl group contributes to the rate observed and in the latter stages of the reaction, the rate decreases to a great degree due to the lesser reactivity of the isocyanate group at the ortho position. Table 3 shows the change in both the rate constants with the structural variations in different diisocyanates.<sup>194</sup>

When all the factors affect both isocyanate groups equally, the reactivities of both the isocyanate groups are equal. This is observed of methylene diisocyanate (MDI) or substituted MDI having equivalent isocyanate groups. However, in the absence of the steric effects, the reactivity of bifunctional monomers is reduced significantly as a result of the reaction of one isocyanate group.

Polycondensation reactions leading to the formation of PPS follow aromatic nucleophilic substitution mechanism. Aromatic polyethers are commercially prepared by aromatic nucleophilic substitution reactions between a diphenoxide and a aromatic dihalide. The reactions are carried out in a highly polar organic solvents.<sup>196</sup> It can be represented in the form,



Denoting [ArO] as the phenoxide and [Ar'X] as the aromatic dihalide in the form of functional moieties, the rate equation can be expressed as,

$$-\frac{d[\text{Ar O}]}{dt} = k[\text{Ar O}][\text{Ar' X}] \quad (18)$$

The above expression on integration becomes,

$$\frac{1}{c} = k t + \frac{1}{c_0} \quad (19)$$

where  $c$  is the concentration of phenoxide [ArO] or the dihalide [Ar'X] functional group at time 't' and  $c_0$ , the initial concentration.

A second order reaction kinetics with respect to the concentration of functional groups is observed. The reaction rate was however bimodal. The uniform initial rate observed was followed by a slower rate beyond 50% conversion. In the investigations of Lenz et al. towards synthesis of PPS, an overall second order reaction rate was observed. In the present investigation, a bimodal rate was observed.

To summarise, polycondensation reactions fall into three categories.

- (i) Uncatalysed reactions that occur with reasonable rate (formation of polyesters and polyamides).
- (ii) reactions that require external addition of catalyst to have reasonable rates of reaction (formation of phenol-formaldehyde resins).
- (iii) reactions with optional addition of catalyst (formation of polyurethane).

The reactions could either be homogeneous or heterogeneous in nature. Most commercially important polycondensation reactions are homogeneous while the generation of PPS is heterogeneous in nature.



#### 1.4 Physico-chemical characterization of polymers

A variety of techniques are available for the physico-chemical characterization of polymers. The widely used techniques and the information generated are summarized below.

	<u>Analysis technique</u>	<u>Information generated</u>
(i)	Infrared spectroscopy (IR)	Functional groups present
(ii)	Nuclear magnetic resonance spectroscopy (NMR)	Chemical structural analysis
(iii)	Volumetric analysis	Estimation of unreacted monomers and side products formed.
(iv)	Microanalysis	Chemical composition/quantitative estimation of end groups in polymer chain
(v)	Solution viscosity	Intrinsic viscosity and molecular weight
(vi)	Differential scanning calorimetry (DSC)	Glass transition temperature, melting point, enthalpy of fusion, crystallization, percent crystallinity and crystallization kinetics
(vii)	Thermogravimetric analysis (TGA)	Thermal stability, weight loss as a function of temperature
(viii)	X-ray diffractometry	Crystal lattice dimensions, crystallite orientation, percent crystallinity
(ix)	Scanning electron microscopy (SEM)	Particle size, shape, crystal growth and morphology

The following techniques have been used in the present investigation.

- (i) Infrared spectroscopy
- (ii) Volumetric analysis
- (iii) Microanalysis
- (iv) Dilute solution viscosity
- (v) Differential scanning calorimetry (DSC)
- (vi) Thermogravimetric analysis (TGA)

- (vii) X-ray diffractometry
- (viii) Scanning electron microscopy

These techniques are discussed briefly in the following sections.

#### 1.4.1 Infrared spectroscopy

Infrared (IR) spectra are generated by the absorption of electromagnetic radiation in the frequency range  $400$  to  $4000\text{ cm}^{-1}$  by polymer molecules. Different functional groups and structural features in the molecule absorb at characteristic frequencies. The frequency and intensity of absorption are indicative of the bond strengths and structural geometry in the molecule. Absorption in the range  $1100\text{ cm}^{-1}$  to  $600\text{ cm}^{-1}$  is specific to each molecule and is termed as 'finger print' region. General infrared spectroscopy is useful to determine functional groups present in the polymer molecule. The substitution pattern in aromatic polymers can also be predicted.

#### 1.4.2 Volumetric analysis

Specific volumetric analysis can be used to evaluate concentrations of reactants and products generated in a reaction. The method involves collection of samples at intermittent reaction times and estimation of the concentration of a reactant. Usually titrimetric methods are followed. In the present investigation, the concentrations of unreacted sodium sulfide and the moles of sodium chloride formed were determined at different reaction times by iodometric and argentometric titrations.

#### 1.4.3 Microanalysis

The method is generally used to evaluate the chemical composition. This estimate can be related to the number average molecular

weight of a polymer, provided the end group differs from the repeating structure of the polymer. The polymer sample is digested with a strong acid in a sealed ampule. The digested sample is then analysed either by gravimetric or volumetric analysis. In the present system, the PPS samples were analysed for chlorine end groups; a gravimetric method was followed, the details of which are given in section 2.

#### 1.4.4 Dilute solution viscosity

Dilute solution viscosity measurement is a widely used indirect method for evaluating the molecular weight of a polymer. The incremental increase in the viscosity of a solvent brought about by the addition of small amounts of polymer forms the basis for intrinsic viscosity determination. It is indicative of the size of the solvated polymer and can be related to the polymer molecular weight by comparison with data based on direct methods such as membrane osmometry and light scattering. A number of capillary viscometers that can be used for the determination of viscosity of dilute polymer solutions exist such as Ostwald, Cannon-Fenske and Ubbelohde viscometers. The viscometers are mounted in precisely-constant temperature bath. The procedure involves the measurement of the flow times of an exact volume of the solvent as well as of polymer solutions of different concentrations at the specific preset temperature. The following viscosity parameters can be determined from the measurements:

$$\text{Relative viscosity } (\eta_r) = \frac{t}{t_0} \quad (1)$$

$$\text{Specific viscosity } (\eta_{sp}) = (\eta_r - 1) \quad (2)$$

$$\text{Intrinsic viscosity } [\eta] = \left( \frac{\eta_{sp}}{c} \right)_0 \quad (3)$$

where  $t$ ,  $t_0$  are flow times for polymer solution and solvent respectively and  $c$ , the concentration of the polymer in gm/deciliter.

The two most widely used equations in relating the intrinsic viscosity with concentration are known as the Higgins<sup>197</sup> and Kramer<sup>198</sup> equations given below:

$$\frac{\eta_{sp}}{C} = [\eta] + k' [\eta]^2 C \quad (4)$$

$$\frac{(\ln \eta_r)}{C} = [\eta] + k'' [\eta] C \quad (5)$$

where  $k'$  and  $k''$  are constants.

A plot of  $\eta_{sp}/C$  against concentration on extrapolation to infinite dilution ( $C=0$ ) gives the intrinsic viscosity  $[\eta]$ , as the intercept. It has units of deciliters per gram. Intrinsic viscosity  $[\eta]$  can be related to the polymer molecular weight by the Mark-Houwink equation<sup>199</sup>

$$[\eta] = K M^a \quad (6)$$

where  $K$  and 'a' are constants characteristic of a polymer and solvent combination at a given temperature and  $M$ , the molecular weight.

Knowing  $K$  and 'a', the polymer molecular weight can be calculated.

An easier, faster method known as the single point intrinsic viscosity measurement has found wide industrial acceptance. Two equations, one proposed by Schultz and Blaschke<sup>200</sup> and the other by Solomon and Ciuta<sup>201</sup> are represented below.

$$[\eta] = \frac{\frac{\eta_{sp}}{C}}{1 + K \eta_{sp}} \quad (7)$$

where  $K$  is constant.

$$[\eta] = \frac{\sqrt{2}}{C} \sqrt{\eta_{sp} - \ln \eta_r} \quad (8)$$

The method involves the evaluation of relative viscosity at a single polymer concentration at an exact temperature. The polymer concentration generally chosen for high molecular weight polymers is 0.5 gm/dl. The intrinsic viscosity is then calculated from equations 7 and 8 .

Equation 7 has been derived from equations 4 and 5 implying that Higgin's and Kramer's equations are obeyed by polymer solutions. However, equation 8 does not involve any constant. Intrinsic viscosity determined from equation 8 match experimental results of Naar et al.<sup>202</sup> They proposed that the right hand side of equation tends to the intrinsic viscosity  $[\eta]$  at infinite dilution ( $C=0$ ). The equation of Solomon and Ciuta (eq.8) was found to be in good agreement with intrinsic viscosity determined by graphical extrapolation method for polycarbonate, poly(phenylene oxide) and poly(ether imide)<sup>203</sup> at polymer concentrations, of  $\eta_{sp} \ll 1$  . Palit and Kar<sup>204</sup> reported that equation can generally be applied for polymer solutions with  $\eta_{sp} < 0.6$ .

Other equations for single point intrinsic viscosity determination have also been proposed. A method proposed by Mortin<sup>205</sup> has been extensively tested.<sup>206</sup> The equation is represented below.

$$\log \left( \frac{\eta_{sp}}{C} \right) = \log (\eta) + k (\eta) C \quad (9)$$

Deb and Chatterjee<sup>207</sup> proposed an equation in the form,

$$[\eta] = \frac{1}{C} \sqrt[3]{3 \ln \eta_r + \frac{3}{2} \eta_{sp}^2 - 3 \eta_{sp}} \quad (10)$$

and have shown the usefulness for a number of polymer-solvent systems. Khan and Bhargava<sup>208</sup> have also proposed an equation for evaluating intrinsic viscosity from single point determinations. The method is sensitive to polydispersity and chemical composition in the case of copolymers.

#### 1.4.5 Thermal analysis

Important thermal analysis techniques include thermogravimetric analysis (TGA), differential thermal analysis (DTA) and differential scanning calorimetry (DSC). The characteristic parameters determined by thermal analysis include, the glass transition temperature, the crystalline melting point in the case of crystalline polymers or softening point in the case of amorphous polymers and the thermal stability of the polymer which determines the temperature and rate of thermal degradation. Several reviews are available.<sup>209-224</sup>

The thermal analysis techniques involve continuous monitoring of a physical property such as the change in mass, enthalpy or specific heat over a temperature range. The techniques offer the advantages of speed, sensitivity and precision. Preliminary thermal analysis would include qualitative determinations such as the use of a simple hot stage microscope. It is used to determine the thermoplasticity, softening temperature, crystalline melting point, flow temperature, adhesive properties and thermal stability.

In differential scanning calorimetry (DSC) the physical or chemical

changes that occur as the polymer sample is heated and cooled at a programmed rate is evaluated. The method is quantitative as the thermogram (the output of this technique) can be directly related to the thermodynamic parameters such as changes in specific heat, enthalpy and entropy of the polymer under investigation. The polymer sample and a reference materials (usually aluminium upto 600°C) are separately subjected to a programmed heating. The thermogram is indicative of the excess differential power required to maintain the sample holder at the same temperature as the reference material when the temperature is increased/decreased at a constant rate. A typical thermogram of commercial PPS (Ryton) is shown in figure 1 .

The enthalpy of a polymer is calculated from a knowledge of the area under its first order transition. Similarly, area under the first order transition of a reference of known enthalpy of fusion is determined (Indium). The enthalpy of fusion of the polymer sample is then calculated.

#### Glass transition temperature

The glass transition temperature is an apparent second order transition and signifies the onset of large scale motion of chain segments at the molecular scale. It is the temperature above which amorphous polymers exhibit rubbery characteristics and below which are glassy and brittle. The molecular factors affecting glass transition temperature include, the chemical structure of the monomer(s), tacticity, molecular weight, molecular weight distribution, extent of crosslinking and the presence of plasticizers. In addition to other known methods, glass transition temperature can be determined using a differential scanning calorimeter by monitoring the specific heat change with temperature.

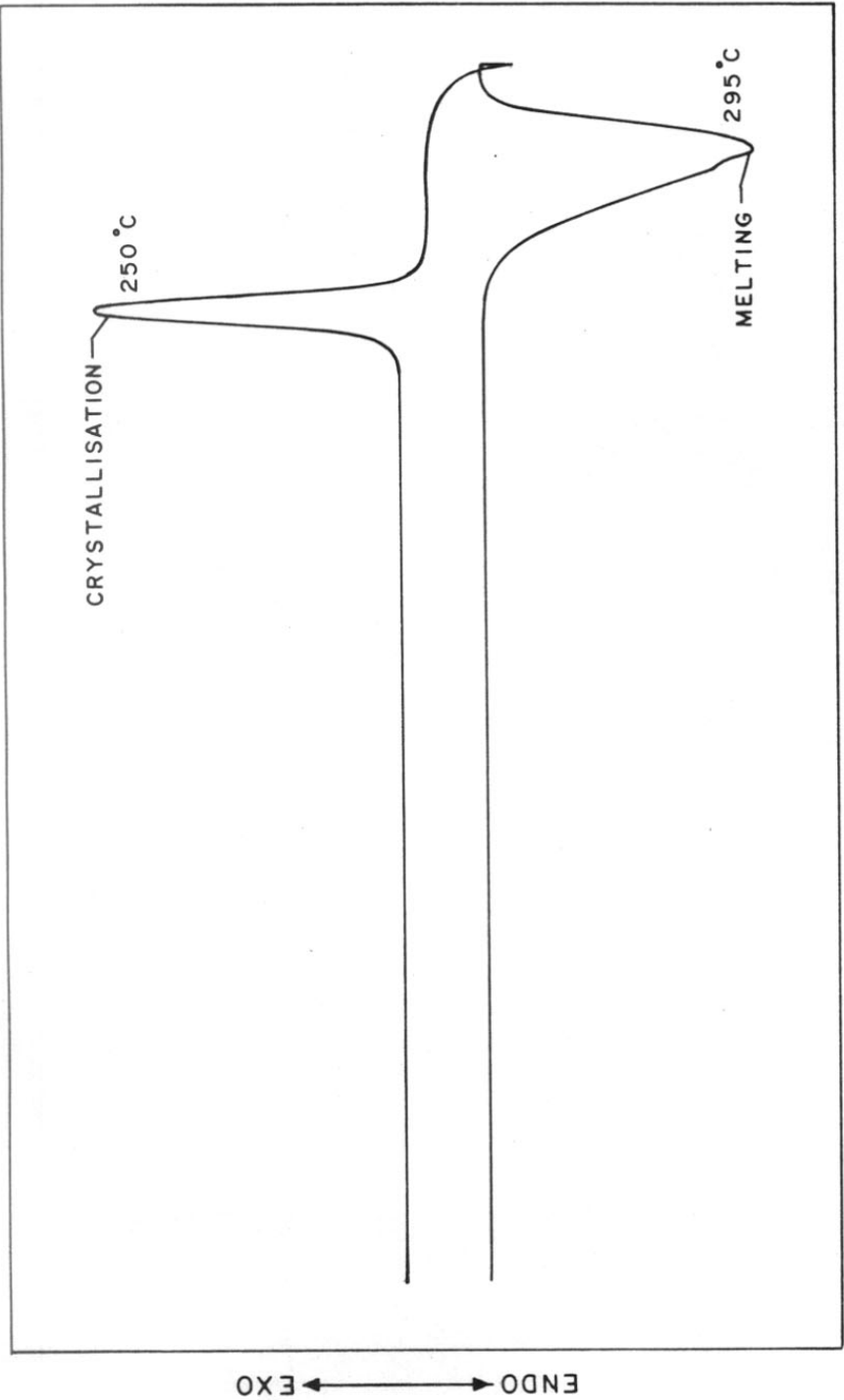


FIG.1: TYPICAL DSC SCAN OF RYTON V-1



### Crystalline melting point

The melting point of a semicrystalline polymer is a first order transition. Due to their polydispersity, polymers generally melt over a temperature range, unlike metals. Also the melting point is not sharp. The factors that affect crystalline melting point and its range are, the degree of crystallinity, crystallite size and perfection, molecular weight, molecular weight distribution and orientation. Crystalline melting point of a polymer sample could conveniently be obtained using either a DSC or an optical microscope.

The DSC thermogram of a polymer shows the glass transition temperature as a shift in the base line, crystallization as an exothermic peak and melting as an endothermic peak.

Other applications<sup>225-229</sup> of the DSC technique include specific heat measurements, estimation of the degree of crystallinity, crystal to crystal transition, liquid crystal transitions, rates of crystallization, crystallization kinetics and curing behaviour of thermosetting polymers.

### Thermogravimetric analysis

Thermogravimetric analysis (TGA) is used to determine the thermal stability of a polymer. This is a dynamic method and involves the determination of the weight loss of a polymer over a temperature range. The analysis is either conducted in an oxidising or inert (nitrogen) atmosphere. The output is a thermogram which is a plot of the weight of the polymer as a function of temperature, at a programmed heating rate. The technique is used primarily to determine the practical upper temperature limit of use for the polymer. The analysis is very useful in the

selection of processing conditions for the polymer. The dependant variables are the sample size, particle size, the rate of heating and the atmosphere (whether oxidising or inert) during analysis.

Other thermal measurements of practical interest include the vicat softening point useful for comparison of the softening characteristics of thermoplastics and heat deflection temperature signifying the thermo-mechanical response of the polymer under load.

#### 1.4.6 Morphological characterization

Polymer morphology involves the study of the arrangement of polymer molecules into crystalline and amorphous phases, the form and structure of these regions and the manner in which they are organized into larger and more complex domains. The morphology of a polymeric article is the result of the interaction of the chemical structure and physical characteristics of the polymer and the processing conditions. Morphological studies make use of techniques such as density measurements, optical and electron microscopy, x-ray diffractometry, birefringence, scanning electron microscopy etc. The two techniques used in the present work, namely x-ray diffractometry and scanning electron microscopy are discussed below.

##### X-ray diffractometry

X-ray diffraction studies of polymer are well reviewed.<sup>230-239</sup> Polymers are either amorphous or semicrystalline. X-ray diffraction studies are extensively used to determine the percentages of the two phases in semicrystalline polymers.

Amorphous polymers can be visualized to consist of molecular

bundles within which some ordered structure is possible. Semicrystalline polymers on the other hand show signs of crystalline order. An increase in crystallinity is signified by denser, stiffer, harder, tougher and solvent resistant characteristics. Amorphous regions offer the advantage of softness and ease in processing.

X-ray diffraction follows Bragg's law represented by,

$$n \lambda = 2 d_{hkl} \sin \theta$$

where  $\lambda$  is the wavelength,  $\theta$  the angle of scattering,  $d_{hkl}$ , the spacing between the planes that cause diffraction, and  $n$  the diffraction order.

X-rays of wavelength  $\lambda = 1.54 \text{ \AA}$  is suitable for x-ray diffraction studies of organic polymers. This is achieved by electron bombardment of a copper target in an evacuated tube and filtration of x-rays generated by using a nickel filter. Normally, the wavelength  $\lambda$  is kept constant and  $\theta$  is varied.

The polymer sample could be in the form of a powder, film or fibre. The diffraction could either be photographed or amplified and recorded by electronic x-ray detectors. A typical output is shown in figure 2 indicating crystalline and amorphous scatterings.

There are a number of methods to determine the percentage of crystallinity by x-ray analysis. The most widely used one involves the measurement of the areas under crystalline and amorphous regions of the x-ray diffraction scans. The degree of crystallinity is calculated from the relation,

$$C_i = \frac{A_c}{A_c + A_a}$$

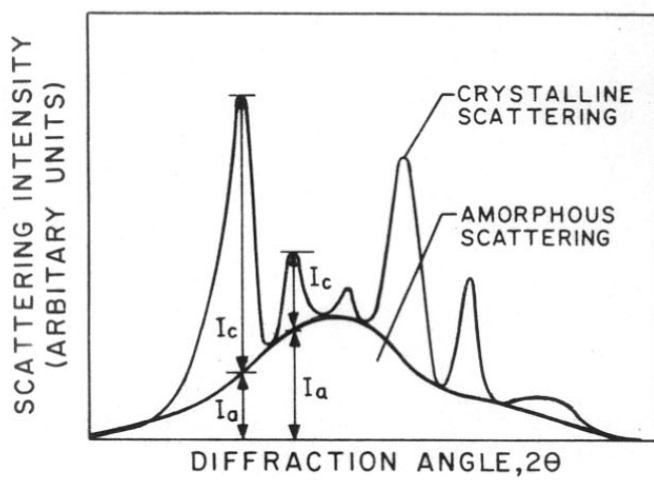


FIG.2: TYPICAL XRD SCAN

where  $A_c$  and  $A_a$  are the areas of crystalline and amorphous phases and  $C_1$ , the crystallinity index.

#### Scanning electron microscopy (SEM)

Scanning electron microscopes were first introduced in 1965 and it has since become a very useful tool in polymer research for studying surface morphology.<sup>240-243</sup> In this technique an electron beam is scanned across the specimen resulting in back scattering of electrons of high energy, secondary electrons of low energy and x-rays. These signals are monitored by detectors and magnified. An image of the investigated microscopic region of the specimen is thus photographed.

If the specimen under investigation is not a good conductor, it should be coated with a thin layer of conducting material like gold or platinum. This is done by placing the specimen in a high vacuum evaporator, and evaporizing the conducting material held in a tungsten basket (vacuum deposition).

The output of SEM in the form of a photograph can be used to evaluate the level of dispersion of particles, size and morphological features. SEM can be used with greater success to study the surface morphology of polymers, copolymers, polyblends and polymer networks; microstructure in two phase polymers, filled and reinforced plastics, deformation morphology of fibers, fracture studies and weathering of polymers.



---


**CHAPTER 2**  
**EXPERIMENTAL**

---

## 2 EXPERIMENTAL

### 2.1 Materials

#### (i) 1,4-Dichlorobenzene

Empirical formula	$C_6H_4Cl_2$
Molecular weight	146.9
Chemical structure	

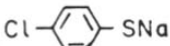
1,4-Dichlorobenzene (commonly known as paradichlorobenzene, PDCB) was obtained from M/s. High Purity Chemicals (New Delhi, India). Its purity was checked by gas chromatographic analysis using a NUCON (AIMIL, India) 5500 series gas chromatograph. The column used was SE30. The injection temperature was 250°C and the oven temperature was maintained at 200°C. A TCD detector was used and the carrier gas was hydrogen with a flow rate of 35 ml/min. PDCB was injected as a 50 weight percent solution in acetone. The purity was determined to be greater than 99.5%. It was used as one of the reactants, without further purification.

#### (ii) Sodium sulfide

Empirical formula	$Na_2S$
Molecular weight	78.04

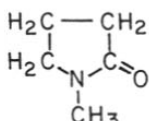
Sodium sulfide flakes were obtained from M/s. Poona Chemicals, (Pune, India). The major impurity was ferric chloride (~2%) which is insoluble in methanol. It was removed by dissolution of the flakes in methanol followed by filtration. The methanolic solution of sodium sulfide was analysed for its concentration by following the procedure discussed in Section 2.5. The filtered methanolic solution of sodium sulfide was used as a reactant. Methanol was distilled off before the other reactant was added.

(iii) Sodium 4-chlorothiophenoxide

Empirical formula	$C_6H_4ClSNa$
Molecular weight	165.5
Chemical structure	

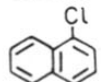
The sodium salt was prepared from 4-chlorothiophenol obtained from M/s. FLUKA (AG BUCHS SG, SWITZERLAND) 4-chlorothiophenol (99.5% purity) was dissolved in warm ethanol. A stoichiometric amount of sodium hydroxide in ethanol was added to it. Ethanol and water were removed in a rotary evaporator to get the sodium salt. It was used in catalytic quantities for mechanistic studies.

(iv) N-methyl pyrrolidone

Empirical formula	$C_5H_9NO$
Molecular weight	99.13
Chemical structure	

N-methyl pyrrolidone (NMP) of 99% purity obtained from GAF Corporation, USA was used as a reaction medium for the solution polymerization.

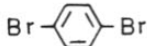
(v) 1-Chloronaphthalene

Empirical formula	$C_{10}H_7Cl$
Molecular weight	162.45
Chemical structure	

1-chloronaphthalene obtained from M/s. FLUKA (AG, BUCHS SG SWITZERLAND) was distilled before use. It was used as a solvent for viscosity measurement.



(vi) 1,4-Dibromobenzene

Empirical formula	$C_6H_4Br_2$
Molecular weight	235.92
Chemical structure	

1,4-dibromobenzene or paradibromobenzene was obtained from M/s. FLUKA (AG, BUCHS, SG SWITZERLAND) as a pure sample. It was used as received as a reactant in place of PDCB for mechanistic studies.

(vii) 1,3-Butane diol

Empirical formula	$C_4H_{10}O_2$
Molecular weight	90.12
Structural formula	$CH_3.CHOH.CH_2.CH_2OH$

1,3-butane diol was obtained from M/s. BDH Chemicals, U.K. The purity was greater than 99%. It was used as received as the medium to maintain a constant temperature in the dilute solution viscosity measurements.

(viii) Methylene chloride

Methylene chloride was obtained from M/s. Lobo Chemie Indo-Austral Co., India. It was distilled before use. It was used to extract cyclic oligomers of phenylene sulfide formed during the course of the reaction.

(ix) Methanol

Empirical formula	$CH_3OH$
Molecular weight	32

The commercial methanol received was distilled before use for purification of the sodium sulfide and for polymer isolation step.

(x) Analytical reagents

Reagents required for chemical analysis were of AR grade and were used without further purification. These included sodium thiosulfate, iodine crystals, silver nitrate, sodium bicarbonate, potassium dichromate, potassium chromate, sodium chloride, potassium iodide, hydrochloric acid, nitric acid etc.

2.2 Polymerization set up

Poly(para phenylene sulfide) was synthesized by the polycondensation of 1,4-dihalobenzene and sodium sulfide in N-methyl pyrrolidone at 195°C using two different reactors. The reactor details are as under:

(i) Stainless steel reactor

A stainless steel pressure reactor of 600 ml capacity was equipped with provision for agitation, heating jacket and cooling coil. The mechanical stirrer with variable speed had a length of 16.7 cm, and a propeller type blade of 6.2 cm width. The reactor top had openings for a thermowell, inlet-outlet valves, pressure gauge and a cooling coil of 3.3 cm diameter surrounding the stirrer. The internal diameter of the reactor was 7.5 cm and the depth was 18 cm.

The reactor was heated electrically by an externally fitting heater assembly. The temperature control was achieved by a temperature controller and a thermocouple introduced into the thermowell opening of the reactor.

(ii) Teflon reactor

A Berghof (W. Germany) autoclave reactor with a teflon sleeve and a magnetic stirrer was also used for the polycondensation reactions.

This reactor had a 250 ml teflon vessel of 6.4 cm internal diameter and a depth of 10.1 cm. The teflon vessel was enclosed in a suitably fitting outside container of stainless steel. A teflon gasket placed between the teflon vessel and the reactor top ensured tight fitting to maintain positive pressure inside the vessel. The reactor top was equipped with inlet-outlet valves, a pressure gauge and a thermocouple to monitor the reaction temperature. The stirring was achieved with a magnetic needle 2 cm in diameter. Heating was done by an externally fitting electrical heater assembly.

### 2.3 Polycondensation procedure

Sodium sulfide flakes (35 gm) were dissolved in 150 ml of methanol and filtered. This step removed ferric chloride impurities. The filtered methanolic solution was analysed for sodium sulfide concentration. Methanolic sodium sulfide solution corresponding to 15 gms (0.1923 mole) sodium sulfide and 50 ml of N-methyl pyrrolidone were charged into the stainless steel reactor. The reactor was closed and placed into the heater assembly. The outlet valve was opened, a distillation head was attached to it and with gentle stirring, the contents were heated to 80°C. The methanol distilling out was collected. The temperature of the reactor contents was gradually raised to 190°C to quantitatively distil off methanol and water. Through the inlet valve, 30 gms (0.2041 mole) of paradichlorobenzene in 50 ml N-methyl pyrrolidone was introduced into the reactor, keeping the outlet valve open. On completion of the addition of the paradichlorobenzene solution, the inlet-outlet valves were closed and the temperature controller was set to 195°C. After an initial drop of 10°C due to addition of paradichlorobenzene solution, the temperature was found

to reach 195°C in approximately five minutes. The reaction time was counted as the time after the attainment of a constant temperature of 195°C. The rate of stirring was maintained at 660 rpm. After a predetermined reaction time, the heating was discontinued, the heater assembly was dismantled and the reaction mixture cooled rapidly by circulating cold water through the cooling coil.

For reactions carried out in the Teflon reactor, the entire quantity of solvent, NMP was added in one lot along with the methanolic solution of sodium sulfide. The reactor contents were then heated to distill off methanol and water.

Before the addition of paradichlorobenzene, the reactor was cooled to a temperature of 130°C. The required quantity of PDCB was added as a solid by opening the reactor. After the addition, the teflon sleeved reactor was closed and placed inside the heater assembly. It took approximately 30 minutes for the contents to attain the reaction temperature of 195°C. The highest possible setting was used for the magnetic needle. At the end of the predetermined reaction time, the reactor was taken out of the heater assembly and cooled under cold water to terminate the reaction.

#### 2.4 Polymer isolation

The procedure followed for polymer isolation step and the wet chemical analysis were the same for reaction products from both the reactors. The polycondensation mixture at the end of a predetermined period was in the form of a cake at ambient temperature containing finely dispersed cream coloured solids. The cake was extracted out of

the stainless steel reactor with 400 ml of methanol in the form of a slurry. This step dissolved the unreacted paradichlorobenzene and sodium sulfide. The slurry contained the polymer (PPS) and byproduct sodium chloride as insolubles. The unreacted sodium sulfide, paradichlorobenzene and oligomers such as dimers were removed as methanol solubles along with NMP.

The slurry was stirred vigorously for ten minutes and filtered through a Buckner funnel. The precipitate containing polymer and sodium chloride generated during the reaction was repeatedly washed with fresh methanol. The filtrate and washings were collected for chemical analysis of unreacted sodium sulfide and recovery of the solvent.

The precipitate was transferred into a two liter beaker, dispersed in 500 ml water to dissolve the sodium chloride, stirred vigorously for 30 minutes and filtered. The precipitate was subsequently washed with fresh warm water. The filtrate and washings containing sodium chloride and traces of unreacted sodium sulfide were collected for chemical analysis. The polymer (polyphenylene sulfide) in the form of precipitate, was obtained as insolubles in methanol and water. It was dried in a vacuum oven at 120°C for 4 hours. The dried polymer was weighed for determining the yield and stored for further characterization.

## 2.5 Wet chemical analysis

Wet chemical analysis was used to determine the purity of sodium sulfide and to estimate the unreacted sodium sulfide and the sodium chloride formed during the reaction. A number of reagents are required to be prepared for these analyses. The procedures followed for standardization

of various reagents required are given in the following section.

### 2.5.1 Preparation of reagents

#### (i) Potassium dichromate solution (0.1 normal)

Potassium dichromate is a primary standard.

The 0.1N solution was prepared by weighing 2.452 gms of dry potassium dichromate in 500 ml volumetric flask. It was dissolved and the volume made up to the mark with distilled water.

#### (ii) Sodium thiosulfate standard solution

Approximately 0.1N solution of sodium thiosulfate was prepared by weighing 24.8 gms sodium thiosulfate crystals. The crystals were transferred to a 1000 ml volumetric flask and dissolved in small amount of distilled water. The volume was then made upto the mark with distilled water. Its exact normality was determined by titration against standard 0.1N potassium dichromate solution.

In a 500 ml iodimetric flask containing 100 ml of cold freshly distilled water, 3 gms of potassium iodide and 2 gms of sodium bicarbonate were dissolved. 6 ml of concentrated hydrochloric acid was added. Exactly 25 ml of the standard 0.1N dichromate solution was added, the flask stoppered, the contents mixed well and kept in the dark for 5 minutes. The contents were then diluted to 300 ml with distilled water and titrated against the sodium thiosulfate solution to be standardized. When the colour of the solution became yellowish green, 2 ml of starch indicator solution (1 wt. percent in water) was added and the titration continued till the blue colour just disappeared. The normality of the thiosulfate is calculated from the relation,

$$N_T = \frac{N_d \times V_d}{V_T}$$

where  $N_D$  and  $V_D$  are the normality and volume of the dichromate solution and  $N_T$  and  $V_T$ , the normality of volume of the thiosulfate solution

(iii) Iodine standard solution (0.1 normal)

In a 1000 ml volumetric flask, 20 gms of potassium iodide were dissolved in 40 ml distilled water. 12.7 gms of pure iodine crystals were then added to the solution and the volume was then made upto 1000 ml mark with distilled water. The exact normality of the iodine solution was determined by titration against standardized thiosulfate solution.

25 ml of 0.1N iodine solution in a 250 ml iodimetric flask was diluted to 100 ml and titrated against standard thiosulfate solution till pale yellow colour developed. 2 ml of starch indicator solution was added and the titration was continued till the developed blue colour just disappeared. The normality of the iodine solution was calculated by using the relation used for thiosulfate normality.

0.1N hydrochloric acid was made by diluting 9 ml of concentrated hydrochloric acid to 1000 ml in a volumetric flask. It was standardized against (standardized) 0.1N sodium hydroxide solution using phenolphthalein as indicator.

(iv) Sodium chloride solution (0.1N)

Freshly dried sodium chloride, weighing 2.974 gm was dissolved in water in a 500 ml volumetric flask and the volume was made up to the mark with distilled water.

(v) Silver nitrate solution (0.1N)

Freshly dried silver nitrate crystals weighing 8.5 gms were dissolved in water in a 500 ml volumetric flask. The volume is made up to the

mark with distilled water. The solution is stored in dark. Its exact normality is determined by titrating against standard sodium chloride solution. A mixed indicator solution made by dissolving 4.2 gms potassium chromate and 0.7 gm potassium dichromate in 100 ml distilled water.

To 25 ml of 0.1N sodium chloride solution in a conical flask, 1 ml of mixed indicator was added and the solution titrated against silver nitrate solution to be standardized. The end point was a distinct permanent red colour. The normality of silver nitrate was calculated as under.

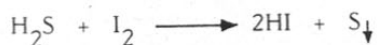
$$N_A = \frac{N_N \times V_N}{V_A}$$

where  $N_N$  and  $V_N$  represent normality and volume of sodium chloride solution and  $N_A$  and  $V_A$  represent normality and volume of silver nitrate solution

### 2.5.2 Sodium sulfide analysis

(i) Purity - The purity of sodium sulfide solution was estimated by iodimetric titration. The titration is based on the principle that sodium sulfide reacts under acidic conditions to liberate  $H_2S$ . Iodine reacts with  $H_2S$  to form HI and sulfur is precipitated. An excess of standardized iodine solution was taken and the unreacted iodine was backtitrated with standard sodium thiosulfate solution.

The series of reactions that occur are represented as follows:





In a one liter iodimetric flask, 40 ml of 0.1N iodine solution was pipetted out. 40 ml of 0.1N hydrochloric acid solution was then added and the volume diluted to 400 ml with distilled water. Exactly 1 ml of the methanolic solution of sodium sulfide to be analysed, was added, stirred vigorously and titrated against standard 0.1N sodium thiosulfate solution till pale yellow colour developed. 2 ml of starch indicator solution was added and the titration continued till the blue colour just disappeared. The titre reading (A) of sodium thiosulfate solution consumed was noted.

A blank titration was run by titrating 40 ml of the acidified iodine solution diluted as earlier with standard sodium thiosulfate solution. The titre reading (B) was noted.

The concentration of sodium sulfide was calculated using the relation,

$$\text{Na}_2\text{S in gm/ml} = (B - A) \times 0.003903 \times N_T$$

where  $N_T$  denotes the normality of thiosulfate solution.

(ii) Unreacted sodium sulfide

Unreacted sodium sulfide at the end of the polycondensation reactions for different reaction times was determined by analysing the methanol and water filtrate and washings collected during the polymer isolation step.

An aliquot of the solution collected (2-5 ml) was titrated iodometrically as per procedure mentioned earlier. The titre reading (C) was noted and the total quantity of unreacted sodium sulfide was computed from the total volume of the solution collected using the relation given below.

$$\text{Unreacted sodium sulfide} = \frac{N_T \times 0.003903 \times (B - C) \times V}{V_a}$$

where  $N_T$ , represent the normality of thiosulfate solution  
 (B-C), the volume of thiosulfate solution consumed  
 $V_a$ , the volume of aliquot taken for analysis and  
 $V$ , the total volume collected.

### 2.5.3 Sodium chloride analysis

The method is based on the principle that in an aqueous solution containing a mixture of chromate and chloride anions, silver cation combines selectively with the chloride ions (due to the lower solubility product of silver chloride formed) as a white precipitate. As soon as all the chloride ions are consumed, the silver cation forms a red precipitate of silver chromate. This can be noted as an accurate end point.

The reactions occurring during the course of the titration are given below.



An aliquot of the solution collected during the polymer isolation step was diluted to 100 ml with distilled water in a 250 ml beaker. 2 ml of dilute nitric acid ( $\sim 6\text{N}$ ) was added. The solution was then heated to boil off  $\text{H}_2\text{S}$  and cooled. Excess nitric acid was neutralized by the addition of solid sodium bicarbonate. 1 ml of the mixed indicator solution of potassium chromate and dichromate was added and the solution was

titrated against standard silver nitrate solution till the first appearance of a permanent red colouration.

The titre value  $V_A$  of the silver nitrate solution consumed was noted and the quantity of sodium chloride generated during the polycondensation was computed from the total volume of the solution collected. The following equation was used for the calculation,

$$\text{Sodium chloride generated} = \frac{N_A \times V_A \times 0.005844 \times V}{V_S}$$

where  $N_A$  and  $V_A$  represent the normality and volume of silver nitrate solution,

$V_S$  the volume of the sample taken for analysis, and  
 $V$ , the total volume collected.

## 2.6 Kinetics and mechanistic investigation

A series of experiments were conducted to elucidate the mechanism of polycondensation of sodium sulfide and paradichlorobenzene. In all the experiments, the nonstoichiometric ratio of the reactants was maintained at 0.2041 moles of PDCB to 0.1923 mole of sodium sulfide. In the first set of experiments, reaction parameters such as the agitation speed and dilution were varied to investigate the effect of diffusion on reaction kinetics. In the second set, a variety of reactants such as sodium thiophenoxide, sodium hydroxide, paradibromobenzene, excess dichlorobenzene were used to study the chemical mechanism of the polycondensation reaction. The details of these experiments are discussed in the respective sections on kinetics and mechanistic studies.

### Chemical analysis for kinetic data

The kinetic analysis of the system was studied by following the conversion as a function of reaction time. The conversion was determined by the analysis of the sodium chloride generated during the reaction by argentometric titration of the filtrate and washings collected during the polymer isolation step. The unreacted sodium sulfide in the reaction mixture was determined by iodimetric titration of the washings and filtration collected. Computation by linear regression method was done to estimate the specific reaction rate. The data of  $1/(1-p)$  versus reaction time were used for the estimation. For reactions where PDCB was used, sodium chloride generated was used to follow the conversion and for reactions where dibromobenzene was used, the rate of generation of sodium bromide was followed.

### 2.7 Microanalysis

The number average molecular weight  $\bar{M}_n$  was determined by end group analysis. The polymer samples were analysed for the percentage of chlorine end groups by microanalysis. The procedure used was the CARIUS method. The polymer sample was digested with concentrated nitric acid in the presence of silver nitrate. The chlorine end groups converted to silver chloride were that estimated gravimetrically.

#### 2.7.1 Evaluation of end groups

The number of -SNa and -Cl groups at different conversions were calculated as described below.

Based on the sodium chloride generated at different conversions,

the moles of -SNa and -Cl groups unreacted at that conversion were calculated. The number of -SNa and -Cl groups at the conversion was the ratio of the group divided by the total number of -SNa and -Cl groups multiplied by 2.

A sample calculation is given below for conversion at 60 minutes.

$$\text{Initial concentration of SS} = 0.1923$$

$$\text{Conversion based on NaCl} = 0.2398$$

$$\text{Unreacted SS + oligomers with -SNa groups} =$$

$$(1-0.2398) \times 0.1923 = 0.1462 \text{ (x)}$$

$$\text{Unreacted PDCB + oligomers with Cl groups} =$$

$$[(1-0.2398) \times 0.1923] + 0.0118 \text{ (y)}$$

Since the reaction is always 1:1 of SS and PDCB the -SNa is calculated as (denoted as z):

$$(z) = \frac{x}{x+y} \times 2$$

$$\text{and -Cl group is } 2 - z$$

The empirical formula becomes-

$$\overline{DP}_n = C_{6n} H_{4n} S_{n-1} Cl_{2-z} SNa_z$$

Since the chlorine end groups present in the polymer is known from microanalysis, the value of 'n' corresponding to chloro groups can be easily computed. In the above example, the chlorine % is 3.99 and the value of 'n' fitting in the equation for  $\overline{DP}_n$  is 8.0.

The empirical formula is therefore given by:



### 2.7.2 Solution viscosity

The polymer is insoluble at ambient temperatures in all solvents. Polyphenylene sulphide is soluble in 1-chloronaphthalene above 160°C. Below 160°C, the polymer precipitates out and is in the form of a solvent swollen gel at ambient temperature. The dilute solution viscosities of the polymer samples were measured in a modified Ubbelodhe viscometer.

The viscometer shown in Figure 3 was kept in a glass container (A) with (B) 50 m joint. This container served as a jacket. A provision (B) for fixing a reflux condenser was made in the viscometer. The viscometer with the glass jacket (A) was insulated with asbestos rope to minimise heat loss. It was placed in a one liter round bottomed flask (C) with B 29 M joint. 1,3-butane diol (BP 196°C) was used as the heating medium. It was added in the flask and the assembly placed on a heating mantle. The vapours of 1,3-butane diol were used to maintain a constant temperature of 195°C. The diameter of the viscometer capillary was 0.4 mm and the flow times were measured at 195°C. The flow time of the solvent 1-chloronaphthalene was 147.2 sec.

The concentration of the polymer solutions were kept at 4 weight percent. The polymer samples were weighed on an aluminium foil and transferred into the viscometer. Exactly 10 ml of the solvent 1-chloronaphthalene was introduced into the viscometer. The slurry was

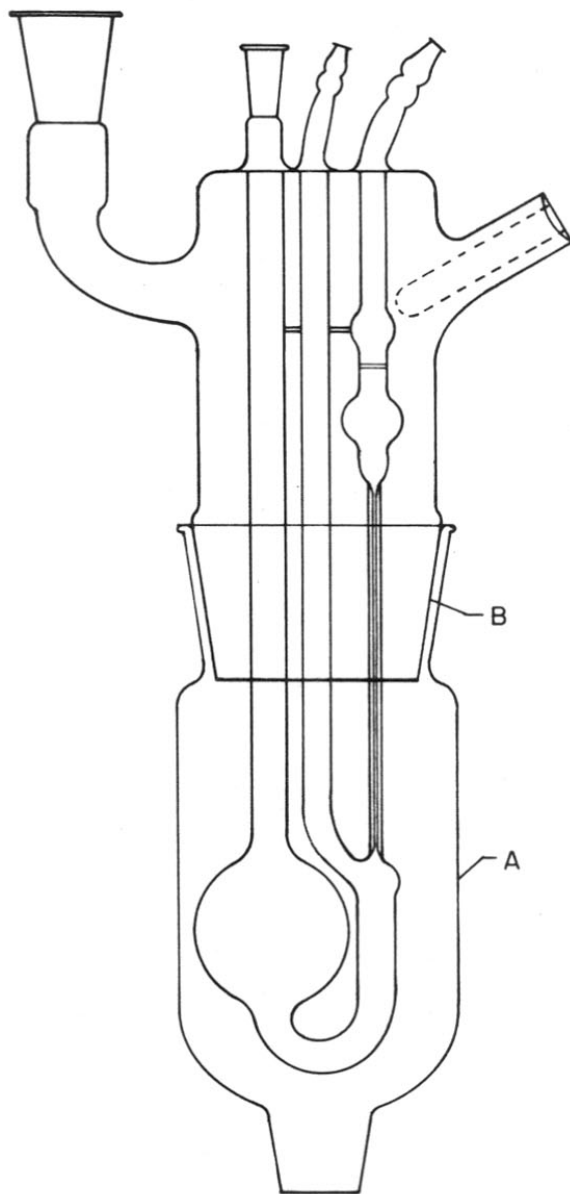


FIG.3: MODIFIED VISCOMETER

warmed to 160°C to dissolve the polymer. The viscometer with the polymer solution was introduced into the hot glass container. The viscometer was allowed to stabilize for 45 minutes at the temperature of 195°C. Efflux times for the polymer solutions were measured at this temperature. Three readings were taken and the mean reading taken for calculations.

The relative viscosity ( $\eta_{rel}$ ), the specific viscosity ( $\eta_{sp}$ ) and the intrinsic viscosity  $[\eta]$  of the polymer samples were calculated as per equation given in Section 1.4.4.

### 2.7.3 Extraction studies

The polymer samples were extracted in a soxhlet extraction unit for 16 hours using methylene chloride. An accurately weighed quantity of the polymer sample was wrapped in a filter paper. The sample was extracted with methylene chloride. After 16 hours of extraction, the solvent methylene chloride was distilled off to get buff white coloured solids. A gravimetric estimation method was followed to evaluate the percent extractable. Infrared spectroscopy was used for comparative studies with published information.

### 2.7.4 Thermal analysis

#### 2.7.4.1 Differential scanning calorimetry

The dried polymer samples were characterized for thermal properties on a PERKIN ELMER DSC-2 differential scanning calorimeter. The unit was calibrated using freshly cut Indium as reference. The



melting temperature and the heat of fusion for Indium were 429.7°K and 6.8 cal/gm respectively. The scanning conditions used for characterization of the polymer samples were as given below.

Polymer sample - 4 mg (exact weight noted)

Heating/cooling rate - 10° /min.

Sensitivity - 5 mcal/sec

Temperature range - 50°C to 290°C.

The polymer sample was heated at the programmed rate of 10°/minute till the melting transition was observed. The sample was then cooled at preset programmed cooling rate of 10°/minute. The heating and cooling cycles were repeated twice. The pan position was adjusted after every cycle to get three clear non-overlapping thermograms. The thermograms observed in the second heating/cooling cycle were used to study transitional properties. The areas corresponding to transitions were measured using a planimeter.

#### 2.7.4.2 Thermogravimetric analysis

The thermogravimetric analysis of the samples were carried using a NERSTZ Thermal analyser model STA 409. The heating rate was 10°C/min. The temperature scale was calibrated in millivolts and the transitions were converted into degrees centigrade using conversion tables supplied along with the unit. The sample used in the analysis was around 25 mg and all the samples were analysed with identical instrument settings, in air.

## 2.8 Infrared analysis

The infrared spectrum of the samples synthesized were compared with the commercial sample V-1. A PYE UNICAM model SP3-300 IR spectrometer was used to record the spectrum. The spectra were recorded in nujol.

## 2.9 X-ray analysis

Amongst the various techniques for the determination of crystallinity, x-ray diffraction method is a reliable and reproducible measurement. The method allows quantitative comparisons. A Philips PW 1730 diffractometer with Cu  $K_{\alpha}$  target and Ni filter was used for the estimation of the crystallinity index of the samples under investigation. The following relation was used ,

$$C_i = [1 + 0.7 (\phi_a / \phi_c)]^{-1}$$

where  $C_i$  = crystallinity index,

$\phi_a$  and  $\phi_c$  = areas under amorphous halo and crystalline peaks

The  $2\theta$  range of  $10-30^\circ$  corresponding to the occurrence of four major peaks of 110, 200, 111, 211 reflections, was chosen for the evaluation of the crystallinity index ( $C_i$ ).

### 2.10 Scanning electron microscopy

The particle morphology of the precipitated polymer was investigated by using a scanning electron microscopy. The samples were placed on a stub and coated with palladium gold alloy using a sputter (Polaron Equipment, UK).

A Cambridge model Steroscan 150 scanning electron microscope was used for these studies. Photographs of the images, obtained as the output were used in the interpretations. The particle size distribution and the growth kinetics of the particle size as a function of reaction time were estimated from the micrographs by manual measurements.



**CHAPTER 3**  
**KINETICS**

### 3.1 KINETICS

The kinetics and structure development during the polycondensation to PPS were investigated by collecting and analysing polymer samples formed at different reaction times. The fractional conversions were evaluated by volumetric analysis and the polymer yields gravimetrically.

Two types of reactors were used for the investigations. One was a stainless steel reactor of 650 ml capacity with provision for mechanical stirring. The other reactor was a 250 ml Teflon sleeve (Teflon reactor) fitting into a stainless steel vessel and had magnetic needle stirring for agitation. The reactors thus essentially varied, in one having an efficient mechanical stirring versus an inefficient magnetic needle agitation in the other. Both reactors had thermocouples for temperature sensing and the desired temperatures were achieved by electrical heating. The effect of physical parameters such as reactor type, agitation speed and dilution on kinetics and structure development were studied.

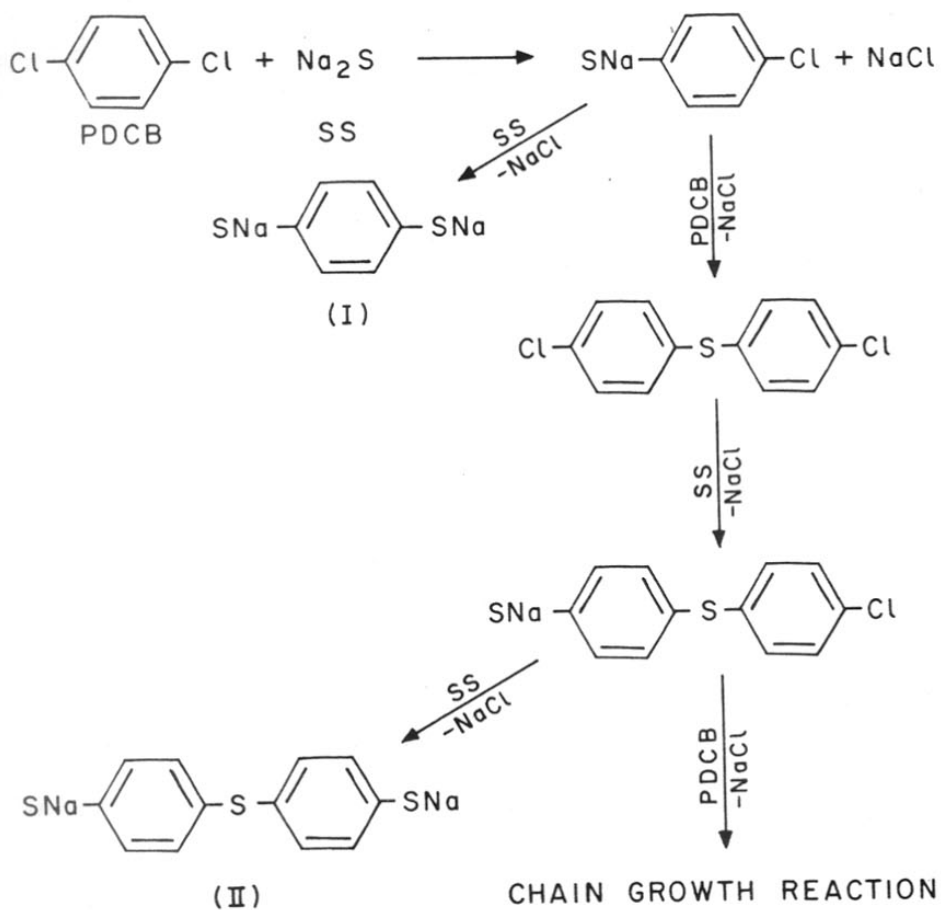
The effect of change in chemical parameters like variation in the concentration of the reactants, use of sodium parachloro thiophenoxide as initiating species and use of dibromobenzene in place of dichlorobenzene, on kinetics were evaluated. The investigations were conducted in the stainless steel reactor.

The objectives of these studies were to evaluate the order of the reaction, the reaction rate constant and compare the behaviour of the systems with conventional polycondensation reactions.

### 3.2 POLYCONDENSATION OF SODIUM SULFIDE WITH PDCB

The polycondensation reactions with PDCB and sodium sulfide were carried out in a 650 ml stainless steel reactor. The experimental details are given in Section 2.3. The molar concentrations of the reactants PDCB and sodium sulfide in the feed were maintained the same in all the experiments. The molar ratio was non-stoichiometric. A slight excess of PDCB was taken to prepare polymers with chlorine end groups. The polymer yields were determined gravimetrically following the polymer separation procedure described in Section 2.4. The rate of the reaction may be determined from the rates of consumption of the reactants, sodium sulfide and PDCB or by the rate of formation of the side product, sodium chloride.

The amount of unreacted sodium sulfide was determined by volumetric titration of the methanol/water extracts collected during the polymer isolation step. The consumption of PDCB was computed from chlorine analysis based on PDCB charged and sodium chloride generated. The consumption of sodium sulfide and PDCB are plotted in Figure 4 as a function of reaction time. For the initial period of reaction upto 2.1/2 hours, the consumption of sodium sulfide appears to be at a faster rate than that of PDCB. This region corresponds to a conversion of 50 percent. This implies the preferential formation of low molecular weight SNa terminated species such as I and II at low conversions as shown below. The course of the reaction could be described to fit the following scheme. Beyond 50 percent conversion, the rates of consumption of the two reactants were comparable indicating reaction of PDCB with SNa terminated species. It is also pertinent to note (Figure 4 ) that even at very high conversions,



REACTION SCHEME

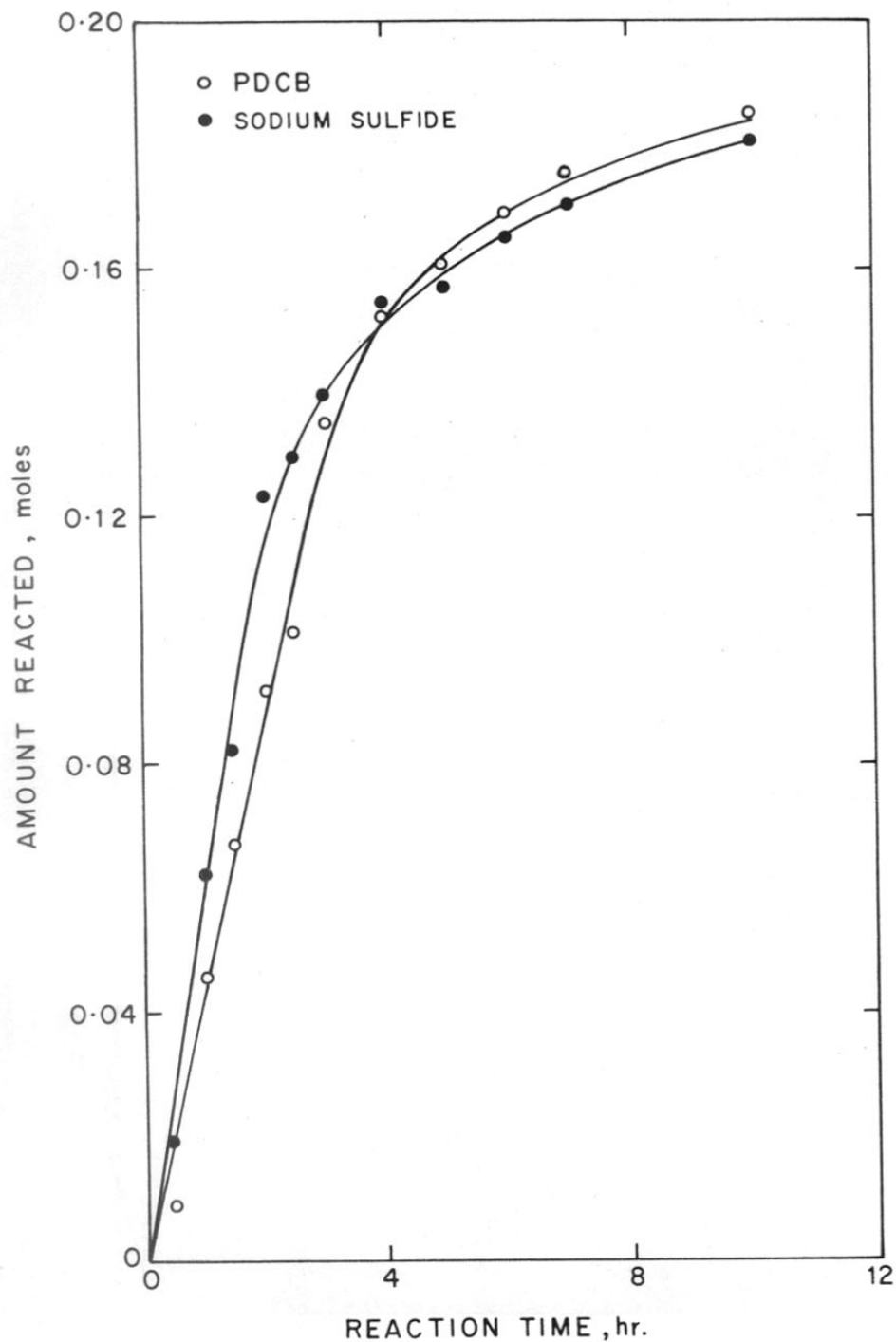


FIG.4: CONSUMPTION OF REACTANTS AS A FUNCTION OF REACTION TIME



unreacted sodium sulfide was present in the system.

The polymer yield reaction time data are plotted in Figure 5. The polymer yield obtained as insolubles in methanol and water was found to increase with reaction time. The increase was gradual after a reaction time of 6 hours.

### 3.2.1 Analysis of the kinetics

The fractional conversion based on sodium chloride generated was followed to evaluate the reaction rate and the rate constants. Analytical procedure described in Section 2.5.3 was followed for estimation of sodium chloride. The computations were done from the data on moles of sodium chloride formed at different reaction times. The theoretical yield of sodium chloride at complete conversion has been taken to be equivalent to twice the moles of the deficient difunctional reactant, sodium sulfide in the feed. The fractional conversion 'p' was evaluated as,

$$p = \frac{\text{sodium chloride formed}}{\text{theoretical yield of sodium chloride}}$$

The results on polymer yield - fractional conversion - reaction time are summarized in Table 4 and illustrated in Figure 6. The fractional conversion, p, varies from zero to 1 with increasing reaction time. The rate of formation of sodium chloride is linear upto a reaction time of 3 hours and then decreases gradually with increasing reaction time. The data were found to fit the second order rate expression over a wide range of conversions

TABLE 4  
TIME CONVERSION DATA

Temperature = 195°C

[sodium sulfide] = 0.1923 moles ,

Pressure =  $\approx$  35 psi

[PDCB] = 0.2041 , [NaCl] theoretical =  
0.3846 moles

No.	Reaction time, min.	Sodium chloride formed, moles	Fractional conversion, p	Polymer yield, gm
1.	30	0.0182	0.0474	0.59
2.	60	0.0922	0.2398	4.33
3.	90	0.1374	0.3572	6.21
4.	120	0.1836	0.4774	9.75
5.	150	0.2060	0.5357	10.72
6.	180	0.2714	0.7056	13.22
7.	240	0.3042	0.7911	16.63
8.	300	0.3220	0.8373	17.25
9.	360	0.3388	0.8809	19.05
10.	420	0.3410	0.8867	19.30
11.	600	0.3720	0.9673	20.90

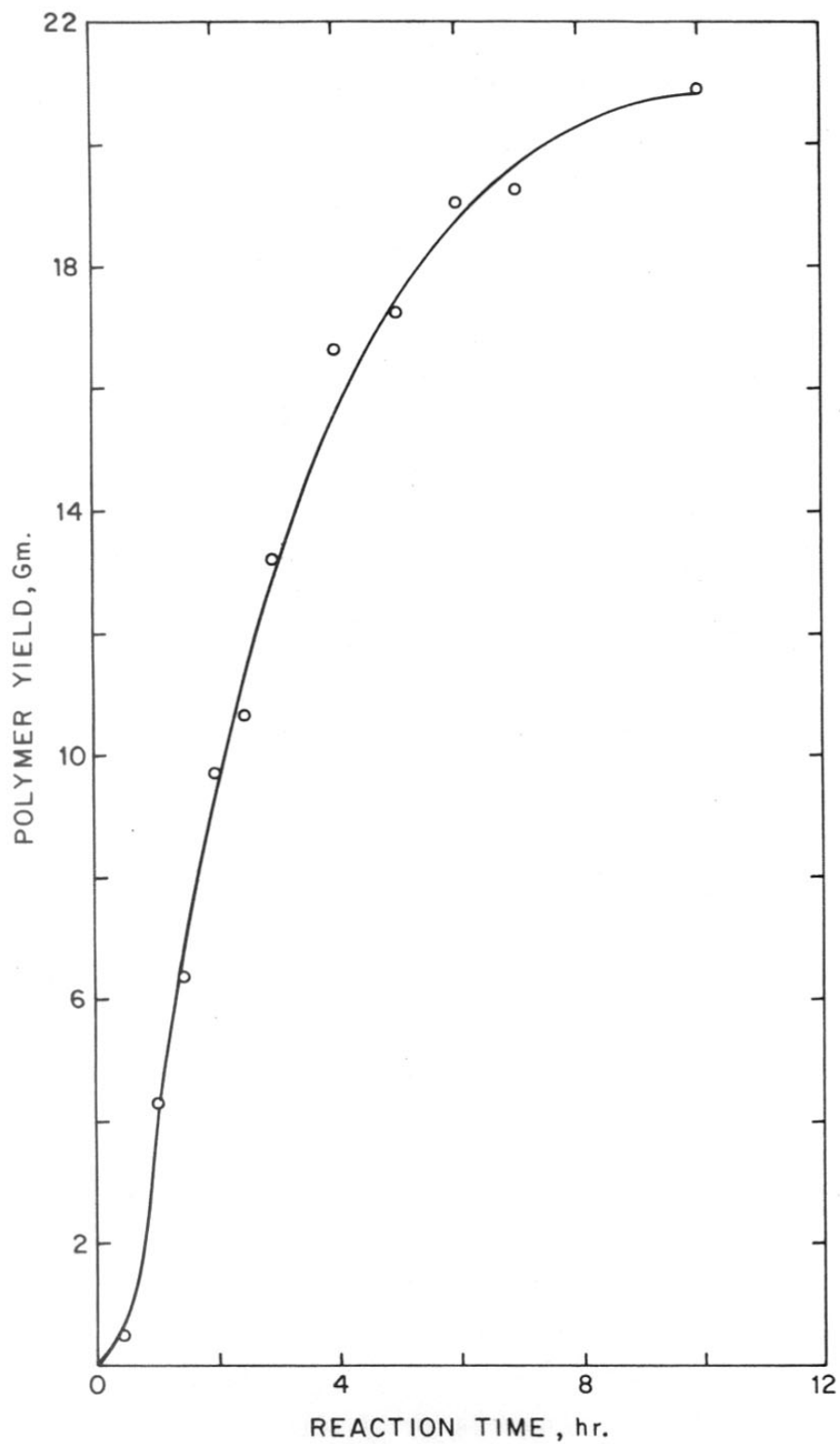


FIG.5:POLYMER YIELD-REACTION TIME DATA

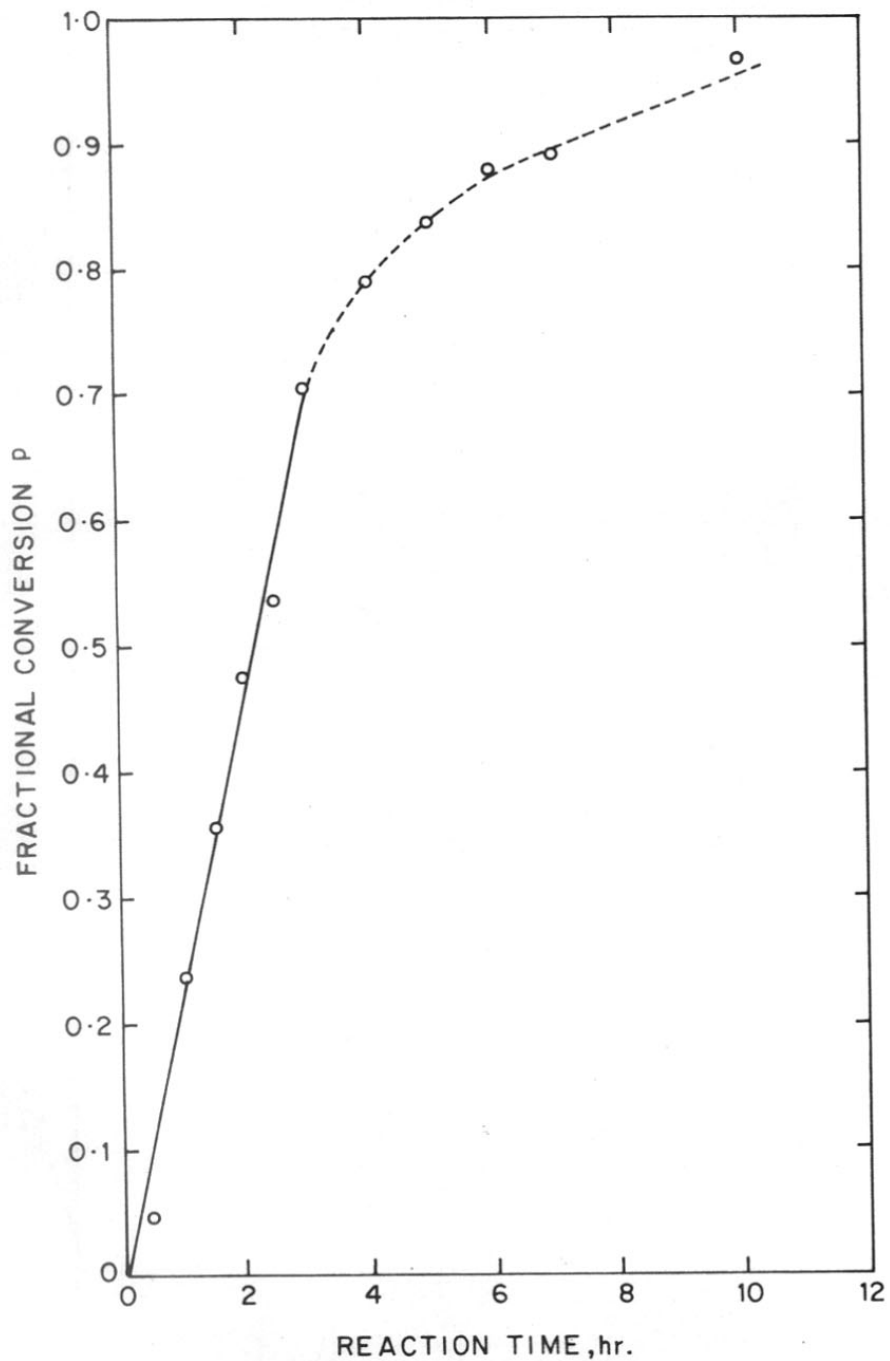


FIG.6:FRACTIONAL POLYCONDENSATION WITH TIME. DETERMINED AS RATE OF FORMATION OF SODIUM CHLORIDE.

(Figure 7). The result is consistent with the other reported kinetic investigation. Lenz et al.<sup>55</sup> had investigated the formation of poly(p-phenylene sulfide) by the self polycondensation of alkali metal salts of parahalo thiophenoxides in pyridine at 250°C. Their results conclusively proved that the reaction followed second order kinetics.

In polycondensation reactants, with identical initial concentrations, the factor  $1/(1-p)$  should vary linearly with the reaction time, to fit second order kinetics. The data are plotted in Figure 7. The figure shows two regions of linearity. A shown rate upto a conversion of 50 percent corresponding to a reaction time of 2.1/2 hours was noted. This was followed by a faster rate between 50 and 90 percent conversions.

In the present investigation, the initial concentrations of the two reactants were non-stoichiometric. In such cases, a second order kinetics would be operational if a plot of  $\frac{(1+r)^{244}}{(1+r-2rp)}$  was linear with reaction time. In the above expression  $r \leq 1$  represents the molar ratio of the two reactants in the feed. The data are summarized in Table 5. The corresponding plot is shown in Figure 8. The experimental data reported in Table 5, fit a second order expression as shown in Figure 8. Again, two similar regions of linearity as observed earlier were noted. A slower rate upto 50 percent conversion was followed by a faster rate between 50 and 90 percent conversions.

The data were subjected to regression analysis to evaluate the rates. The two rates of polycondensation (evaluated as the rate of formation of sodium chloride) corresponding to the two regions thus obtained are given below:

TABLE 5  
FITTING EXPERIMENTAL DATA

Temperature = 195°C, pressure =  $\approx$  35 psi

$$p = [\text{NaCl}]/[\text{NaCl}]_{\text{Theo}}, \quad r = [\text{Na}_2\text{S}] / [\text{PDCB}] = 0.9422$$

Time, min	p	$1/(1-p) = \bar{X}_n$	$\bar{X}_n = \frac{(1+r)}{(1+r-2rp)}$
30	0.0474	1.0498	1.0482
60	0.2398	1.3154	1.3032
90	0.3572	1.5557	1.5304
120	0.4774	1.9135	1.8629
150	0.5357	2.1538	2.0823
180	0.7056	3.3967	3.1706
240	0.7911	4.7870	4.3021
300	0.8373	6.1463	5.3300
360	0.8809	8.3963	6.8816
420	0.8867	8.8261	7.1588

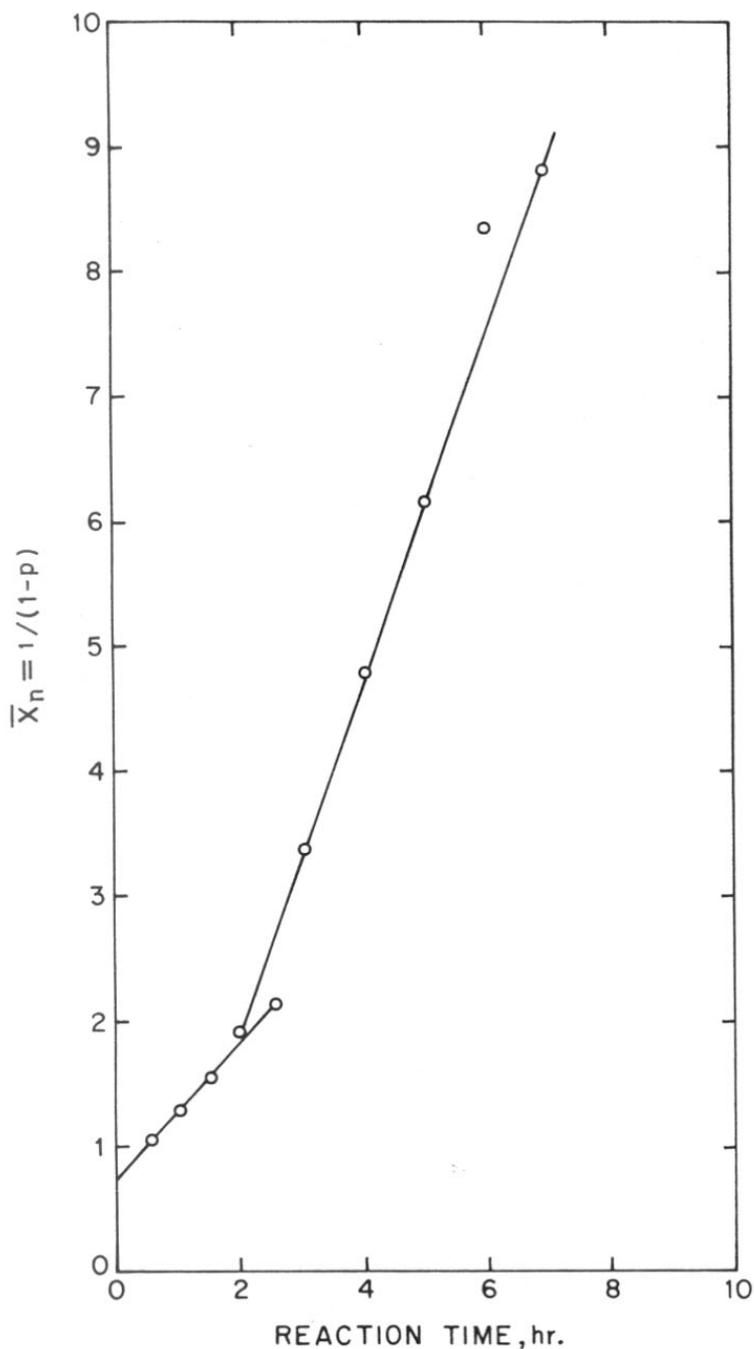


FIG.7: PLOT OF THE NUMBER-AVERAGE DEGREE OF POLYMERIZATION OF POLY (p-PHENYLENE SULPHIDE) AS A FUNCTION OF REACTION TIME, ASSUMING STOICHIOMETRIC EQUIVALENCE OF THE REACTANTS.

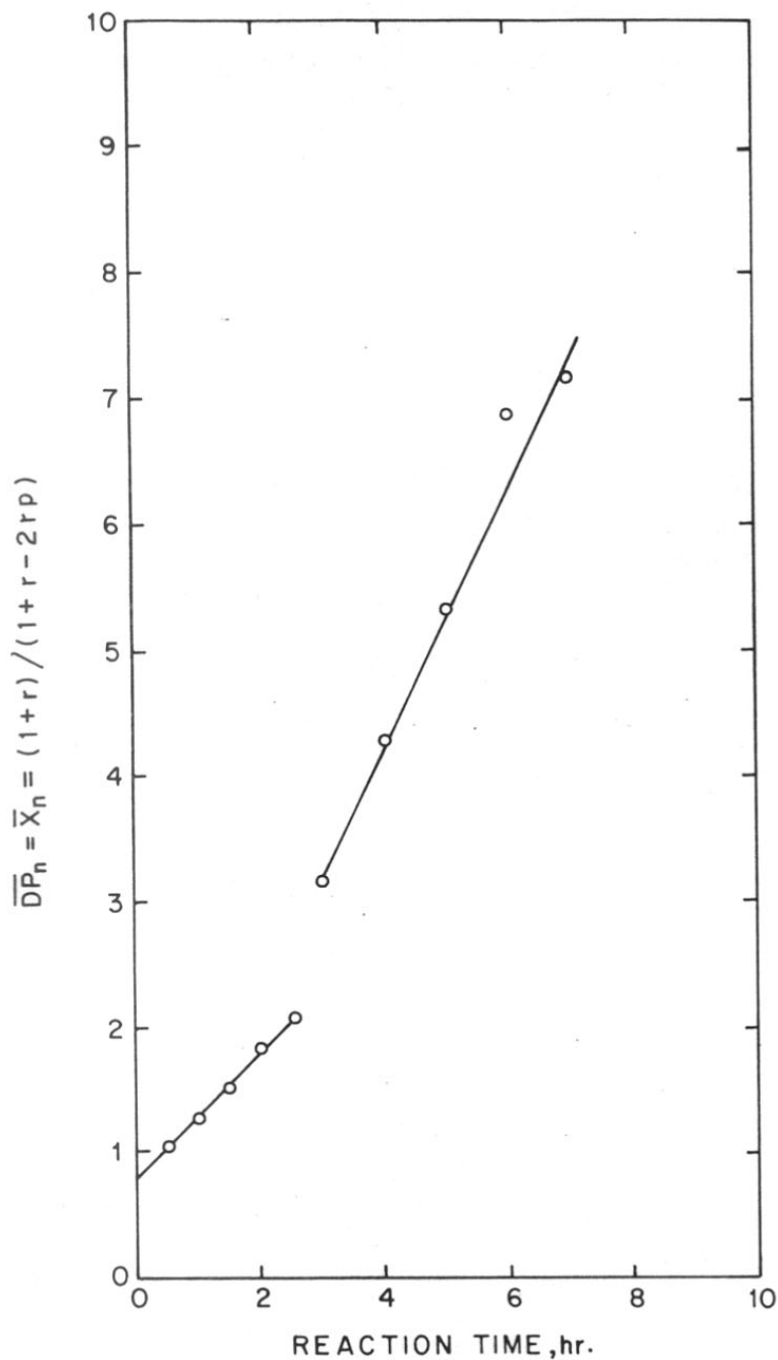


FIG.8: PLOT OF  $\overline{DP}_n$  OF POLY (p-PHENYLENE SULPHIDE) AS A FUNCTION OF REACTION TIME. PLOT ASSUMING STOICHIOMETRIC NONEQUIVALENCE BETWEEN THE TWO REACTANTS



Rate =  $3.00 \times 10^{-5} \text{ m l}^{-1} \text{ s}^{-1}$  upto 50 percent conversion

Rate =  $3.85 \times 10^{-5} \text{ m l}^{-1} \text{ s}^{-1}$  beyond 50 percent conversion

The specific reaction rate constant is defined as:

$$\text{Specific reaction rate constant} = \frac{\text{rate}}{\text{concentration of reactants}}$$

The two specific reaction rates were,

$$8.11 \times 10^{-4} \text{ l m}^{-1} \text{ s}^{-1} \text{ and } 4.16 \times 10^{-3} \text{ l m}^{-1} \text{ s}^{-1}$$

respectively for the two regions of conversion.

There is atleast one documented evidence for the occurrence of variable rates at different conversion levels in polycondensation by nucleophilic substitution reaction. The reactions between alkali salts of aromatic diols and aromatic dihalides in dimethyl sulfoxide<sup>196</sup> follow a second order kinetics. Here an initial faster rate was followed by a slower rate at higher conversion.

In the system investigated, compounds with differing reactivities are formed as the reaction proceeds as illustrated in the reaction scheme. The differing rates in the two regions of conversions could be ascribed to the different reactivities of the species formed at different conversions. The presence of significant amount of unreacted sodium sulfide at high conversions was noted in the system. This observation differs from the features of conventional polycondensation reaction. This could possibly be due to the solubility limitation of sodium sulfide in NMP. Another

notable deviation from conventional polycondensation reactions is the formation of polymers at low conversions.

### 3.2.2 Molecular weight development

#### (a) Polymer yield

The polymer formed was collected as an insoluble product of methanol and water extractions. The initial products of substitution reaction (refer to the reaction scheme in 3.2.1) such as sodium parachloro thiophenoxide are soluble in methanol. Oligomers above a critical molecular weight are insoluble in methanol were collected together with the high molecular weight material, as the polymer formed. This represented the actual polymer yield obtained. The critical molecular weight above which the oligomer was rendered insoluble could not be evaluated.

The theoretical yield of the polymer at total conversion was calculated as follows:

The molar ratio of the reactants was non-stoichiometric. The theoretical yield would depend on the number average degree of polymerization  $\bar{X}_n$  at 100 percent conversion. The relation to be used for non-stoichiometric molar ratio of the reactants is given by,

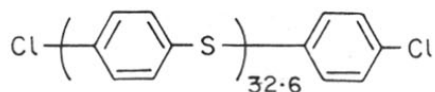
$$\bar{X}_n = \frac{1 + r}{1 + r - 2rp}$$

where,  $r$  is the molar ratio of the reactants and  $p$ , the fractional conversion.

In the system investigated  $r = 0.9422$  and for total conversion  $p = 1$ . The above equation in substituting these values becomes,

$$\bar{X}_n = \frac{1 + 9422}{1 + 0.9422 - (2 \times 0.9422 \times 1)} = 33.5932$$

The polymer formed at 100 percent conversions, on a statistical average would be,



The moles of -Cl end group would be,

$$\frac{2}{33.6} \times 0.1923 = 0.01145 \quad \text{where } 0.1923 \text{ is the molar concentration of the deficient difunctional reactant, sodium sulfide}$$

The theoretical yield (T.Y) of polymer becomes,

$$\begin{aligned} \text{T.Y.} &= 0.1923 \times \text{C}_6\text{H}_4\text{S} + 0.01145 \times \text{Cl}_2 \\ &= 0.1923 \times 108.15 + 0.01145 \times 70.9 \\ &= 21.61 \text{ gm s} \end{aligned}$$

The fractional yield of the polymer is defined as,

$$\text{fractional yield} = \frac{\text{polymer yield obtained}}{\text{theoretical yield at 100 percent conversion}}$$

The data on fractional yield with reaction time of this system which forms the reference set are summarized in Table 6. A plot of the fractional yield based on the polymer formed with reaction time is shown in Figure 9. Two regions could be noted. An initial region upto 50 percent conversion where the yield increased linearly with reaction time was followed by a gradual increase beyond 50 percent conversion. It was observed that

TABLE 6  
FRACTIONAL YIELD DATA OF REFERENCE SET

Reaction time, min.	Fractional conversion	Polymer yield, gm	Fractional yield
30	0.0474	0.59	0.0273
60	0.2398	4.33	0.2004
120	0.4774	9.75	0.4512
180	0.7056	13.22	0.6118
240	0.7911	16.63	0.7695
300	0.8373	17.25	0.7982
360	0.8809	19.05	0.8815
420	0.8867	19.3	0.8931
600	0.9673	20.9	0.9672

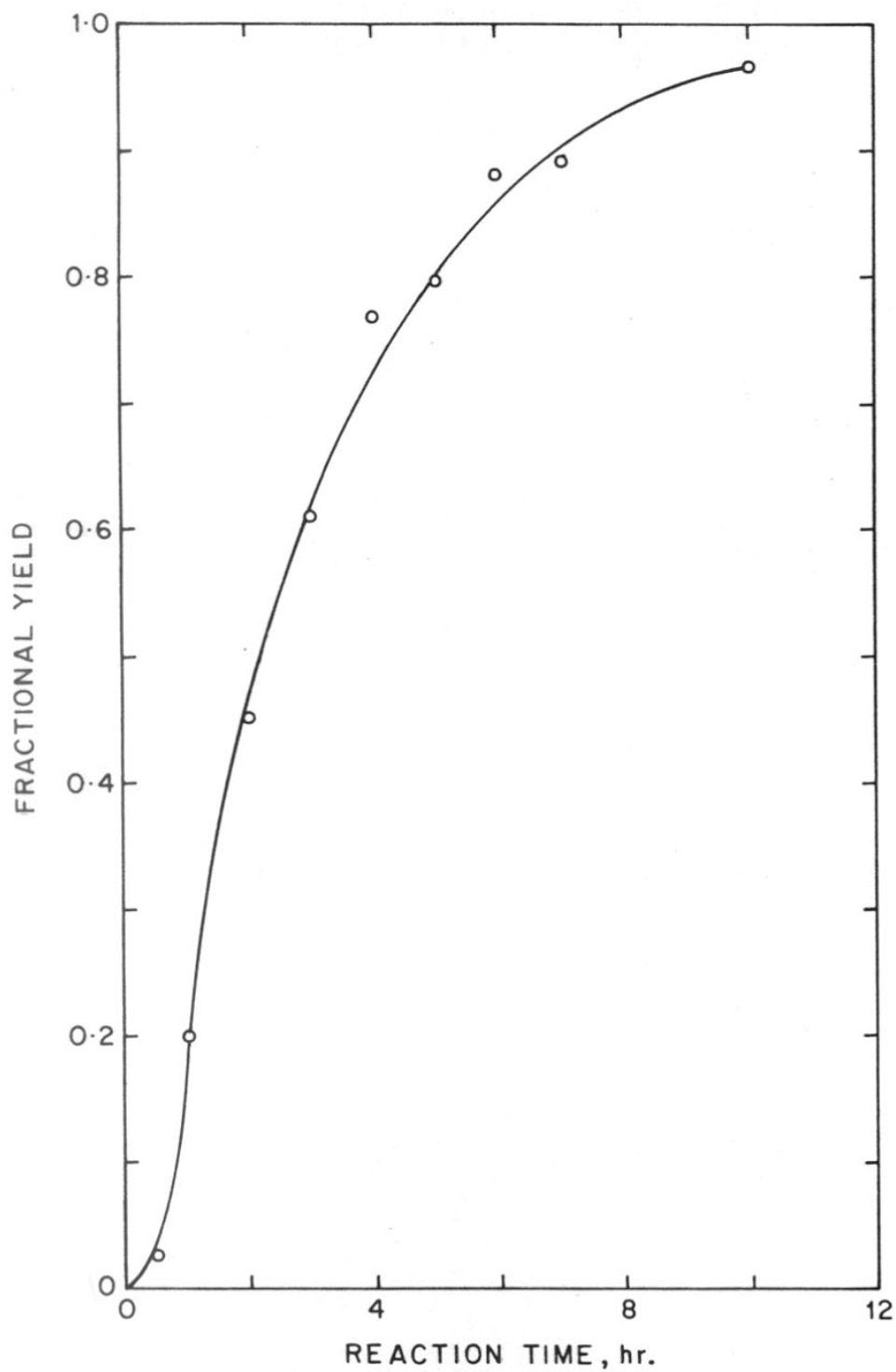


FIG.9:FRACTIONAL YIELD-REACTION TIME DATA

even for short reaction times of 30 and 60 minutes corresponding to very low conversions, polymer was formed unlike conventional polycondensation reactions where polymer formation is noted only at high conversions (above 90 percent).

(b) Degree of polymerization

The amount of chloro end groups present in the polymers was determined by elemental micro analysis. At complete conversion, the polymer will be exclusively chlorine terminated at both ends, as the reactions were conducted with a slight excess of PDCB. At lower fractional conversions SNa end groups will also be present. The relative ratio of the chloro (x) and SNa (2-x) end groups and the empirical formula at different conversions were evaluated as per procedure described in Section 2.7. The number average degree of polymerization  $\overline{DP}_n$  and the molecular weight of the polymer formed at different fractional conversions were determined from the elemental analysis and the empirical formula of the polymer at the respective conversions. Low molecular weight oligomers are present in the isolated polymer due to insolubility in methanol. Thus the molecular weight distribution in the polymer samples isolated at different reaction times is wide. The number-average degree of polymerization of the polymer formed at very low conversions is significantly larger ( $\overline{DP}_n = 8.00$  at 24 percent conversion) than that noted at similar conversions in polycondensations ( $\overline{DP}_n$  theoretical = 1.05). The data on  $\overline{DP}_n$  evaluated with reaction time is presented in Table 7. The  $\overline{DP}_n$  of the polymer formed increased with reaction time and conversion. This data is illustrated in Figure 10, of  $\overline{DP}_n$  with conversion. The increase in  $\overline{DP}_n$  with reaction time was

TABLE 7  
 $\overline{DP}_n$  - CONVERSION DATA

Reaction time, min.	Fractional conversion, 'p'	Chlorine in polymer % (micro analysis)	End group (Section 2.7.1) - Cl	Empirical formula (Section 2.7.1)	$\overline{DP}_n$ (based on micro analysis)	$\overline{M}_n$	
1	2	3	4	5	6	7	8
60	0.2398	3.99	1.0606	0.9394	$C_6H_{4n}S_{(n-1)+0.9612Cl_1.0388}$ Na <sub>0.9612</sub>	8.00	9 22
120	0.4774	3.88	1.0751	0.9249	$C_6H_{4n}S_{(n-1)+0.9445Cl_1.0555}$ Na <sub>0.9445</sub>	9.00	9 67
180	0.7056	2.14	1.1067	0.8933	$C_6H_{4n}S_{(n-1)+0.9056Cl_1.0944}$ Na <sub>0.9056</sub>	18.50	20 36
240	0.7911	1.91	1.1791	0.8209	$C_6H_{4n}S_{(n-1)+0.8719Cl_1.1281}$ Na <sub>0.8719</sub>	18.85	20 92
300	0.8374	1.76	1.2398	0.7602	$C_6H_{4n}S_{(n-1)+0.8414Cl_1.1586}$ Na <sub>0.8414</sub>	20.90	23 09

contd.....

Table 7 contd....

1	2	3	4	5	6	7	8
360	0.8867	1.47	1.2943	0.7057	$C_{6n} H_{4n} S_{(n-1)+0.7869} Cl_{1.2131}$ Na <sub>0.7869</sub>	26.60	29 27
600	0.9673	1.26	1.8027	0.1973	$C_{6n} H_{4n} S_{(n-1)+0.516} Cl_{1.484}$ Na <sub>0.516</sub>	38.25	41 80



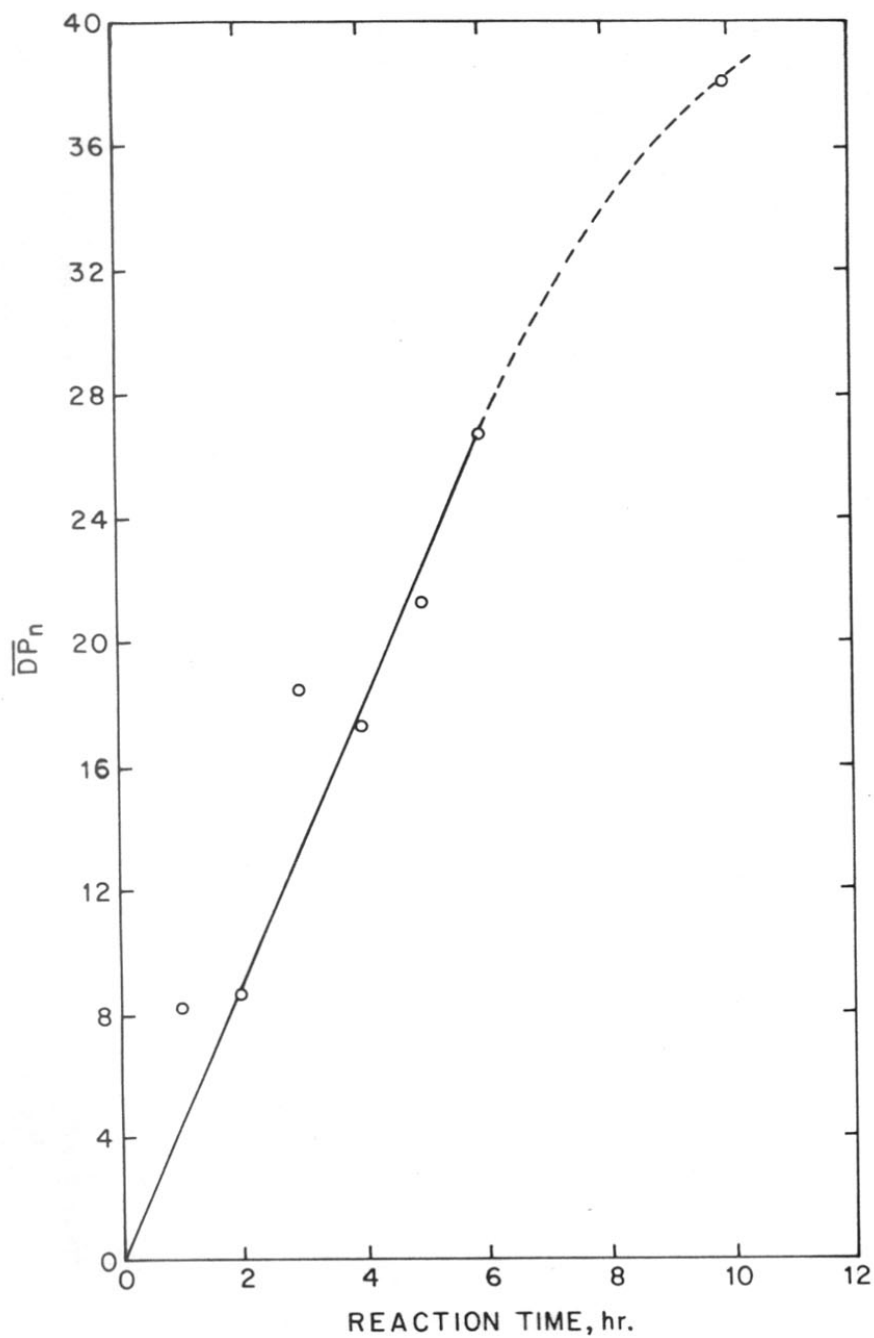


FIG.10:  $\overline{DP}_n$  OF POLY (p-PHENYLENE SULPHIDE) FORMED AS A FUNCTION OF REACTION TIME, BASED ON MICRO ANALYSIS

less dramatic than that observed in polycondensation reactions. The overall number-average degree of polymerization at different conversions ( $p$ ) for this system, with the molar ratio of the reactants  $r = 0.9422$  were calculated using the expression,

$$\bar{X}_n = \frac{1+r}{1+r-2rp}$$

The data on  $\bar{DP}_n$  of the precipitated polymers at different conversions as evaluated from microanalysis and the  $\bar{DP}_n$  overall calculated as per equation given above are presented in Table 8. The  $\bar{DP}_n$  of as-precipitated polymers were much higher than the overall  $\bar{DP}_n$ . In addition, the presence of unreacted sodium sulfide at conversions as high as 97 percent indicated the occurrence of a wide molecular weight distribution in the system.

(c) Solution viscosity measurements

The intrinsic viscosity  $[\eta]$  of the polymers formed at different conversions were evaluated from single point relative viscosity measurements of 4 weight percent solutions of the polymer in 1-chloronaphthalene at 195°C. The experimental details are given in Section 2.7.2. The following relationships were used for evaluation of intrinsic viscosity.

$$[\eta] = \frac{\sqrt{2}}{C} \sqrt{\eta_{sp} - \ln \eta_r} \quad (1)$$

and

$$[\eta] = \frac{\eta_{sp}}{C(1+K\eta_{sp})} \quad (2)$$

where,  $K = 0.302$

$\eta_r$  = relative viscosity,

TABLE 8

$$\overline{DP}_n \text{ (ANALYSED)} - \overline{DP}_n \text{ OVERALL DATA}$$

Reaction time, min.	Fractional conversion, 'p'	$\overline{DP}_n$	$\overline{DP}_n$ overall = $\frac{1+r}{1+r-2rp}$
60	0.2398	8.00	1.0482
120	0.4774	9.00	1.8629
180	0.7056	18.50	2.0823
240	0.7911	18.85	3.1706
300	0.8373	20.90	4.3021
360	0.8867	26.60	5.3300
600	0.9673	38.25	7.1588

$\eta_{sp}$  = specific viscosity and

C = the polymer concentration in gm/deciliter

The relationships ( 1 ) and ( 2 ) are generally valid for very dilute ( 0.5 weight percent) polymer solutions. The polymers obtained in the present investigations were of low molecular weight with the number average degree of polymerization less than 40. Hence the relationships were found to be valid even at high polymer concentrations in the present system. The evaluated data are presented in Table 9. The intrinsic viscosity of the various polymer samples collected at different conversions was found to increase initially and level off after a reaction time of 6 hours corresponding to 88 percent conversion. A plot of intrinsic viscosity with reaction time is shown in Figure 11. In precipitation polymerizations, it is generally observed that the polymer would precipitate out once a critical molecular weight is attained. However, in the case of PPS, the  $\overline{DP}_n$  gradually increases with reaction time indicating that the polymer chain keeps on growing even after precipitation. The further growth could be due to the solvation of the reactive end of the polymer chain or by the occurrence of polymerization on the solid surface of the precipitated polymer. This phenomenon is thus different from other precipitation systems, like in the formation of polycarbonates, wherein the polymer ceases to flow after precipitation. The molecular weight of the polymer requires enhancement in molecular weight for commercial applications. The polymer isolated after a reaction time of 10 hours has a  $\overline{DP}_n$  of 38 ( $M_n \approx 4200$ ), a level which is still too low for most commercial applications. The higher value of intrinsic viscosity for the commercial sample is a pointer in this direction.

TABLE 9

## INTRINSIC VISCOSITY OF PPS FORMED AT DIFFERENT CONVERSIONS

$t_0 = 147.2$  sec, Temperature = 195°C, Solvent = 1-chloro naphthalene

Reaction time, min.	Polymer concn. gm/deciliter	relative viscosity	$[\eta]^a$ dL/g	$[\eta]^b$ dL/g
60	4.12	1.181	0.0415	0.0416
120	4.08	1.398	0.0867	0.0871
180	4.08	1.527	0.1116	0.1115
240	3.36	1.373	0.0996	0.0998
300	4.11	1.599	0.1239	0.1234
360	4.02	1.618	0.1301	0.1295
420	4.00	1.620	0.1311	0.1306
600	3.95	1.629	0.1344	0.1338
Ryton*	4.07	1.855	0.1692	0.1669

$$a = [\eta] = \frac{2}{C} \sqrt{\eta_{sp} - \ln \eta_r}$$

$$b = [\eta] = \frac{\eta_{sp}/C}{(1 + K \eta_{sp})}, \quad K = 0.302$$

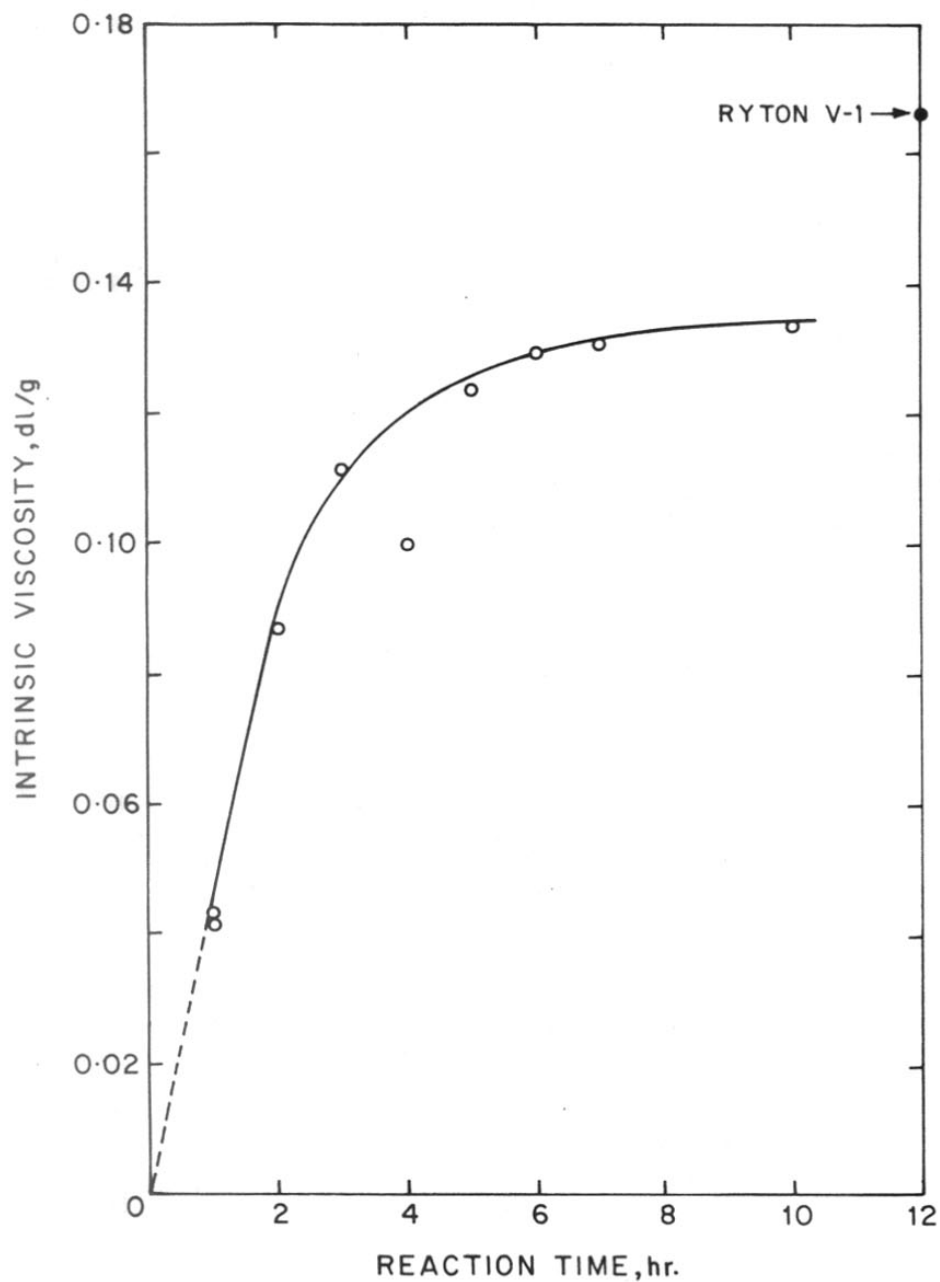


FIG.11 : INTRINSIC VISCOSITY OF POLYMER FORMED AT DIFFERENT CONVERSIONS. INDUSTRIAL GRADE PPS (RYTON) SHOWN FOR COMPARISON

(d) Melting point determination

The melting points of the polymers isolated were determined by capillary method. The variation of the m.p. with conversion is shown in Figure 12 . The melting point was found to rise rapidly till a conversion of 75 percent, followed by a slower rate of increase. This trend is identical to that observed with the intrinsic viscosity of the polymer, thus confirming the gradual increase in the polymer molecular weight with increasing reaction time and conversion.

### 3.3 EFFECT OF PHYSICAL PARAMETERS ON KINETICS

#### 3.3.1 Polycondensation experiments in Teflon reactor

These reactions were carried out in a Bergof autoclave. The description of the unit is given in Section 2.2. The experimental procedure for this reactor varied from that followed for the stainless steel reactor. The total volume of the solvent NMP required for the reaction and required amount methanolic solution of sodium sulfide were added initially and the mixture heated to 190°C to distil off methanol and water. The reactor contents were then cooled to about 135°C, the reactor top was opened and PDCB (0.2041 mole) was introduced in a solid form into the reactor. The vessel was then closed and again placed in the heater assembly. The maximum achievable stirring rate was maintained with the magnetic stirrer. The reaction time was counted from the time, the thermocouple registered the attainment of 195°C. The reaction was conducted for different pre-decided times. Once the preset reaction time was reached, the reactor assembly was taken out and cooled rapidly under running water to arrest the reaction. The procedures for polymer isolation and chemical analysis were identical to those followed for the experiments conducted in the stainless steel reactor.

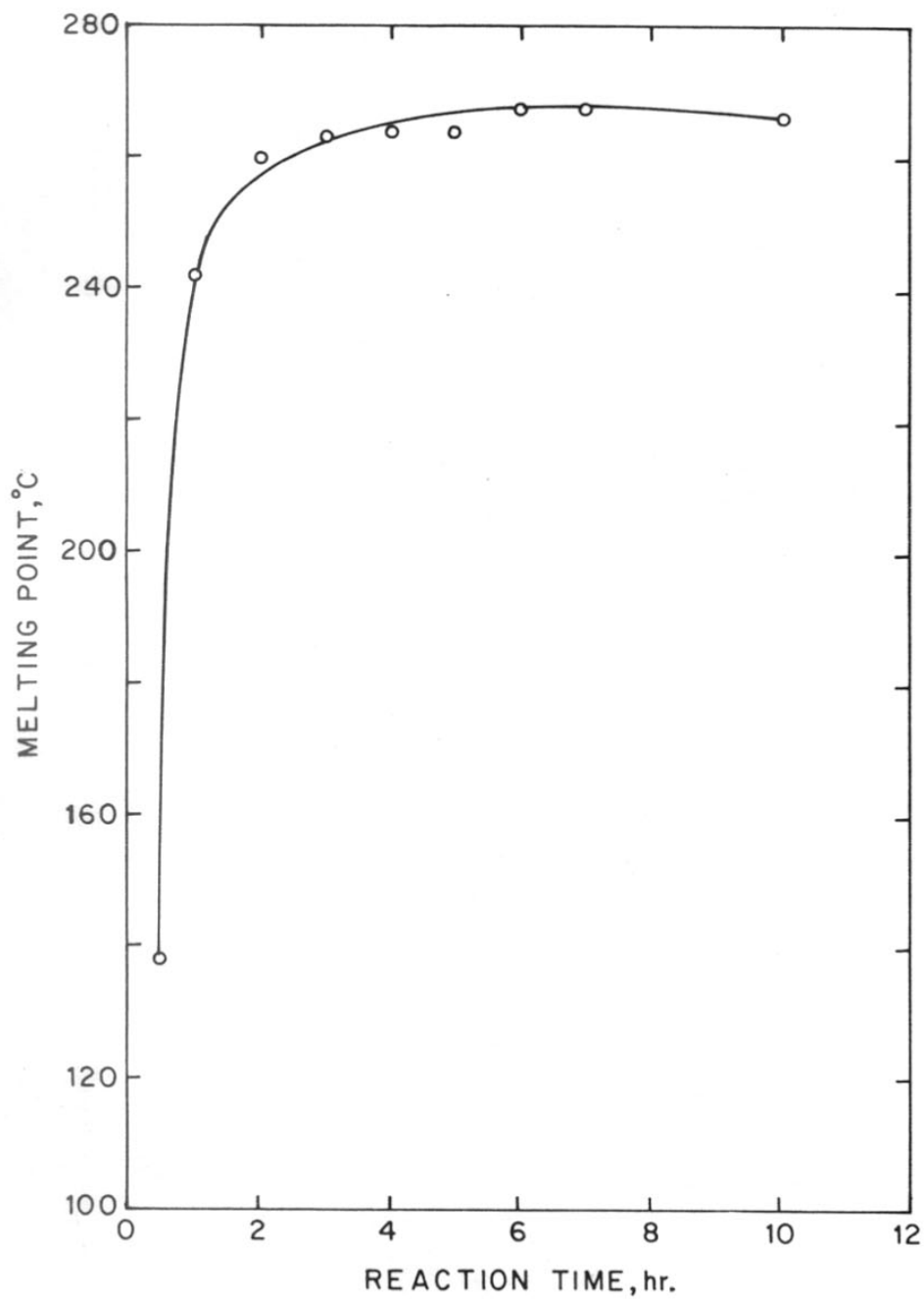


FIG.12 : MELTING POINT-REACTION TIME DATA



The extent of the reaction was calculated from the moles of sodium chloride formed. The data on variation of the fractional conversion, polymer yield with reaction time are summarized in Table 10. The observed trends are similar to those noted for the PDCB-sodium sulfide polycondensation in the stainless steel reactor. The polymer yield-fractional conversion data with reaction time are plotted in Figures 13 and 14. The data obtained from stainless steel reactor are also plotted in the same figures for comparative evaluation showing that the trends are similar within experimental limitations. This system also followed a second order kinetic scheme over a wide range of conversions. The fractional yield data are plotted in Figure 15 along with reference set.

The experimental data were subjected to regression analysis to evaluate the overall rate and the specific rate constant. The data on  $1/(1-p)$  and  $(1+r)/(1+r-2rp)$  (for non-stoichiometric ratio of the reactants) with reaction times are represented in Figures 16 and 17. Two regions of linearity are observed in this set also as in the case of reaction in stainless steel reactor. However, the regions of linearity differed. The initial slower rate constant till 75 percent conversion was followed by faster rate beyond this conversion.

The rate and the specific rate constants evaluated for this system are tabulated in Table 11 along with results for the stainless steel reactor. The difference in initial higher rate in Teflon reactor is within experimental limits. The latter slower rate could be attributed to differences in reactor geometry and variation in agitator speed. The change in linearity to 75 percent versus 50 percent in stainless steel reactor could be due to the formation of more SNa terminated species in Teflon reactor. The

TABLE 10  
FRACTIONAL CONVERSION-POLYMER YIELD DATA

Reactor : Teflon, Temperature = 195°C, [sodium sulfide] = 0.1923 mole,  
[PDCB] = 0.2041 mole, NMP = 100 ml

Reaction time, min.	Sodium chloride formed, mole	Polymer yield, gm	Fractional conversion	Fractional polymer yield
30	0.0571	2.68	0.1486	0.1240
60	0.0900	4.14	0.2340	0.1916
90	0.1967	9.05	0.5116	0.4188
150	0.2371	12.64	0.6165	0.5849
180	0.2772	13.70	0.7206	0.6340
240	0.2895	14.31	0.7527	0.6617
300	0.3114	17.52	0.8096	0.8107
360	0.3336	18.50	0.8674	0.8561
420	0.3415	19.18	0.8879	0.8875

TABLE 11  
RATE AND SPECIFIC RATE CONSTANT DATA IN TEFLON  
AND STAINLESS STEEL REACTORS

Reactor	Conversion range	Rate, $\text{m l}^{-1} \text{s}^{-1}$	Specific rate constant, $\text{l m}^{-1} \text{s}^{-1}$
Stainless steel	upto 50 percent	$3.00 \times 10^{-5}$	$8.11 \times 10^{-4}$
	beyond 50 percent	$3.85 \times 10^{-5}$	$4.16 \times 10^{-3}$
Teflon	upto 75 percent	$4.67 \times 10^{-5}$	$1.26 \times 10^{-3}$
	beyond 75 percent	$2.26 \times 10^{-5}$	$9.78 \times 10^{-3}$

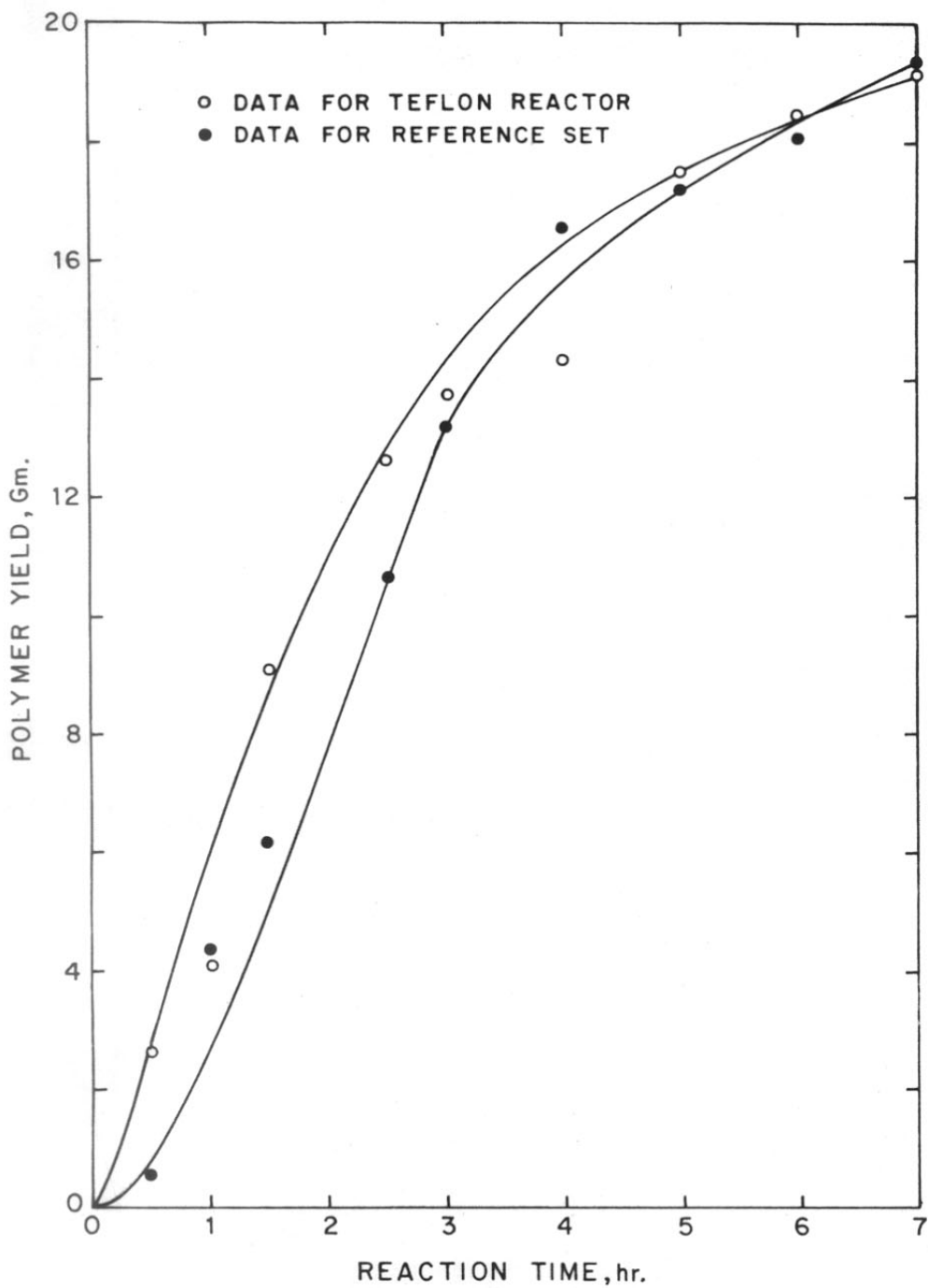


FIG.13: POLYMER YIELD - REACTION TIME DATA

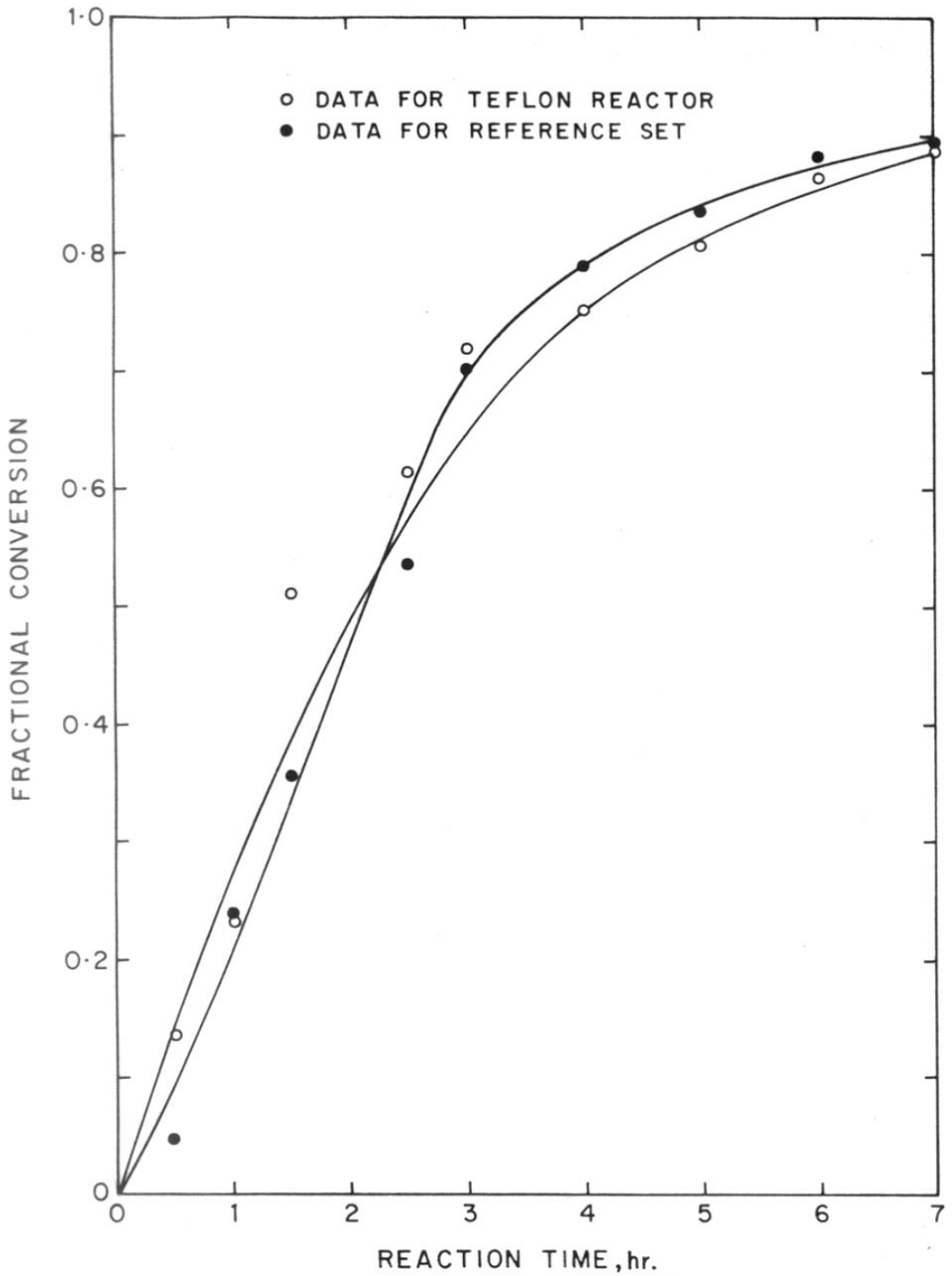


FIG.14: FRACTIONAL CONVERSION - REACTION TIME DATA

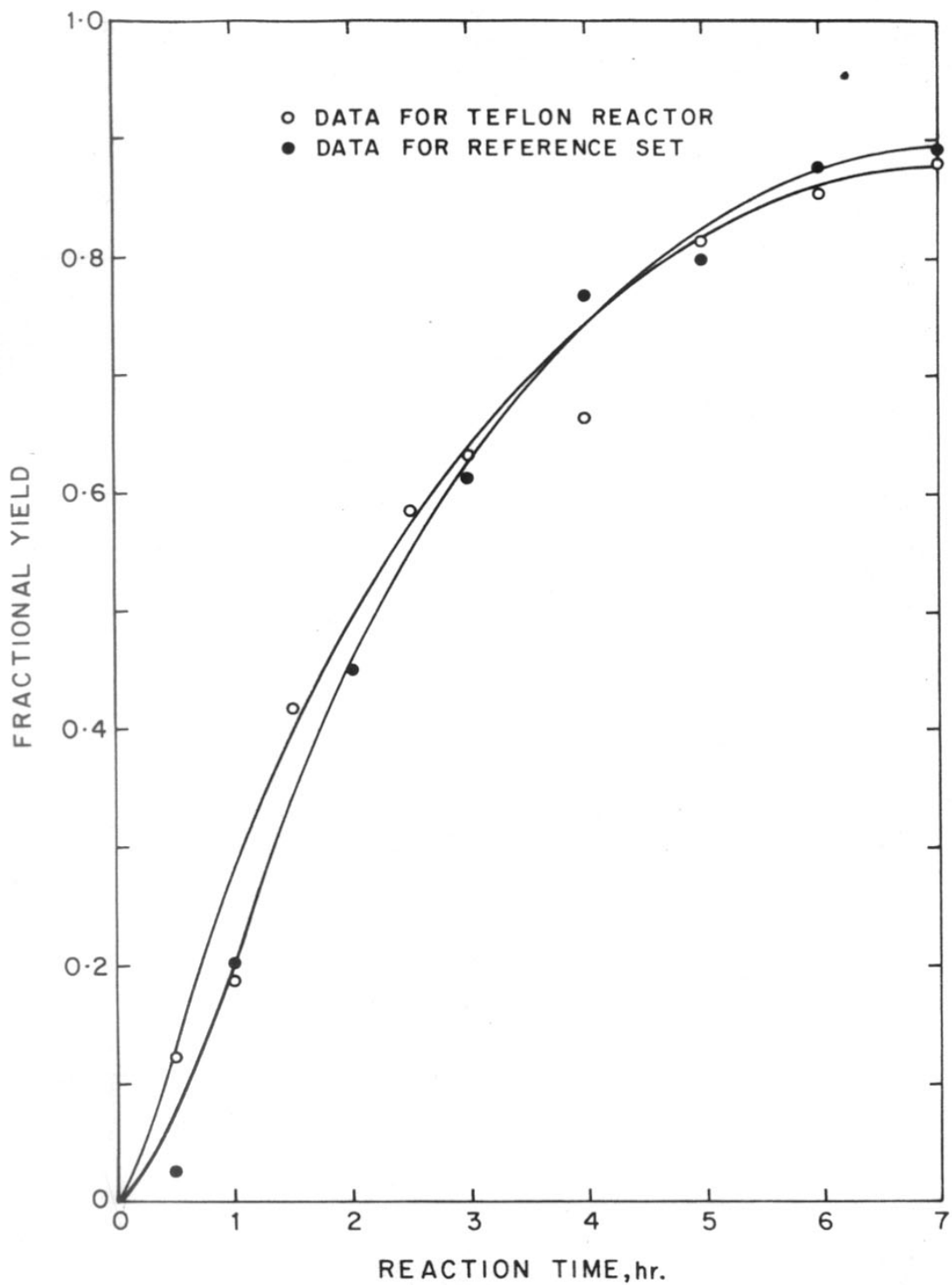


FIG.15:FRACTIONAL YIELD-REACTION TIME DATA

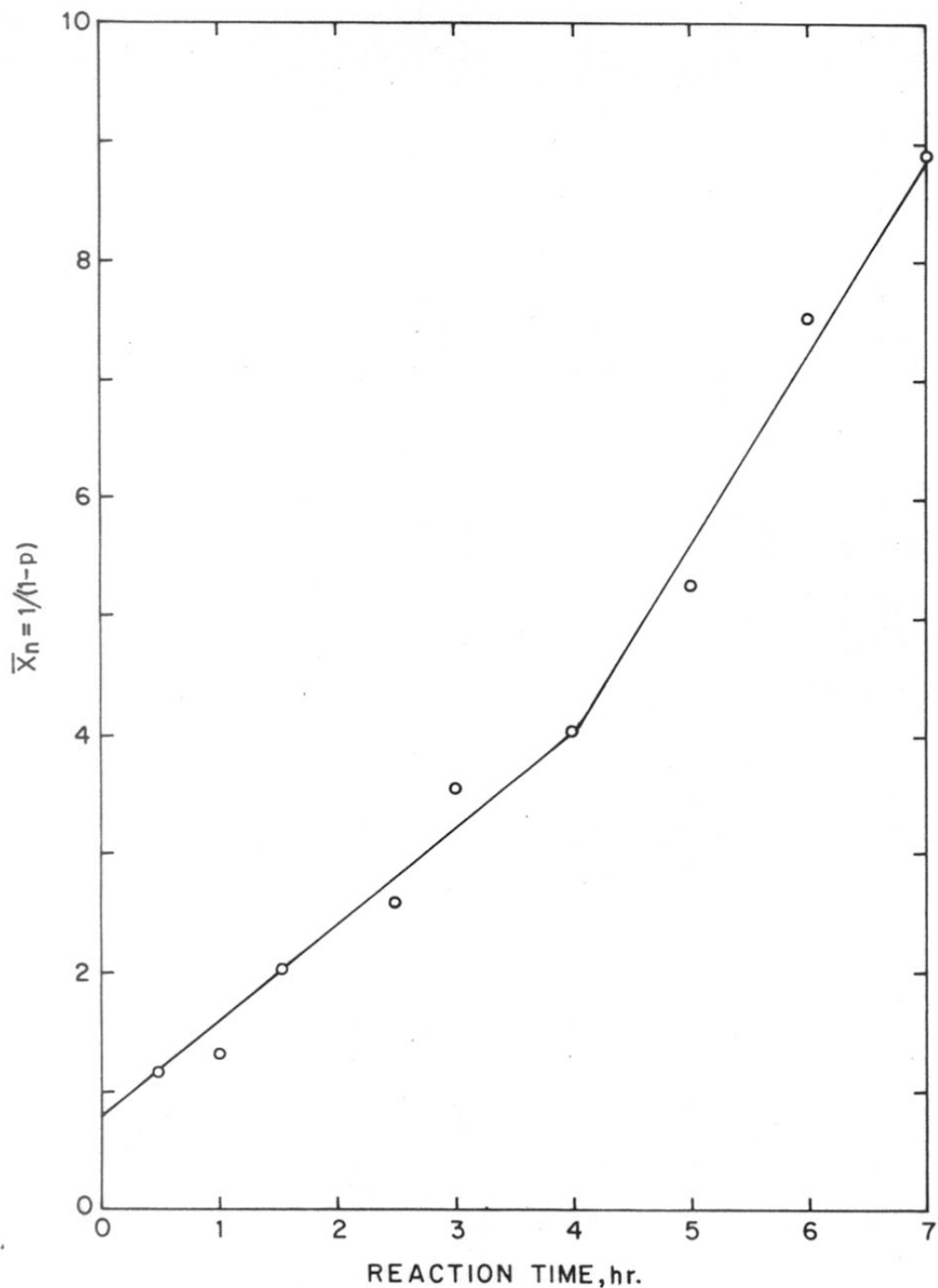


FIG.16: FITTING EXPERIMENTAL DATA - TEFLON REACTOR  
 $\bar{X}_n = 1/(1-P)$  AS A FUNCTION OF REACTION TIME

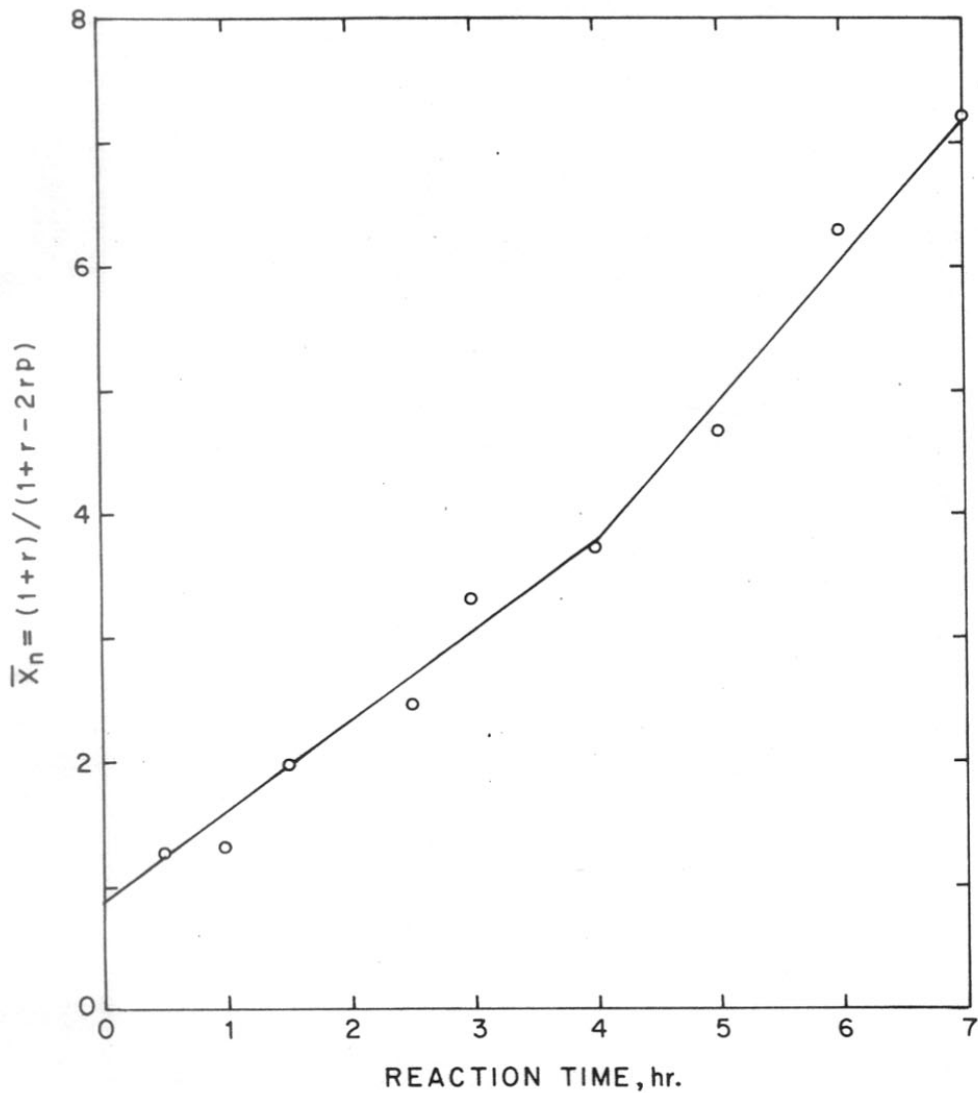


FIG.17: FITTING EXPERIMENTAL DATA-TEFLON REACTOR  
 $\bar{X}_n = (1+r)/(1+r-2rP)$  AS A FUNCTION OF REACTION  
TIME.



molecular weight distribution in this system could be wider than the one for stainless steel reactor. Lower intrinsic viscosity values show a pointer in this direction. The yield differences are within experimental limits and at higher reaction times the results from the two reactors are comparable. The observed differences could also be due to diffusion constraints in the heterogeneous nature of the system. These variations were analysed by conducting experiments at different stirrer speeds and dilution in the stainless steel reactor.

The intrinsic viscosity of the polymer samples at different conversions were evaluated by single point relative viscosity measurements in 1-chloronaphthalene at 195°C as done in the case of samples from stainless steel reactor. The data are presented in Table 12 and the plot is shown in Figure 18. The values on comparison were found to be lower than that obtained for stainless steel reactor.

The melting point of the samples collected at different reaction times were determined using capillary method (Table 12). The data is plotted in Figure 19. The trend is similar to that noted for samples from stainless steel reactor. The high melting point observed for 30 minutes could be due to reaction being initiated earlier. The time taken for the temperature to attain 195°C after PDCB addition is about 30 minutes as compared to 5 minutes in stainless steel reactor. Once the polymer precipitates after reaching a critical molecular weight, the melting point difference as a function of reaction time is insignificant.

TABLE 12

## INTRINSIC VISCOSITY DATA OF PPS FROM TEFLON REACTOR

Solvent = 1-chloronaphthalene, temperature = 195°C,  $t_0 = 147.2$  sec.

Reaction time, min.	Polymer concentration, gm/dl		$[\eta]^a$ dL/dl	$[\eta]^b$ dL/dl	M.P. °C
30	4.19	1.219	0.0489	0.0491	229
90	4.16	1.359	0.0777	0.0779	269
150	4.04	1.464	0.1007	0.1008	274
180	3.94	1.441	0.0987	0.0989	275
240	3.965	1.573	0.1236	0.1232	277
300	4.05	1.590	0.1241	0.1237	279
360	4.02	1.620	0.1305	0.1300	281
420	4.01	1.627	0.1321	0.1315	282

$$[\eta]^a = \frac{2}{C} \sqrt{\eta_{sp} - \ln \eta_r}$$

$$[\eta]^b = \frac{\eta_{sp}/C}{1 - K \eta_{sp}} \quad K = 0.302$$

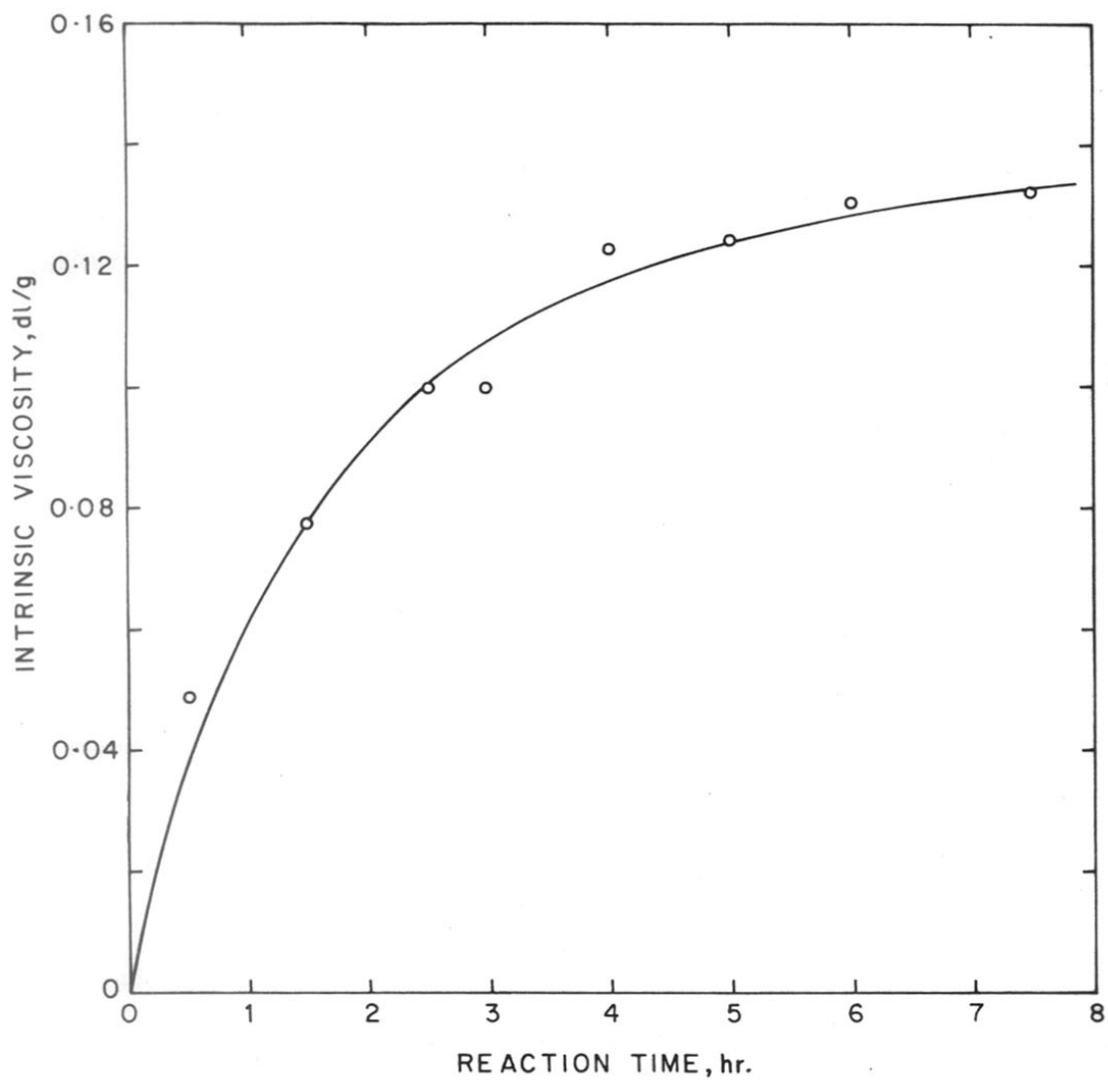


FIG.18 : INTRINSIC VISCOSITY-REACTION TIME DATA

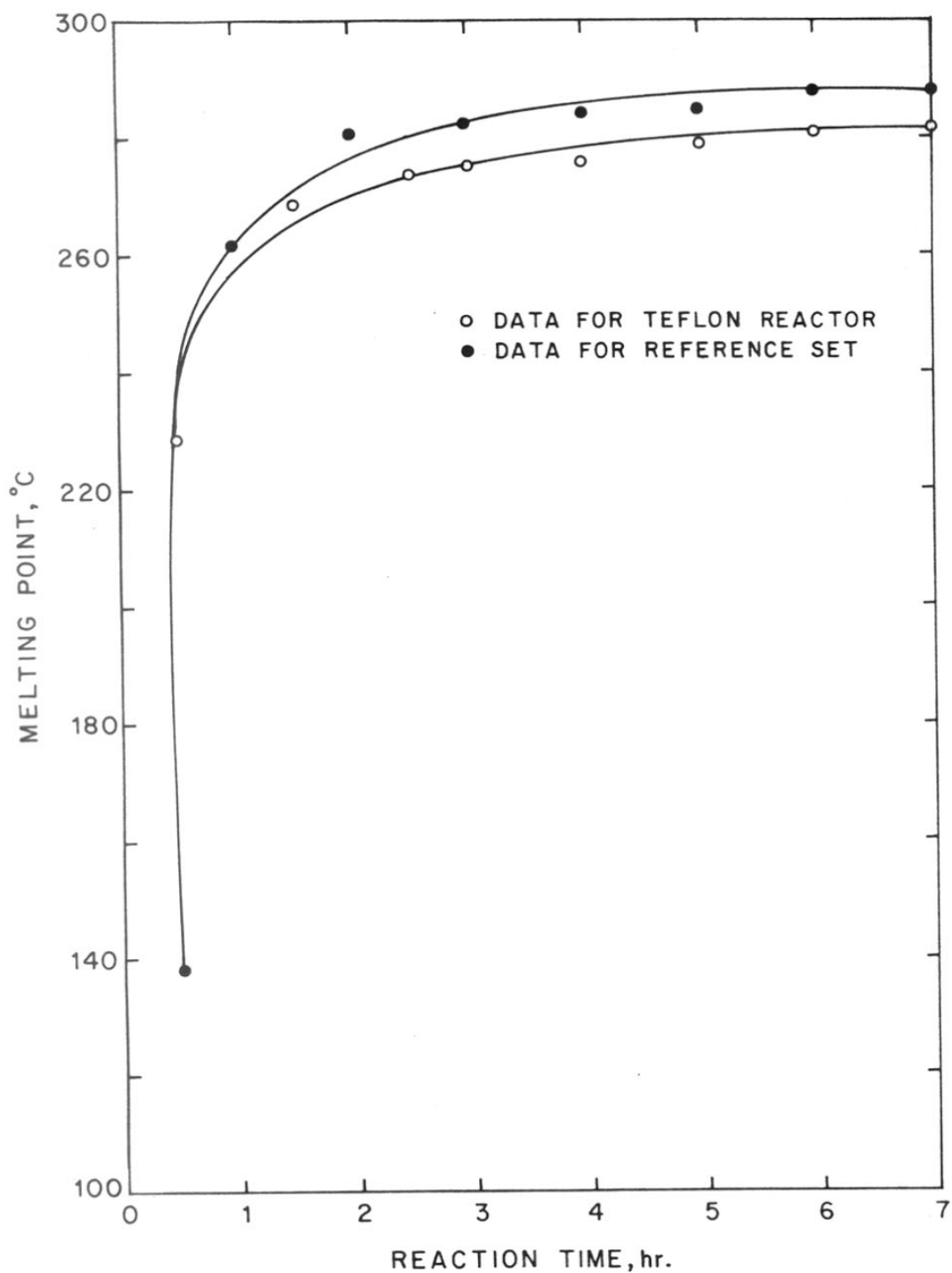


FIG. 19: MELTING POINT - REACTION TIME DATA

### 3.2.2. Effect of stirring speed and dilution

A comparison of the results on kinetics of polycondensation obtained in Teflon reactor indicated that the course of the reaction and the overall rate of polycondensation may be influenced by physical parameters. This is to be expected in view of the heterogeneous nature of the reaction and the limited solubility of sodium sulfide in the solvent NMP. The polymer also precipitates during the course of polycondensation, once a critical molecular weight has been achieved. The reaction kinetics and structure development would thus be affected by parameters that influence the physical processes of dissolution, transport of reactants, scale of mixing and precipitation. The growth of the polymer chain would therefore be expected to be dependent on parameters such as stirring speed and dilution of the reactants in the reaction mixture.

#### (a) Effect of stirring speed

Sodium sulfide is only marginally soluble in NMP at 195°C. This was confirmed by visual observation of the methanolic solution of sodium sulfide in NMP at 195°C under an optical microscope. Tiny particles of size less than 1 micron were found floating in NMP. In order to facilitate the reaction of sodium sulfide, it has to first get solvated in NMP. Both the dissolution and reaction would be influenced by the stirring speed. Experiments were conducted at different stirrer speeds in the stainless steel reactor under identical conditions. The experiments were carried out with the molar ratio of the reactants at 0.9422, the quantity of NMP at 100 ml and a reaction temperature of 195°C. Polymer samples were collected only at one reaction time. Based on the earlier results, it may be concluded that a reasonable degree of polymerization

and conversion are achieved at 6 hours. Therefore, the reaction time of 6 hours was selected for this set of experiments. The stirring speeds were kept at 660 and 400 rpm for two experiments while no mechanical stirring was maintained for the third experiment. The polymer isolation and chemical analysis steps were identical to the procedures followed in earlier experiments. The polymer samples were characterized for intrinsic viscosity to investigate the molecular weight development.

The variation of fractional polymer yield, fractional conversion and intrinsic viscosity with stirring speed are summarized in Table 13. The data are illustrated in Figures 20 and 21. The fractional polymer yield and fractional conversion were found to increase with stirring speed. The intrinsic viscosity of the samples was determined in 1-chloronaphthalene as was done for earlier samples. The results plotted in Figure 21 show an increase in intrinsic viscosity with increasing rpm. From these results, it is concluded that the reaction rate is accelerated and the degree of polymerization increases with increasing stirring speed.

(b) Effect of dilution

In solution polymerization, the concentration of the reactants in the solvent would have an influence on the probability of encounter of the two reacting species, particularly if the chemical reaction between the two species is relatively fast. To evaluate the effect of dilutions, a set of experiments were carried out wherein the volume of the solvent NMP was maintained constant. The molar concentrations of PDCB and sodium sulfide were varied, keeping their molar ratio constant at 0.9422. The reaction time in this set of experiments was also maintained at 6 hrs.

TABLE 13

RPM-CONVERSION-VISCOSITY DATA

Reaction temperature = 195°C, Reaction time = 6 hours

[sodium sulfide] = 0.1923 mole, [PDCB] = 0.2041 mole, NMP = 100 ml

RPM	Sodium chloride formed, mole	Fractional polymer conversion	Fractional polymer yield, gm	Fractional polymer yield	Intrinsic viscosity dL/g
0	0.2917	0.7585	16.07	0.7436	0.097
400	0.3182	0.8274	17.78	0.8228	0.104
660	0.3387	0.8808	19.05	0.8815	0.130

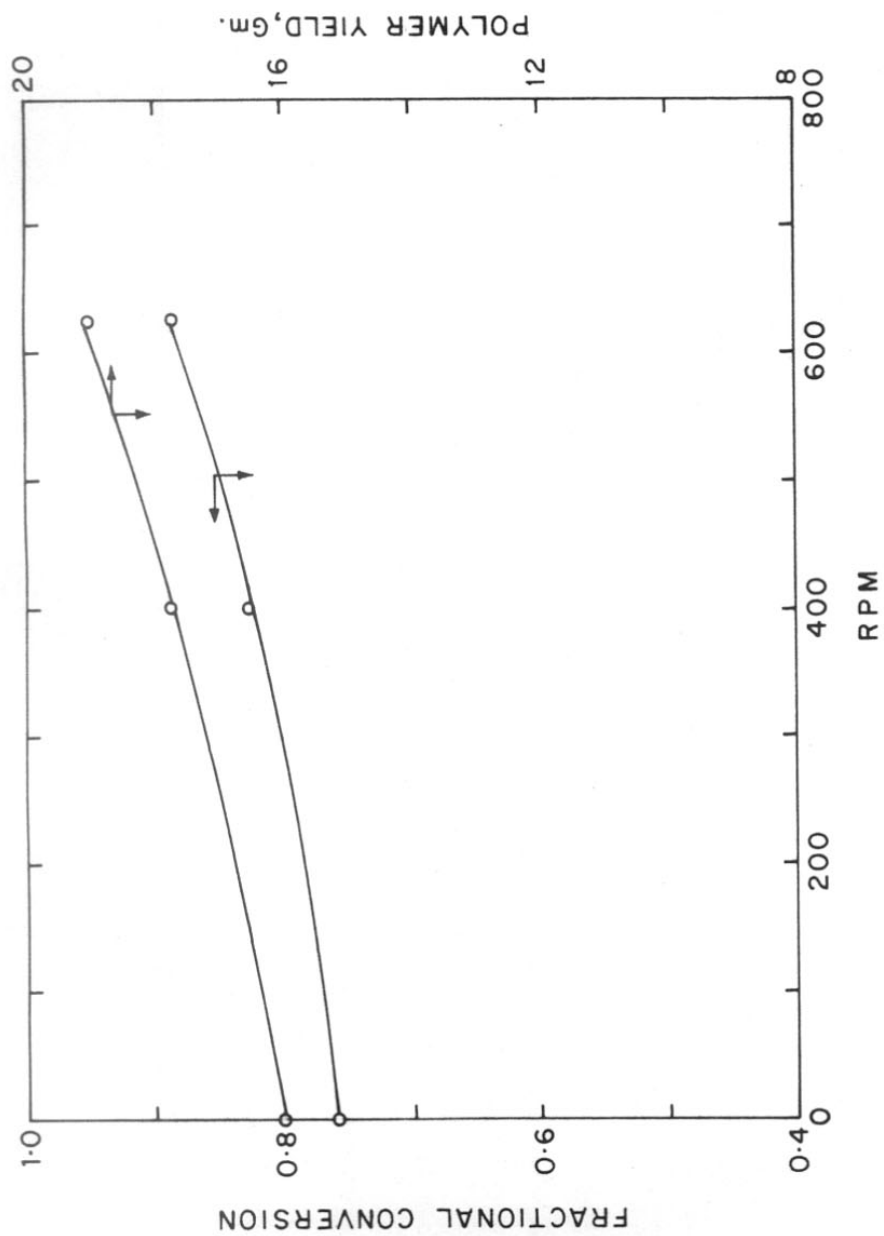


FIG.20: FRACTIONAL CONVERSION - POLYMER YIELD - RPM DATA



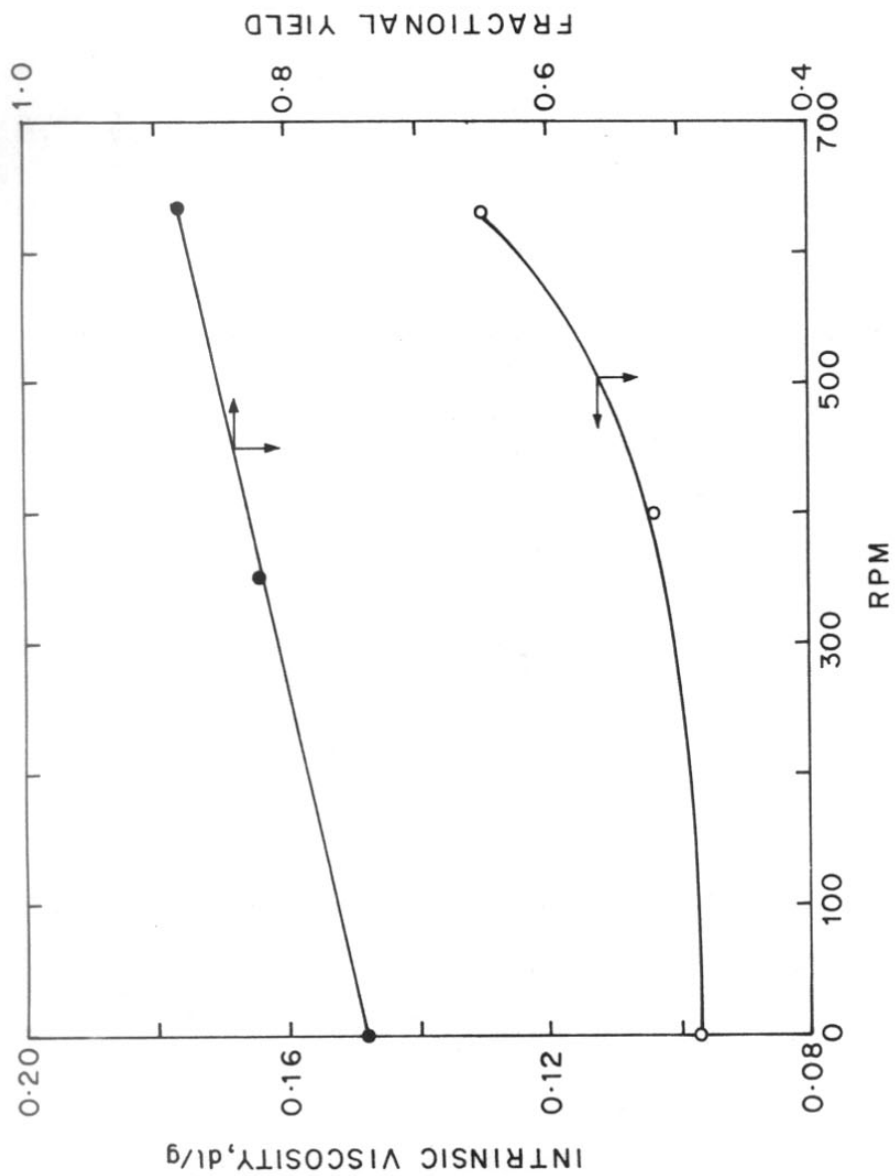


FIG. 21: INTRINSIC VISCOSITY - FRACTIONAL YIELD - RPM DATA

The process of polycondensation, polymer isolation step and the chemical analysis procedures were identical to those followed for earlier experiments.

A dilution factor of 1 was assigned to the system where the feed of reactants was as under:

PDCB = 2.041 molar

sodium sulfide = 1.923 molar

NMP = 200 ml.

This set of conditions in the feed was maintained as standard recipe for the investigation. The concentrations of the reactants PDCB and sodium sulfide were decreased proportionately to get dilution factors of 2, 4 and 10. The polymer yield and fractional conversion data with respect to dilution are summarized in Table 14. The polymer yield, fractional conversion data are plotted in Figure 22 while the fractional polymer yield data is shown in Figure 23. The intrinsic viscosity of the polymer samples isolated was determined by the method followed in earlier experiments. The variation of intrinsic viscosity with dilution is illustrated in Figure 23.

The probability of encounter of the sodium sulfide and PDCB molecules in the dissolved state would decrease with increasing dilution. As a result, both the fractional yield and conversion decreased with increasing dilution. However, the drop in yield is gradual and substantial, whereas the fractional conversion levelled off between 0.65 and 0.70 beyond a dilution factor of 2.5 to 3. This implies that, with increasing dilution, only the initial condensation reactions occur without subsequent chain growth reactions, resulting in the formation of low molecular weight, methanol soluble oligomers. The polymer yield as isolated, are the insolubles in methanol and water extractions. This conclusion is confirmed by the

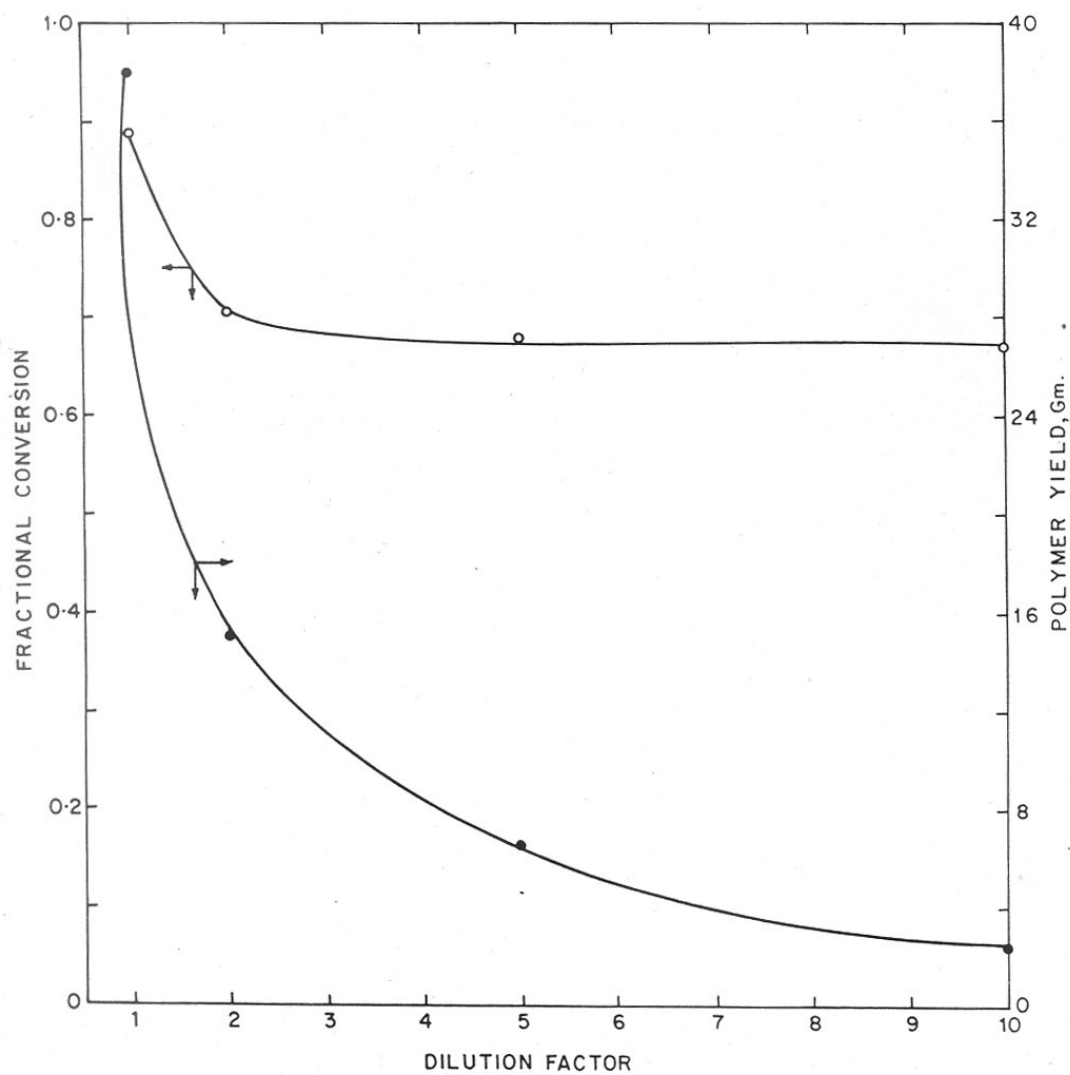


FIG.22: FRACTIONAL CONVERSION-POLYMER YIELD - DILUTION DATA

TABLE 14  
DILUTION-CONVERSION-VISCOSITY DATA

Reaction temperature = 195°C, reaction time = 6 hours

$$\frac{[\text{Sodium sulfide}]}{[\text{PCDB}]} = 0.9422$$

Dilution factor	Sodium chloride, mole	Fractional conversion	Polymer yield, gm	Fractional polymer yield	Intrinsic viscosity, dL/g
1	0.6775	0.8808	38.10	0.8815	0.130
2	0.2712	0.7051	15.06	0.6969	0.092
4	0.1312	0.6823	6.75	0.6247	0.081
10	0.0517	0.6719	2.43	0.4507	0.050

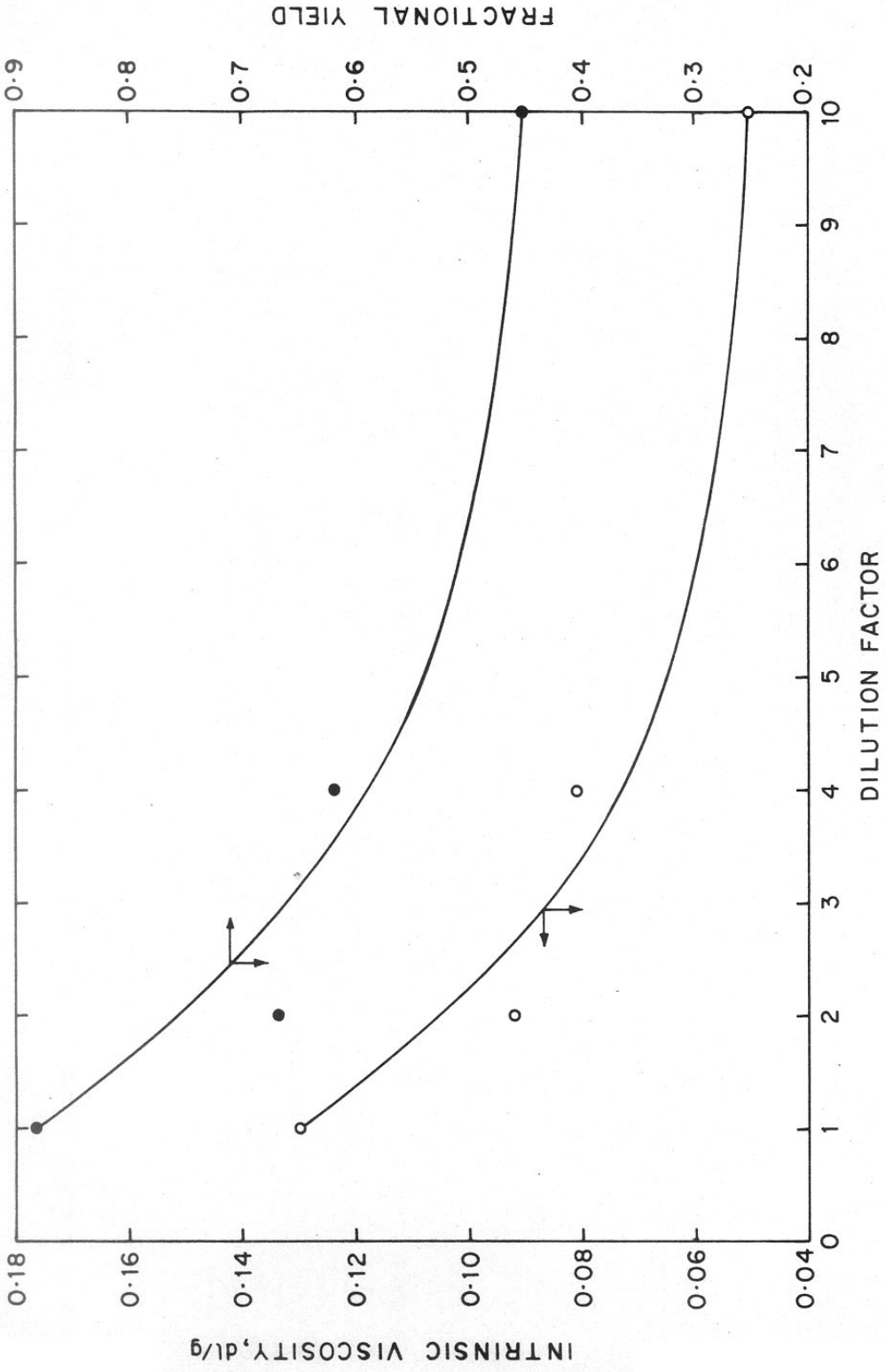


FIG.23: INTRINSIC VISCOSITY - FRACTIONAL YIELD - DILUTION DATA

steady, significant drop in the intrinsic viscosity of the polymer formed with dilution.

A comparison of the results in the two sets of experiments (see Table 13, 14), wherein the effect of stirring speed and dilution were investigated, indicate that the kinetics and structure development in polycondensation reactions to synthesize PPS are considerably more sensitive to the extent of dilution than to the stirring speed.

### 3.4 EFFECT OF CHEMICAL PARAMETERS ON KINETICS

#### 3.4.1 Reactions with excess PDCB

Experiments were conducted with a large excess of PDCB to evaluate the influence of a higher PDCB concentration on the rate as well as the properties of the polymer formed. In this set of experiments, the molar concentration of PDCB was maintained at 4.082 versus 2.041 used in the reference set of experiments (Section 3.1). The molar concentration of the other reactant, sodium sulfide was however maintained at 1.923 as in the other experiments. The polycondensation reactions were carried out in the stainless steel reactor for varying reaction times. The experimental procedures followed for polymerization, polymer isolation and chemical analysis were as per detailed described in Section 2.

The variation of polymer yield and fractional conversion with reaction time are summarized in Table 15. The data are graphically compared to the reference set in Figures 24 and 25. The conversion corresponding to a reaction time of 2 hours was 85 percent. Thus the initial part of the reaction appears to be very fast compared to the reference discussed earlier. The increase in conversion with reaction time after this period

TABLE 15  
REACTION TIME - CONVERSION DATA

Reaction temperature = 195°C, [PDCB] = 0.4082 ,  
[Sodium sulfide] = 0.1923, NMP = 100 ml, [NaCl] theoretical= 0.3846 moles

Reaction time min.	Polymer yield, gm	Sodium chloride formed, mole	Fractional conversion	Fractional yield
20	0.1	0.0306	0.0796	0.0041
40	2.41	0.0382	0.0993	0.0938
60	4.01	0.1172	0.3047	0.1560
90	13.91	0.2725	0.7085	0.5412
120	17.20	0.3259	0.8474	0.6692
180	18.67	0.3302	0.8586	0.7264
270	19.01	0.3404	0.8851	0.7396
360	20.10	0.3559	0.9254	0.7820

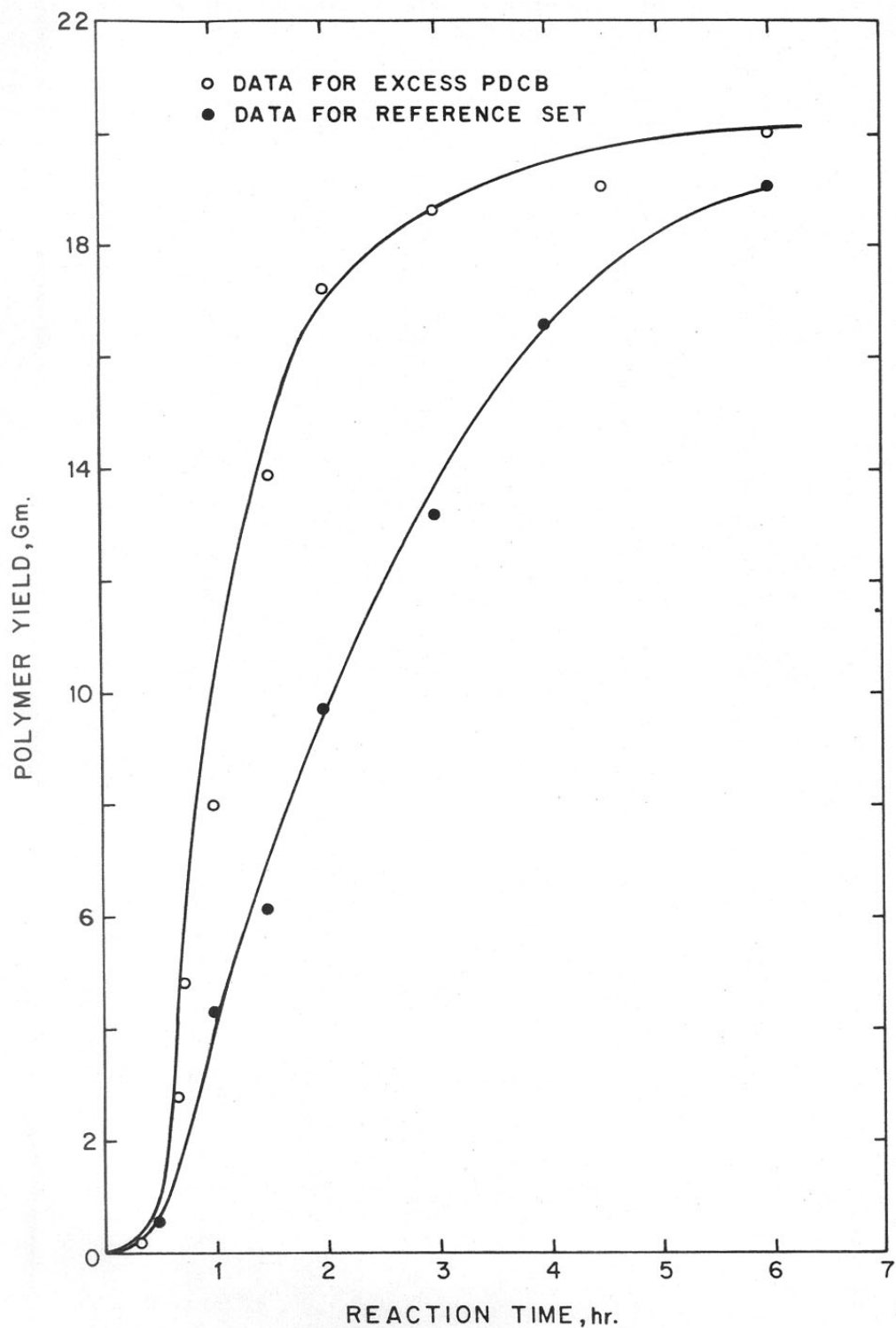


FIG.24: POLYMER YIELD - REACTION TIME DATA



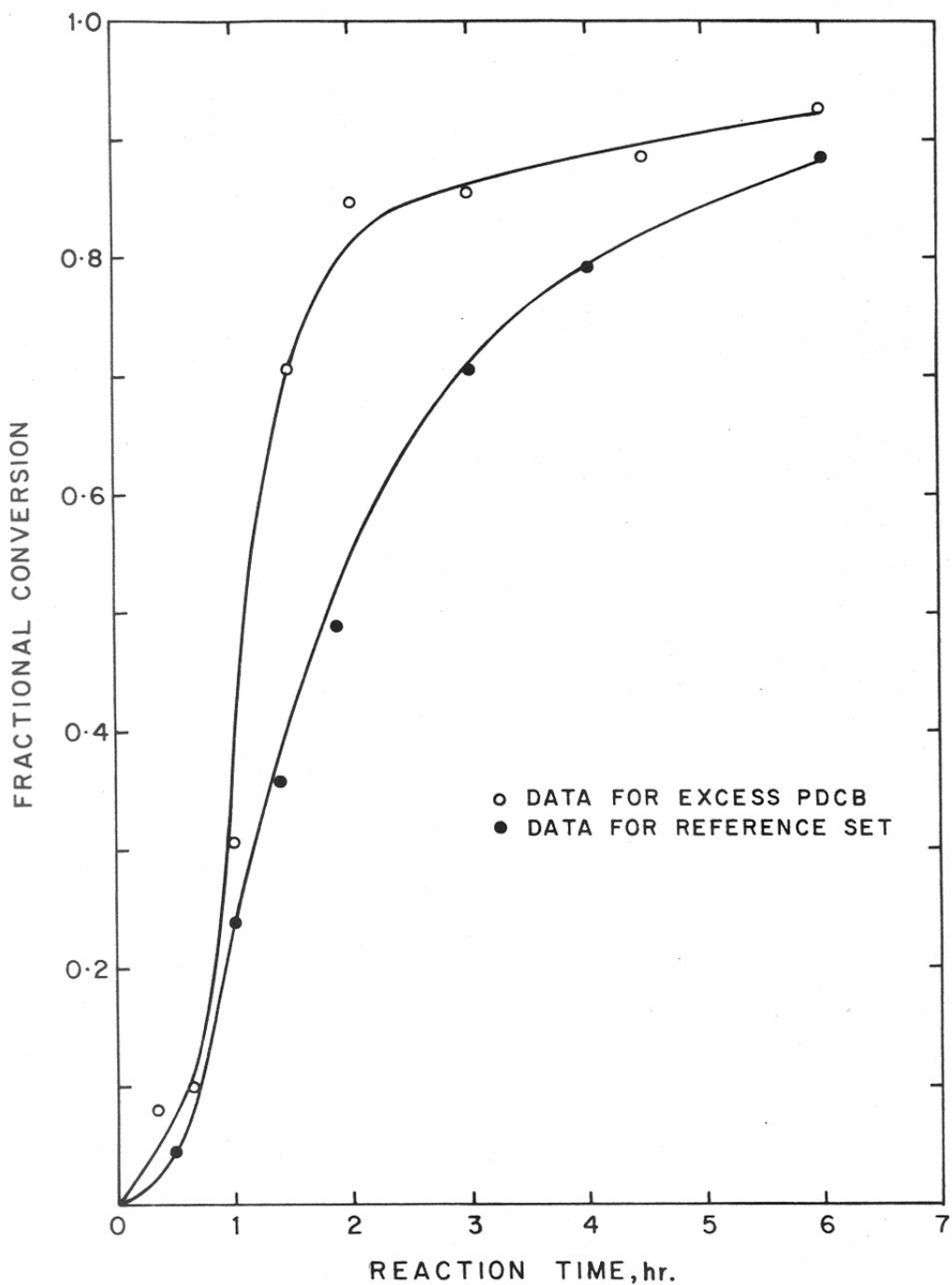


FIG.25: FRACTIONAL CONVERSION WITH TIME, WITH EXCESS PDCB. DETERMINED AS RATE OF FORMATION OF SODIUM CHLORIDE.

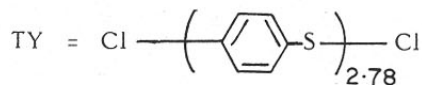
was very gradual. The polymer yield determined as methanol insoluble is high compared to the reference set (Figure 22). The theoretical yield for this system was calculated as follows:

$$X_n \text{ at 100\% conversion} = \frac{(1 + r)}{(1 + r - 2rp)}$$

$$\text{here } r = \frac{0.1923}{0.4082} = 0.4711$$

$$X_n = \frac{1 + 0.4711}{1 + 0.4711 - (2 \times 0.4711 \times 1)} = 2.781$$

Structure (on statistical average) of polymer formed as theoretical yield (T.Y.) would be,



$$\begin{aligned} \text{TY} &= 0.1923 \times 108.15 + 2 \times \frac{0.1923}{2.78} \times 35.45 \\ &= 25.70 \text{ gms} \end{aligned}$$

The fractional polymer yield calculated as the ratio of the polymer yield obtained gravimetrically and the theoretical equivalent (Table 15). The plot of fractional yield with reaction time is shown in Figure 26 along with the data for the reference set. Though the polymer yields by weight are high, the fractional yields follow the trend seen for the yield reaction time data.

The concentrations of the two reactants in this system were highly non-stoichiometric. The kinetics could not be accurately evaluated on the basis of the change in  $1/(1-p)$  with reaction time. The corresponding relation for non-stoichiometric proportion of the reactants was applied

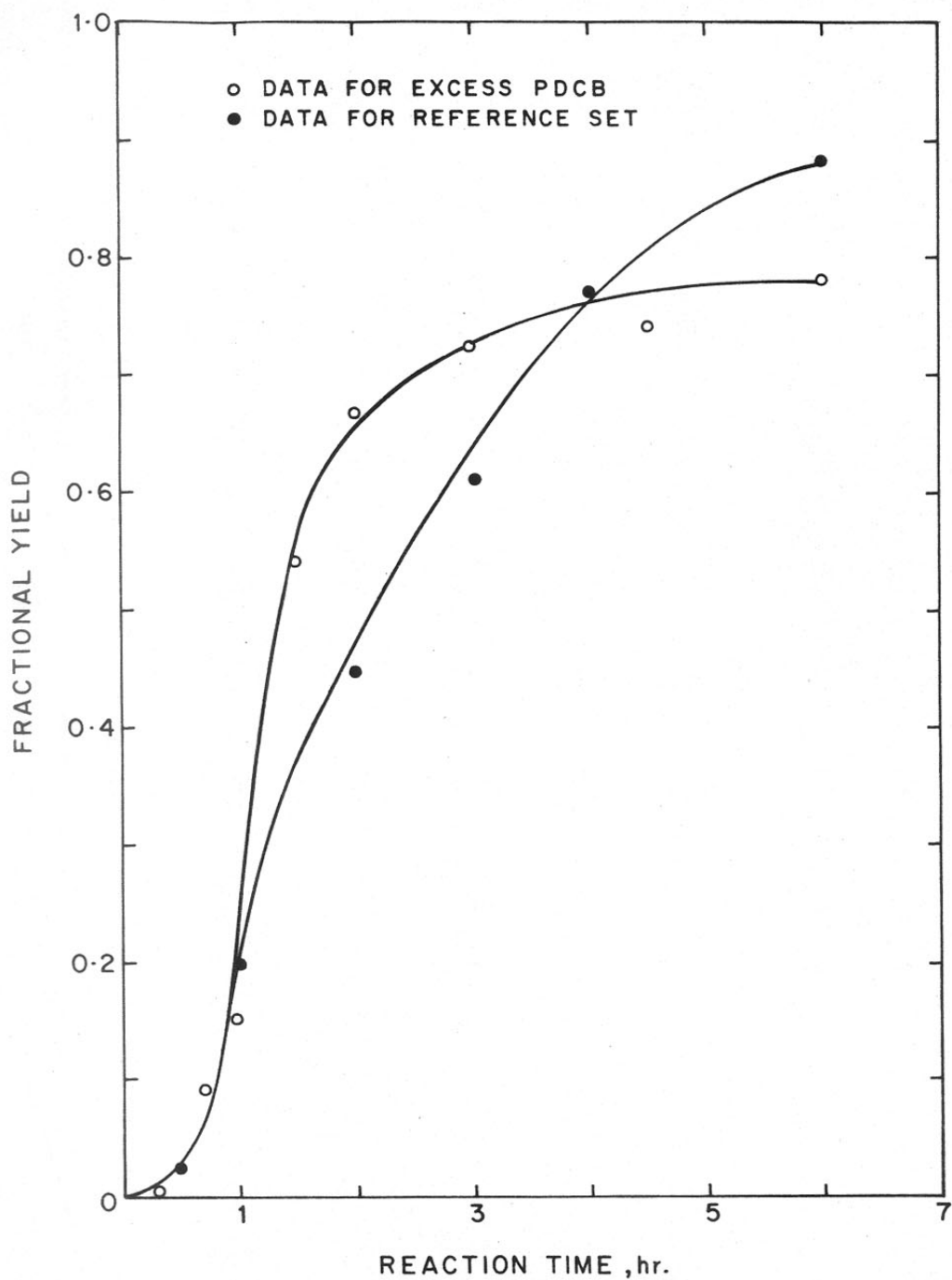


FIG.26: FRACTIONAL YIELD - REACTION TIME DATA

for this system. The data are presented in Figure 27. In this system also, two regions of linearity are observed. The reaction rates were evaluated for the two regions, first region upto 70% conversion and the second one from 70 to 93% conversion. The evaluated rates were  $3.96 \times 10^{-5} \text{ m l}^{-1} \text{ s}^{-1}$  and  $1.07 \times 10^{-5} \text{ m l}^{-1} \text{ s}^{-1}$  for the two regions. Interestingly, the trends in the rates of polycondensation were reversed in this system. An initial faster reaction rate was followed by a slower rate beyond 70 percent conversion. The reaction rate was an order of magnitude slower in the later part of the reaction, when compared to the reference set, wherein the reactants were used in almost stoichiometric proportion.

#### 3.4.2 Reactions with sodium parachloro thiophenoxide

A series of experiments were designed to evaluate the role (if any) of sodium parachloro thiophenoxide (SPCTP), the initial product of the condensation of PDCB and sodium sulfide (see section 3.1). The experimental procedure for these reactions was identical to 3.1.1 except that 1.47 mole percent of SPCTP was added along with PDCB. The polycondensations were run for different predetermined reaction times and the reaction products were analysed for the conversions achieved. The post reaction work up procedures and the analyses were identical to that followed in experiments 3.1.

The fractional conversions 'p' were calculated from the moles of sodium chloride generated. It was assumed for the calculations that at the start of the reaction sodium chloride equivalent to the moles of SPCTP used had already been generated. In this series of experiments 0.003 moles of SPCTP were taken. Hence the fractional conversion were calculated using the formula,

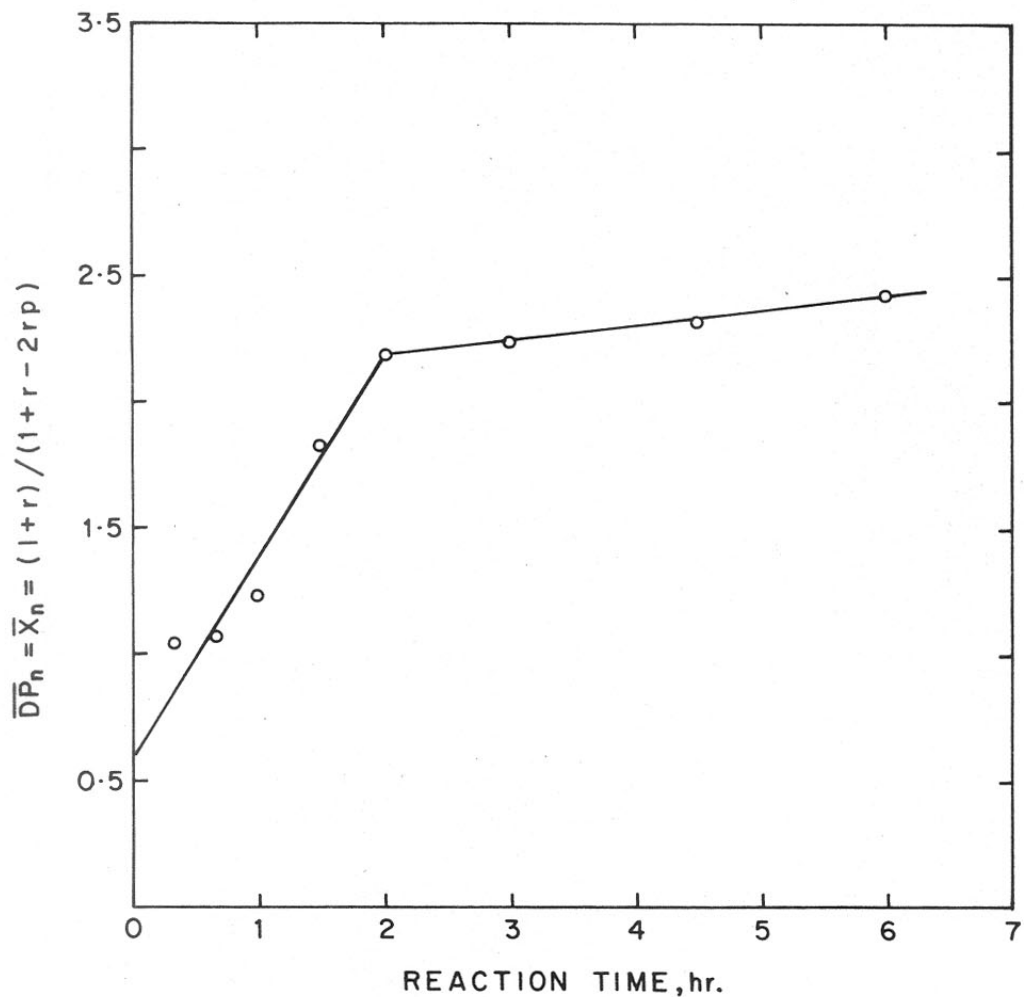


FIG.27: PLOT OF  $\overline{DP}_n$  AS A FUNCTION OF REACTION TIME. PLOT ASSUMING STOICHIOMETRIC NONEQUIVALENCE BETWEEN THE TWO REACTANTS.

$$P = \frac{0.003 + \text{moles of sodium chloride formed}}{0.003 \times (0.1923 \times 2)}$$

The data generated in terms of fractional conversion and polymer yield with reaction time are summarized in Table 16. The trend observed for this system was very similar to that seen for the system of PDCB-sodium sulfide reaction. The fractional conversion and polymer yield data with reaction time are shown in Figures 28 and 29. The experimental data for this system were found to fit a second order kinetic scheme over a wide range of conversions. Polymer was formed at low conversion and the yield was found to increase with reaction time. The data are presented along with that for reference set.

The data were subjected to regression analysis similar to that for PDCB - sodium sulfide system. The data on  $1/(1-p)$  and  $\frac{(1+r)}{(1+r-2rp)}$  (for non-stoichiometric ratio) with reaction time are graphically represented in Figures 30 and 31. Two regions of linearity were noted for this system also.

The rate and specific rate constants were evaluated as,

$$\begin{array}{ll} \text{Rate} = 2.75 \times 10^{-5} \text{ m l}^{-1} \text{ s}^{-1} & ) \\ & ) \text{ upto 36 per-} \\ & ) \text{ cent} \\ \text{specific rate constant} = 7.44 \times 10^{-4} \text{ l m}^{-1} \text{ s}^{-1} & ) \text{ conversion} \end{array}$$

$$\begin{array}{ll} \text{Rate} = 8.34 \times 10^{-5} \text{ m l}^{-1} \text{ s}^{-1} & ) \\ & ) \text{ beyond 36} \\ \text{specific rate constant} = 5.51 \times 10^{-3} \text{ l m}^{-1} \text{ s}^{-1} & ) \text{ percent} \\ & ) \text{ conversion} \end{array}$$

The values evaluated above differ marginally on comparison with the system PDCB-sodium sulfide (section 3.1). The variations are within the errors of experimentation and analysis. This leads to the conclusion

TABLE 16

REACTION TIME - CONVERSION, POLYMER YIELD DATA

[PDCB]= 0.2041 mole, [sodium sulfide]= 0.1923 mole, [SPCTP]= 0.003mole

NMP = 100 ml, reaction temperature = 195°C

Reaction time, min.	Sodium chloride formed, mole	Fractional conversion	Polymer yield gm	Fractional polymer yield
30	0.0099	0.0333	0.31	0.0141
60	0.0469	0.1287	2.01	0.0916
90	0.1003	0.2664	4.45	0.2029
120	0.1362	0.3591	6.24	0.2845
160	0.2069	0.5415	11.25	0.5129
180	0.3054	0.7957	16.71	0.7619
360	0.3499	0.9105	19.70	0.8982

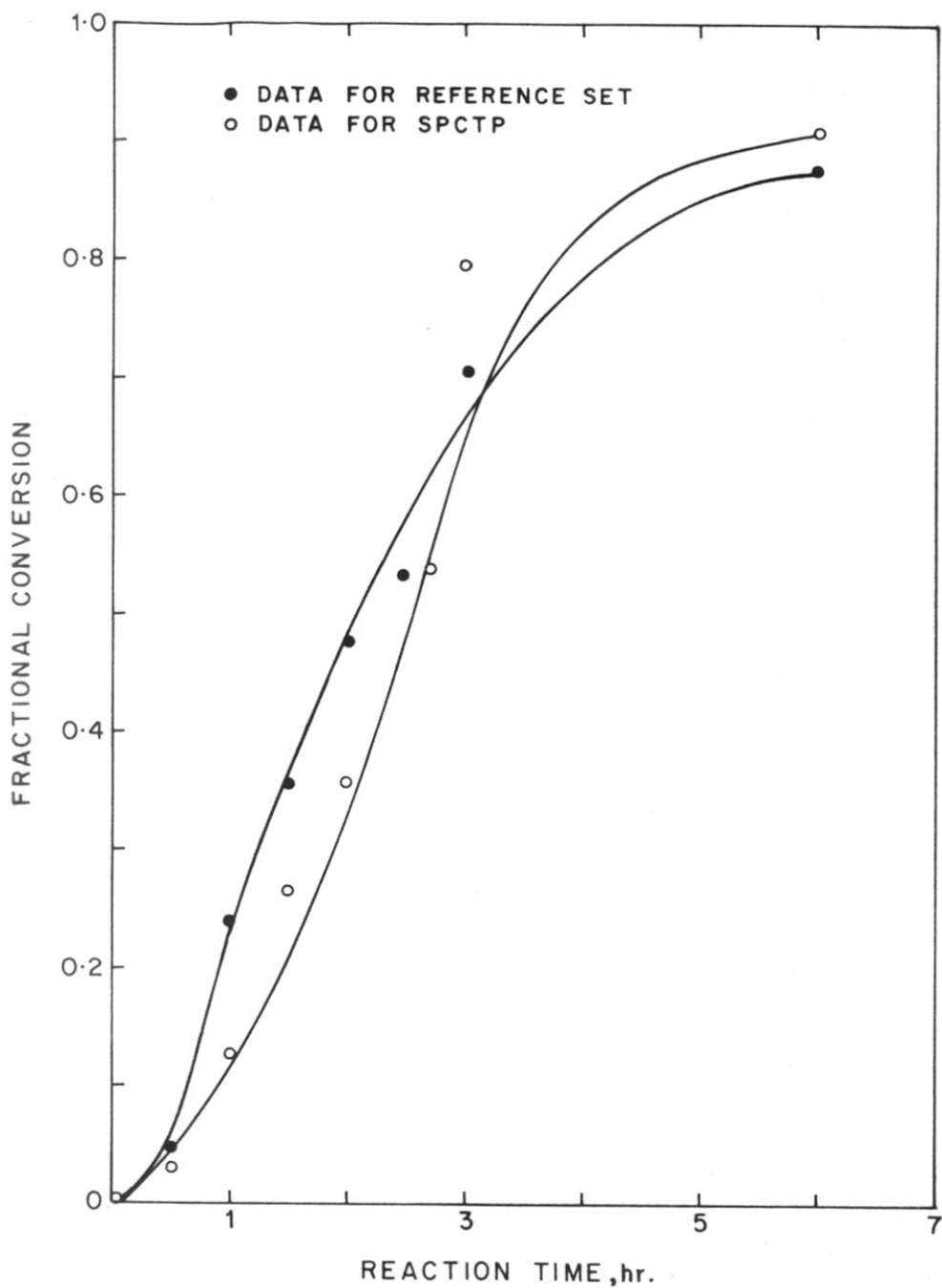


FIG.28:FRACTIONAL CONVERSION DETERMINED BASED ON SODIUM CHLORIDE GENERATED.



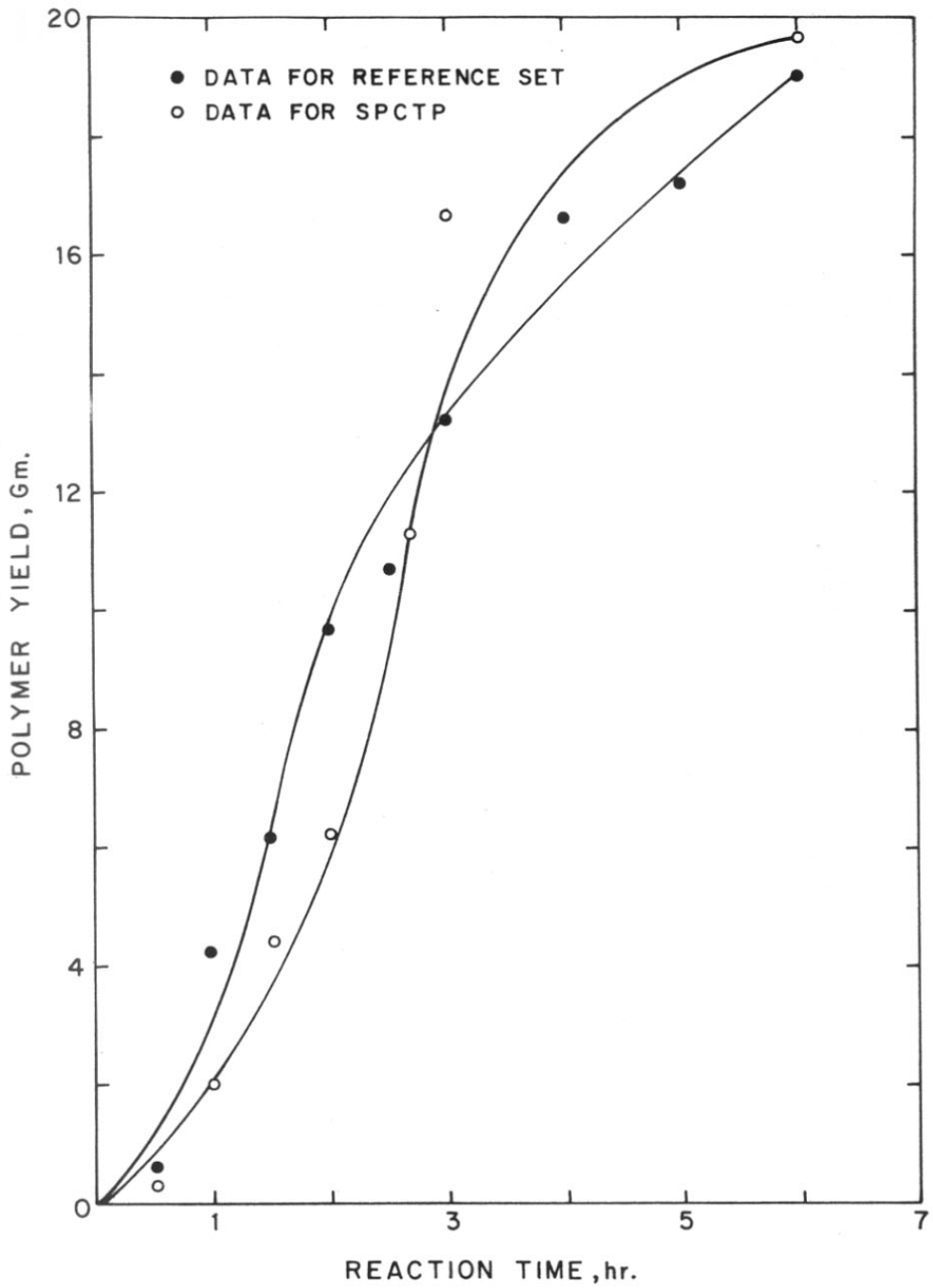


FIG.29 : POLYMER YIELD -REACTION TIME DATA

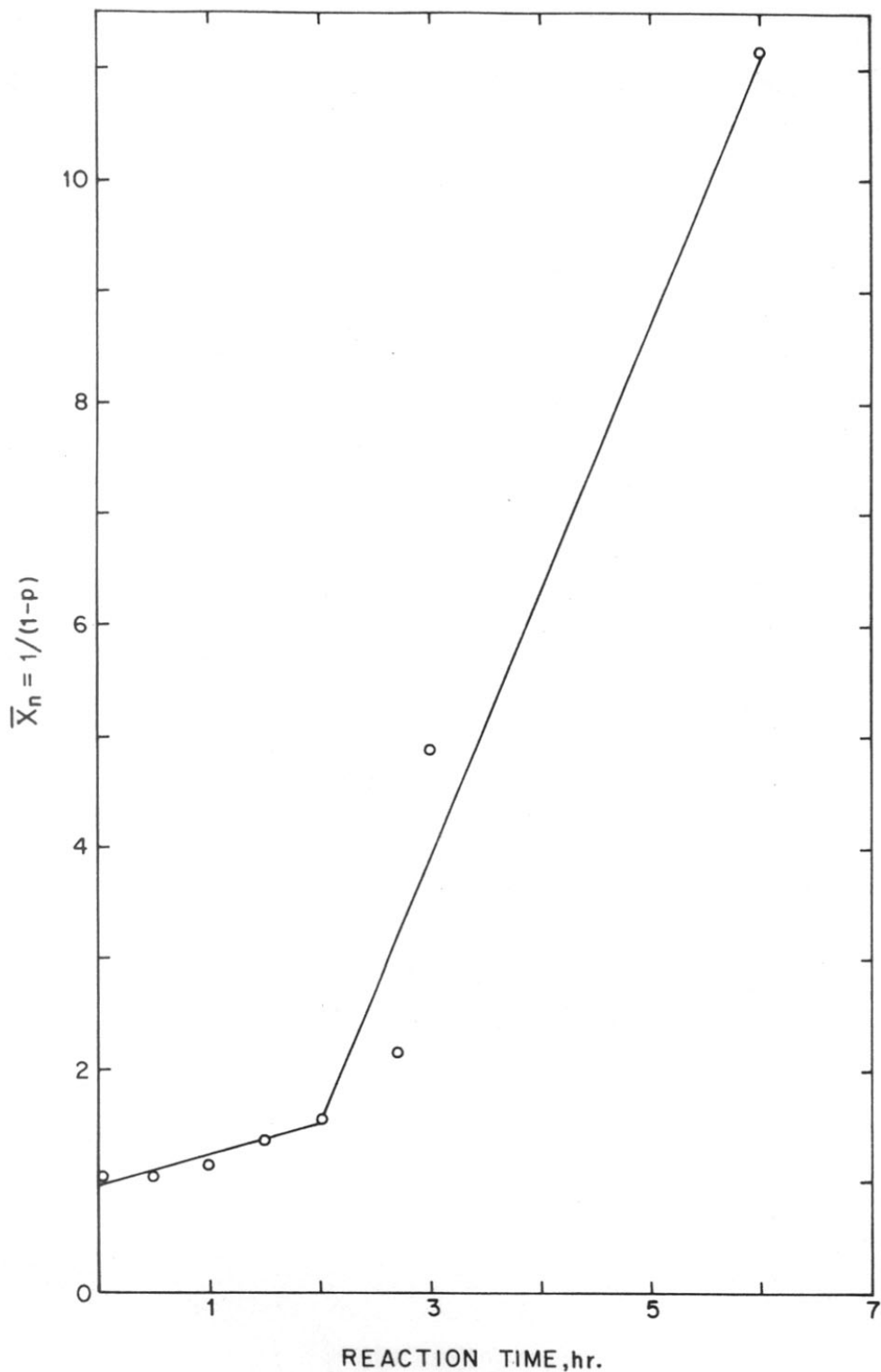


FIG.30: PLOT OF THE NUMBER-AVERAGE DEGREE OF POLYMERIZATION AS A FUNCTION OF REACTION TIME, ASSUMING STOICHIOMETRIC EQUIVALENCE OF THE REACTANTS.

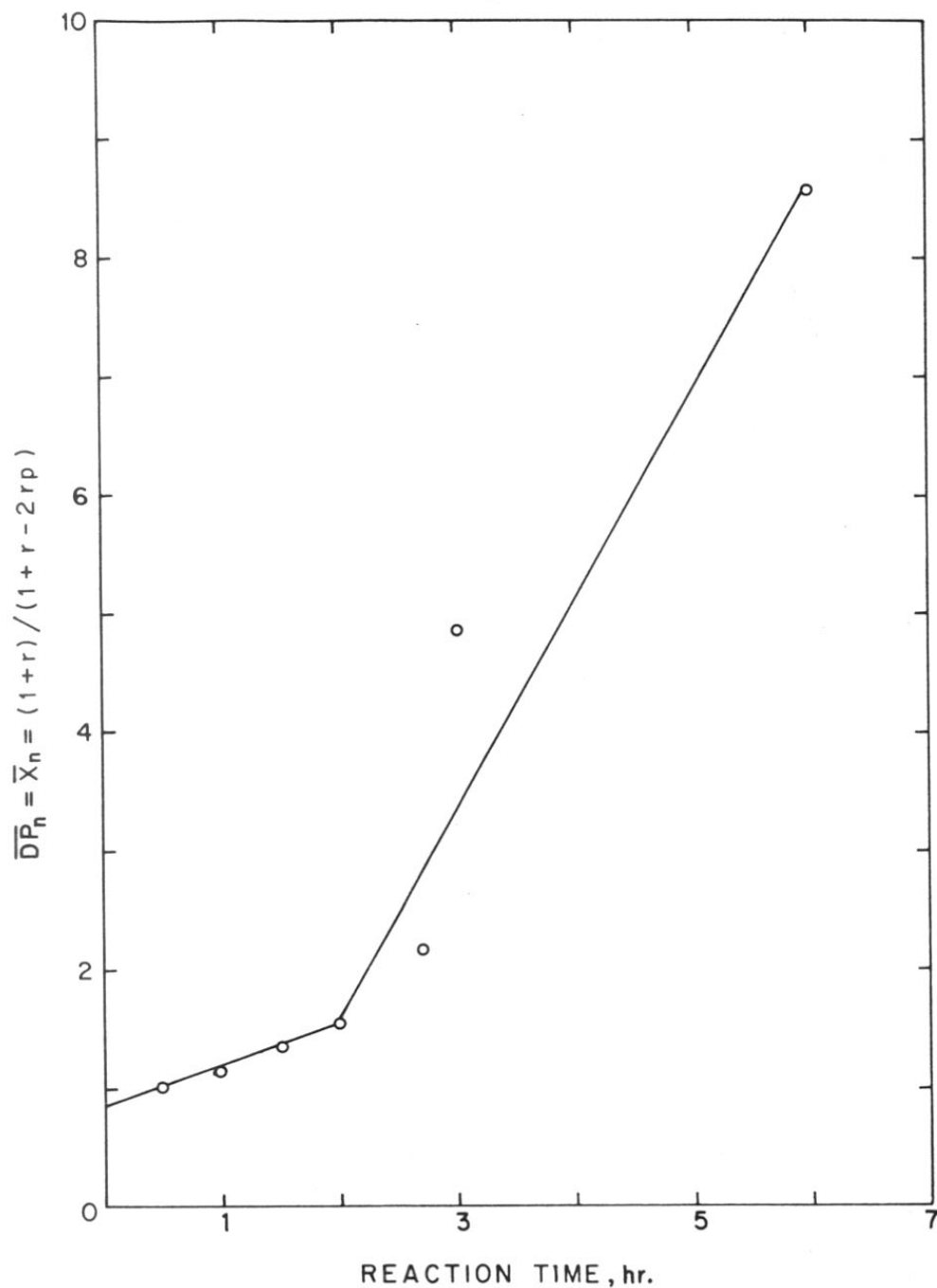


FIG.31: PLOT OF  $\overline{DP}_n$  AS A FUNCTION OF REACTION TIME. PLOT ASSUMING STOICHIOMETRIC NONEQUIVALENCE BETWEEN THE TWO REACTANTS

that SPCTP does not function as a possible catalyst. Its presence does not enhance the rate of the polymer yield to an appreciable extent. It is also probable that the kinetic step involving reaction between PDCB and sodium sulfide to generate sodium parachloro thiophenoxide is not the rate determining step.

In the calculation of fractional polymer yield, the concentration of SPCTP was taken into consideration. The polymer yield in this case becomes,

$$(0.003 + 0.1923) \times 108.15 + 0.01144 \times \text{Cl}_2 = 21.933 \text{ gm.}$$

where 0.003 is the molar concentration of SCPTP. The data are presented in Figure 32 in comparison with the reference set.

Studies with SPCTP thus indicated that the initial linear region where the reaction is slow could be advantageously shifted to lower conversion. Concrete results required homopolycondensation kinetics.

The intrinsic viscosity of the samples were evaluated in 1-chloronaphthalene as done for the reference set. The data are presented in Figure 33 along with the data for the reference set. The intrinsic viscosity values obtained for this set are consistently lower than those obtained in the reference set.

The melting point of the samples were determined by capillary method. The data are plotted in Figure 34 along with the data for reference set. After a reaction time of 3 hours, no significant difference was observed in the case of reference set.

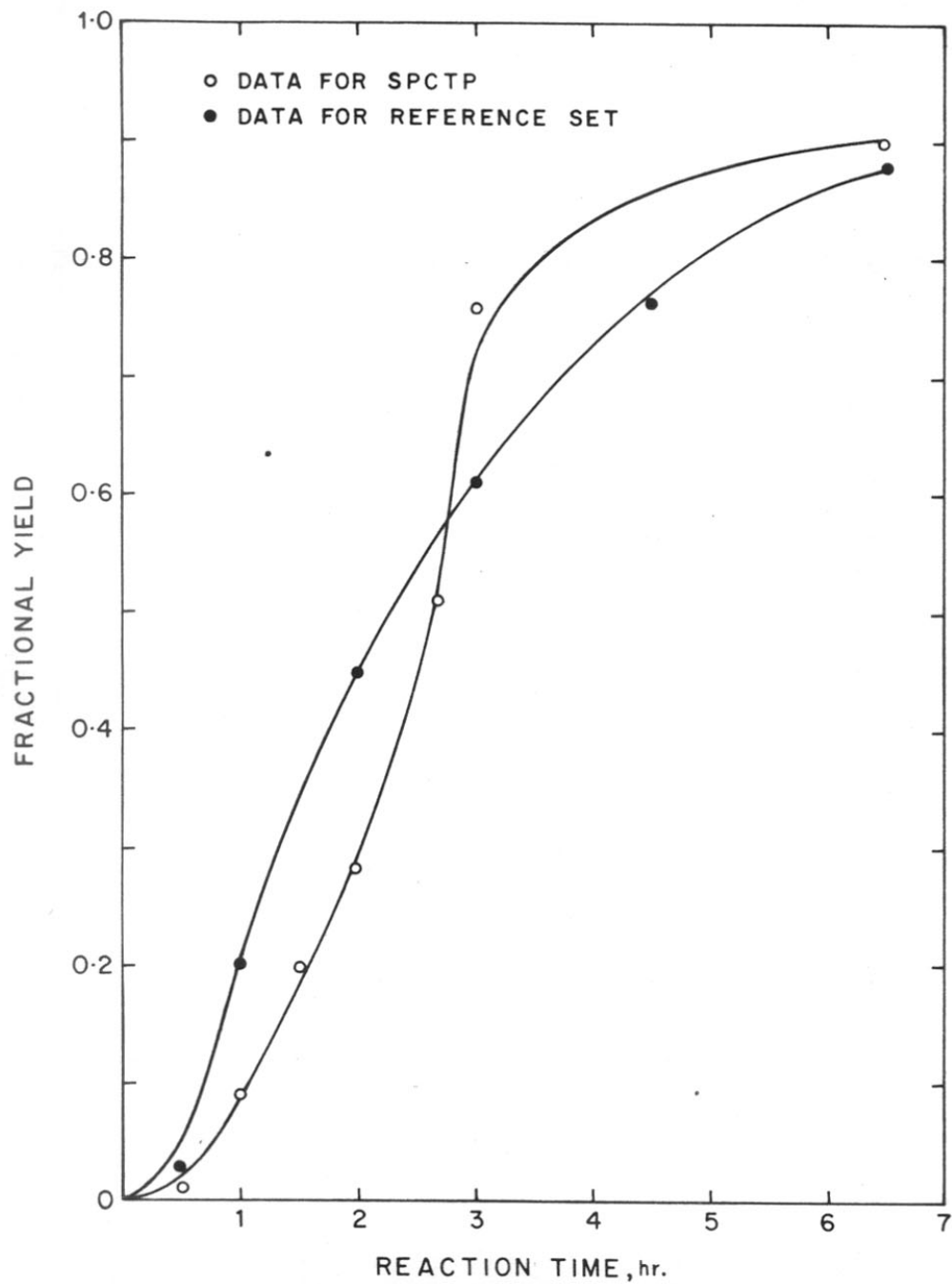


FIG.32: FRACTIONAL YIELD - REACTION TIME DATA

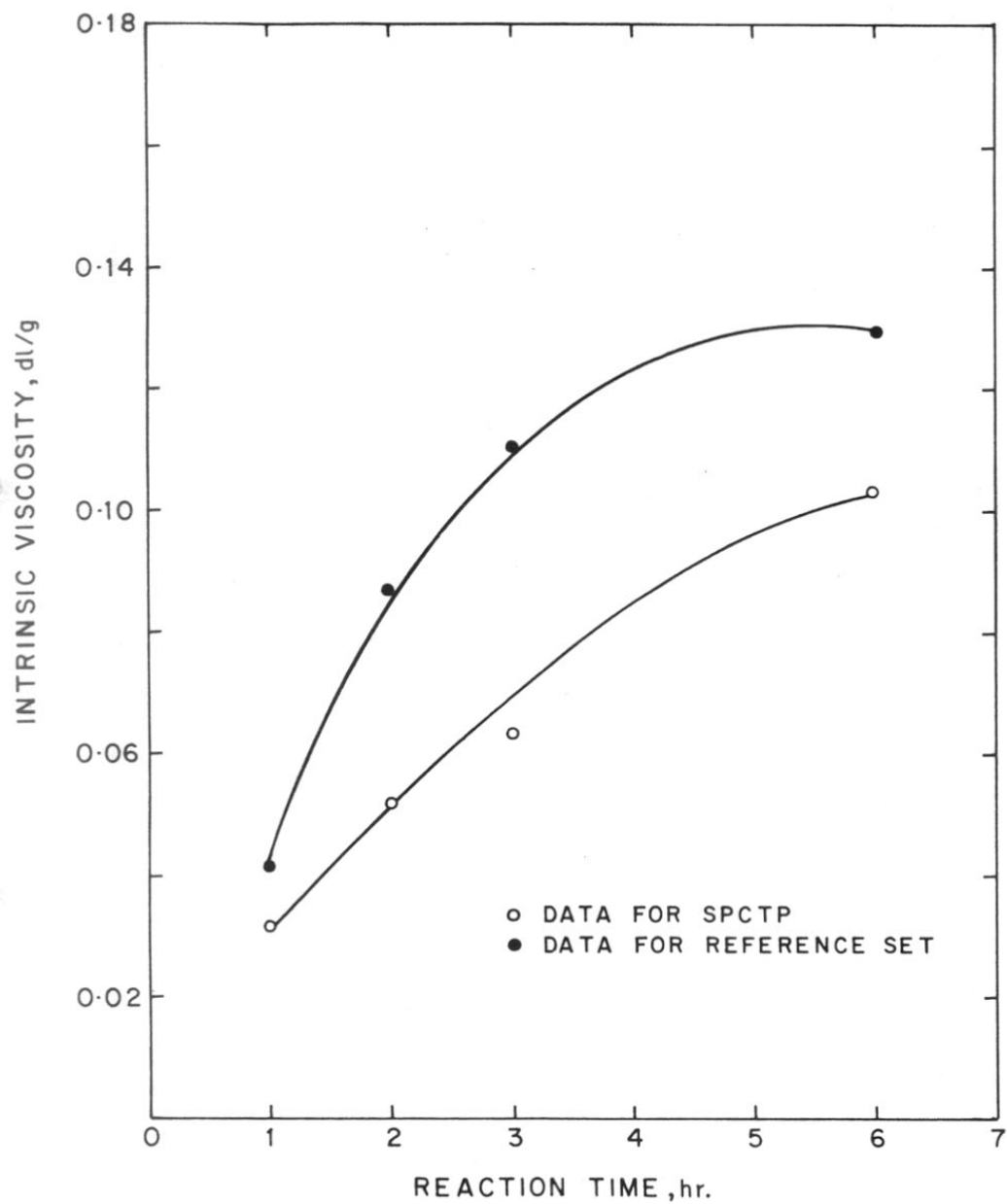


FIG.33: INTRINSIC VISCOSITY - REACTION TIME DATA

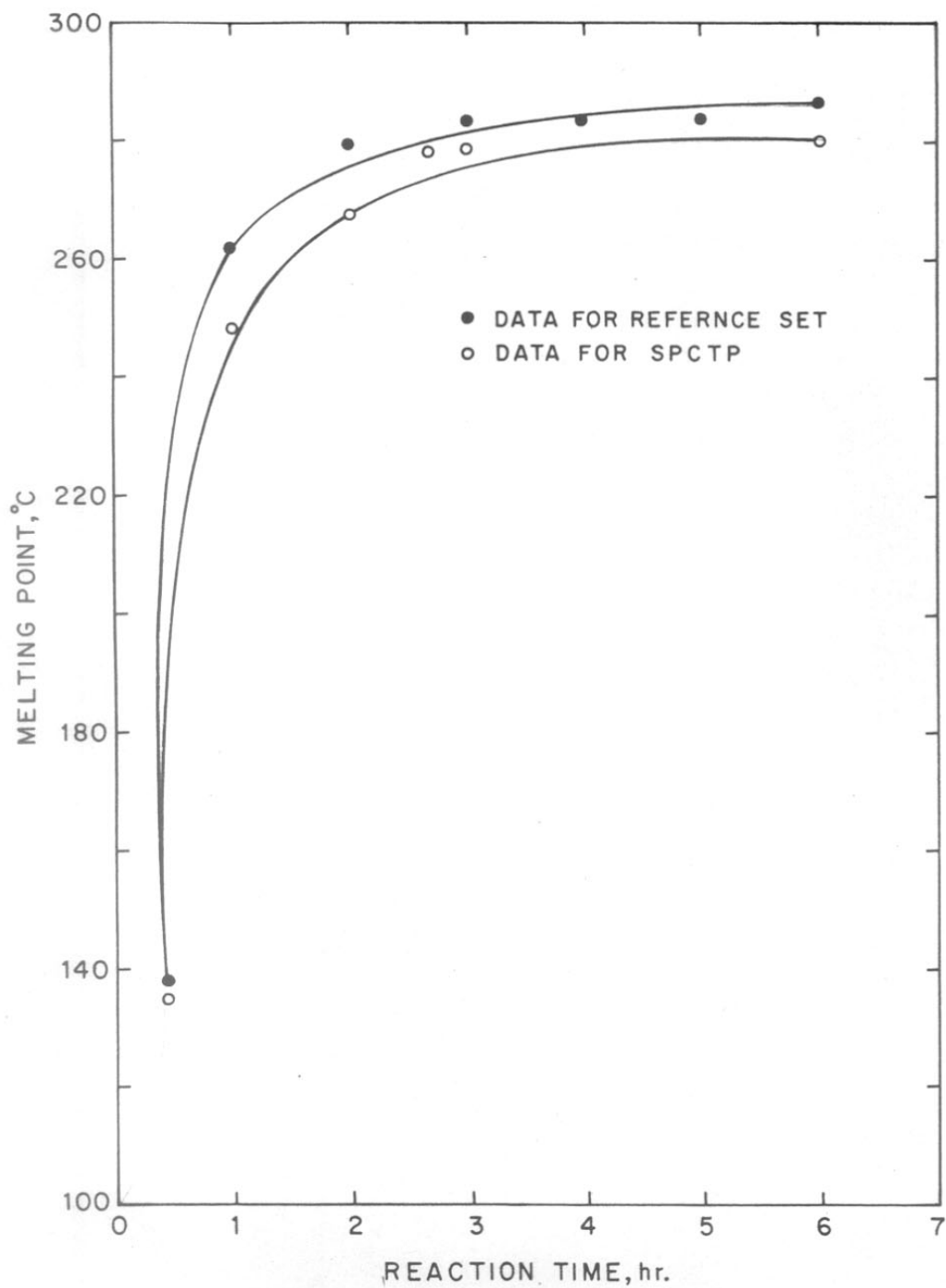


FIG. 34: MELTING POINT - REACTION TIME DATA

### 3.4.3 Reaction with paradibromobenzene

Aromatic nucleophilic substitution reactions occur by the attack of a nucleophile on the aromatic nucleus (see section 4.1). An alternate route for the synthesis of PPS with the use of dibromic benzene was investigated. PDCB was substituted by 1,4-dibromobenzene (PDBB). The other relevant parameters were unaltered. Thus, the molar ratio of the reactants, the amount of solvent, the reaction temperature, the reactor geometry, the agitator speed as well as the work up procedures after the polymerization were all kept identical to the reference set of experiments with PDCB (Section 2.3.).

The reactions were conducted for preset reaction times. The data generated as the extent of reaction and the overall rate were computed from the moles of the side product formed, in this case sodium bromide. The moles of sodium bromide that would be generated at complete conversion was again equated to correspond to twice the moles of the deficient difunctional reactant, sodium sulfide. The reactions were stopped at preset times and sodium bromide was estimated from the methanol/water extractions. The data as fractional conversion and the polymer formed with reaction time are presented in Table 17. The data are compared with the reference set in Figures 35 and 36. For the initial part of the reaction, the reaction was found to be faster than the reference set. The fractional conversion and the polymer yield are much high indicating the possibility of a different reaction scheme as compared to the reference set. The experimental data of this system were found to fit a second order kinetic scheme over a wide range of conversions.



TABLE 17  
TIME-CONVERSION DATA OF REACTION BETWEEN PDBB AND  
SODIUM SULFIDE

$$\text{Reaction temperature} = 195^{\circ}\text{C}, \frac{[\text{Na}_2\text{S}]}{[\text{PDBB}]} = 0.9422$$

Reaction time, min.	Polymer yield, gms	NaBr formed, moles	Fractional conversion, p	Fractional yield
2.5	3.82	0.0821	0.2135	0.1688
5	7.30	0.1286	0.3343	0.3227
7	8.35	0.1577	0.4102	0.3691
10	10.16	0.1850	0.4810	0.4491
15	11.15	0.2422	0.6298	0.4928
22	13.73	0.2623	0.6820	0.6068
45	15.25	0.2772	0.7208	0.6740
90	16.37	0.3094	0.8045	0.7235
180	17.82	0.3536	0.9194	0.7876

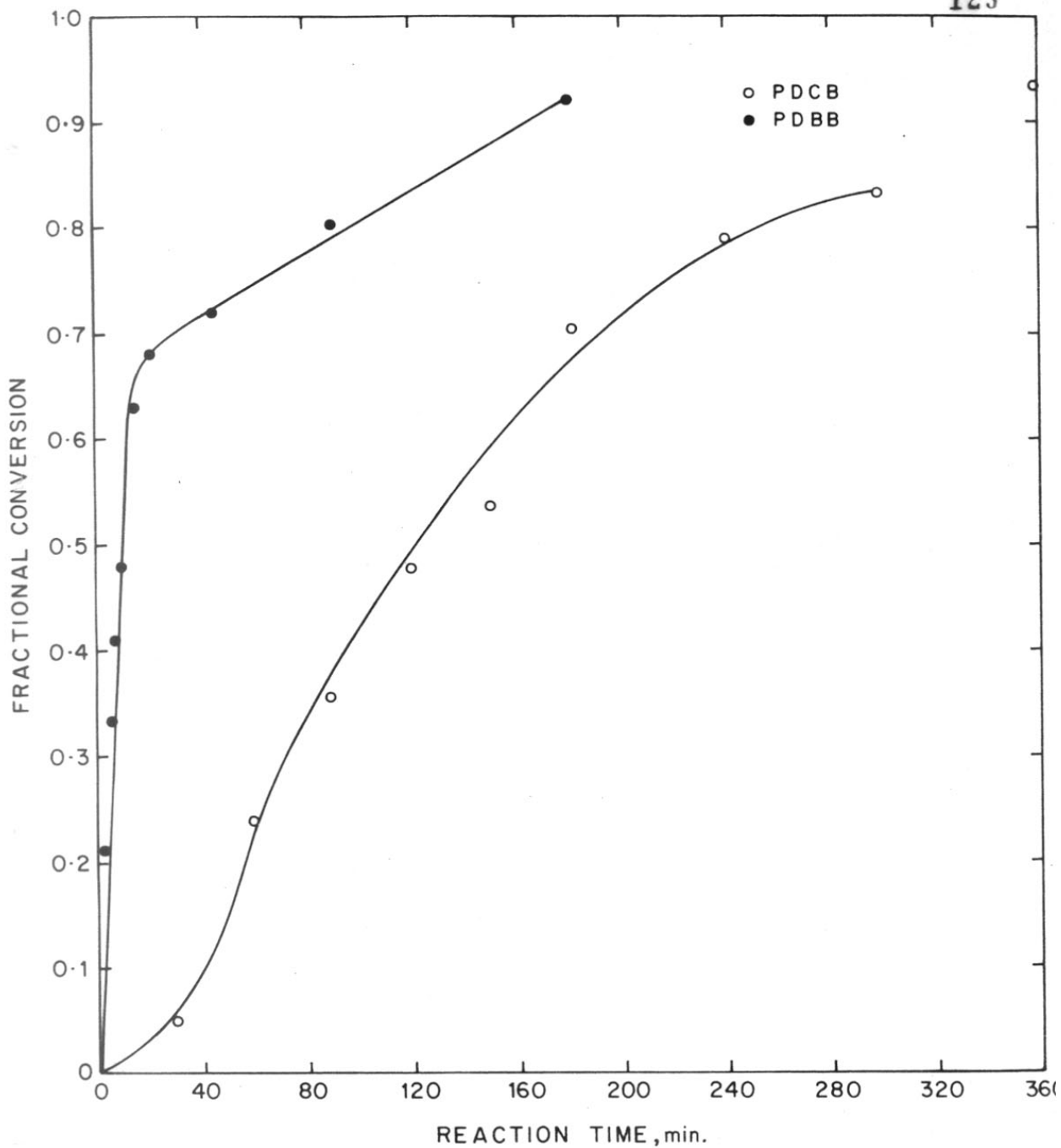


FIG.35: FRACTIONAL CONVERSION - REACTION TIME DATA

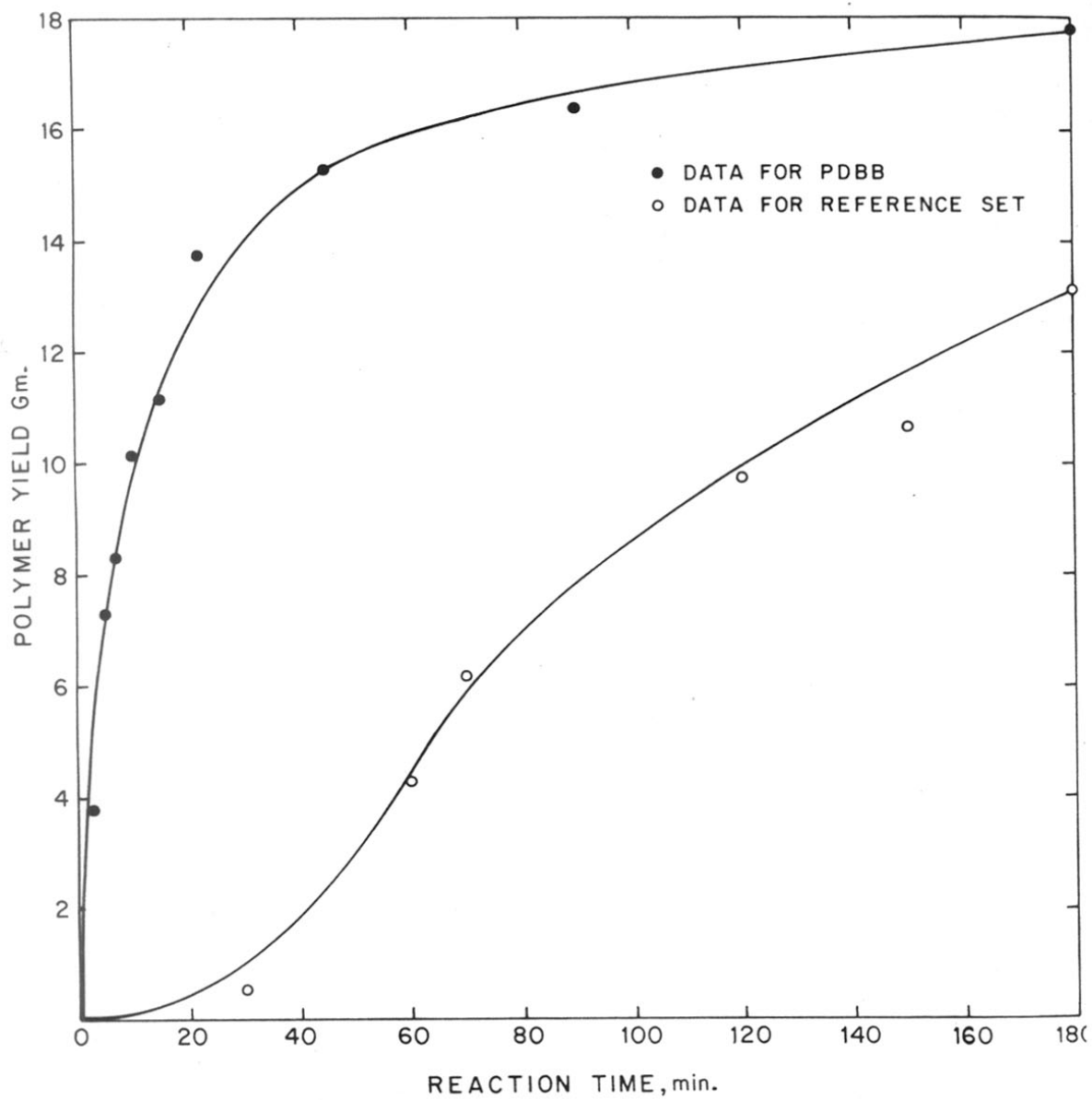


FIG.36 : POLYMER YIELD-REACTION TIME DATA

The data on PDBB-sodium sulfide systems was subjected to the same regression analysis as for PDCB. Two regions of linearity were again observed for this system. The data on  $1/(1-p)$  and  $\frac{(1+r)}{(1+r-2rp)}$  (for non-stoichiometric ratio of reactants) as a function of reaction time are presented in Figures 37 and 38. The overall reaction rate and the specific rate constant data obtained by regression analysis are presented in Table 18. The data for the reference set are also presented in the table. In the case of the reaction between PDCB and sodium sulfide, the initial rate of reactions was slow till 50 percent conversion, followed by a faster rate from 50 to 90 percent conversion. On the other hand, the reaction between PDBB and sodium sulfide exhibited an initial fast reaction upto 50 percent conversion, followed by a relatively slower rate equivalent to that observed in the range beyond 50 percent for the system PDCB-sodium sulfide.

This dramatically different behaviour between the two systems could be related to a number of factors including the relative rates of substitution of the two halide groups. The presence of chloro group at a position para to the substitution center retards the rate of nucleophilic substitution, whereas the bromo group relatively enhances the rate in the initial stage to a conversion of about 50 percent. After this range of conversion, when on a statistical average one of the two halide groups on the same benzene ring would be substituted, the rates of the two reactions were identical. Also on a statistically averaged situation, after 50 percent conversion, the position para to the substitution point in both the systems is -SNa group. The presence of bromo group enhances the rate relative to the -SNa groups as seen by the relative rates till 50 percent conversion

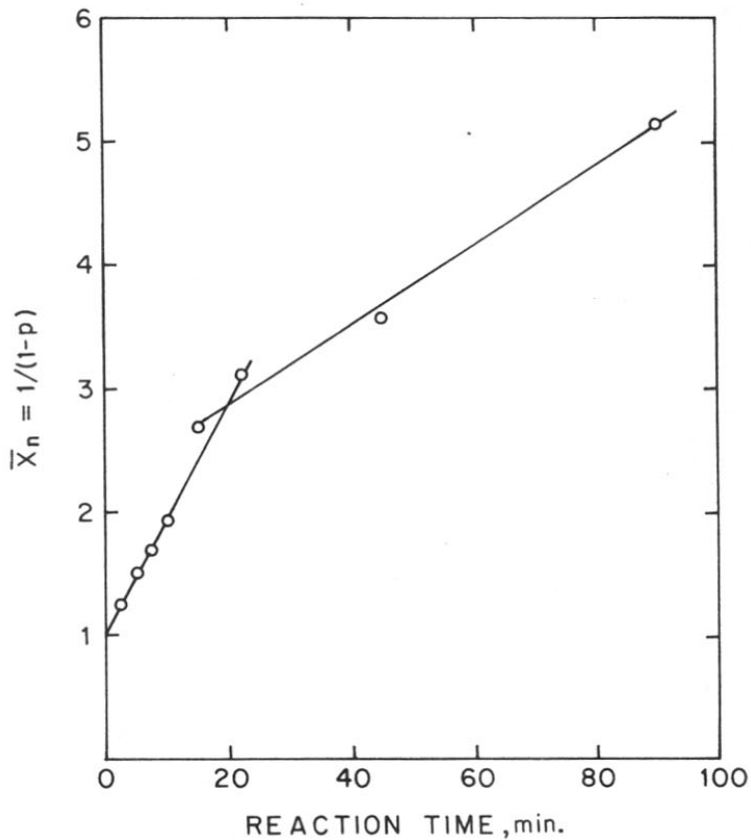


FIG.37: PLOT OF THE NUMBER-AVERAGE DEGREE OF POLYMERIZATION AS A FUNCTION OF REACTION TIME, ASSUMING STOICHIOMETRIC EQUIVALENCE OF THE REACTANTS

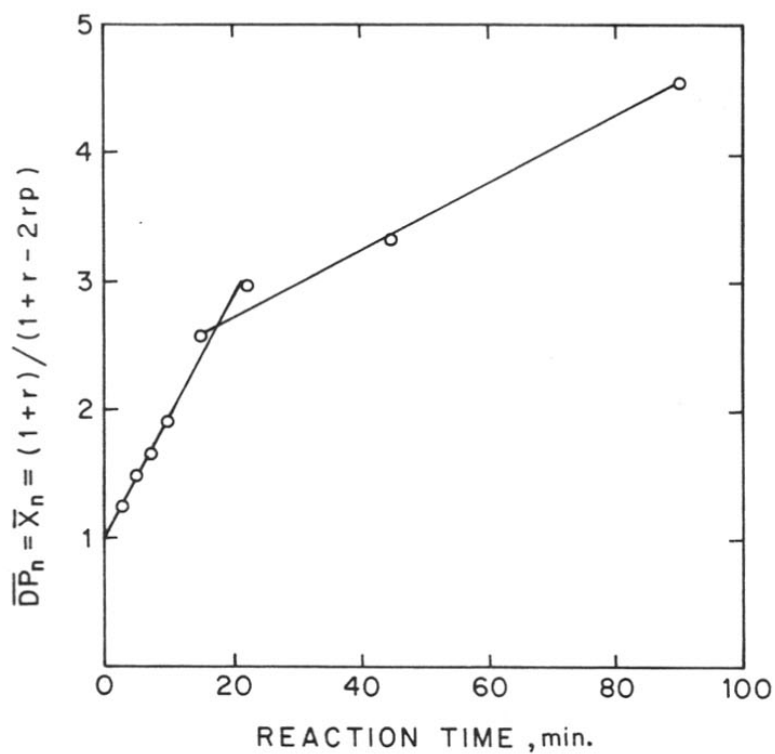


FIG.38: PLOT OF  $\overline{DP}_n$  AS A FUNCTION OF REACTION TIME. PLOT ASSUMING STOICHIOMETRIC NONEQUIVALENCE BETWEEN THE TWO REACTANTS.

in comparison to that observed after 50 percent conversion. The initial rate in the system PDBB-sodium sulfide was found to be an order of magnitude faster than the system PDCB-sodium sulfide.

The theoretical yield of polymer at 100 percent conversion was calculated as given in section 4.2.2. The value for chlorine was replaced with for bromide. The theoretical yield (TY) thus becomes,

$$\begin{aligned} \text{TY} &= 0.1923 \times \text{C}_6\text{H}_4\text{S} + 0.01145 \times \text{Br}_2 \\ &= 0.1923 \times 108.15 + 0.01145 \times 159.82 \\ &= 21.627 \text{ gms} \end{aligned}$$

The fractional yield-reaction time data are represented in Figure 39 along with the data in that for the reference set. The fractional yields are larger as compared to the reference set.

The intrinsic viscosity of the polymers formed were evaluated in 1-chloronaphthalene. The procedure followed was identical to that for the reference set. The evaluated data are presented in Table 18. The intrinsic viscosity values are much lower than that observed for the reference set indicating that the molecular weights of these samples would be very low. The microanalysis data could not be obtained to definitely prove this point. The relative values of intrinsic viscosity with the reference set are shown in Figure 40. While a steady increase in viscosity was noted in reference set, the values in the PDBB system remained steady till a conversion of about 50 percent. The increase with conversion was gradual till 80 percent conversion. The value again levelled off after this stage indicating that the maximum molecular weight perhaps is achieved in this range.

TABLE 18  
COMPARISON OF THE REACTION RATES OF THE TWO SYSTEMS  
PDCB-SODIUM SULFIDE AND PDBB-SODIUM SULFIDE

System	Conversion range, %	Rate, $\text{m l}^{-1} \text{ s}^{-1}$	Specific reaction rate, $\text{l m}^{-1} \text{ s}^{-1}$
PDCB sodium sulfide	upto 50 50-90	$3.11 \times 10^{-5}$ $3.85 \times 10^{-5}$	$8.11 \times 10^{-4}$ $4.16 \times 10^{-3}$
PDBB sodium sulfide	upto 50 50-92	$3.21 \times 10^{-4}$ $3.87 \times 10^{-5}$	$8.68 \times 10^{-3}$ $4.18 \times 10^{-3}$

Reaction conditions:

Reaction temperature = 195°C

Molar ratio of reactants = 0.9422

NMP = 100 ml.



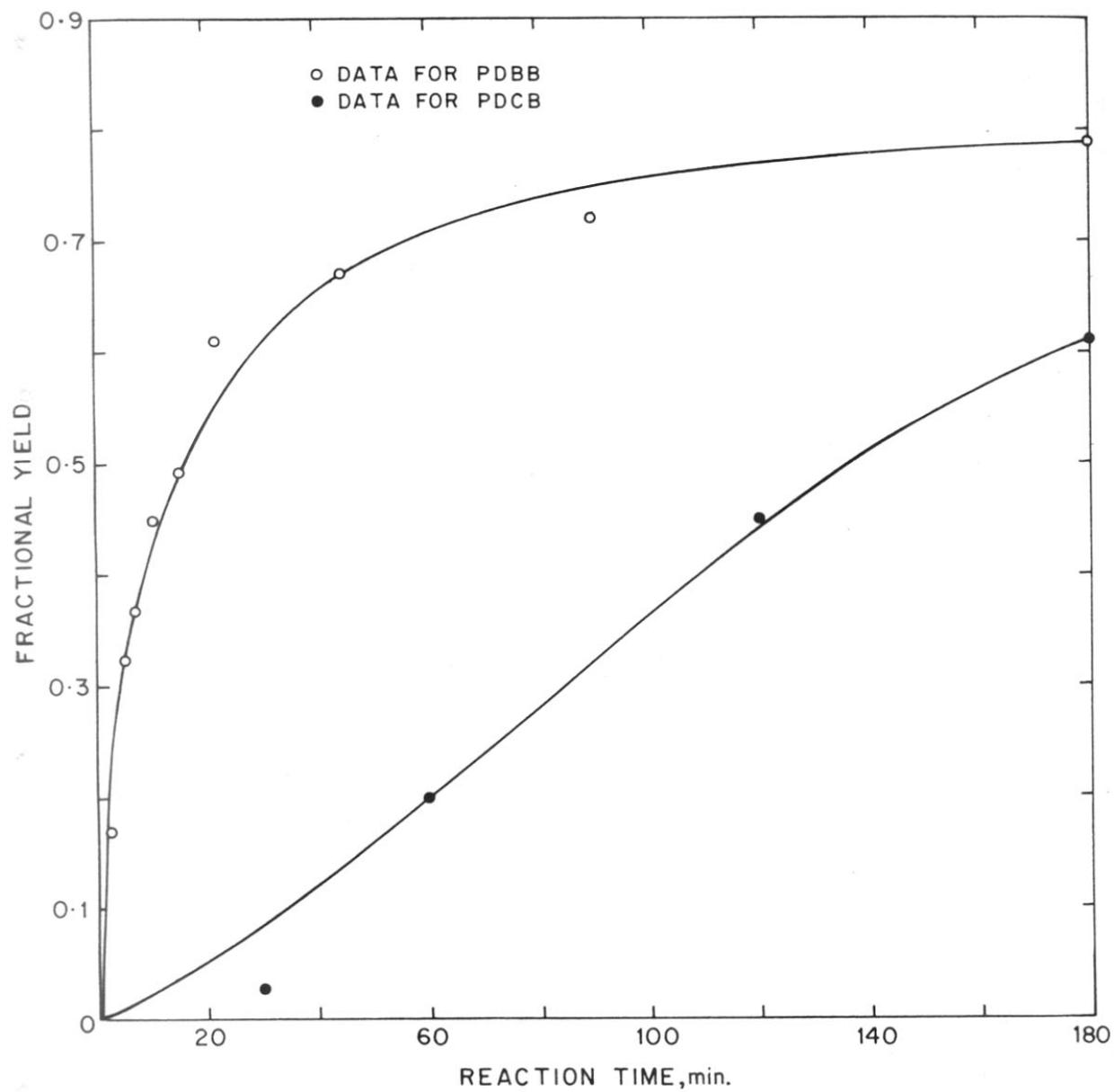


FIG.39 : FRACTIONAL YIELD-REACTION TIME DATA

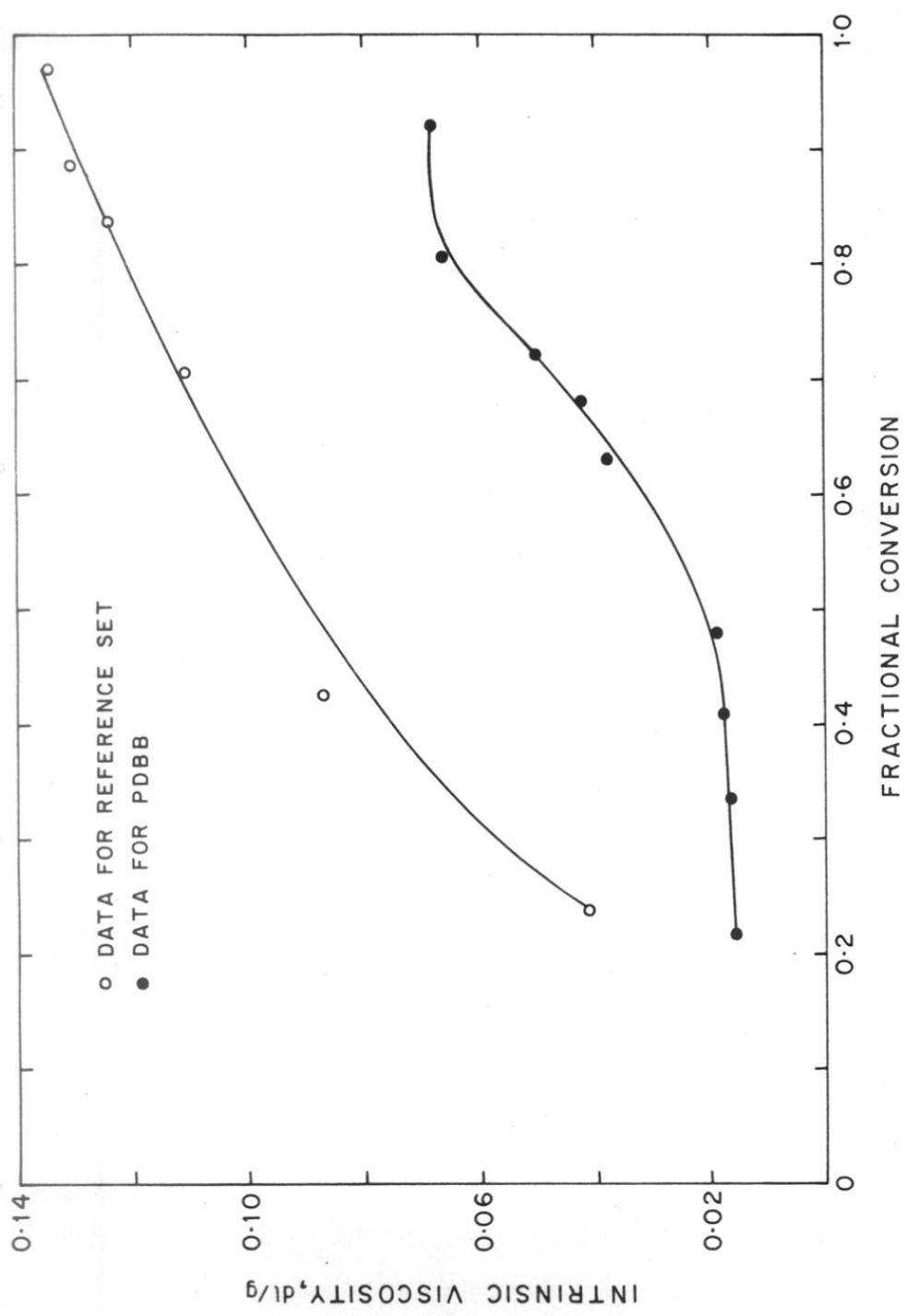


FIG.40: INTRINSIC VISCOSITY - FRACTIONAL CONVERSION DATA

The melting points of the samples obtained in the PDBB system were determined by capillary method. The variation of the melting point with reaction time is shown in Figure 41 (Table 19). The values for the reference set are also included in the plot. The melting point increase in the system with PDBB was gradual and were consistently lower than the reference set. The intrinsic viscosity values also followed a similar trend. These indicate that PPS synthesized with PDBB reach a maximum molecular weight around 180 minutes of reaction time and that the molecular weights are lower than those obtained by using PDCB under identical conditions.

To summarize, the kinetic studies of the reaction between PDCB and sodium sulfide at a molar ratio of 1.0641:1 were conducted at 195°C in NMP as the reference set. The analysis of the data indicated that the formation of polyphenylene sulfide follows a second order kinetics, exhibiting two distinct regions of constant rates. In the first region upto 50% conversion the rate is slower, followed by a region wherein the rate constant is approximately five times faster. The condensation reaction between PDCB and sodium sulfide to form PPS exhibited the following features which are different from the conventional polycondensation reactions:

- (a) Unreacted monomers were present at conversions as high as 97%.
- (b) Polymeric species were formed even at very low conversion (5%).
- (c) The polymer precipitates out during the course of the reaction but continues to grow in the solid state with increase in reaction time.
- (d) The melting point of the polymer formed increased rapidly till a reaction time of 3 hours. At high reaction times no significant increase in the melting point was noted.

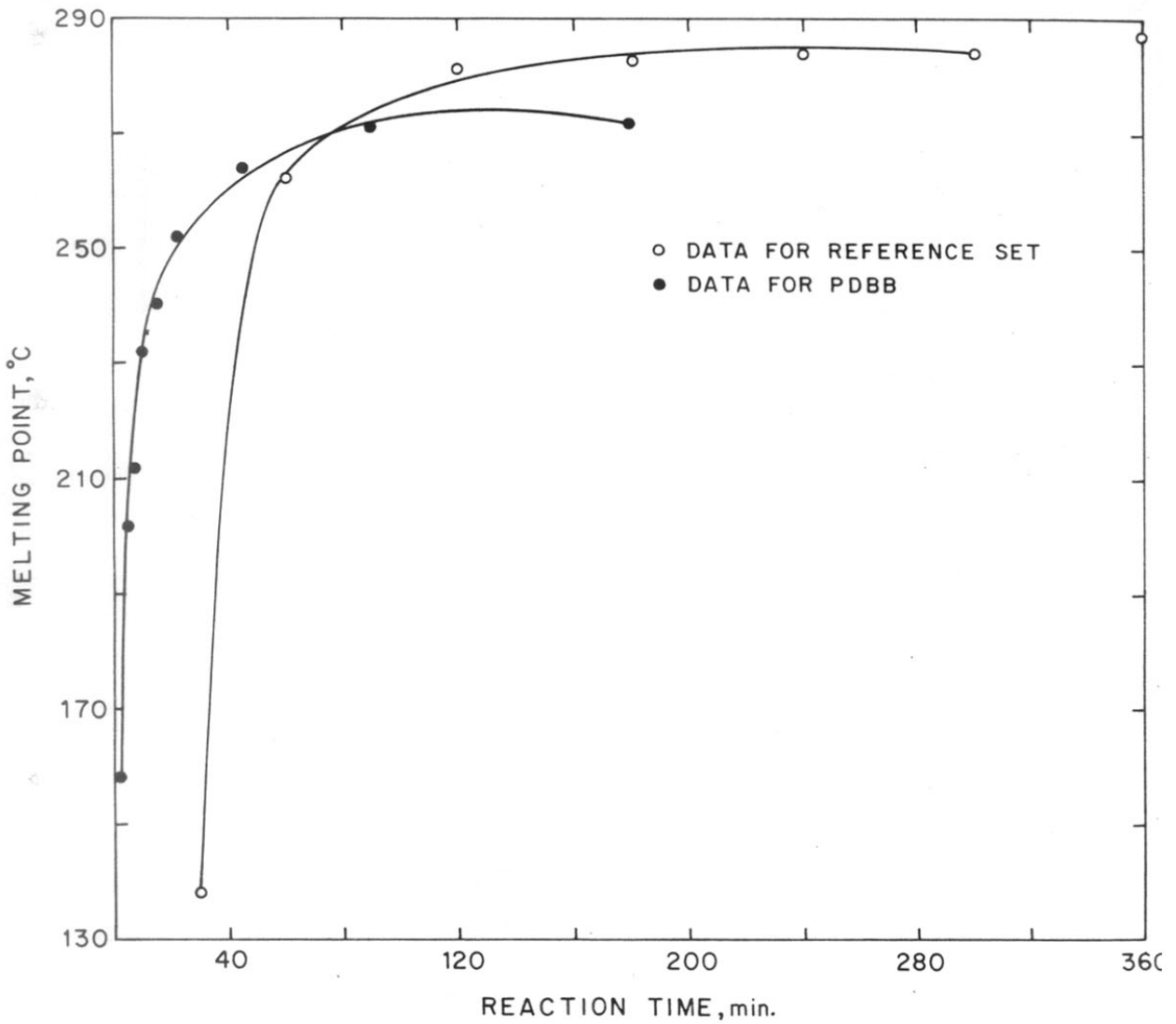


FIG.41: MELTING POINT - REACTION TIME DATA

TABLE 19  
INTRINSIC VISCOSITY M.P. DATA AT DIFFERENT REACTION TIMES

Temperature = 195°C , Solvent = 1-chloronaphthalene

Reaction time, min.	Polymer concentration, gm/dl	Relative viscosity	$[\eta]^a$ dL/g	$[\eta]^b$ dL/g	MP, °C
2.5	4.00	1.0645	0.0158	0.0158	158
5	4.14	1.0693	0.0164	0.0164	202
7	4.00	1.0706	0.0173	0.0173	212
10	4.03	1.0774	0.0187	0.0188	252
15	4.04	1.1630	0.0383	0.0385	241
22	4.15	1.1830	0.0423	0.0424	252
45	4.19	1.2280	0.0508	0.0509	264
90	3.97	1.2880	0.0667	0.0666	271
180	3.945	1.2942	0.0685	0.0683	272

$$[\eta]^a = \frac{2}{c} \sqrt{\eta_{Sp} - \ln \eta_r}$$

$$[\eta]^b = \frac{\eta_{Sp}}{1 + K \eta_{Sp}} \quad K = 0.302$$

The effect of physical parameters such as reactor type, the speed of agitation and the extent of dilution on yield conversion and intrinsic viscosity of the polymer were investigated. The speed of agitation had a marginal effect on the yield, conversion and intrinsic viscosity. The fractional conversion at 6 hours dropped from 0.88 to 0.67 when the speed was reduced from 660 rpm to 0; the fractional yield was reduced from 0.88 to 0.74, whereas the intrinsic viscosity reduced by 30 percent. On the other hand, the extent of dilution seems to have a much more significant effect on the kinetics and structure development in PPS formation. When the dilution factor was increased from 1 to 10, the fractional yield at 6 hours decreased from 0.88 to 0.45, the fractional conversion decreased from 0.88 to 0.67, whereas the intrinsic viscosity exhibited a steep drop from 0.13 to 0.05 dL/g.

The kinetic experiments were conducted in two types of reactors, namely, stainless steel and Teflon. Little change in the kinetics of the reaction was observed, other than the fact that the initial specific reaction rate in the Teflon reactor was extended upto 75 percent versus 50 percent in the stainless steel reactor. The yield values and the reaction rates were comparable. The major difference between the two reactors is in the type of agitation, the agitation in the stainless steel reactor being more effective. The other difference in the experiments was the mode of addition of reactants.

The effect of chemical parameters on the kinetics and structure development in PPS formation were studied by conducting the following experiments.

TABLE 3.4.3

## POLYMER YIELD - CONVERSION RATE DATA

		Reference set	Teflon	SPCTP	Excess PDCB	PDBB
Polymer yield, gm.	3 hrs	13.22	13.7	16.71	18.67	10.16 (10 min.)
	6 hrs	19.05	18.5	19.70	20.1	17.82 (180 min.)
Fractional conversion	3 hrs	0.7056	0.6165	0.7957	0.8586	0.4810 (10 min.)
	6 hrs	0.8867	0.8674	0.9105	0.9254	0.9194 (180 min.)
Regions of linearity	I	upto 50%	upto 75%	upto 36%	-	upto 50
	II	beyond 50%	beyond 75%	beyond 36%	-	beyond 50
Rates $\text{ml}^{-1} \text{s}^{-1}$	I	$3.00 \times 10^{-5}$	$4.67 \times 10^{-5}$	$2.75 \times 10^{-5}$	-	$3.21 \times 10^{-4}$
	II	$3.85 \times 10^{-5}$	$2.26 \times 10^{-5}$	$8.34 \times 10^{-5}$	-	$3.87 \times 10^{-5}$
$[\eta]$ at 6 hrs dL/g		0.13	0.13	0.117	0.085	0.068 (180 min.)

- a. addition of 1.1 percent (by weight) of sodium parachlorothiophenoxide (SPCTP)
- b. use of 100% excess of PDCB
- c. reaction of sodium sulfide with paradibromobenzene (PDBB) in place of paradichlorobenzene (PDCB).

The details of the experimental data are summarized in Table 3.5.1. Both the addition of SPCTP and use of excess PDCB were found to improve the yield significantly.

However, the intrinsic viscosity of the polymer was considerably lower. Also, in the case of experiments with SPCTP, the initial region of slower rate was shortened to about 36 percent versus 50 percent in the reference set. Therefore, it is concluded that the addition of SPCTP or the use of excess PDCB enhances the rate of initiation, thereby probably leading to the formation of a greater amount of oligomers.

The reaction between  $\text{Na}_2\text{S}$  and PDBB exhibited a significantly higher rate (by a factor of 10) in the initiation region upto 50% conversion, relative to the reference set with PDCB. The reaction rates in the second region beyond 50 percent conversion were comparable for both the reactions involving PDBB and PDCB. The reaction between  $\text{Na}_2\text{S}$  and PDBB resulted in a lower yield of the polymer and a lower intrinsic viscosity at comparable conversion, relative to the reaction with PDCB. Therefore, it is concluded that the formation of the intermediate species is faster with PDBB, because bromine is a better leaving group from a mechanistic view point.

The reactions followed a second order kinetics in all the cases, irrespective of the changes in the physical or chemical parameters.





**CHAPTER 4**  
**THERMAL CHARACTERIZATION**

#### 4. THERMAL CHARACTERIZATION STUDIES

The thermal behaviour of the polymer formed at different conversions was evaluated by Differential Scanning Calorimetry (DSC) and thermogravimetric analysis (TGA). The results were analysed to elucidate the development of polymer structure with polymerization time. The molecular weight of the polymer formed increases with reaction time as illustrated by microanalysis and solution viscosity measurements. Thus, the analysis brought out the variation of thermal characteristics with molecular weight and molecular weight distribution. The thermal stability and DSC results of PPS samples synthesized were compared with the commercial polymer Ryton, grade V-1.

##### 4.1 Differential Scanning Calorimetry (DSC)

These studies were carried out to elucidate the changes in physical structure as a function of reaction time. The experimental details are presented in the experimental section 2.7.4. The instrumental settings were kept identical for all the samples. The samples were subjected to three heating and cooling cycles. The first heating scan of the polymer sample represents the physical structure of the polymer as precipitated in the reaction mixture. It would thus signify the interaction between the precipitation and the continuing polymerization at the solid-liquid interface and its influence on the crystallite size and crystallite size distribution. Once the polymer is heated beyond the melting point in the first scan, the as-precipitated morphology is destroyed. The thermal parameters derived from the subsequent cooling and heating scans would therefore represent the effect of molecular weight and molecular weight distribution

of the polymer samples, as crystallized from melt.

The DSC thermograms of the polymer samples at different reaction times are shown in Figures 1 to 9. The thermal behaviour of the samples is discussed below with reference to the respective DSC scans. The DSC scan of commercial sample Ryton V-1, is shown in Figure 51.

(a) 1/2 hour sample

The DSC scan is shown in Figure 42. The initial melting peak was sharp with high  $\Delta H_m$  in the first heating cycle. In the subsequent heating scans, the  $\Delta H_m$  was found to reduce significantly. The melting peaks were also not as sharp compared to the first heating scan. This indicates that the melt crystallized sample has considerably lower crystallinity than the as-precipitated product. The cooling scans did not reveal a sharp crystallization peaks. The average particle size was in the range of 0.5 microns.

(b) 1 hour sample

The DSC scan is shown in Figure 43. In the first heating scan, three multiple melting peaks were observed for this sample. The multiple peaks, however disappear in the subsequent scans. This indicates that the morphology of the as-precipitated polymer is different from the melt crystallized sample. The as-precipitated sample appeared to have three distinct crystallite size distributions. The average size of the particles was 1.1 microns and the total number of particles were less than that for 1/2 hour reaction. Unlike the 1/2 hour reaction product, the 1 hour sample exhibited a clear crystallization peak in the cooling scans with

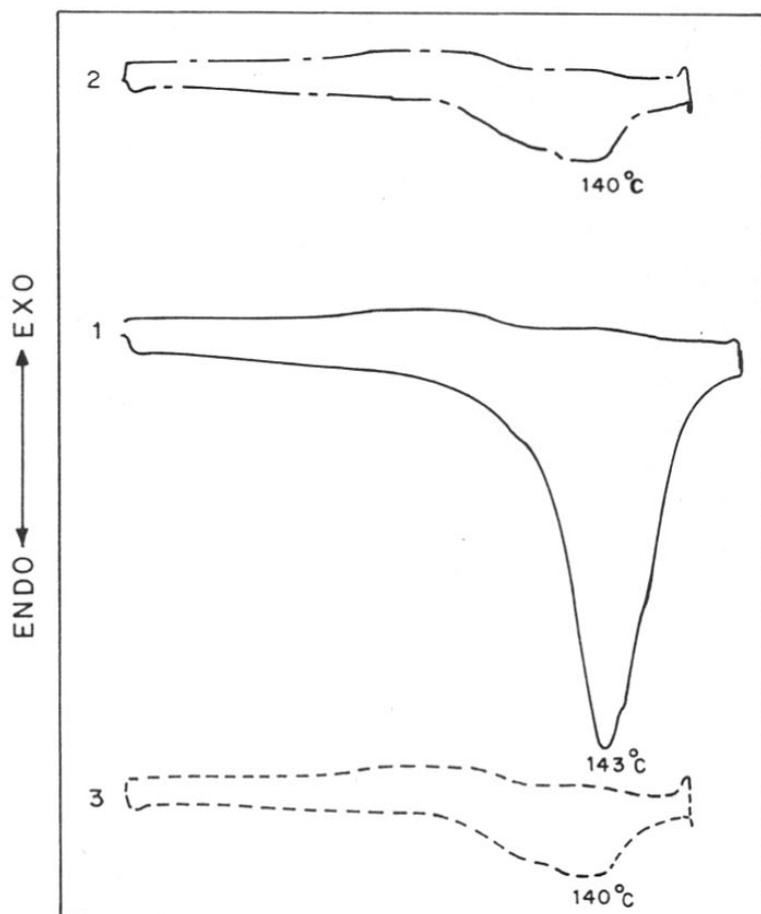


FIG.42: DSC SCAN - 1/2 hr SAMPLE

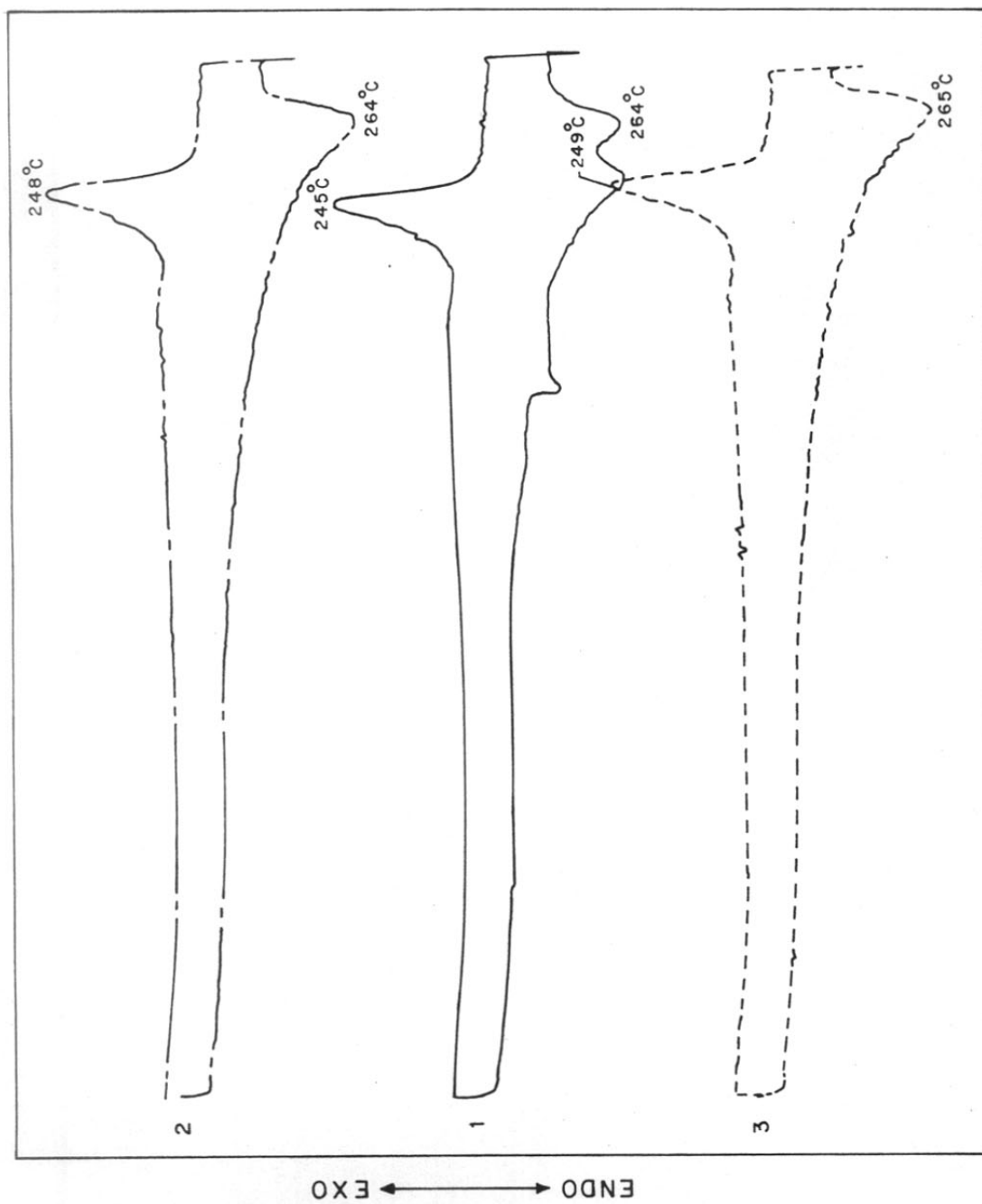


FIG.43: DSC SCAN - 1 hr SAMPLE

a broad shoulder. The crystallization occurred over a broad temperature range of 56°C (256 °C to 240°C). This would lead to a broad crystallite size distribution as reflected in the broad melting range of 66°C (from 210°C to 278°C).

(c) 2 hour sample

The DSC scan is shown in Figure 44. This scan does not exhibit multiple peaks in the first heating scan. However, the melting transition in the first scan suggested of a different shape in the as-precipitated sample. The second and third heating scans show a single peak for the melting transition. This suggests the existence of different morphologies before and after the polymer is heated through the melting range. The cooling scans of the samples follow the same trend as for the 1 hour sample including a sharp crystallization peak and a broad crystallization range.

(d) 3 hour sample

The DSC scan shown in Figure 45 for this sample, exhibits two multiple peaks during the first heating cycle. This indicates a bimodal crystallite size distribution in the as-precipitated sample. The cooling scan for this sample exhibits a crystallization behaviour similar to the earlier sample.

(e) 4 hour sample

The DSC scan is shown in Figure 46. This sample also exhibits two melting peaks suggestive of a bimodal crystallite size distribution. The melting transition peaks are however sharper in the as-precipitated state. The second and third heating scans shows a single peak. In the

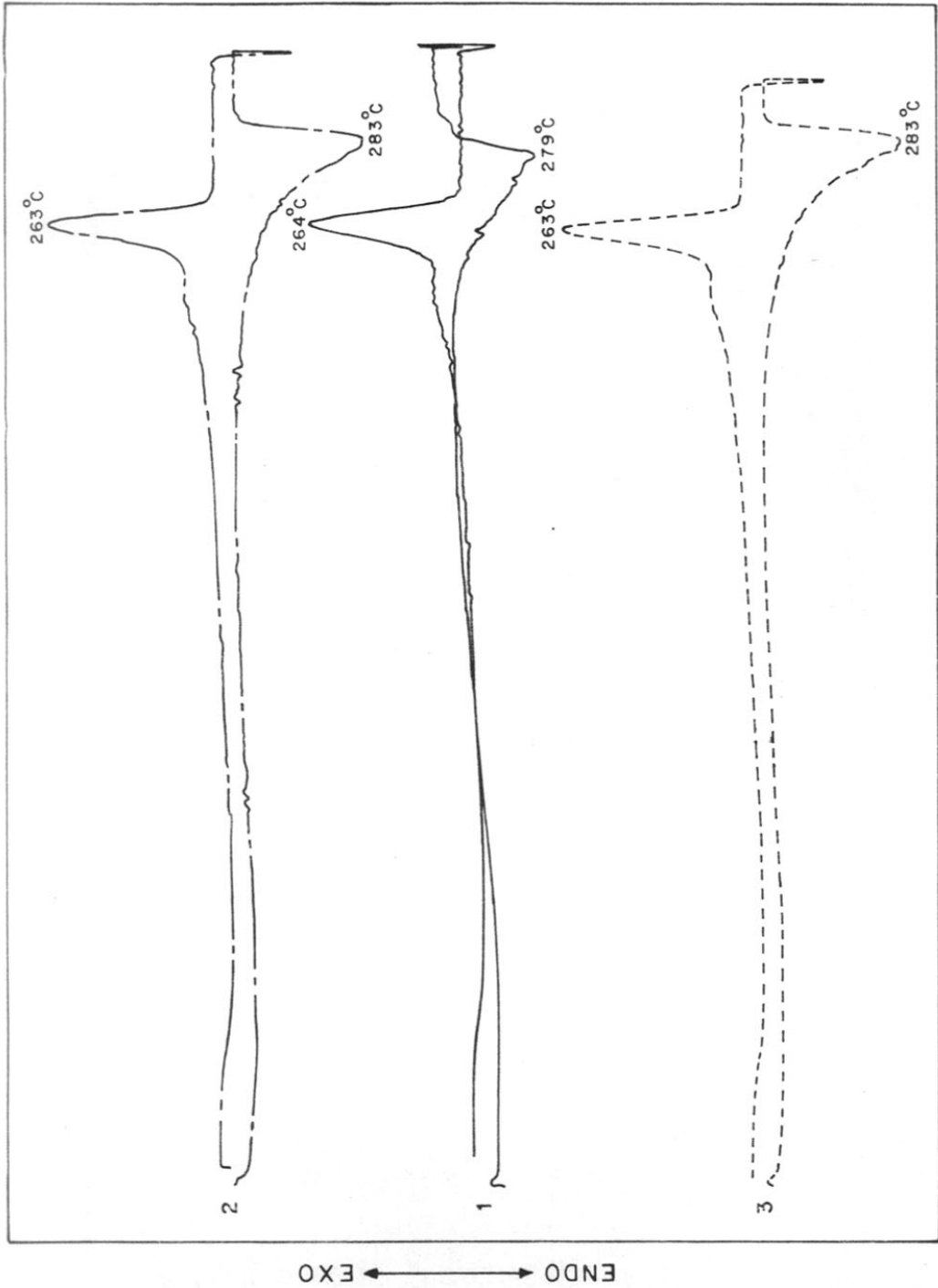


FIG.44 : DSC SCAN - 2 hr SAMPLE

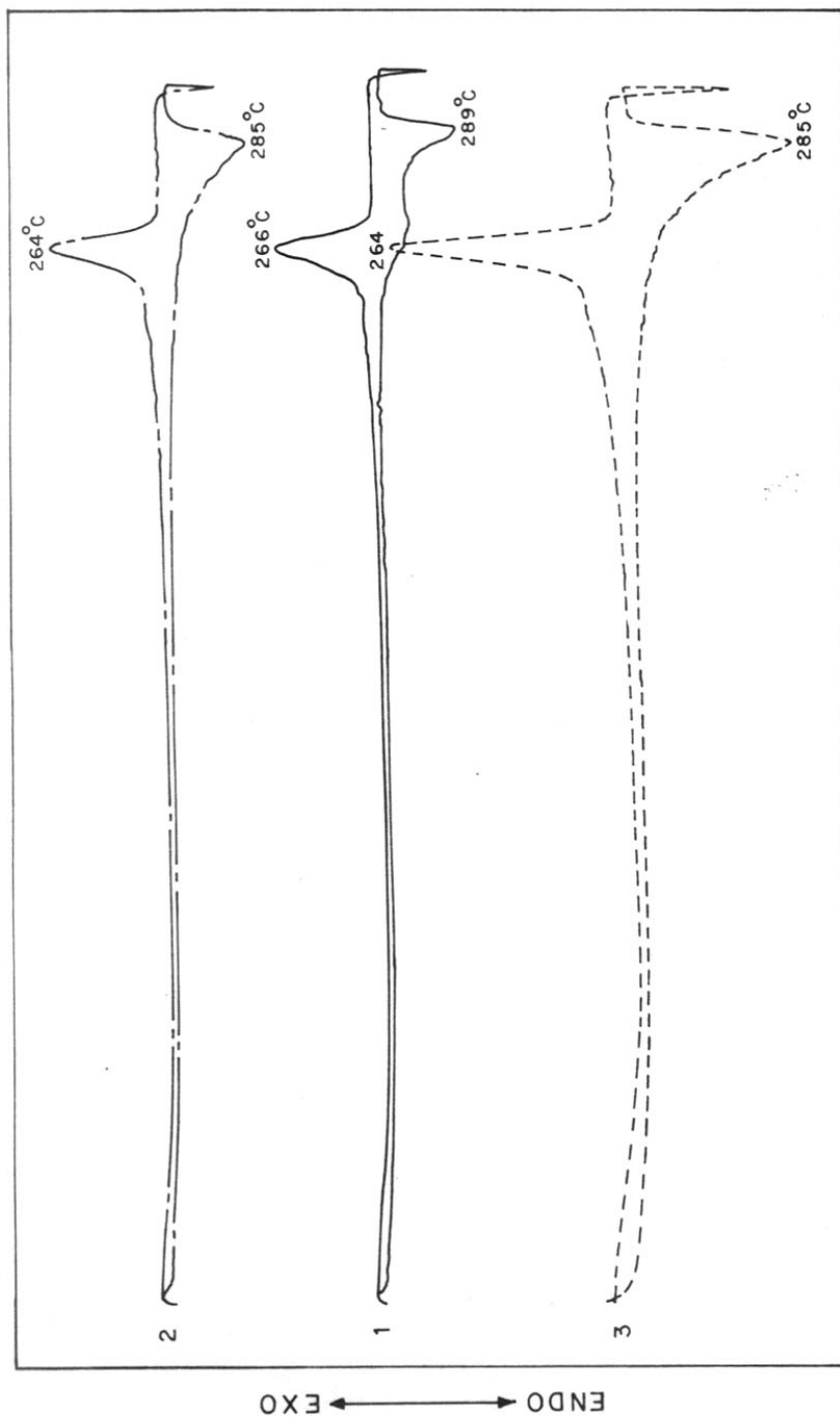


FIG.45 : DSC SCAN - 3 hrs SAMPLE



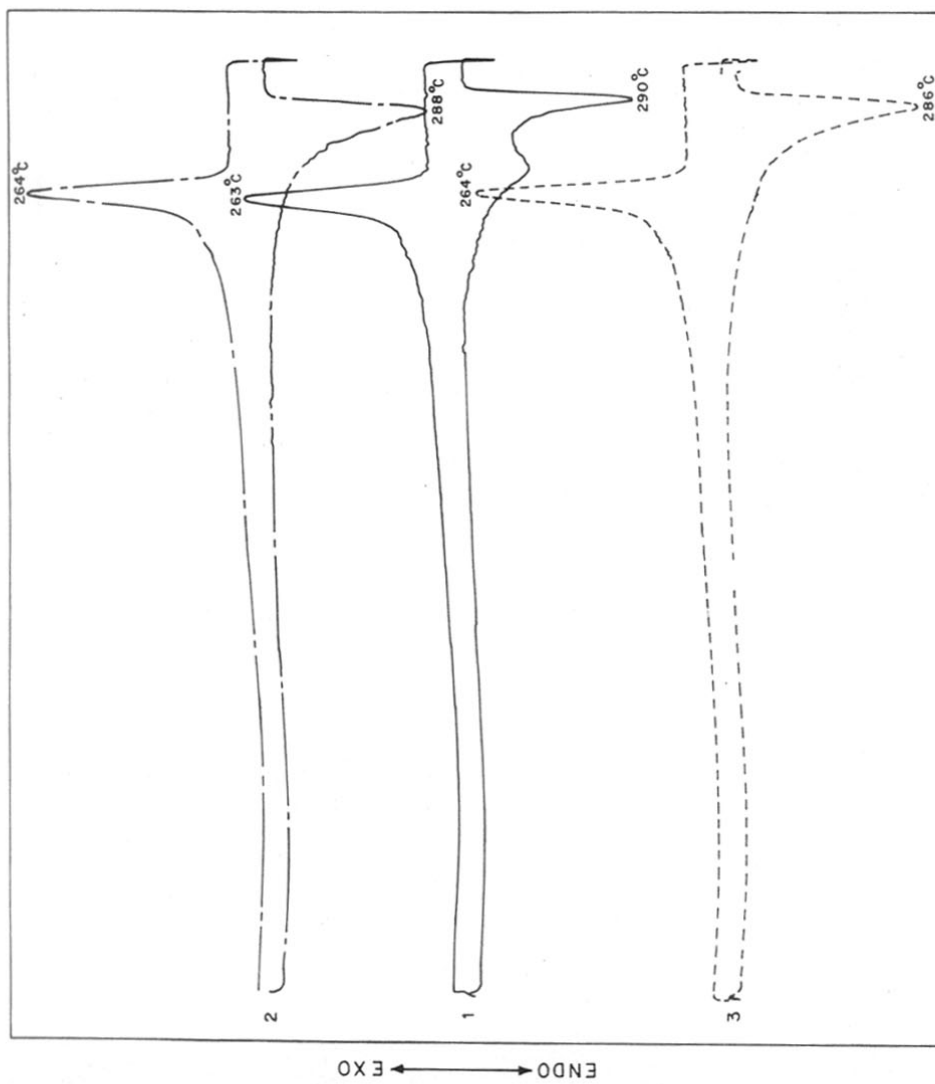


FIG. 46: DSC SCAN - 4 hrs SAMPLE

cooling scans, the crystallization behaviour is identical to the 3 hour sample.

(f) 5 hour sample

The DSC scan is shown in Figure 47 . The behaviour of this sample is identical to that of 4 hour sample, both in the heating and cooling cycles.

(g) 6 hour, 7 hour and 10 hour samples

The DSC scans of these samples are shown in Figures 48,49 and 50 respectively. The scans in the first heating cycle in the as-precipitated state do not show clear multiple peaks. However, the melting peaks exhibit a shoulder which disappears in the second heating cycle. This is suggestive of a predominantly single crystallite size distribution unlike the 3,4 and 5 hour samples. The particle size increases as a function of reaction, but the total number of particles decreased with increase in reaction time. The morphology details are discussed in section 5.

The cooling scans of these samples exhibit an identical crystallization behaviour. The crystallization range was also much narrower as compared to the short reaction time products.

(h) Commercial polymer sample

The DSC scan of the commercial polymer, Ryton grade V-1 is shown in Figure 51. The scan shows no difference in the first, second and third heating scans. This is due to a different morphology of the polymer as the sample was not in the as-precipitated state. It also had a different thermal history. The cooling scan exhibiting the crystallization

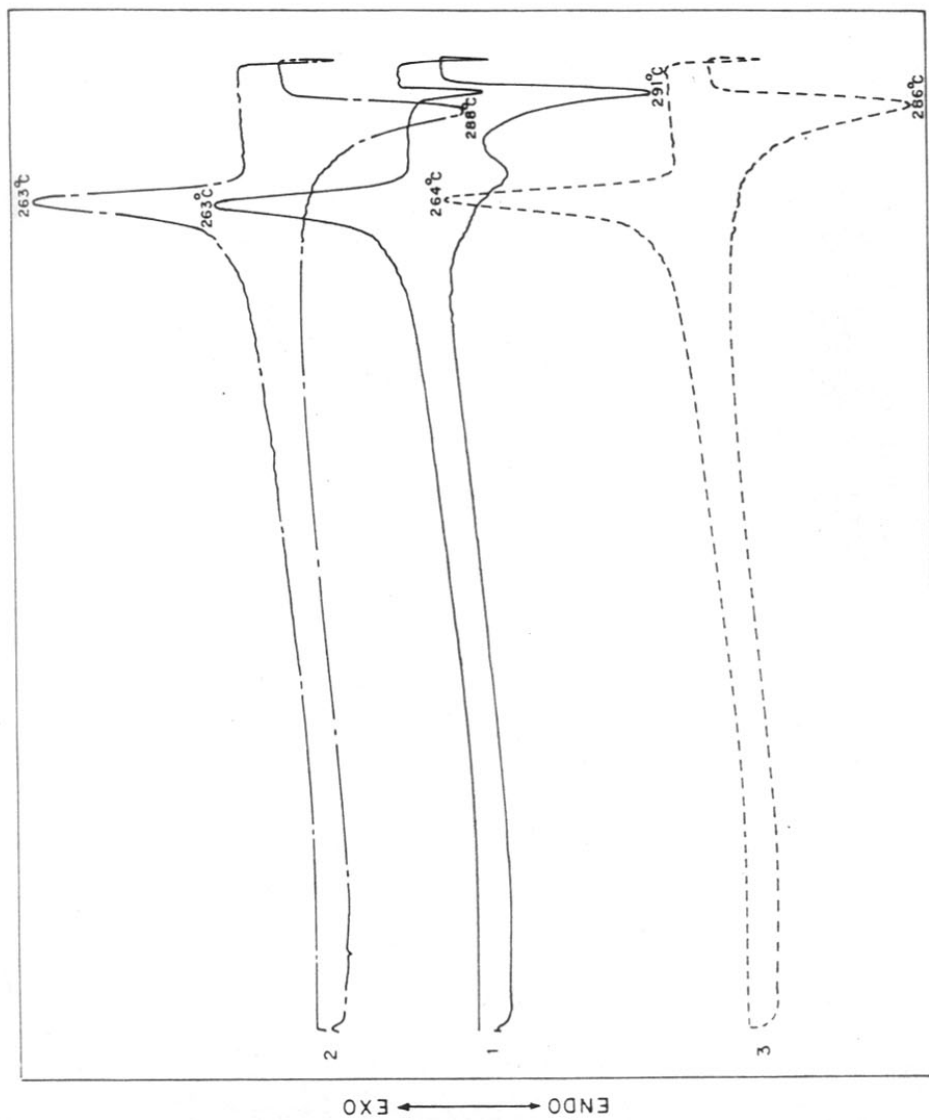


FIG.47 : DSC SCAN - 5 hr SAMPLE

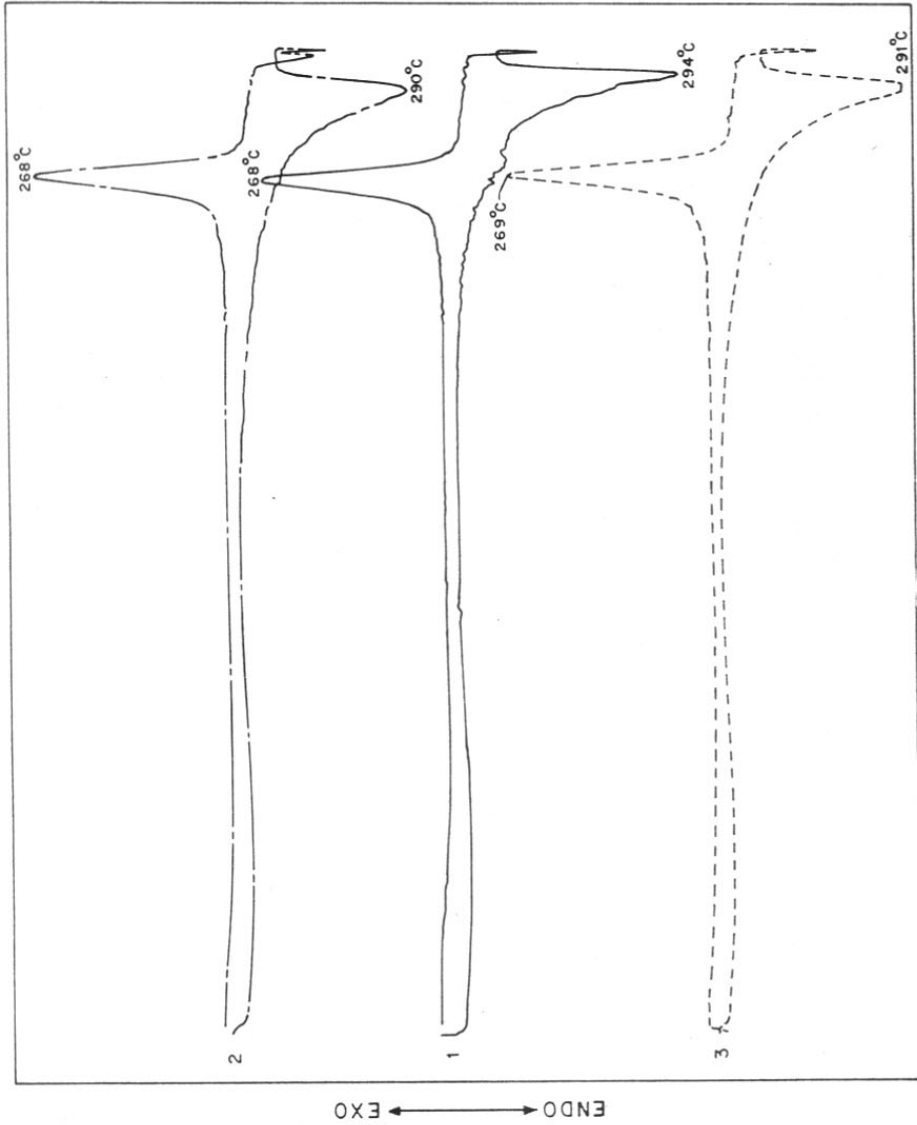


FIG.48 : DSC SCAN - 6hr SAMPLE

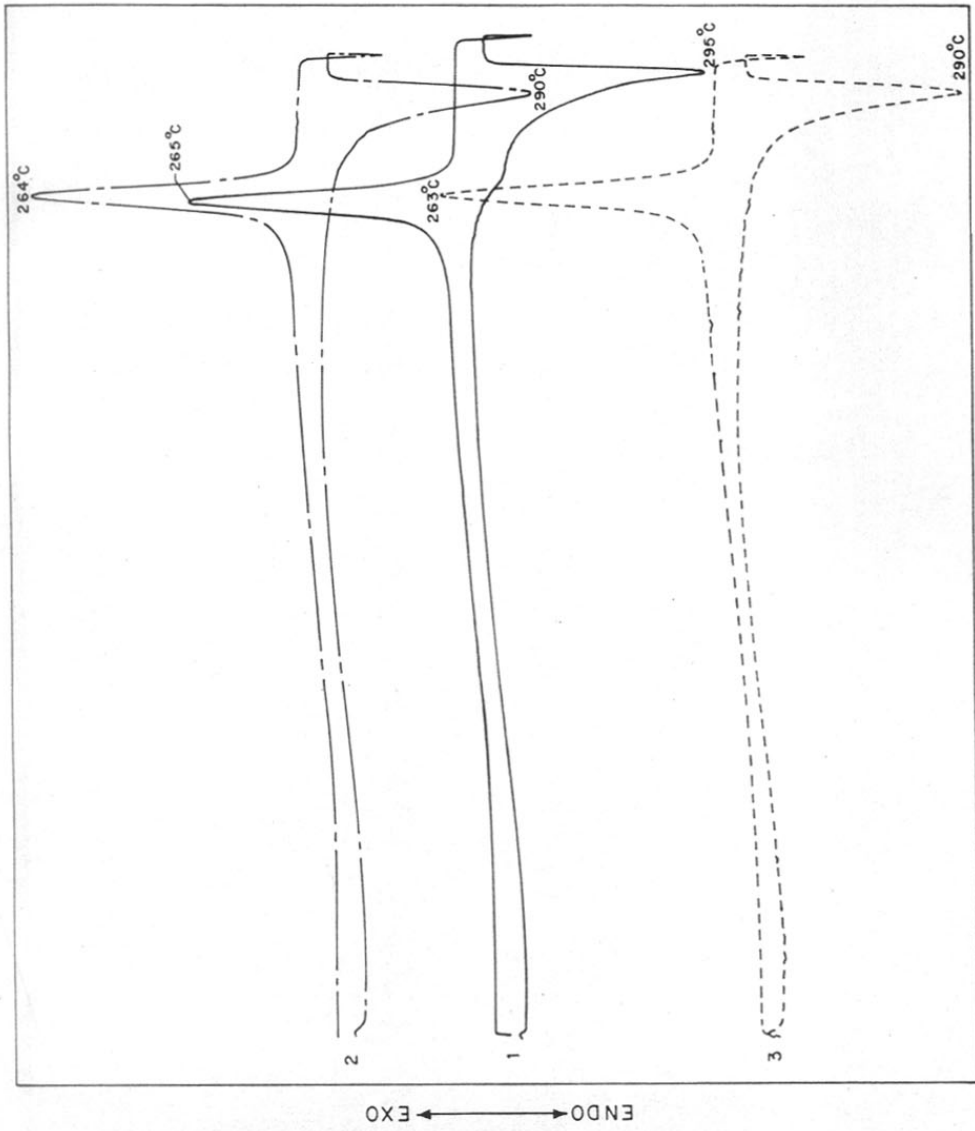


FIG. 49: DSC SCAN - 7 hr SIMPLE

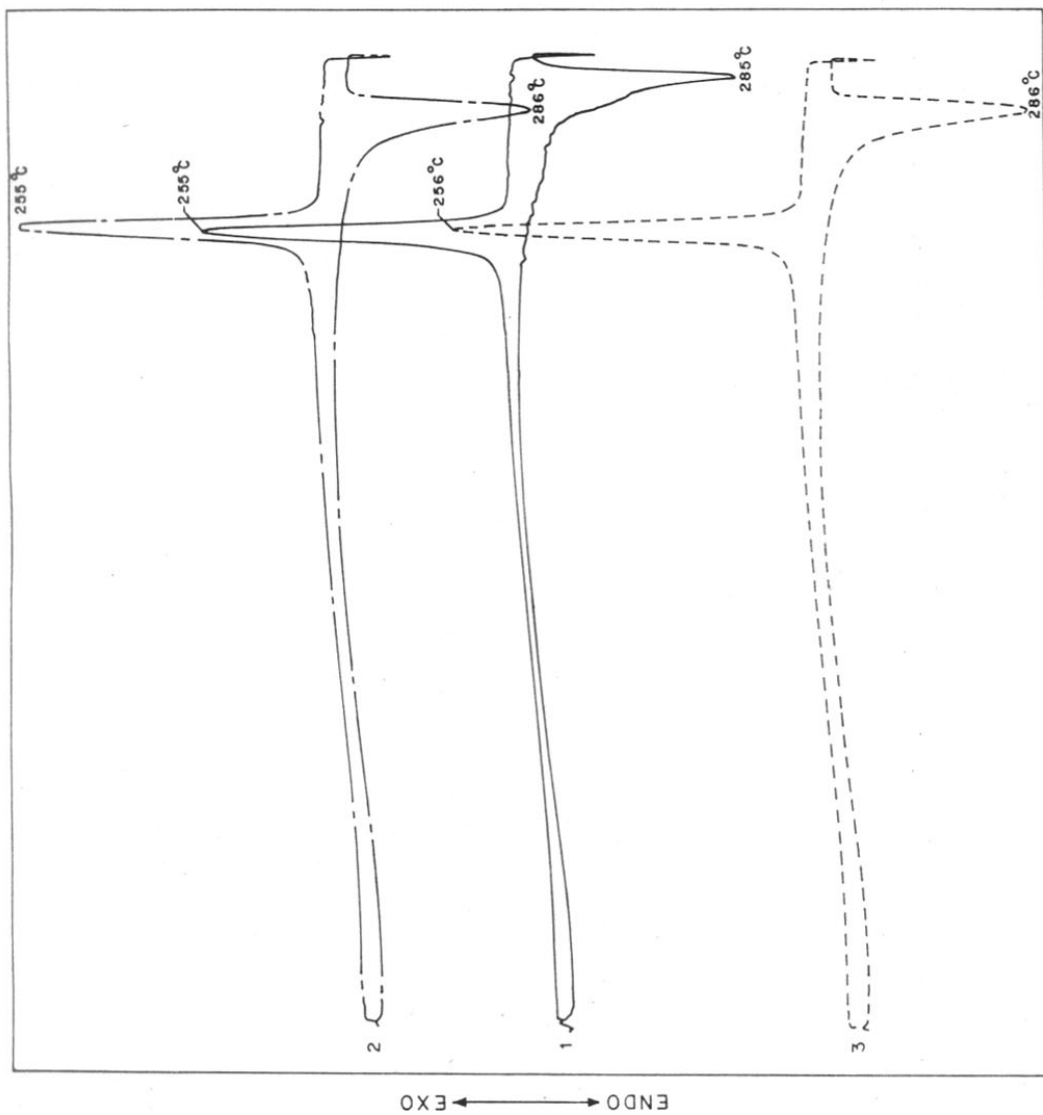


FIG.50 : DSC SCAN-10hr SAMPLE

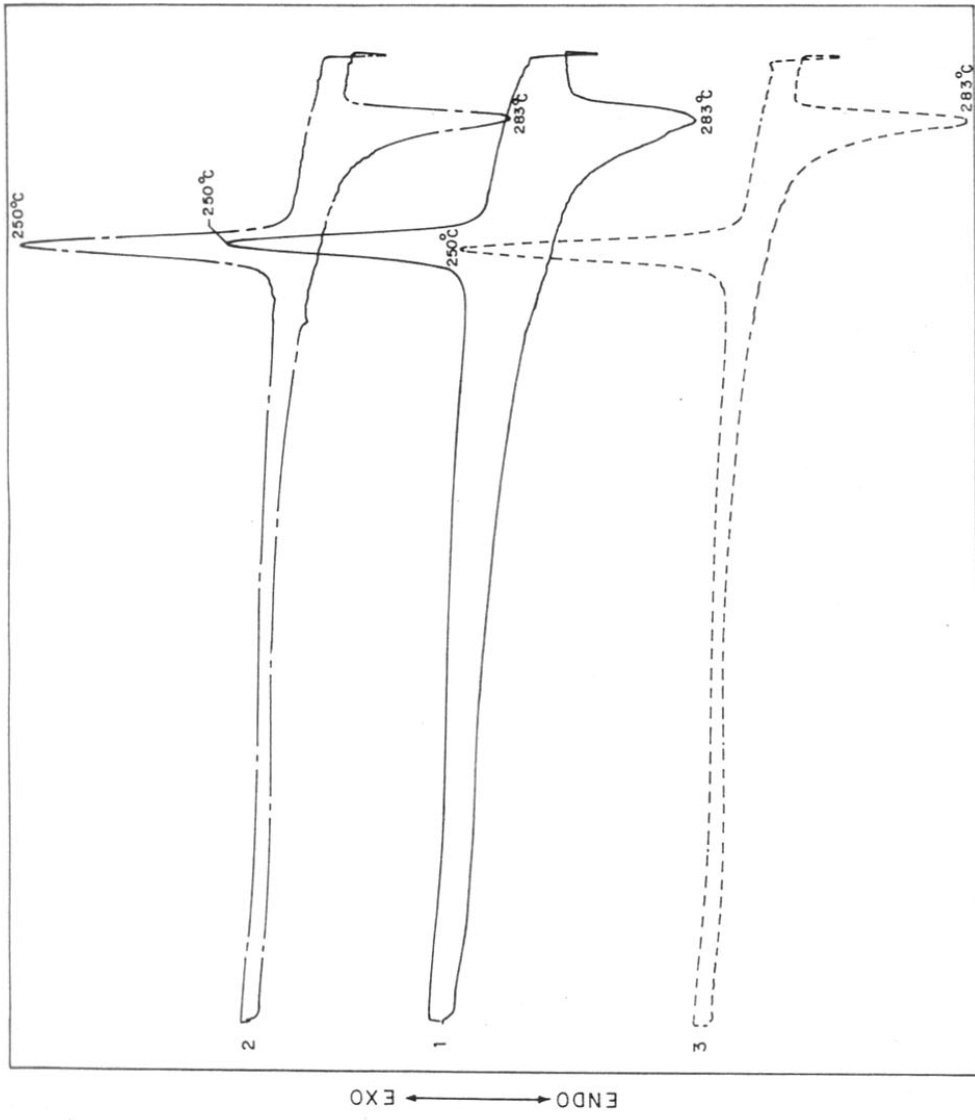


FIG. 51: DSC SCAN-RYTON V-1

behaviour was identical to that of the 6,7 and 10 hour samples.

The notable feature of the DSC scans (Figures 42-51) is the presence of multiple first order transitions in the first heating scan. These disappear in the subsequent heating scans in the melt crystallized state. The polymer was isolated after the preset reaction times by precipitation into methanol followed by water washing to remove unreacted PDCB, sodium sulfide, oligomers as well as the side product sodium chloride generated during the reaction. Thus the thermogram from the first heating cycle corresponds to the morphology of the as-precipitated polymer. The thermograms of the subsequent scans are defined by the crystallization from the polymer melt. However, the thermograms from the first, second and third cooling cycles are identical since the morphology of the as-precipitated polymer is lost on melting.

In PPS synthesis, the polymer formed precipitates after a critical molecular weight is attained. End group analyses results indicate that the precipitated polymer continues to grow even after precipitation from the reaction medium.<sup>245</sup> The molecular weight of the polymer increases with conversion unlike other heterogeneous polycondensation reactions. As a result of the continuing polymerization after precipitation, a wide particle and crystallite size distribution may be generated in this system. The particle size was found to increase with increasing reaction time while the total number of particles decreased with increase in reaction time.<sup>246</sup> This trend was noted in the melting behaviour of the polymers. The melting endotherms were uniformly broad.

The thermal data based on the heating scans by DSC are summar-



zed in Table 20. The peak temperature ( $T_m$ ) may be used for comparison of the results. For the first heating scan with multiple peaks, the  $T_m$  corresponding to the large prominent peak was used for comparison. The temperature of onset of melting and the melting peak temperature were lower for the first heating cycle relative to the second and third heating cycles. There was little change in the completion temperature of melting in the three cycles. The peak width in the first heating scan was wider as compared to the subsequent scans.

The thermograms of all the polymer samples synthesized show, on the first heating cycle two first order transitions either distinctly or as a shoulder. These merge into a single first order transition in the subsequent heating cycles except for the 1/2 hour sample where the fractional conversion was only 0.0474. This behaviour could be attributed to the initial presence of a broad crystallite size distribution in the as-precipitated state, which is destroyed on melting. The melting range in the second and third heating cycles was still very broad. This may be attributed to the broad molecular weight distribution in these samples.

The data on  $T_m$  and the number of peaks observed in the first heating cycle are presented in Table 21. The  $T_m$ -fractional conversion data are presented in Figure 52. The  $T_m$  was found to increase rapidly till a conversion of about 50 percent. The increase in  $T_m$  with conversion was gradual after this stage. Molecular weight determination by end group analysis and morphology studies by scanning electron microscopy indicated that this trend could be attributed to the increase in molecular weight and particle size with conversion.

TABLE 20  
DSC-DATA ON HEATING CYCLE

Reaction time, hr.	Fractional conversion	SCAN No.	Transition temperature °C			Melting range °C
			Onset	Peak	Terminal	
1	2	3	4	5	6	7
1/2	0.0474	I	106	143	171	65
		II	111	140	159	48
		III	111	140	159	48
1	0.2398	I	204	262	270	66
		II	210	264	276	66
		III	211	265	278	67
2	0.4774	I	250	279	289	39
		II	249	283	289	40
		III	248	283	288	40
3	0.7056	I	256	289	291	35
		II	260	285	290	30
		III	260	285	290	30
4	0.7911	I	243	290	293	50
		II	250	286	291	41
		III	259	288	293	34
5	0.8373	I	239	291	295	56
		II	253	286	293	40
		III	255	288	293	38
6	0.8809	I	260	294	299	39
		II	260	290	297	37
		III	260	291	298	38

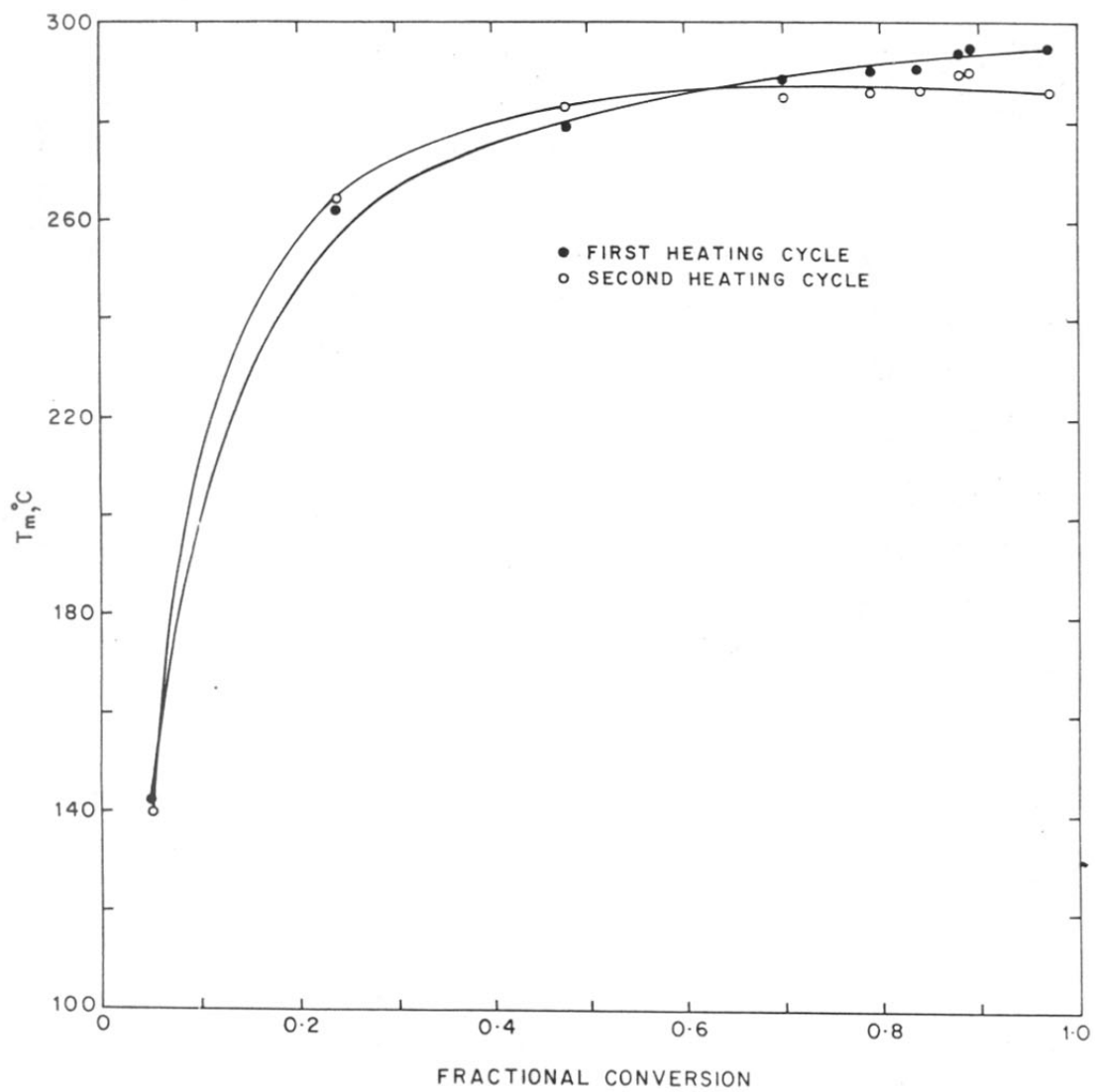
.....

Table 20 contd...

1	2	3	4	5	6	7
		I	256	295	300	44
7	0.8867	II	263	290	295	32
		III	269	290	295	26
		I	248	295	300	52
10	0.9673	II	261	286	291	30
		III	261	286	291	30
		I	256	283	291	35
Ryton V-1	-	II	261	283	289	38
		III	261	283	289	38

TABLE 21  
FRACTIONAL CONVERSION - T<sub>m</sub> DATA (BASED ON DSC)

Reaction time, hr.	Fractional conversion	T <sub>m</sub>		No. of peaks in 1st heating
		1st heating	2nd heating	
1/2	0.0474	143	140	1
1	0.2398	262	264	3
2	0.4774	279	283	1 and broad shoulder
3	0.7056	289	285	2
4	0.7911	290	286	2
5	0.8373	291	286	2
6	0.8809	294	290	1 and shoulder
7	0.8867	295	290	"
10	0.9673	295	286	"
Ryton	-	283	283	1

FIG.52 :  $T_m$  - FRACTIONAL CONVERSION DATA

The DSC data based on the cooling cycles for the samples are summarized in Table 22. The thermograms based on the first, second and third cooling cycles are comparable. A single peak was observed in all the cases. The crystallization temperature was broad for low conversion sample. The range narrows as the molecular weight increases with conversion. The data on the onset of crystallization with fractional conversion is shown in Figure 53. After 2 hours reaction time or a conversion of about 50% there is little change in the temperature of onset of crystallization. Similarly the degree of supercooling also reaches a plateau value at 0.5 fractional conversion. The degree of crystallinity was found to decrease marginally from 71 to 66 percent with increasing reaction time on the basis of XRD studies discussed in section 5.1. These trends are consistent with the analysis that the polymer molecular weight continues to grow with conversion inspite of precipitation after a critical molecular weight was attained.

The transition energy data based on the second heating cycle are presented in Table 23. The transition energies were calculated per monomer repeat unit. No clear trend was seen in the transition energies either in melting or cooling.

The commercial PPS sample Ryton V-1, in comparison, showed a single first order transition peak on the first heating cycle itself. The thermal history of the commercial sample differed from the samples in this investigation. The commercial sample had lower  $T_m$  but the degree of super cooling was higher as compared to the samples synthesized. The melting range of Ryton was also narrower. These observations indicate

TABLE 22  
DSC DATA ON COOLING CYCLE

Reaction time, hr.	Fractional conversion	SCAN No.	Crystallisation temp.°C			Crystallisation range temp. °C	Degree of super-cooling
1	2	3	4	5	6	7	8
1/2	0.0474	I	125	No distinct peaks, but only a broad shoulder	91	34	18
		II	125		91	34	15
		III	125		91	34	15
1	0.2398	I	256	245	195	61	16
		II	256	248	200	56	8
		III	256	249	199	57	9
2	0.4774	I	271	264	238	33	8
		II	270	263	235	35	13
		III	268	263	235	33	15
3	0.7056	I	270	264	241	31	19
		II	270	264	238	32	19
		III	270	264	237	33	15
4	0.7911	I	270	263	235	35	20
		II	270	264	231	39	16
		III	270	264	236	36	16
5	0.8373	I	270	263	234	36	28
		II	270	263	238	32	16
		III	271	264	238	33	17
6	0.8889	I	278	268	238	40	16
		II	278	268	239	39	12
		III	277	269	244	37	14

.....

Table 22 contd...

1	2	3	4	5	6	7	8
7	0.8867	I	274	263	246	28	21
		II	274	264	245	29	16
		III	274	264	245	29	16
10	0.9673	I	263	255	230	33	32
		II	264	255	239	25	22
		III	264	256	237	27	22
Ryton	-	I	260	250	239	21	23
		II	258	250	238	20	25
		III	258	250	239	19	25



TABLE 23  
TRANSITION ENERGY DATA BY DSC

Reaction time	Fractional conversion	$H_f$ kcal/mfu	$H_c$ kcal/mru
60	0.2398	1.23	2.28
120	0.4774	1.32	2.38
180	0.7066	1.67	3.03
240	0.7911	1.67	3.03
300	0.8373	1.54	2.81
360	0.8809	1.25	2.27
420	0.8867	1.57	2.81
600	0.9673	1.67	3.03
Ryton		1.31	2.38

mru = monomer repeat unit

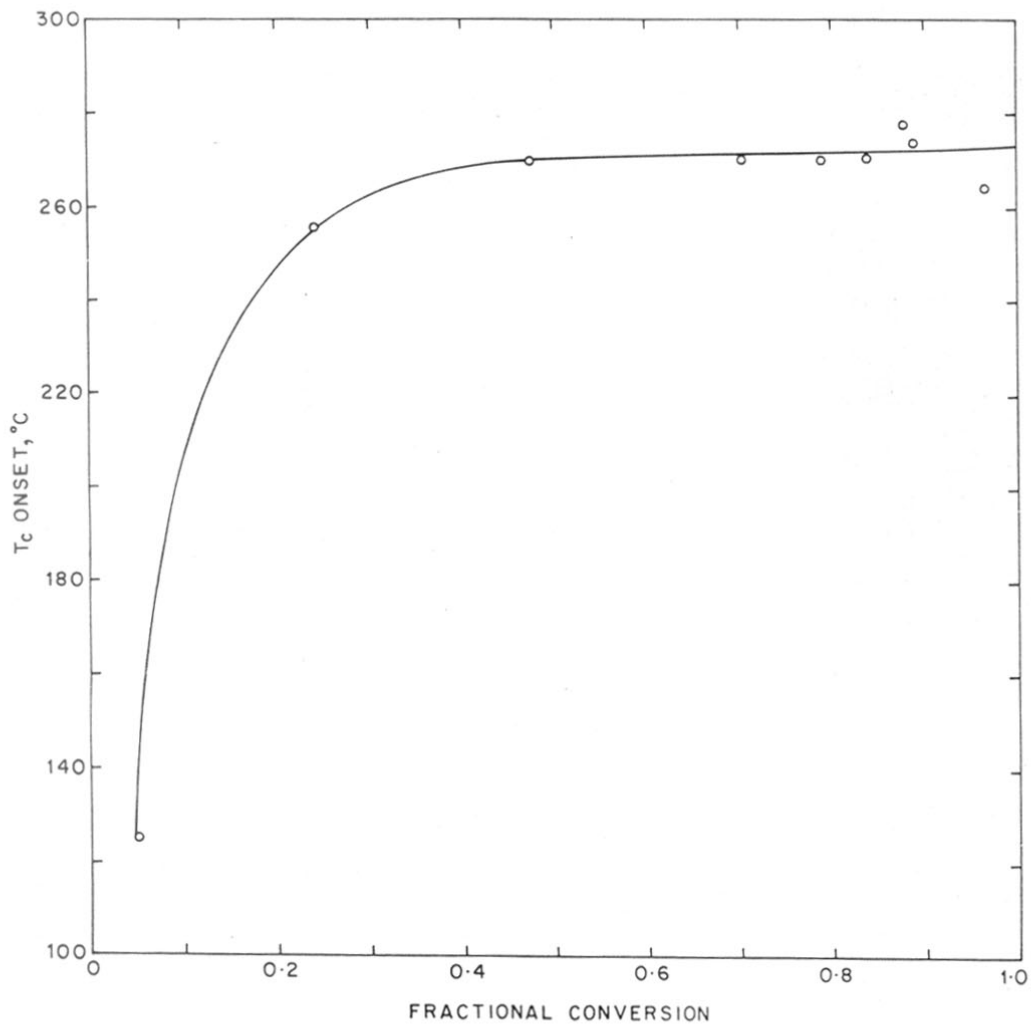


FIG.53:ONSET CRYSTALLIZATION-FRACTIONAL CONVERSION

the presence of a narrower molecular weight distribution in the commercial sample.

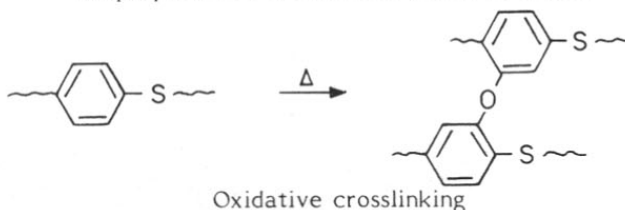
### Thermogravimetric analysis (TGA)

The changes in the physical structure of the polymer with reaction time were studied by DSC. The TGA studies were carried out to elucidate the changes in the chemical structure with reaction time. The high temperature behaviour of the polymer samples is relevant to the curing process. The PPS powder transforms into a thermoset on curing in the temperature range of 375 to 425°C for extended period. It is therefore necessary that the polymer should be stable atleast upto this temperature for the material to be useful as a coating grade polymer.

The curing reaction of PPS is not completely understood. The initial thermal studies were directed towards the stability of the material at high temperatures. Both chain extension and some degree of crosslinking are known to take place during this step. The notable contribution in this aspect has been made by Hawkins.<sup>247</sup> His proposed scheme involves the following steps:

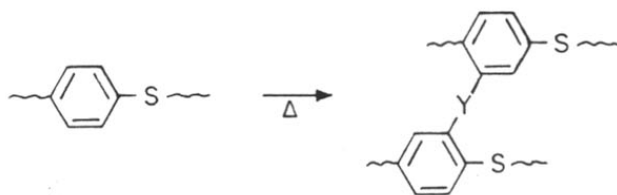


Disproportional reaction for chain extension



Oxidative crosslinking

or



where  $Y = S$  or  $Ar$

, Thermal crosslinking

Volatiles and low molecular weight products are formed during the curing reaction of PPS in air. In the present investigation the TGA of PPS samples were done in air. The experimental details are given in section 2 .

In PPS, the polymer chain is interlinked by carbon-carbon, carbon-sulfur and carbon-hydrogen bonds. These bonds are thermally stable resulting in the overall excellent thermal stability of the polymer.

The thermal behaviour and decomposition profile of the polymers synthesized were determined by thermogravimetric analysis (TGA) and differential thermogravimetry (DTG). A typical output from the NETZCH thermal analyser model STA 409 used in the investigation is shown in Figure 54. The dependance and variation if any, in the mode of thermal decomposition in air with molecular weight were evaluated. The thermal stability parameters derived from the TGA/DTG scans are presented in Table 24. The decomposition profiles of the selected polymer samples collected at reaction times of 1/2, 1,2,3 and 6 hours are shown in Figure 55. The corresponding DTG curves are illustrated in Figure 56. Referring to these figures, it is clear that different decomposition mechanisms are operational depending on the structure of the polymer formed at that particular conversion level. The changes in TGA indicated that the

TABLE 24  
TRANSITION ENERGY DATA BY DSC

Reaction time,hr.	Fractional conversion	H <sub>g</sub> kcal mru	H <sub>c</sub> kcal mru
1	0.2398	1.23	2.28
2	0.4774	1.32	2.38
3	0.7066	1.67	3.03
4	0.7911	1.67	3.03
5	0.8373	1.54	2.81
6	0.8809	1.25	2.27
7	0.8867	1.57	2.81
10	0.9673	1.67	3.03
Ryton	-	1.31	2.38

mru = monomer repeat unit

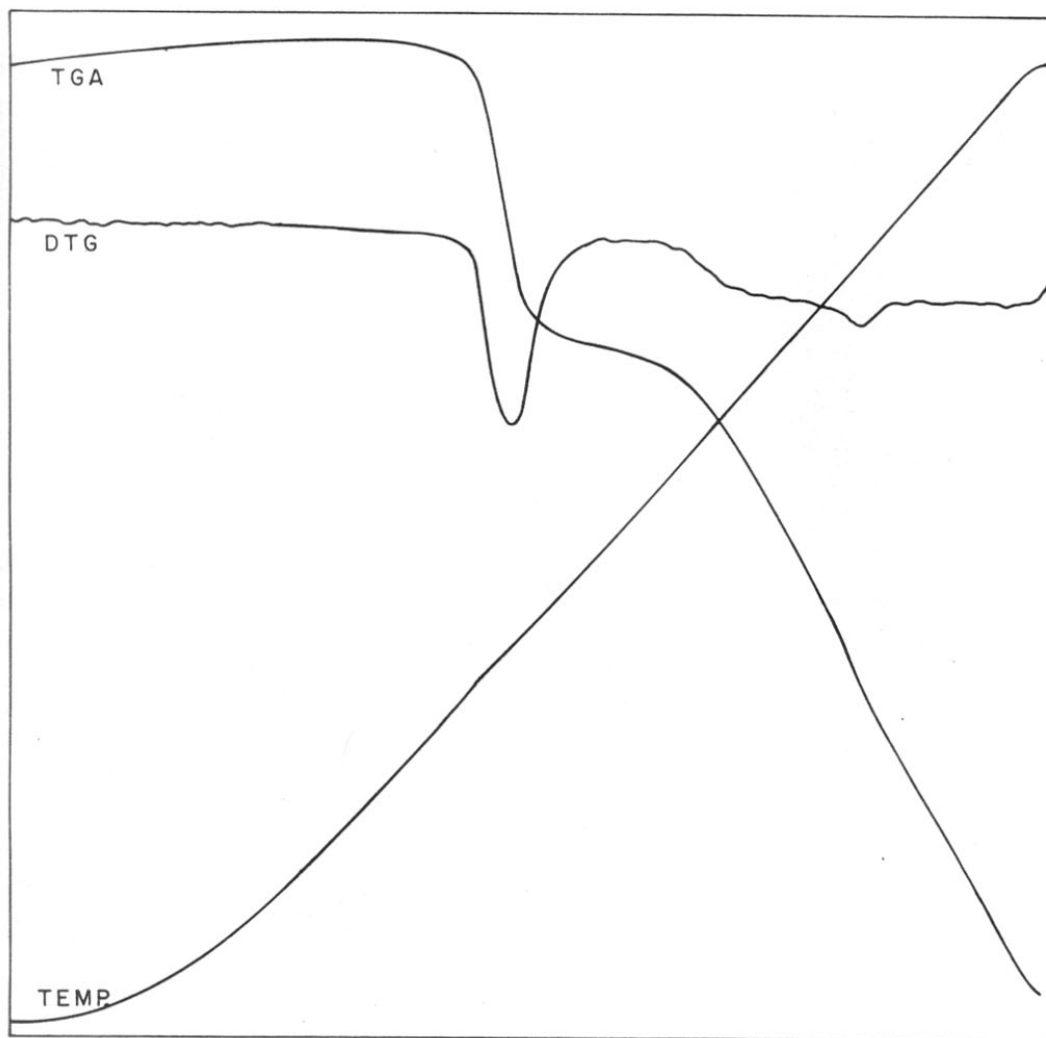


FIG. 54: TYPICAL OUTPUT OF TGA SCAN-6 hr. SAMPLE

chemical structure of the polymer was also changing with reaction time. While it is difficult to present their exact nature in the absence of post-decomposition product analysis, some general trends can be noted and these related to the differences in the molecular weight, molecular weight distribution, difference in the end group populations, and possibly to the varying levels of cyclic moieties in the polymer samples collected at different reaction times.

The polymers differ in the concentration of end groups. The polymers formed initially were of a low molecular weight and have a high concentration of SNa end groups.<sup>246</sup> This concentration decreases with increasing polymerization time and degree of polymerization. Clear trends are noted in the comparative study of the TGA curves. Polymer samples generated at low conversions were thermally less stable as indicated by the lower temperatures of onset of degradation. The thermal stability increases with molecular weight. The initial decomposition occurs probably close to the end group. A polymer with thermal stability comparable to that of commercial polymer Ryton was attained after a polymerization time of 6 hours.

The data on percent decomposition and the temperature are summarized in Tables 25,26. After 20-41 percent decomposition (temperature range 304 to 544°C), the decomposition mechanism shifts and probably involves random positions along the polymer chain. The synthesized polymer samples are more stable to oxidative degradation than the commercial Ryton after 40 percent decomposition. This is reflected in the broad shoulder in the TGA curves shown in Figure 55.

TABLE 25  
DEGRADATION DATA BY DTG

Reaction time, hr.	Fractional conversion	Degradation °C			Range °C
		Onset	Peak	Completion	
1/2	0.0474	304	450/541	635	331
1	0.2398	331	544	902	571
2	0.4774	323	541	899	576
3	0.7056	329	559	664	335
6	0.8809	477	544	618	141
Ryton V-1	-	440	554	827	387



TABLE 26  
DECOMPOSITION-TEMPERATURE RANGE DATA

Reaction time, hr.	Fractional conversion	Decomposition %	Temperature range °C
1/2	0.0474	16 to 48	304 to 450
1	0.2398	10 to 37	331 to 544
2	0.4774	8 to 34	323 to 541
3	0.7056	38 to 45	329 to 559
6	0.8809		477 to 544
Ryton	-	3 to 31	440 to 554

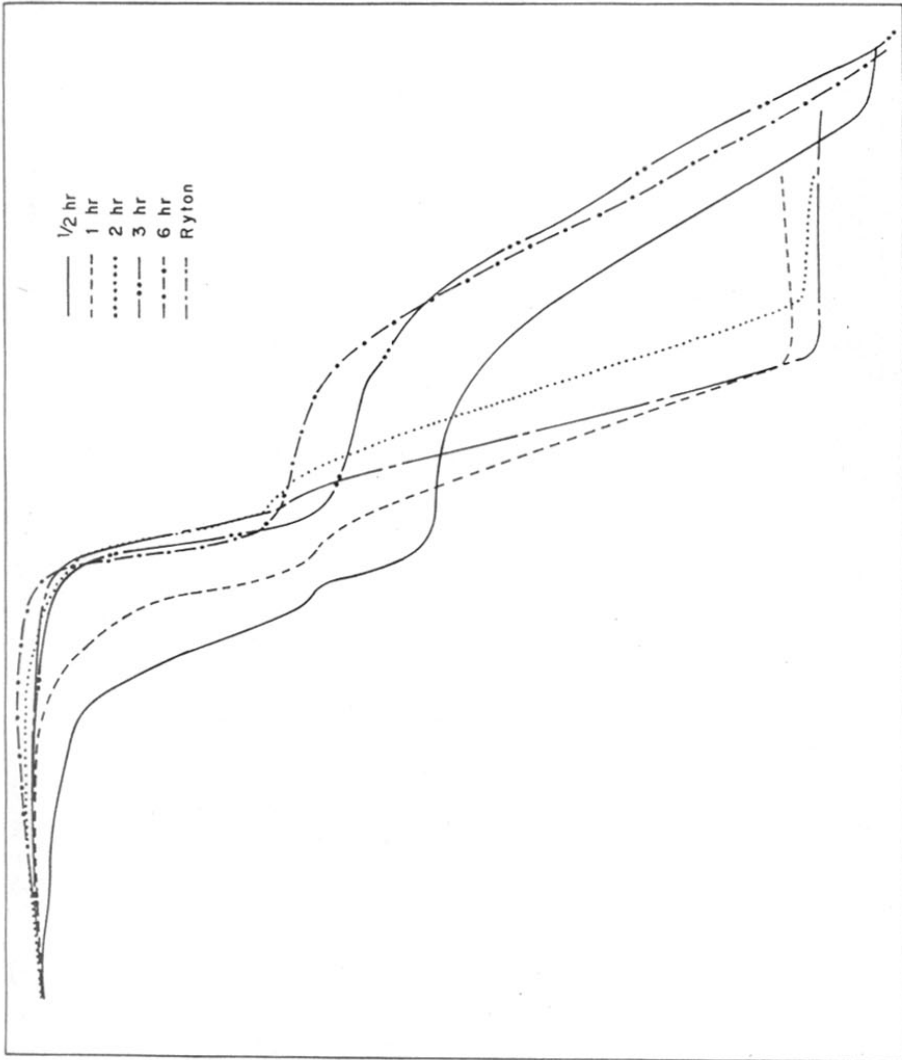


FIG. 55: TGA SCANS OF REFERENCE SET

The DTG curves of the reference set samples are shown in Figure 56. It could be noted that a polymer of comparable thermal stability is obtained after a reaction time of 3 hours. The data on percent residue and fractional conversion are summarized in Table 27. After decomposition was complete, the residue left was much higher in the low conversion samples than that noted in other polymer samples. The data are plotted in Figure 57. This probably consisted extensively inorganics such as sodium chloride and sodium sulfide generated from end groups or from cyclic moieties formed. The high thermal stability of even oligomeric PPS was uniformly brought out in this investigation.

To summarize, the thermal transitions of the reference set samples were studied using a DSC. The notable feature of the thermograms was the presence of multiple first order transitions in the first heating cycle, which disappeared in the subsequent heating cycles. The thermograms from the first heating cycle corresponds to the morphology of the as-precipitated state versus the morphology in the melt crystallized state in the subsequent scans. The crystallization peaks were however identical.

The thermogravimetric analysis of the samples were evaluated in air. While polymers formed at low conversions had high concentration of  $-SNa$  end groups, those formed at higher conversions would be relatively richer in  $-Cl$  end groups. This was reflected in the residue formed as a function of reaction time. The polymer samples formed at lower conversions were thermally less stable as compared to Ryton. A polymer of comparable thermal stability with Ryton V-1 was obtained after a reaction time of 3 hours. The kinetic studies revealed a change in the rate after a reaction time of 3 hours.

TABLE 27  
RESIDUE-FRACTIONAL CONVERSION DATA

Reaction time, hr.	Fractional conversion	Residue %
1/2	0.0474	12
1	0.2398	8.76
2	0.4774	6.98
3	0.7056	7.2
6	0.8809	7.1
Ryton	-	4.5

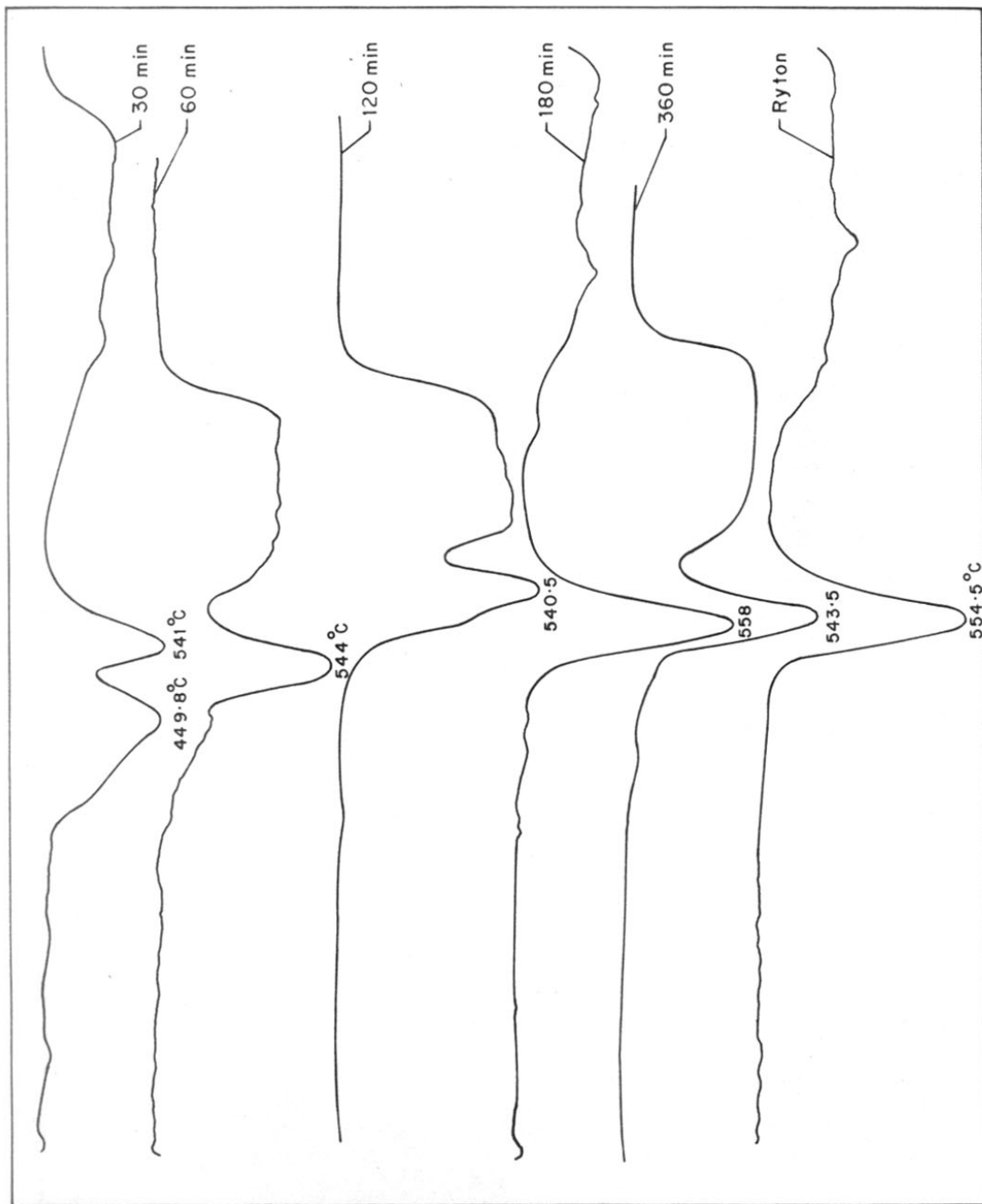


FIG 56: DTG CURVES OF REFERENCE SET

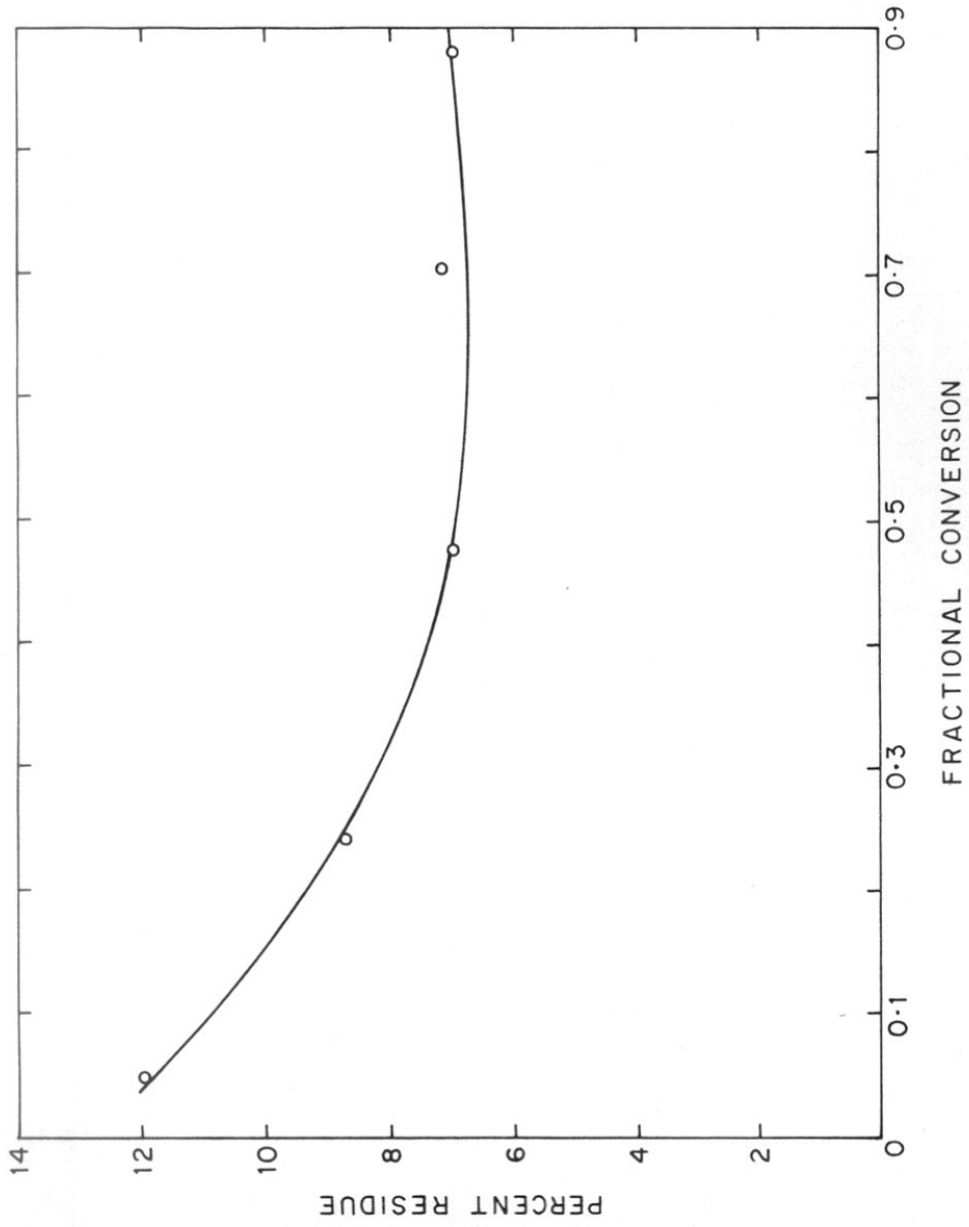


FIG.57 : PERCENT RESIDUE - FRACTIONAL CONVERSION DATA



**CHAPTER 5**  
**MORPHOLOGICAL STUDIES**

## 5. MORPHOLOGICAL STUDIES

Most high temperature polymers are based on aromatic units. Amongst these, those based on para phenylene type such as polyphenylene oxide (PPO), polyphenylene sulfide (PPS), polyether ether ketone (PEEK) and polyether sulfone (PES) have attracted much attention in the recent years due to their excellent thermal/chemical stability and resistance to corrosive materials.<sup>248</sup> The unique feature of PPS is its thermal stability in air upto 400°C and the ability to be transformed into fine insoluble, chemical resistant coating by thermal curing process. The adhesive properties of PPS towards various metal substrates are excellent and is an extremely useful material in high temperature coatings.

It is well known that growth, structure and morphology of the polymer play an important role in governing the various properties for end use application of the processed articles. In particular, the size, shape and structure of the polymeric powders are critical factors influencing their processibility in solid state compaction and sintering processes and also the coating properties. These powder metallurgical processing techniques are used extensively for PPS coatings.<sup>249</sup> The studies on growth and morphology of PPS samples polymerized under different conditions would be useful in a better understanding of its behaviour in subsequent processing steps. The crystallinity, particle size and morphology of PPS synthesized under varying conditions have been investigated by x-ray diffraction and scanning electron microscopy.



### 5.1 X-RAY DIFFRACTION STUDIES

The experimental details for obtaining the XRD-scans are described in Section 2.9. The polymer samples collected at different reaction times in the reference set were chosen for the investigation. The dried powder samples were used for these investigations.

Figures 58, 59 and 60 show the wide angle diffraction scans (WAXS) for PPS samples collected at 1/2 hr, 1 hr, 2 hr, 3 hr, 6 hr and 10 hr reaction product samples in that order. It is seen that the region of diffraction angle ( $2\theta$ ) indicated, there are four major peaks occurring at 18.8, 20.5, 25.5 and 27.4 degrees which correspond to crystalline form of PPS. There are two additional reflections seen in the WAXS of samples collected at low reaction time (1/2 hr and 1 hr). However, the intensity of these peaks decreases rapidly with increase of reaction time and for reaction times higher than 2 hr, these additional peaks are totally absent in the WAXS data.

It is well known that PPS would crystallize in orthorhombic configuration<sup>250</sup> with unit cell dimensions of  $a = 8.67\text{\AA}$ ,  $b = 5.61\text{\AA}$  and  $c = 10.26\text{\AA}$ . The analysis of the WAXS data showed that most of the reflections could be assigned according to this crystalline structure. For example, the four major peaks shown in Figures 58-60 were assigned as reflections from the planes corresponding to Miller indices

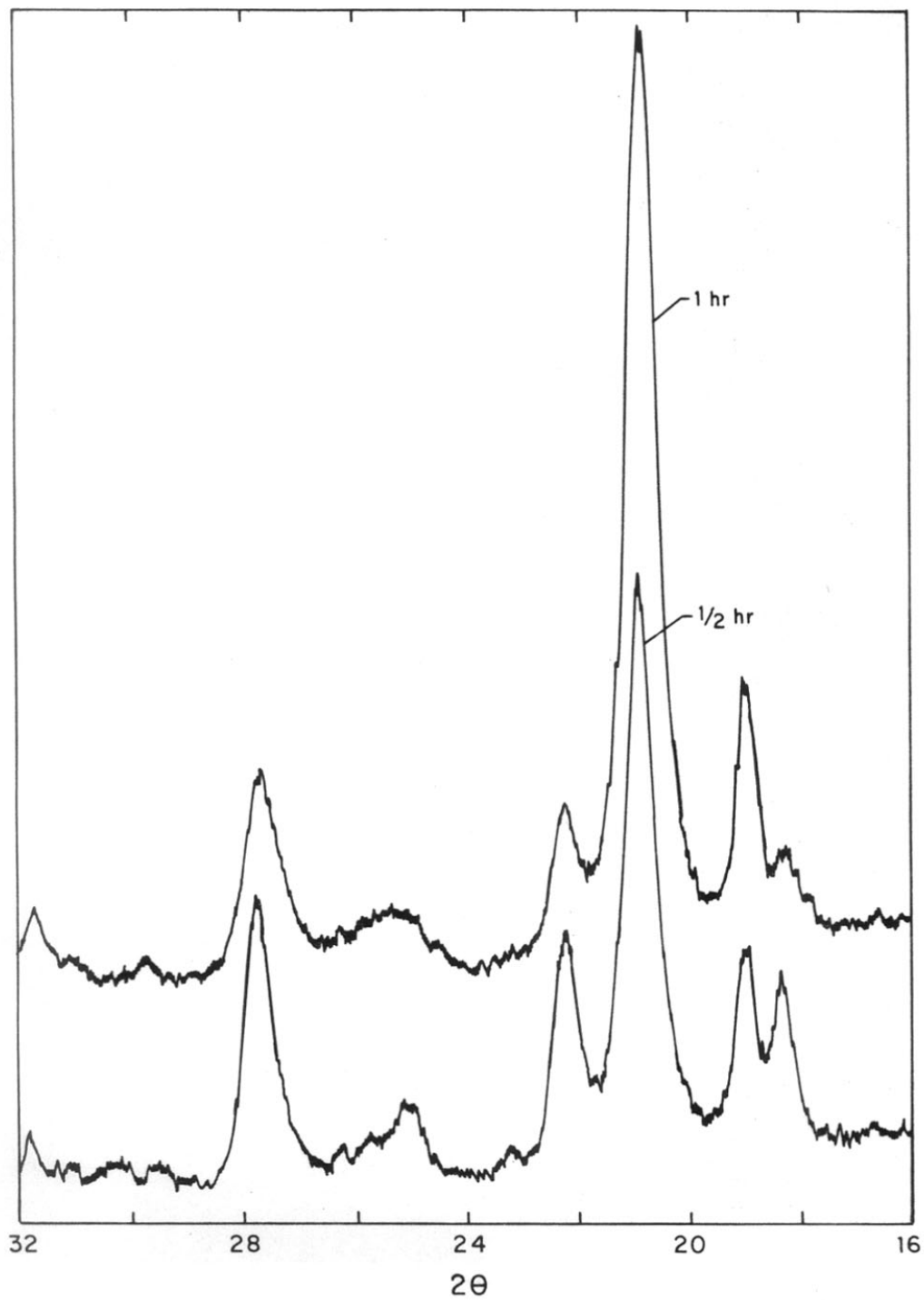


FIG.58 : XRD SCANS - 1/2 hr, 1 hr SAMPLES

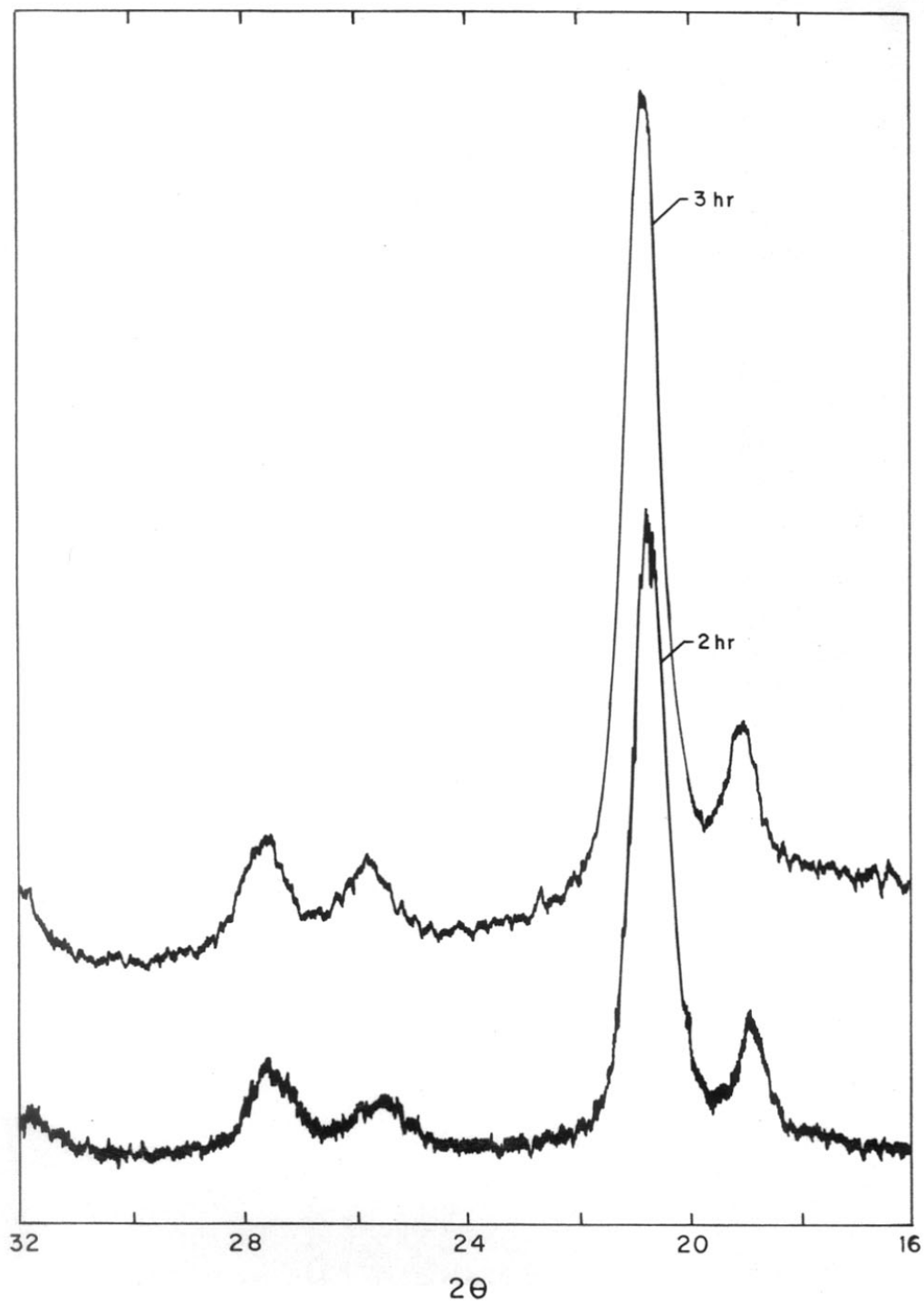


FIG.59: XRD SCANS—2 hr, 3hr SAMPLES

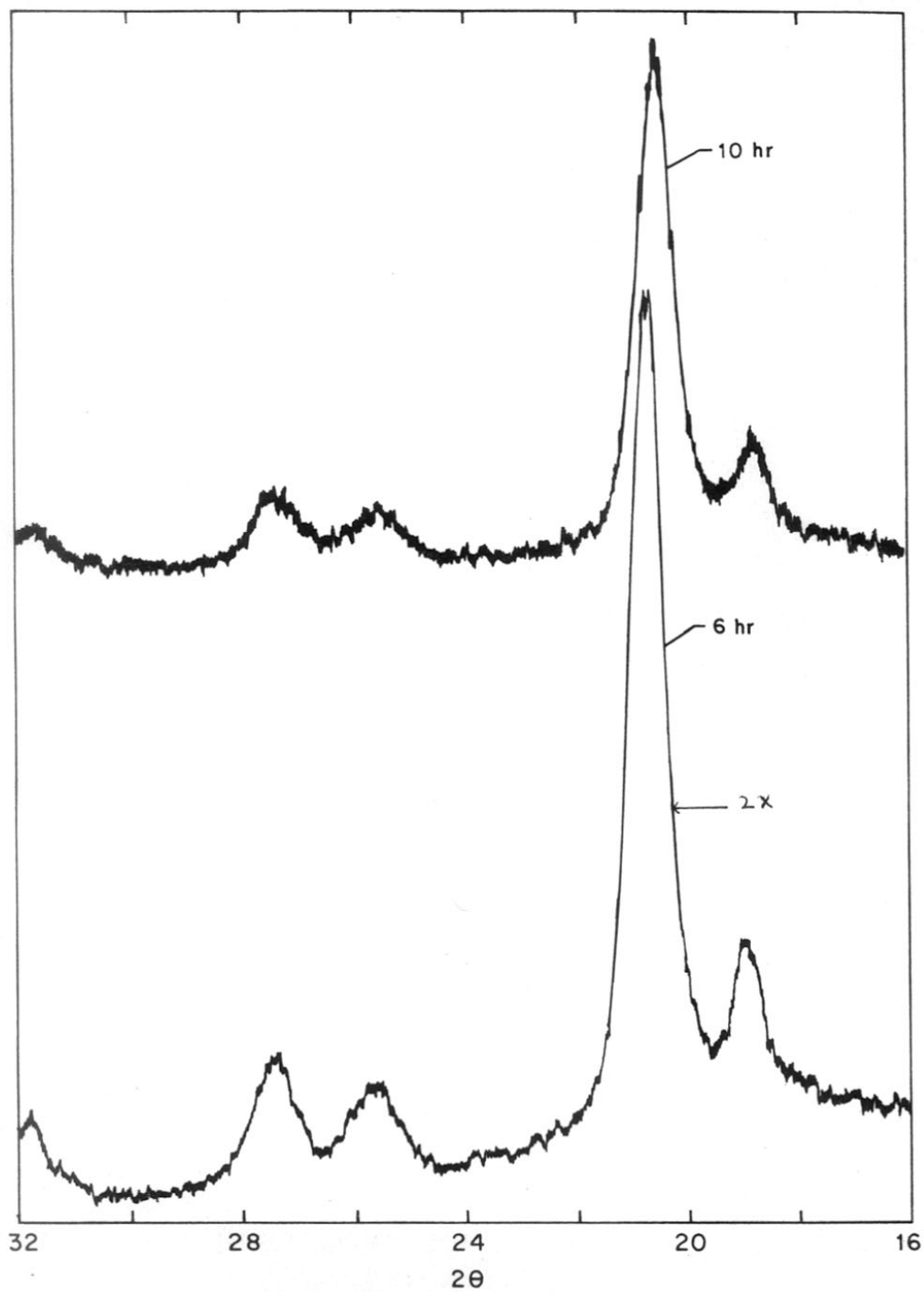


FIG.60: XRD SCANS - 6 hr ,10 hr SAMPLES

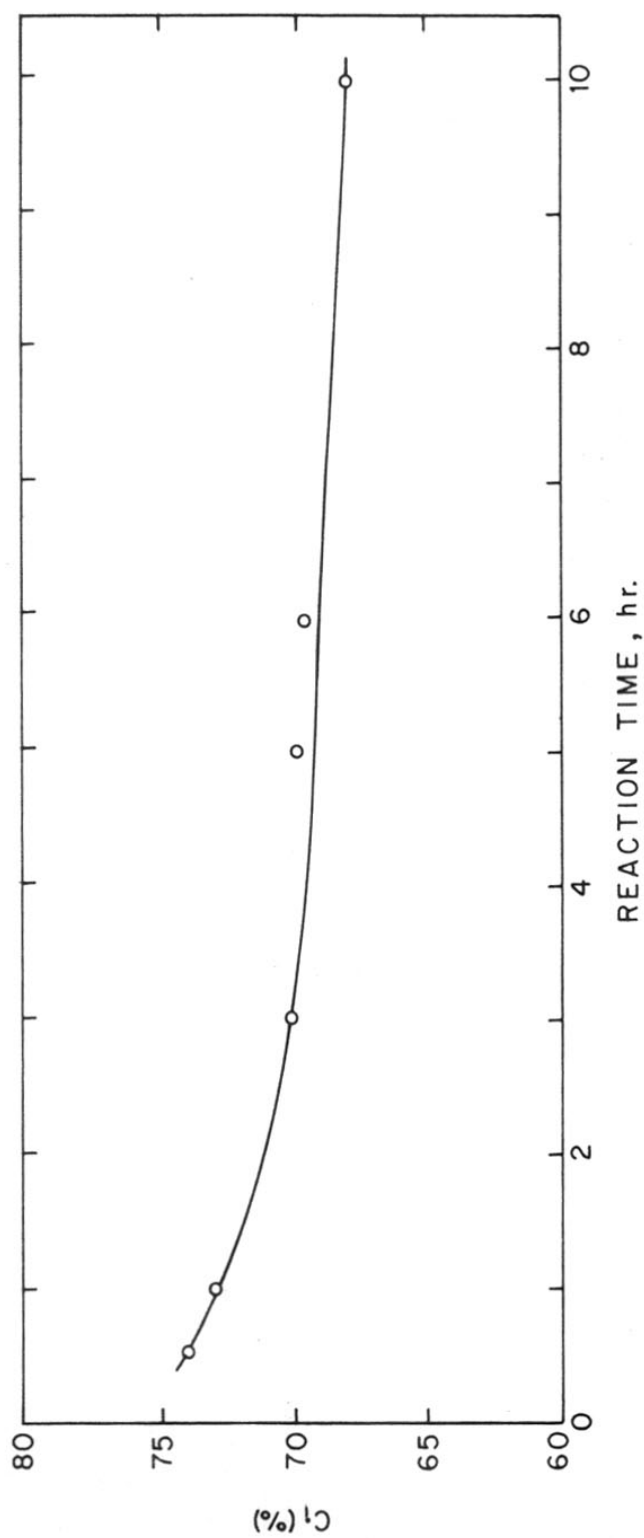
110, 110/200, 112/003 and 211 respectively. This was found to be the case for all the samples investigated, irrespective of the differences in reaction conditions such as reaction time, variation in stirring speed and dilution of the reactants.

The crystallinity, on the other hand, was dependant on the reaction time to some extent. The crystallinity was determined from the regression curve analysis<sup>251</sup> of the diffractometer scans as per the following relation:

$$C_i = [ 1 + 0.7 (\phi_a + \phi_c)^{-1} ]$$

where,  $C_i$  is the crystallinity index,  $\phi_a$  and  $\phi_c$  are the areas under the amorphous halo and crystalline peaks.

The data on the variation of  $C_i$  with reaction time, evaluated from the four prominent peaks corresponding to 110, 200, 111 and 211 reflections in the  $2\theta$  range 10-30 degrees are illustrated in Figure 61. It is seen from the figure that as the reaction time is increased, the crystallinity decreases slightly from 74 % to a value of 68 % upto

FIG. 61 :  $C_1$ - VARIATION WITH REACTION TIME

a reaction time of 6 hours. There is no significant change in  $C_1$  beyond 6 hours reaction time. The low molecular weight fractions are known to have higher crystallization rate and hence crystallinity as compared to high molecular weight polymers. The PPS samples synthesized have a wide molecular weight distribution. The crystallinity values noted for low reaction times could be due to these species in the polymers isolated.

## 5.2 SCANNING ELECTRON MICROSCOPE STUDIES

The particle size distribution and average particle size were evaluated using a scanning electron microscope. The instrumental details are described in Section 2.10. Counts were taken for the existing particles of various sizes in the electron beam scanned area ( $0.5 \text{ mm}^2$ ) and the spot was shifted to various locations of the sample. Percentage average values for each size was then determined from these. The average particle size was taken as the weighted mean value. The data on the average particle size growth variation with reaction time are presented in Table 28. The data in particle size-polymer yield and reaction time are shown in Figure 62. It is seen that the particle size, which is initially less than a micron, increases rapidly upto 3 hours and more gradually for higher reaction times, tending to the asymptotic limit of 11 microns for very large reaction time. The polymer yield data also follows a similar trend.

Figure 63 shows the actual distribution of particle size obtained after polymer isolation at different reaction times. In the early stages of the reaction, the distribution curve is sharp and shows a maximum at about 1 micron particle size. As the reaction time is increased, the

TABLE 28

## GROWTH BEHAVIOUR OF POLYPHENYLENE SULFIDE

Reaction time, ( $t_r$ hrs)	Average particle size, ( $S_t$ microns)	Yield, ( $Y_t$ gms)	Total number of particles, ( $N_t$ )
0.5	0.5	0.59	$8.13 \times 10^{11}$
1.0	1.1	4.33	$7.46 \times 10^{11}$
2.0	3.0	6.2	$3.95 \times 10^{10}$
3.0	4.75	13.2	$2.1 \times 10^{10}$
4.0	6.0	16.63	$1.32 \times 10^{10}$
5.0	6.8	17.25	$9.4 \times 10^9$
6.0	7.5	19.05	$7.7 \times 10^9$
7.0	8.2	19.3	$6.0 \times 10^9$
10.0	10.0	20.9	$3.6 \times 10^9$



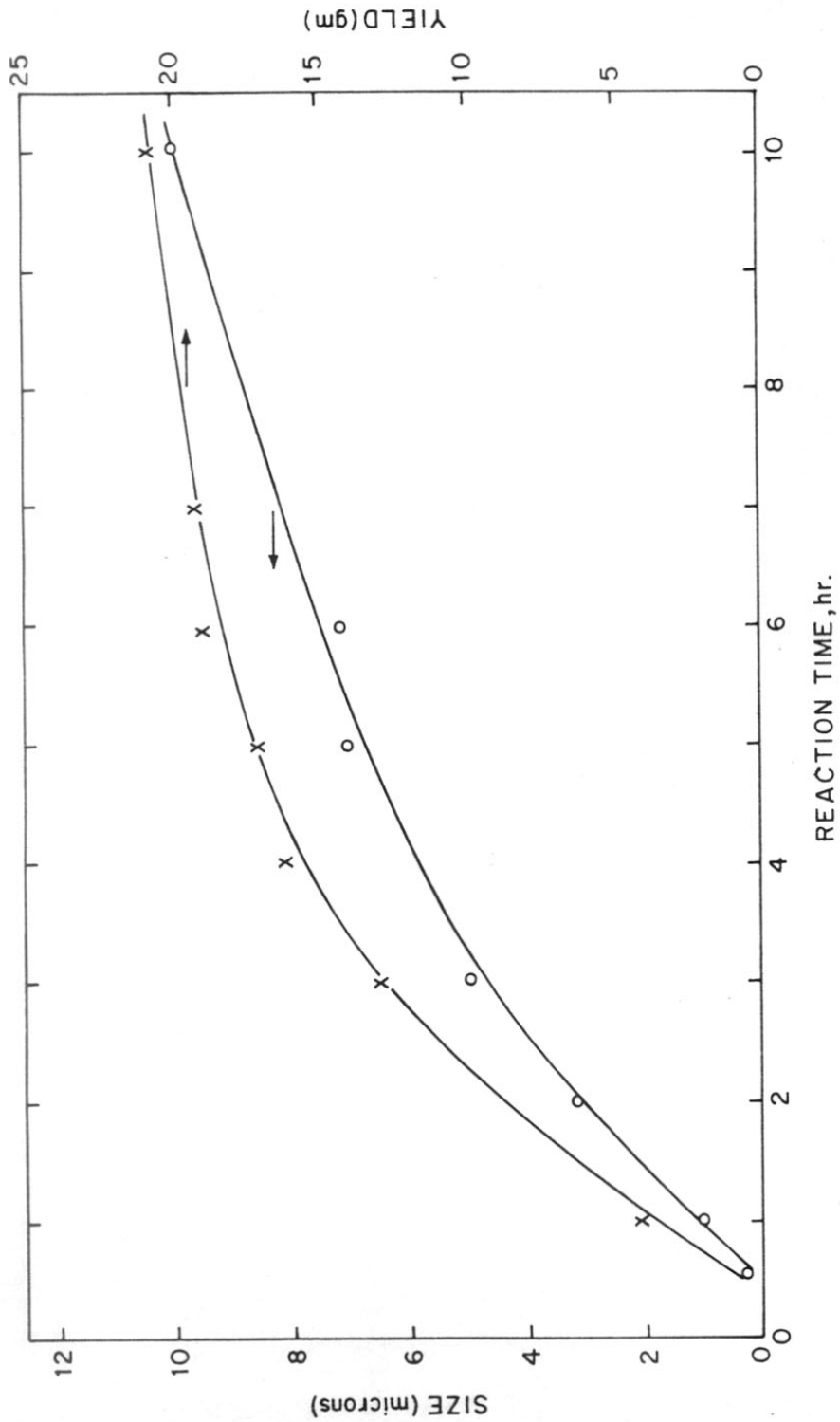


FIG. 62 : PARTICLE SIZE - YIELD-REACTION TIME DATA

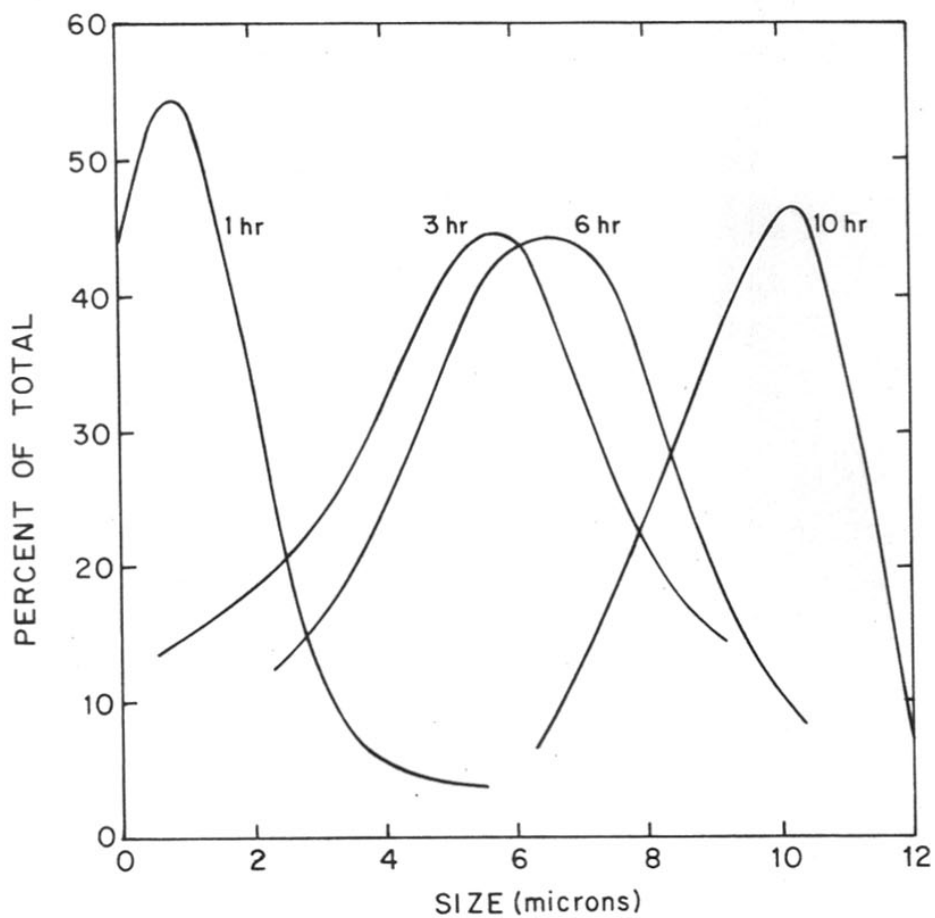


FIG.63: PARTICLE SIZE DISTRIBUTION - REACTION TIME DATA

distribution curve becomes increasingly broader and the maximum peak value shifts towards higher particle size region. Figure 71 shows the typical SEM of particles obtained at  $t_r$  of 6 hours. It is seen that there are a large number of particles with varying sizes ranging from 3 to 10 microns. At reaction times beyond 6 hours, however, the curve again tends to become sharp centering about 11 microns though it is asymmetric in the higher particle region indicative of upper limit of the size can be achieved under the reaction conditions investigated.

In order to investigate the exact time dependance of the growth phenomena, a plot of  $\log (S_t - S_f)$  with reaction time was made where  $S_t$  is the saturation limit of the particle size and  $S_f$ , the average particle size at time 't'. The data are shown in Figure 64. It could be seen that the plot is a linear one with a negative slope suggesting that the growth equation is of the type,

$$S_t = S_f (1 - e^{-\alpha t})$$

where, the slope  $\alpha$  has a value of  $2.6 \times 10^{-5}/\text{sec}$ . Figure 64 also shows the plot of  $\log (m_f - m_t)$  with reaction time where  $m_f$  and  $m_t$  represent the mass of polymer obtained at asymptotic limit (reaction time  $\infty$ ) and reaction time 't' respectively. This graph interestingly is also a linear one with a slope of  $3.8 \times 10^{-5}/\text{sec}$ . The build up of the total mass also follows a similar time dependance as shown below.

$$m_t = m_f (1 - e^{-\alpha t})$$

where,  $\alpha$  has a value  $3.8 \times 10^{-5}/\text{sec}$ .

It thus seems that the build up of the polymer mass is accompanied by growth of the original particles rather than reaction of new number

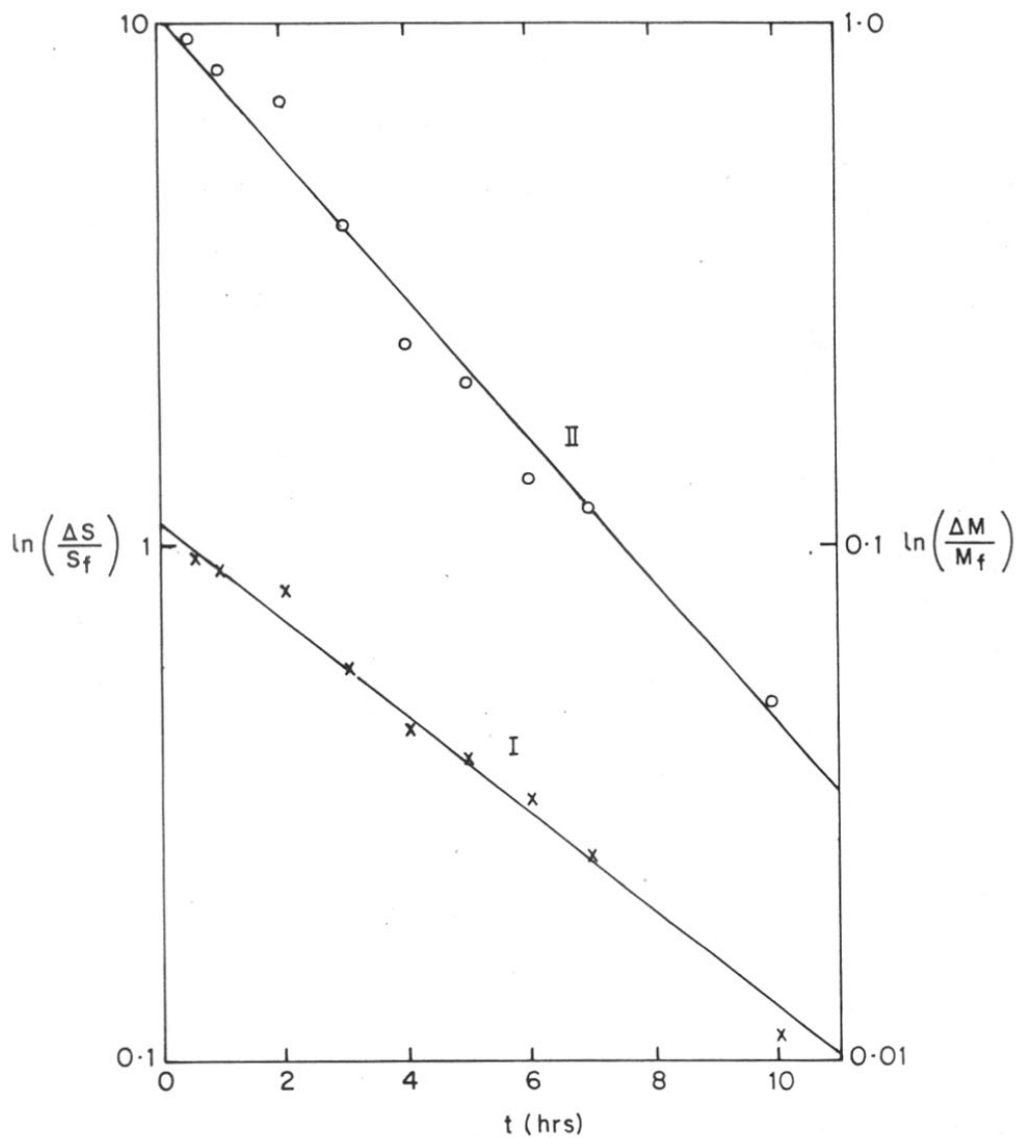


FIG.64: PLOT OF  $S_f - S_t / S_f$  AND  $M_f - M_t / M_f$  VERSUS REACTION TIME

of particles. This may be further confirmed by estimating the total number of particles in polymer mass obtained at different reaction times. The total number of particles can be estimated by calculating the mass of the particle from average particle size giving volume and crystallinity giving effective density (crystalline + amorphous) and dividing the total mass by it. These calculations are summarized in Table 28. The total number of particles are found to decrease with increase in reaction time.

Figures 65, 66 and 67 show the scanning electron microscopes of PPS obtained under identical reaction conditions but at different reaction times of 1, 3 and 10 hours respectively. It could be noted that the particles at reaction time of 1 hour are small, well defined and having (crystal-like) sharp boundaries indicative of high crystallinity. As the reaction time is increased, the particles not only grow in size but also develop complex structure as seen from Figures 67 and 68. It may be noted from these figures that as the reaction proceeds, the polymer mass develops on top of the existing particles from all directions giving rise to generally spherical shape but containing 'sheaf-like' structure (opened cabbage analogy). The most interesting feature of these observations is that the sheaf-like structure continues to grow even at large reaction times.

The growth behaviour of the polymer amongst the various possibilities, under a given set of reaction conditions, depends upon the nucleation and termination rates,<sup>252</sup> the type of polymerization reaction<sup>253</sup> (condensation, addition etc.) and the phase of the monomers<sup>254</sup> (solid, liquid or vapour). For example, if the nucleation rate remains steady for a given time period but the termination rate is high, then one would expect the polymer mass to contain small particles with sharp distribution curve.

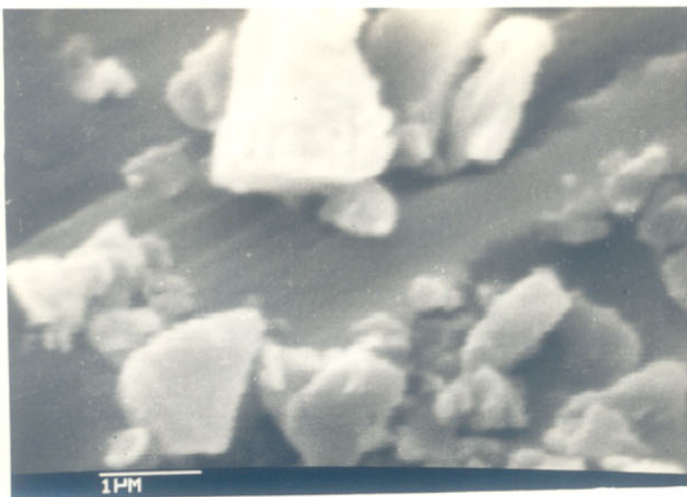


FIG. 65



FIG. 66



FIG. 67

SEM OF PPS PARTICLES 1hr, 3hr AND 10hr

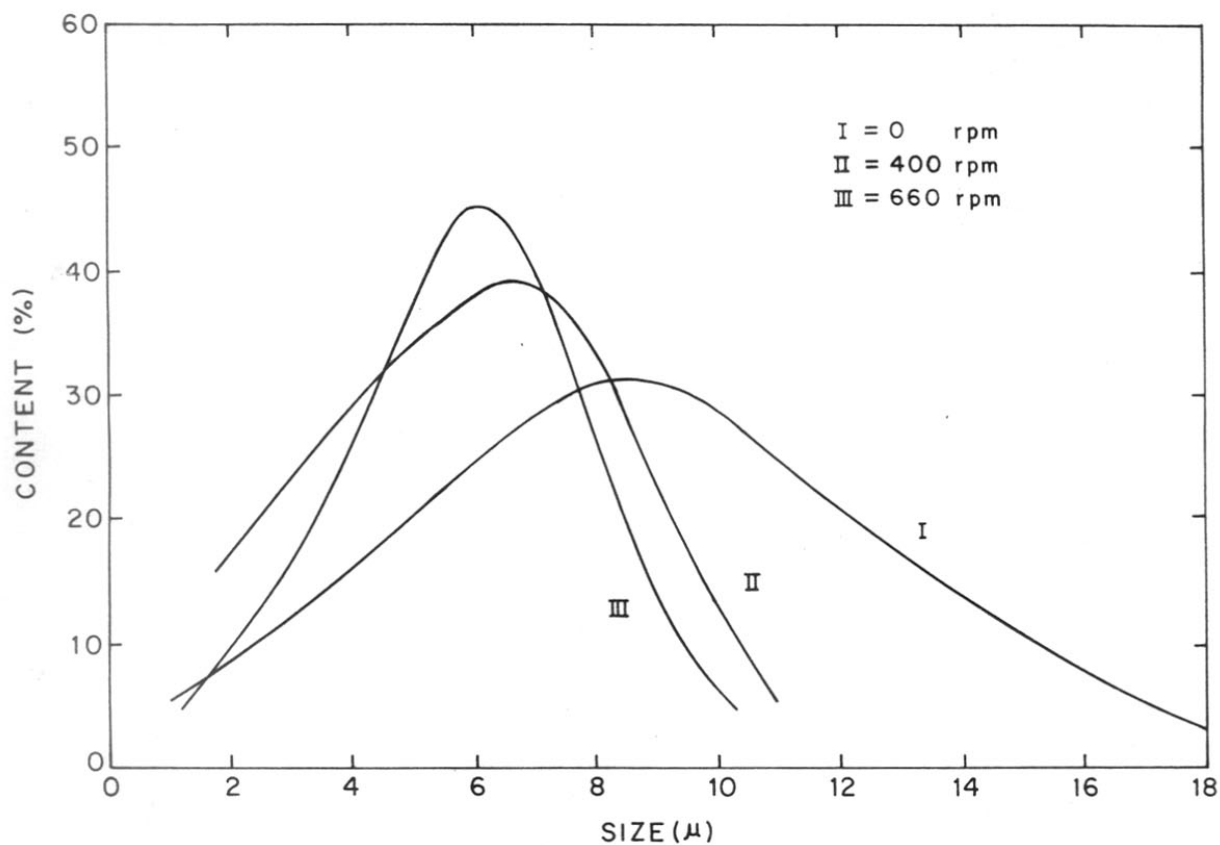


FIG.68: PARTICLE SIZE DISTRIBUTION FOR VARIOUS STIRRING SPEEDS.

The rate of growth of the polymer mass depends upon the reaction kinetics or the type of reaction such as whether the type is condensation or addition. The crystallinity, orientation etc. depend upon the form of the monomers used, as for example in the solid phase one can expect high crystallinity and even epitaxy to develop. Extensive studies on the particle formation for polyvinyl chloride have revealed<sup>255-257</sup> that the particle size and shape not only depend upon the mode of reaction such as suspension, emulsion or bulk polymerization but also the process variables like the reaction temperature, stirring speed, suspension medium etc. However, such studies have not been reported for other polymers. In particular, no data are available on PPS. Nevertheless, one may well understand that the various parameters are bound to play an important role in the type of polymer particles produced.

As already indicated in Section 3.1, sodium sulfide is not completely soluble in the solvent used for the reaction. The state of sodium sulfide at the reaction temperature in NMP, is as tiny particles of less than 1 micron floating in the medium representing a suspension system in a solution of the other reactant PDCB. As the polycondensation reaction progresses, the growth takes place mainly on the solid-liquid interface with the solid particles acting as nuclei, the concentration of which is very high in the initial stages but drops at the latter stages of the reaction. However, it was noted that the total number of particles decreased with an increase in reaction time, indicating the possibility of considerable amount of coalescence taking place internally. This process seems to be present at the microscopic level rather than macroscopic one since the particle morphology did not give any indications of agglomerate formation.



### 5.3 EFFECT OF STIRRING SPEED ON POLYMER MORPHOLOGY

The polymer samples collected at the same reaction time of 6 hours but with different stirring speeds of 0, 400 and 660 RPM were analysed for their morphology. The particle size distribution is shown in Figure 68 for samples obtained at varying stirring speeds represented by curve nos. I, II and III. A comparison of these curves indicates that as the stirring speed is increased, the average particle size decreases and the distribution becomes progressively sharp. This seems to suggest that the coalescence process which has been outlined earlier is greatly affected by the agitation created in the medium. However, since the polymerization processes are also dependant on the stirring speeds, their correlation is not a simple one.

Figures 69, 70 and 71 show the scanning electron micrographs on the particles obtained in the polymer samples at 0, 400 and 660 rpm respectively. It is seen that large amount of polymer can build up as a single particle ( $> 12$  microns) with very complex internal structure, as revealed in Figure 70, at low stirring speeds (small amount of internal convectional currents exist in the case where no mechanical stirring was used). With the increase in stirring speed, the particles seem to develop more and more sheaf-like structure. There was practically no change in the crystallinity ( $\sim 66$  percent) with increase in stirring speed suggesting that crystallization rates were quite high. On the other hand, the particles obtained at high speeds (660 rpm), seem to have less porosity.

### 5.4 EFFECT OF DILUTION ON POLYMER MORPHOLOGY

In this set of experiments, the reaction time was set at 6 hours, but the concentration of the reactants were varied, keeping the stoichiometric

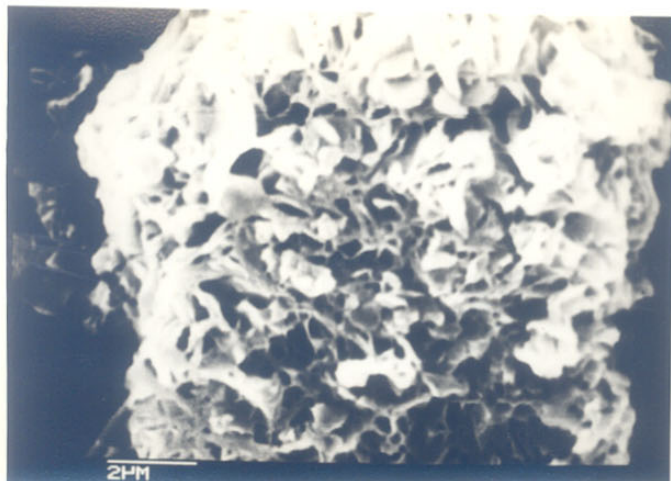


FIG.69

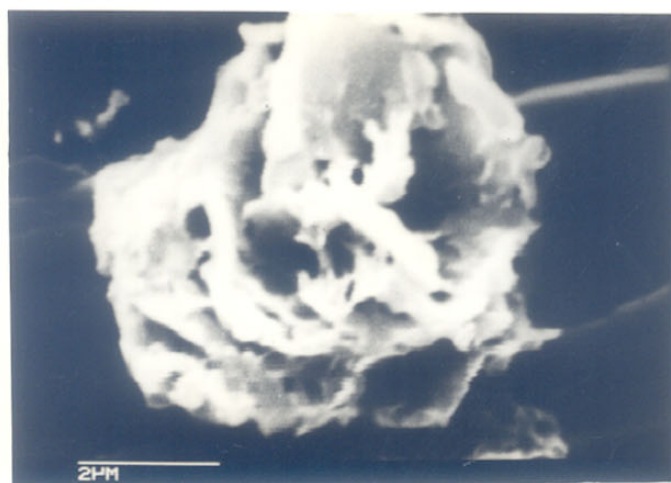


FIG.70



FIG.71

and reaction parameters identical. Some remarkable changes were noted in the morphology of PPS samples taken for analysis. Figures 73, 74 and 75 show the particle morphology, as revealed by SEM, when the initial concentration was decreased from 100 to 50 and 25 percent respectively representing a dilution factor of 1,2 and 4. In the normal case (dilution factor 1), the particles have more or less spherical boundaries but with internal sheaf-like structure, those for diluted reactants have an entirely different morphology and particle size. In the case where the dilution factor is 4 (Figure 75), the particle growth is very much restricted and their shape is oblong platelet like giving almost two dimensional appearance. It is interesting to note that this morphology is entirely different from that observed at low reaction time. This suggests that the neighbouring nuclei have a strong influence on the growth pattern of the polymer in the particular state. Further, the shape of the particles obtained under dilute conditions is almost two dimensional one while that for high concentrations of the reactants is a three dimensional one. The particle size distribution is also extremely sharp in the former case than in the latter, suggesting that the termination of the particle growth i.e. the upper limit of the size ( $S_t$ ) is mainly set by concentration of the reactants rather than other parameters.



FIG. 73

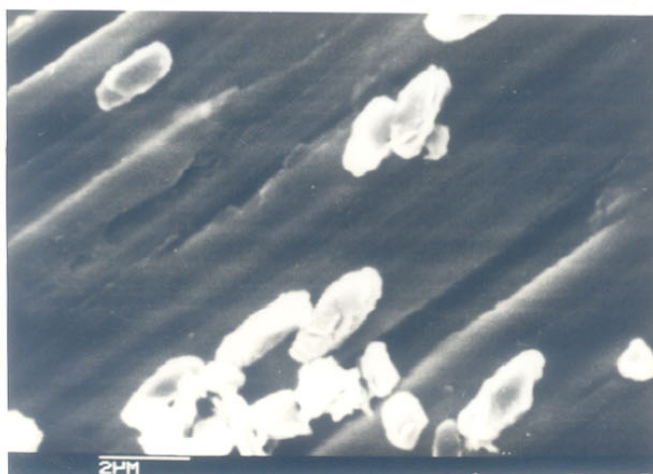


FIG. 74

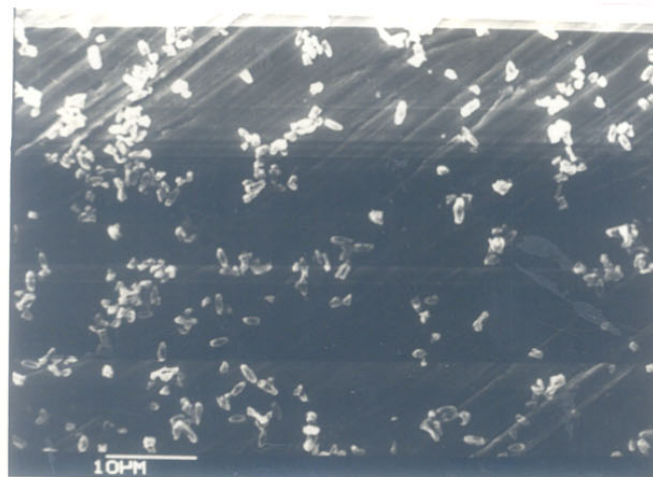


FIG. 75

SEM OF PPS PARTICLES WITH INCREASING DILUTION

### 5.5 CHARACTERIZATION OF STRUCTURE, CRYSTALLINITY AND MORPHOLOGY OF PPS FROM PDBB

The PPS polymer synthesized using PDBB as the reactant in place of PDCB was characterized for structure, crystallinity and morphology by means of x-ray diffraction and scanning electron microscopy in the same way as described earlier.

Figures 76 to 78 show the WAXS scan for the polymer obtained after the reaction time of 2.1/2, 7, 22, 45 and 180 minutes respectively. By comparing these curves, it is seen that the intensities of reflections occurring at  $2\theta$  18.6, 22.5, 25 and 28 degrees progressively decrease while those for the reflections at 19.2, 21 and 26 degrees increase with the increase in the reaction time ( $t_r$ ). These findings suggest that there is a reordering of the crystalline structure for the polymer with the increase in reaction time. These results are discussed later in the chapter.

The crystallinity ( $C_i$ ) was determined from the WAXS data in the same manner as for PPS synthesized from PDCB. The variation of crystallinity with the reaction time for the same concentration of reactants and stirring speed is shown in Figure 79 (curve I). It is seen that  $C_i$  increases slightly first from 62 percent to 68 percent with increase of  $t_r$  upto 45 minutes but with the further increase of reaction time, the crystallinity decreases gradually. This is in contrast to the findings in the case of PPS synthesized from PDCB where the crystallinity from the high value (74 percent) was found to decrease continuously with the increase of reaction time.

The growth of the particles was studied by means of SEM as before and curve II of Figure 79 shows increase of average particle size as a function of reaction time. It is seen that the particle size ( $S_t$ ) increases



---

**CHAPTER 6**  
**MECHANISTIC STUDIES**

---

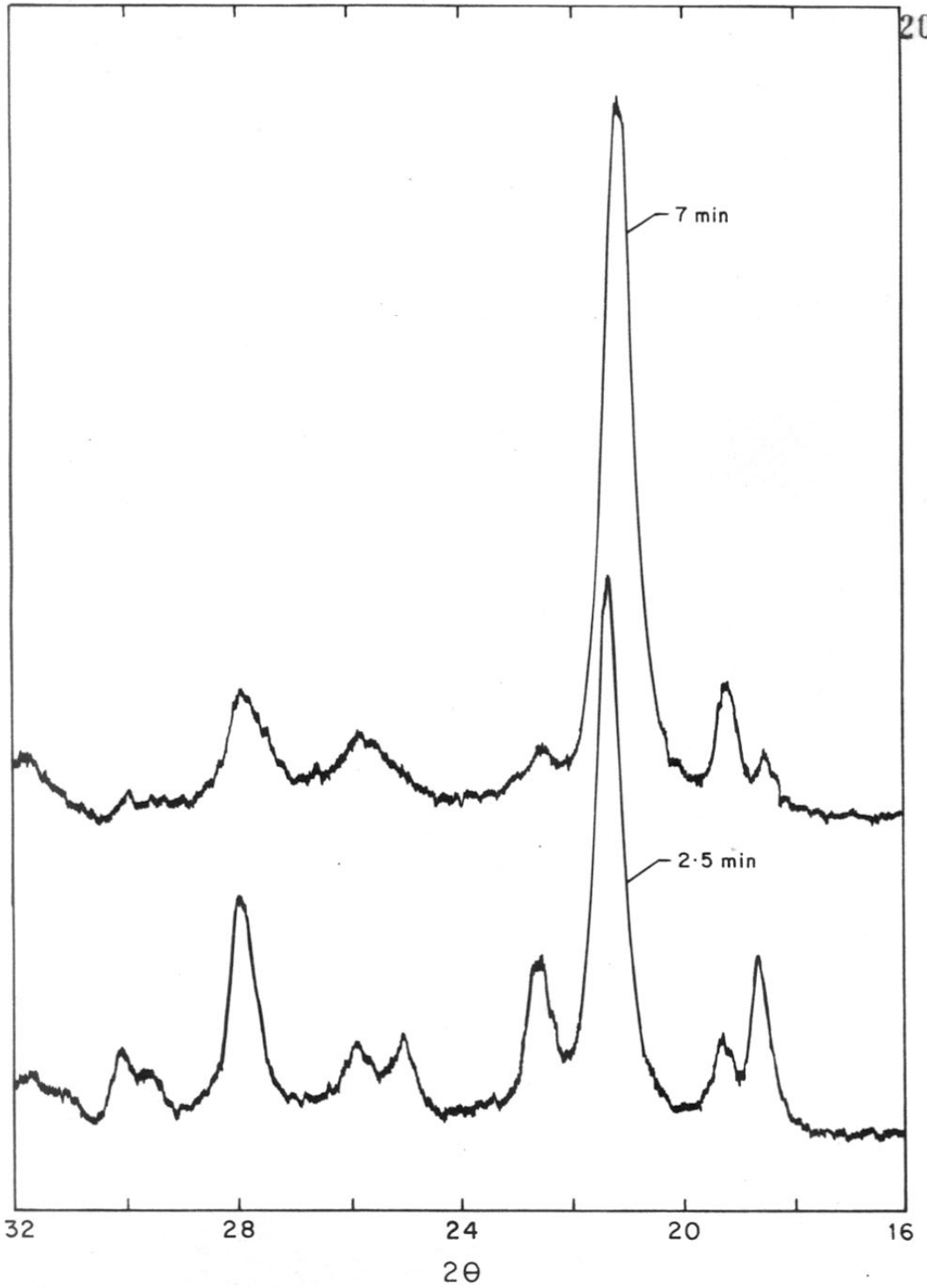


FIG.76 : XRD SCANS-2.5min, 7 min SAMPLES

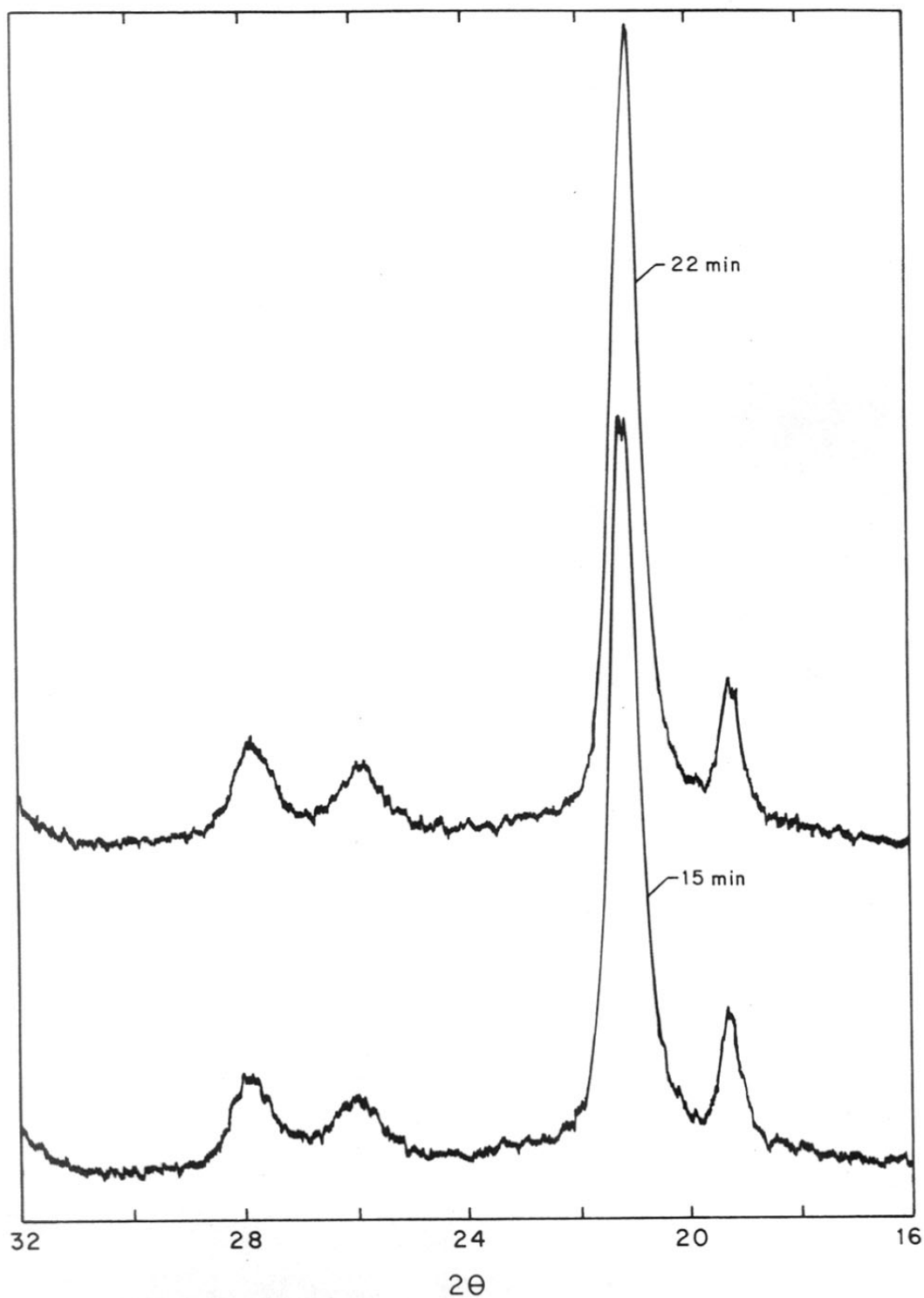


FIG.77 : XRD SCANS - 15 min, 22min SAMPLES



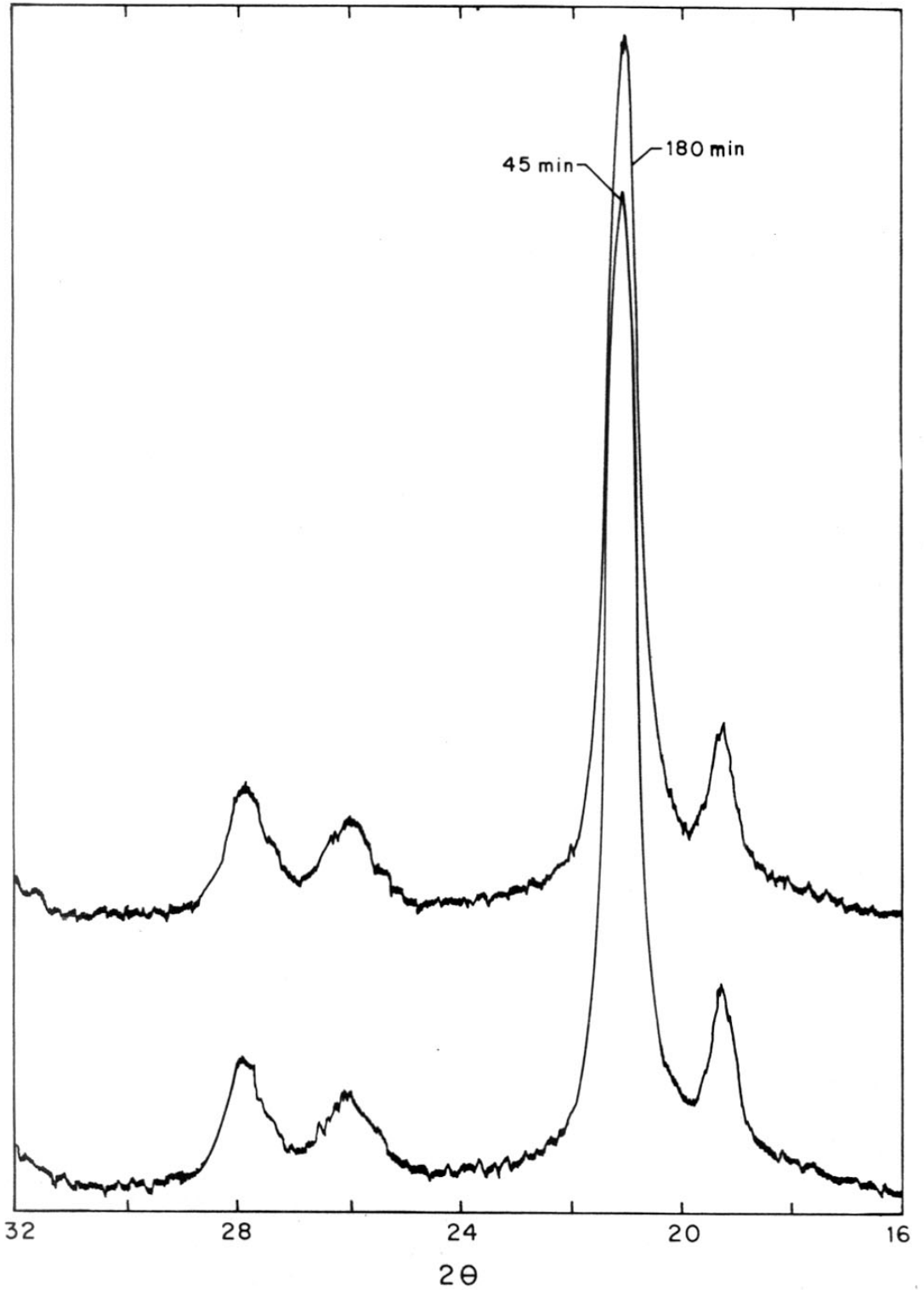


FIG. 78: XRD SCANS - 45 min, 180 min SAMPLES

rapidly with increase of reaction time upto a  $t_r$  of 60 minutes above which the particle size increases slowly to obtain a limiting value ( $S_\infty$ ). This behaviour is very similar to that noted for PPS synthesized from PDCB only with a difference that the time scales in the present case are very small (minutes) as compared to the former case (hours). Curve III in Figure 79 shows the variation of total polymeric mass obtained as a function of reaction time, other reaction parameters being maintained the same. In this case too, it is seen that the polymer yield ( $M_t$ ) increases rapidly with increase in  $t_r$  upto a reaction time of 45 minutes above which it gradually tends to a constant value (18 grams). These observations clearly indicate the polymerization reaction proceeds at a very rapid rate in the case of PDBB giving a large polymeric yield. However, the particle growth takes place at a slower rate and proceeds more or less uniformly over the reaction period studied.

In order to study the time dependance of the growth phenomena for both particle size as well as polymer yield, a plot was made as before of  $\ln(\Delta S/\Delta S_f)$  and  $\ln(\Delta M/\Delta M_f)$  versus  $t_r$  on a semilog scale as shown in Figure 80.  $\Delta S$  and  $\Delta M$  are defined as,

$$\Delta S = (S_f - S_t)$$

and  $\Delta M = M_f - M_t$  respectively.

Curve I is for the particle size growth while curve II is for the polymer yield. It is seen that the graph for the particle size growth is a linear one with a single slope suggesting that the time dependance for the particle size follows the equation,

$$S_t = S_f (1 - e^{-\alpha t})$$

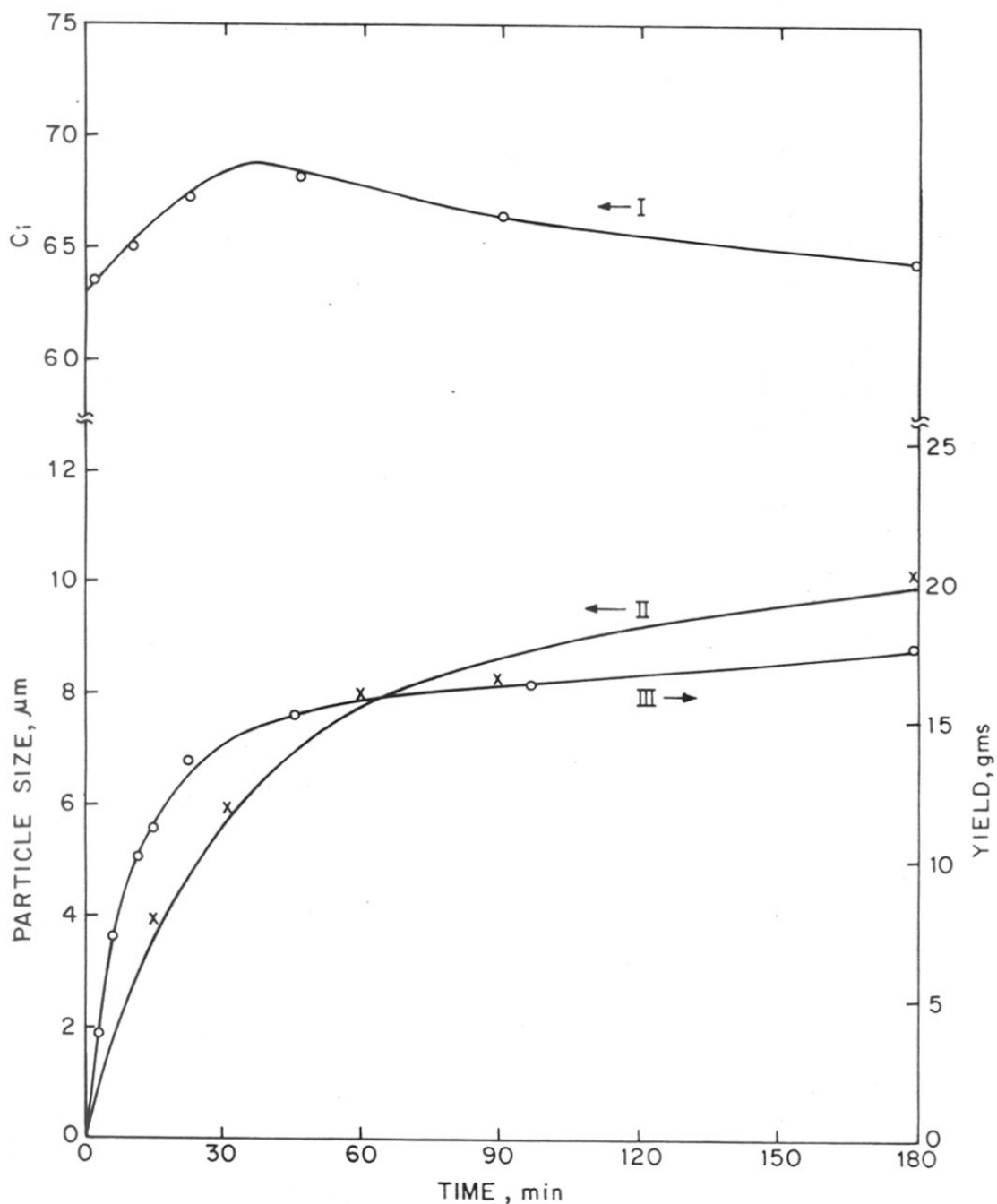


FIG.79: VARIATION OF CRYSTALLINITY (I), AVERAGE PARTICLE SIZE (II) AND TOTAL POLYMER YIELD(III) FOR PPS SYNTHESIZED FROM PDBB

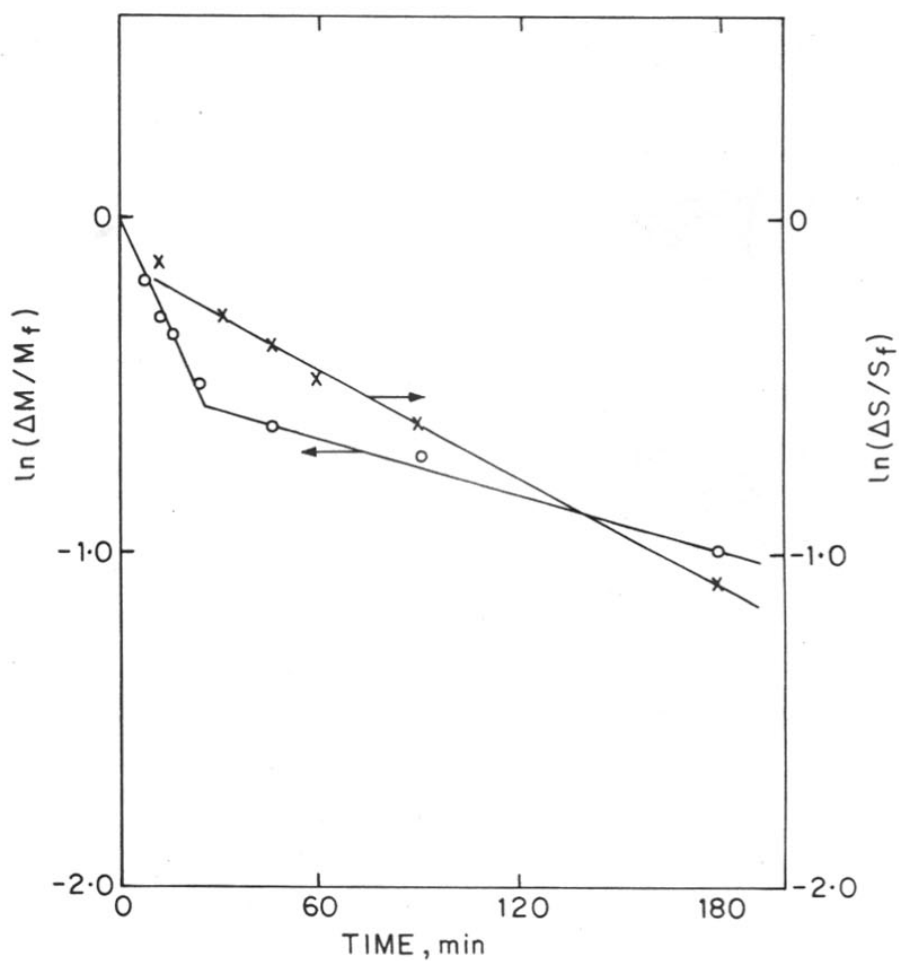


FIG.80: PLOT OF  $(S_f - S_t) / S_f$  AND  $(M_f - M_t) / M_f$  AGAINST REACTION TIME ON SEMILOG SCALE - PPS FROM PDBB

where  $\alpha$  is constant with a value of  $8.8 \times 10^{-5} \text{ sec}^{-1}$ .

The graph for the time dependance of the yield (curve II) on the other hand, does not appear to be a simple linear one. However, one may represent the graph in terms of two straight lines having different slopes as shown in the Figure 80. The slope in the initial region is estimated to be  $3.5 \times 10^{-4} \text{ sec}^{-1}$  while that in the high  $t_r$  region is seen to be  $4.7 \times 10^{-5} \text{ sec}^{-1}$ . Thus the reaction is seen to proceed at two distinct rates giving different yields with increase in reaction time. The time dependance of the yield nevertheless can be represented by the equation,

$$M_t = M_f (1 - e^{-\beta t})$$

with  $\beta = 3.5 \times 10^{-4} \text{ sec}^{-1}$  for  $t_r < t'$

and  $\beta = 4.7 \times 10^{-5} \text{ sec}^{-1}$  for  $t' > t'$

where  $t'$  is the delineating time (35 minutes) between the fast and slow processes.

The particle size distribution for PPS synthesized PDBB for various reaction times is shown in Figure 81. Curves I, II and III correspond to reaction time of 15, 30 and 180 minutes respectively. It is seen that the distribution of particles is quite sharp in all cases - namely the initial, intermediate and the final stages of the reaction (large  $t_r$ ). The peak position however is seen to shift to higher values of particle size with increase in reaction time. Figure(81a) shows the typical SEM of PPS particles obtained at a reaction time of 30 min. and it is clearly seen that most of the particles have similar shape and size indicative of very sharp particle size distribution. In the case of PPS synthesized from PDCB (page186), it was found that the particle size distribution was sharp at small reaction

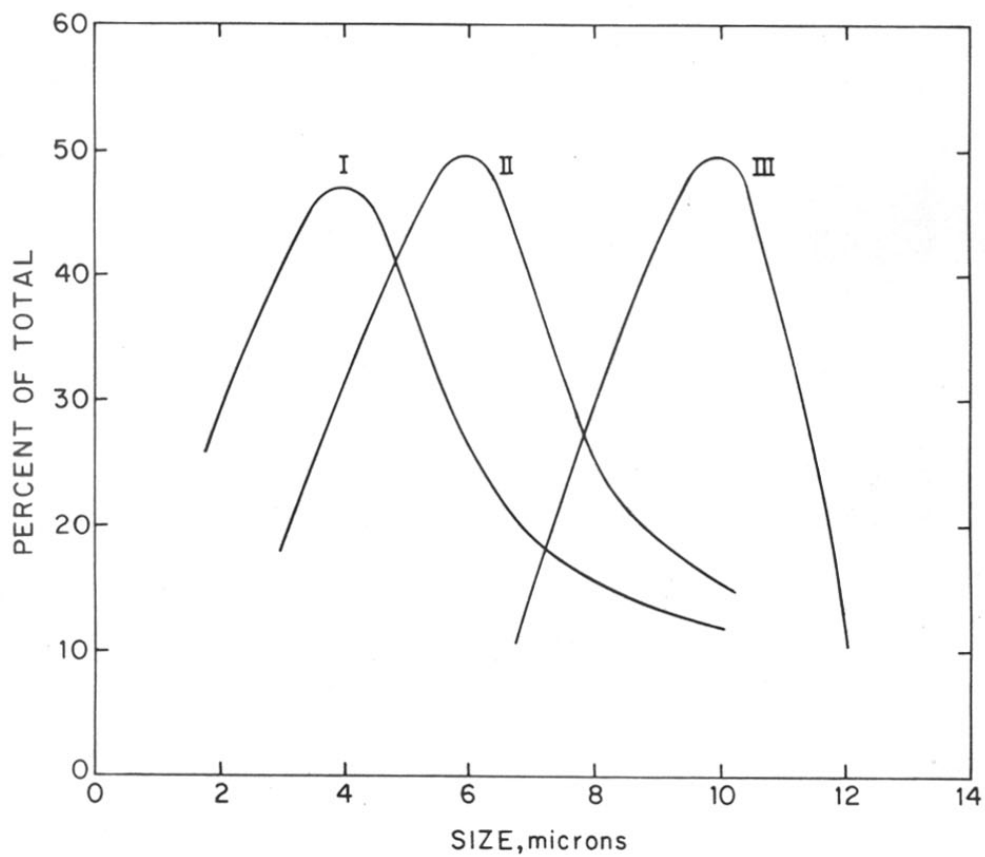


FIG.81: PARTICLE SIZE DISTRIBUTION IN PPS SYNTHESIZED FROM PDBB



FIG. 81(a)

SEM OF PPS FROM PDBB

times as well as for very large  $t_r$  while for the intermediate stages (3-6 hours), the particle size distribution was a broad one. In the present case, it has already been shown that the reaction is faster by an order of magnitude (see Chapter 3) and hence the growth is expected to be much faster than in the case of PPS synthesized from PDCB. However, since the particle size distribution is also sharp, it appears that either the termination rate is fast or the number of nucleating centers is large. Since the particles continue to grow even at large reaction times at which the maximum yield of polymer is obtained, the former possibility seems to be unlikely. On the other hand, the second possibility of large number of nucleating centers with high growth rate can give not only sharp distribution in particle size but also large number of particles in the total polymer mass. This has been confirmed during the SEM studies on the morphology of these particles.

Figure 82 shows the morphology of the PPS particles obtained at various reaction times. The photographs (a), (b) and (c) are for reaction times of 15, 30 and 180 minutes respectively. It can be clearly seen that the particles in all cases have more or less similar morphology consisting of flat, round disc shaped platelets with practically no variation in their shape but only in size. Further these morphological features were observed even for very large reaction times. By comparing these figures with Figures 65-68, it is seen that there is a remarkable change in morphology by the use of PDBB for the synthesis of PPS. While in the former case (PPS synthesized from PDCB) very intricate morphology of lettuce type, sheaf like or even peeled onion type was noted, that in the later case it was more or less uniform disc type. It is interesting to note that morphological features observed in the present case are somewhat similar



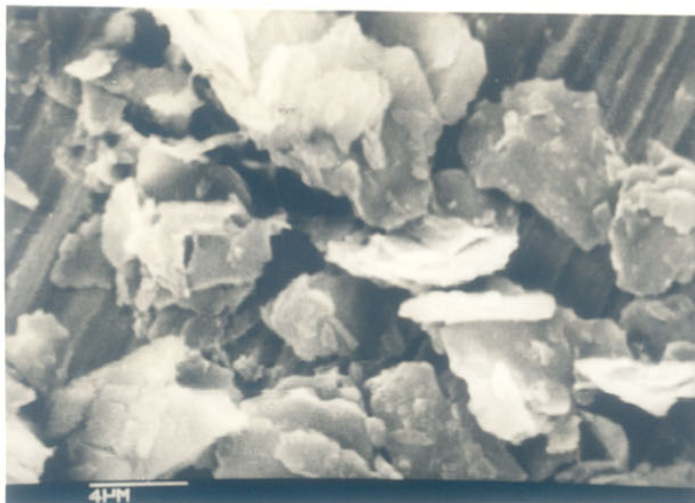


FIG.82(a)

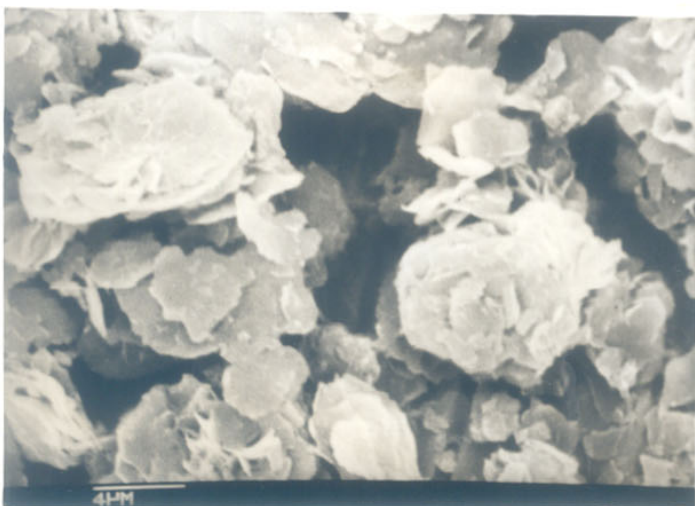


FIG.82(b)

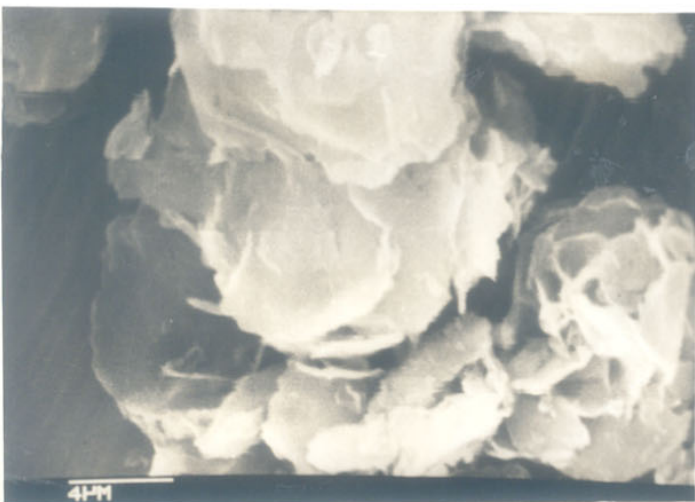


FIG.82(c)

SEM OF PPS FROM PDBB

to those seen in very dilute conditions of PPS synthesized from PDCB. (Figure 73-74), wherein the particles were also platelet shaped. However, the particle size noted there was very much smaller ( $< 2\mu\text{m}$ ) than in the present case.

Now, the growth and morphology of the polymer depend upon the nucleation and termination rate, type of polymerization, kinetics of reaction, the phase of the monomer and also on factors such as the presence of ionic impurities, aggregation, clustering or coalescence of polymer molecules/particles etc. Amongst these various factors, the dominating ones for the present studies seem to be related to the rate of reaction and presence of ionic species. Since these parameters are essentially varied by using PDBB instead of PDCB for the PPS synthesis. In the early stages ( $t_r < 15$  min.) of the reaction with PDBB, the rate being high, one would expect a large number of end groups to be present. These end groups would have to be incorporated in the subsequent growth of crystals. In order to accommodate such groups, the polymer crystal lattice would be distorted/modified. Such a modified lattice would give rise to additional peaks in the WAXS data which indeed have been observed by us (see Figure 76). As the polymerization reaction proceeds and the molecular weight builds up, the defects in the crystalline structure gradually reduce and more perfect crystals are available giving rise to increase in crystallinity and sharp diffraction peaks corresponding to the single orthorhombic type crystal structure of PPS described earlier (page 180). With further increase of reaction time, there would be corresponding increase of molecular weight and same processes which lead to the decrease of crystallinity as mentioned earlier would operate. Thus one finds the increase in  $C_i$  upto a reaction time of 35 minutes but a decrease in  $C_i$  for higher reaction times.

The time dependence of growth of polymer particle was found to be essentially similar to that for PPS synthesized from PDCB excepting for the fact that the constant  $\alpha$  had much higher value (four times) in the present case. On the other hand, increase of the polymer yield with reaction time showed two regions; one where the rate was very high having an order of magnitude higher than the PDCB case and the second region where the rate was comparable to that of the PDCB case. These findings correlate well with the reaction kinetics for the polymerization process of PPS synthesized from PDBB (see Chapter 3). It has been shown in that chapter, that the polymerization reaction with PDBB follows a two step process with rate constants of  $3.21 \times 10^{-4} \text{ l m}^{-1} \text{ s}^{-1}$  and  $3.87 \times 10^{-5} \text{ l m}^{-1} \text{ s}^{-1}$  for two regions. By comparing these values with that the values of the constant B in the two regions, it is seen that there is a good correlation between these values.

In addition to the polymerization process, the growth of the PPS particle also depends upon the termination rate as well as coalescence and other such phenomena. It was seen earlier that there was a considerable amount of coalescence taking place in the particle growth of PPS synthesized from PDCB. This was evidenced by the fall in the total number of particles with the increase of reaction time. In the present case the total number of particles ( $M_t$ ) in the polymer mass was estimated by taking into account the disc shaped morphology (cylinder shape) with known dimensions (from SEM), density of the polymer and yield for each reaction time. Table 29 shows the various values of  $M_t$ ,  $S_t$  and  $M_t$  for the various reaction time  $t_r$ . It can be seen from the table that the total number of particles decreases slightly with increase of reaction time but still remains within the same order of magnitude. It is interesting

TABLE 29  
GROWTH BEHAVIOR OF PPS FROM PDBB

$t_r$ (min)	Size $S_t$ ( $\mu$ m)	Yield $M_t$ (gms)	Total No. of particles $N_t$
15	4	9	$9.8 \times 10^{11}$
30	6	14	$9.7 \times 10^{11}$
60	8.0	15.5	$4.5 \times 10^{11}$
90	8.5	16.4	$4.0 \times 10^{11}$
180	10.5	17.8	$3.0 \times 10^{11}$

to note here that for PPS synthesized from PDCB on the other hand  $N_t$  decreased considerably (for same  $t_r$ ), much more than an order of magnitude (see Table 28). This clearly suggests that in the present case the polymer mass builds up by continuous nucleation of fresh particles and their growth as the reaction time is increased rather than the growth of the already nucleated particles as observed for PPS synthesized from PDCB. These observations together with the sharp well defined boundaries of the PPS particles noted in the SEM photographs reveal the important role played by the ionic species and the type of the group in governing the morphology of PPS.

#### Summary

To summarize, the structure, growth and morphology of PPS samples synthesized under various conditions were investigated by using x-ray diffraction and scanning electron microscopic techniques. The studies revealed that although the crystal structure remained the same, there is a slight variation in the crystallinity. The crystallinity was found to decrease from 71 percent to 66 percent with increase in reaction time. The growth of the particle size as well as the total polymer mass formed (yield in gms) follow the dependence represented

by an equation of the form,

$$X_t = X_0 (1 - e^{-\alpha t})$$

where,  $X_t$  represents the particle size or polymer mass at time 't' and  $X_0$  represents the value of these parameters at very large reaction times ( $t_r > 10$  hours). On the other hand, the total number of particles decreases with increase in reaction time.

The particle size distribution has been found to be dependant on the reaction time, stirring speed and the concentration of reactants in the feed. The distribution curve was noted to be sharp and centering at small particle size for short time, high speed and low concentration of the reactants. This was also the case for very large reaction times when the upper limit of the particle size was reacted, but there was asymmetry in the curve.

The particle size morphology showed a very strong dependance on various reaction parameters. In the initial stages, the particles have sharp well defined shapes reminiscent of crystalline materials but with increase of reaction time these develop into complex morphologies with sheaf-like structure. This is found to be true even for the polymers grown at different stirring speeds. In fact, the most intricate morphology was noticed in the PPS grown at very low rpm. The dilution of the reactants in the feed cause the particles to decrease in size and also to develop an oblong platelet type two dimensional morphology.

These results have been explained on the basis of the formation of nuclei for the growth of polymer and their subsequent growth and also to some extent coalescence with the neighbouring ones. Sodium sulfide

seems to give rise to the initial nucleating centres and the polymer growth phenomena are not yet well understood due to the complexities of the morphological features.

PPS as obtained from the reaction, is usually heat treated in air (oxygen atmosphere) below the melting point of the polymer for various end applications.<sup>258</sup> It is also treated with vapour of  $AsF_5$  for producing conducting grade compounds.<sup>259</sup> In these processes, the diffusion of gases into the polymer will be of great importance in deciding not only the various parameters such as temperature, partial pressure, time etc. used during the process, but also the ultimate properties that can be obtained after such treatment. On the other hand, in powder processing steps of PPS such as free sintering or coating, where powder compaction behaviour is involved, the particle size and shape will play an important role. Thus, it could be concluded that the control of the reaction time, stirring speed and the concentration of the reactants are essential to produce a proper polymer mass suitable for specific applications.

The results obtained above are consistent with the data obtained in the kinetic studies and thermal characterization. The change in rate observed after 3 hours of reaction, the optimum thermal properties attained after 3 hours of reaction time and the steady increase in viscosity upto 6 hours are consistent with the particle size growth upto 6 hours reaction time. It was also noted that optimum properties are obtained with a reaction time of 6 hours using the reference set conditions. The other notable observation that the dilution of the reactants has an important bearing on the PPS formed, rather than the change in stirring speeds, is clearly brought out in the morphological studies.

In the case of PPS synthesized using PDBB, it was noted that there was a reordering of crystalline structure with increase in reaction time. An initial increase in crystallinity from 62 to 68 percent upto a reaction time of 45 minutes is followed by a decrease in crystallinity with further increase in reaction time.

The particle size attained a limiting value after a reaction time of 60 minutes similar to PPS from PDCB except that the reaction times are very small. The particle size growth was linear following the equation:

$$S_t = S_f (1 - e^{-\alpha t}), \text{ where } \alpha = 8.8 \times 10^{-5} \text{ s}^{-1}$$

The distribution of particles was very sharp. SEM photographs show the morphology to be consisting of flat round disc shaped platelets while PPS synthesized from PDCB had intricate morphology like lattice type, sheaf like or pealed onion type. Other notable difference observed was that the total number of particles remained of the same order while that in the case of PPS from PDCB, there was a decrease in increasing reaction time by an order of magnitude.

The time dependance on yield followed an equation of the form,

$$M_t = M_f (1 - e^{-\beta t})$$

where  $\beta = 3.5 \times 10^{-4} \text{ s}^{-1}$  upto 35 minutes

and  $\beta = 4.7 \times 10^{-5} \text{ s}^{-1}$  beyond 35 minutes

The time dependance on yield exhibited two regions as a function of reaction. This was noticed in the kinetics also where two regions with different rates were observed.



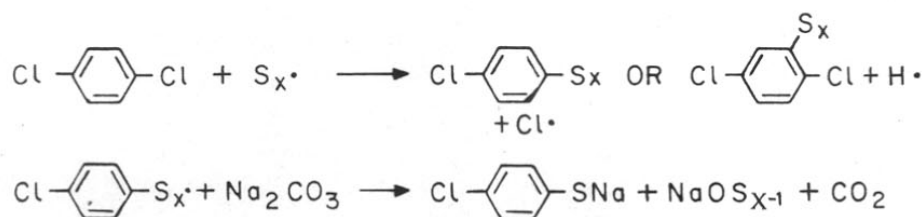
## 6. MECHANISTIC STUDIES

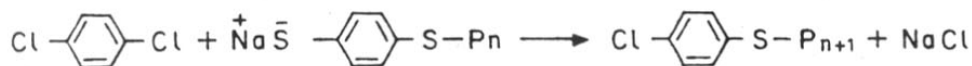
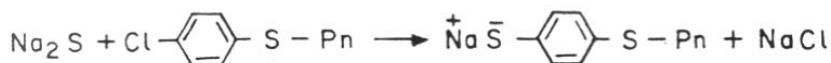
6.1 Polycondensation reactions leading to the formation of PPS have not been studied in detail. The different synthetic routes include the Macallum polymerization involving melt reaction of PDCB, sulfur and sodium carbonate;<sup>50</sup> solution polymerization of parahalothiophenoxide in pyridine at 250°C;<sup>54</sup> the homopolycondensation reaction of thiophenol in sulfuric acid at ambient temperature;<sup>132</sup> and the commercial route which involves the reaction of PDCB with sodium sulfide in NMP at high temperature and pressure.<sup>56</sup> In the present investigation PPS has been synthesized with PDCB-sodium sulfide reaction in NMP at 195°C. The substitution at the halide group, in unactivated aryl halides like PDCB is very difficult and the reaction conditions required are vigorous including high temperature and use of a polar solvent. It is therefore probable that the reaction takes place by aromatic nucleophilic substitution.

Published literature concerning the mechanism of the reactions for PPS synthesis is very limited. The reaction conditions in the various reported studies have not been identical and the mechanisms postulated are thus different. These are briefly discussed below.

The Macallum polymerization was postulated<sup>53</sup> to follow a free radical initiation (as the mechanism for the melt reaction of PDCB, sulfur and sodium carbonate) followed by nucleophilic substitution of aryl halide. The initiation and propagation reactions are represented below.

### Initiation

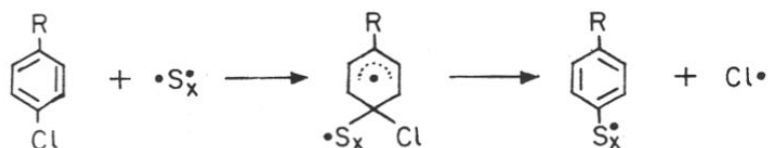




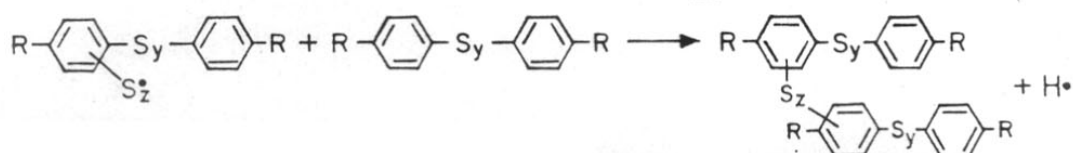
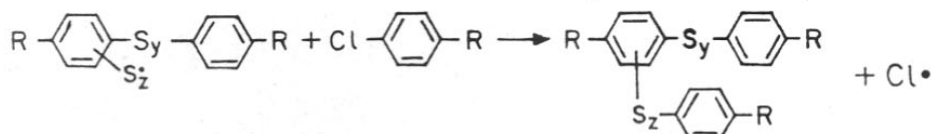
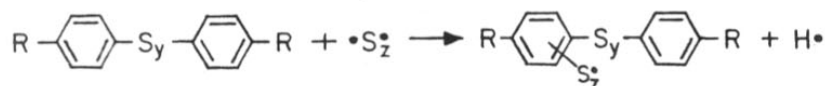
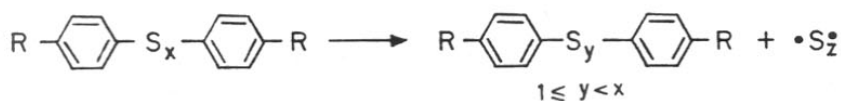
Sodium carbonate and sulfur react in the melt to form sodium sulfide during the course of the reaction.

Hortling and Lindberg<sup>260</sup> postulated an electrophilic radical reaction as the initial step in the reaction for the formation of PPS. The reactions were carried out by reacting substituted chlorobenzenes, sulfur and sodium carbonate in ampoules sealed under nitrogen at 300°C. The sulfur diradicals are not selective in their substitution reactions. The weaker bond C-Cl, in the benzene nucleus is attacked first followed by the C-H bonds leading to branched structures. The reactions are represented below.

#### Initiation

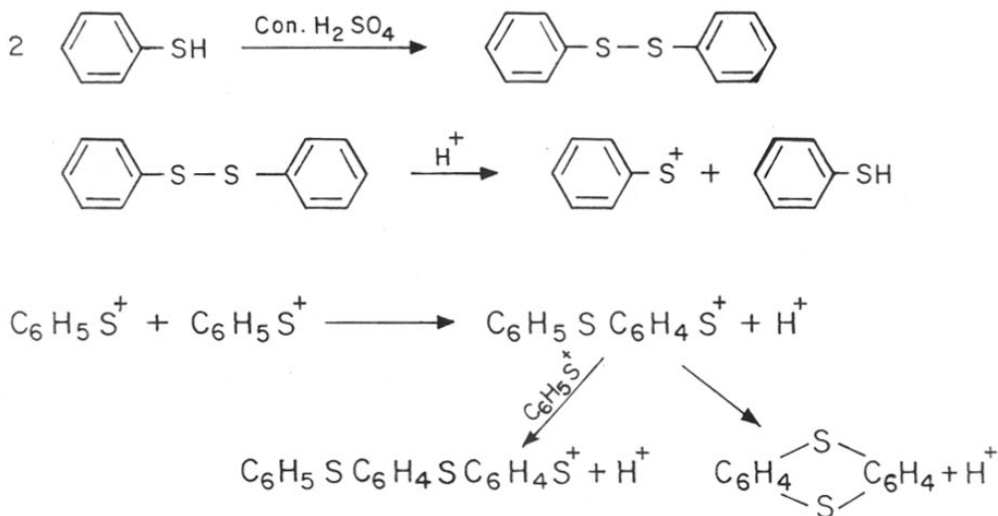


#### Propagation

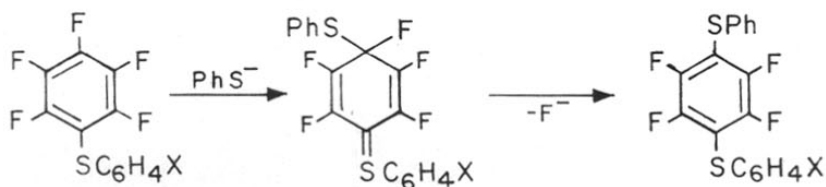


Aleksander Zuk<sup>261</sup> and coworkers proposed a free radical mechanism for the homopolycondensation reaction of thiophenol in sulfuric acid to generate PPS. The reaction scheme is as follows.

In the first stage diphenyl disulfide was formed, which heterolytically dissociated to generate sulphenyl ion and mercaptan. The latter steps involved p or o-substitution by elimination of a proton in each and thiantrene was formed as a by-product.



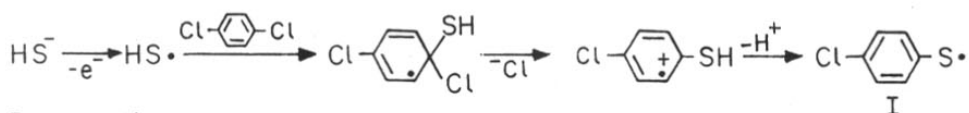
Birchall and coworkers<sup>262</sup> postulated an intermediate complex formation as the initial step in reactions involving fluorobenzenes. The reactions were reported to follow nucleophilic substitution reaction mechanism to yield polyfluoroarenes. With  $\text{PhS}^-$  as the nucleophile, the initial reaction could be represented as,



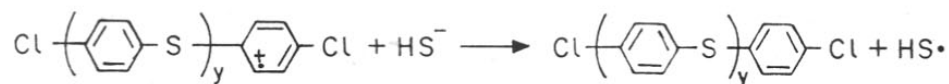
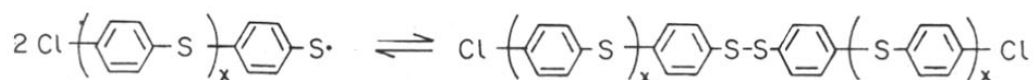
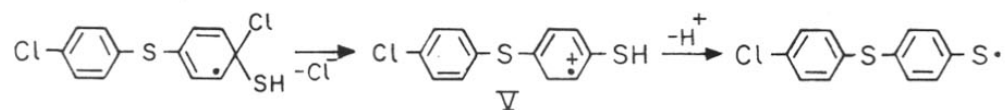
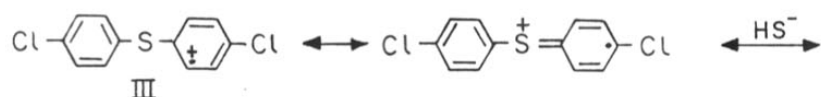
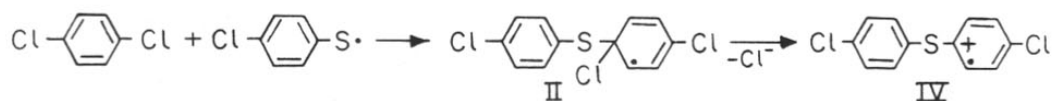
It was noted that the nucleophile attacked only the para position. It was suggested that compounds of the type  $C_6F_5H$ ,  $C_6F_5.SMe$  and  $C_6F_5.SH$  react with thiophenoxides by an addition - elimination type of mechanism and that nucleophilic substitution reactions of polyfluorinated aromatic compounds follow  $SN_2$  mechanism.

Although the commercial route for producing PPS involves the reaction of PCB with sodium sulfide in a polar organic solvent, there is little published information on the chemical mechanism of the process.

Recently Koch and Heitz<sup>263</sup> reported that PPS formation does not follow the conventional polycondensation process. They proposed a one-electron-transfer with radical-cations as the reactive intermediates. The initiation and propagation reactions were represented as follows:



Propagation



Thus five types of reactive intermediates I-V are formed and the presence of any of these species propagates the chain growth. It was also noted that the usual order of nucleophilic substitution namely  $\text{Aryl F} \gg \text{Aryl Cl} \approx \text{Aryl Br} > \text{Aryl I}$  is not followed. This contradictory results were also observed in the studies by Lenz and coworkers.<sup>54</sup>

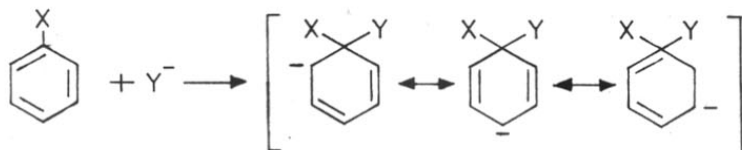
In the present investigation when PDCB was replaced by the bromo derivative PDBB, the order of the reaction was an order of magnitude faster as compared to PDCB. The studies also revealed that the reaction does not conform to the features of a conventional polycondensation and exhibits polymer formation at low conversion and presence of unreacted monomers at high conversions.

Aromatic nucleophilic substitution reactions may be categorized into three types from mechanistic considerations. These include  $\text{S}_\text{N}\text{Ar}$ ,  $\text{S}_\text{N}1$  and the Benzyne mechanisms and are discussed below.

(a) The  $\text{S}_\text{N}\text{Ar}$  mechanism

Most aromatic nucleophilic substitution reactions follow this mechanism, also referred to as the addition - elimination,  $\text{S}_\text{N}2$  and the intermediate complex mechanism. This reaction involves two steps.

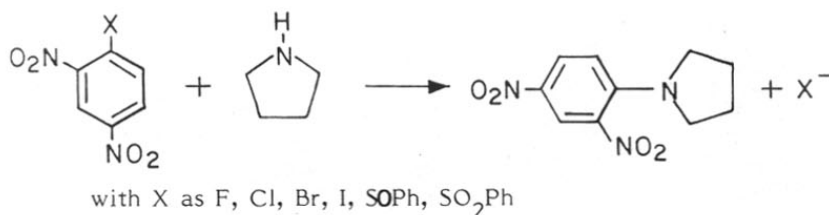
Step-1



Step-2



The first step generally, though not always, is the slower and hence the rate determining step. The second step becomes rate determining in only isolated cases where the aromatic nucleus is deactivated as in the case of trinitro ethoxy benzene with the ethoxy group as the leaving group. The rate of the reaction is only marginally affected by the nature of the leaving group.<sup>264</sup> A factor of about 5 was found in the reaction between the fastest and the slowest reactions shown below.



The reaction was the fastest with fluoride as the leaving group.

This type of reaction is catalysed by bases, only when a poor leaving group is present and the attacking nucleophiles are bulky amines.<sup>265</sup>

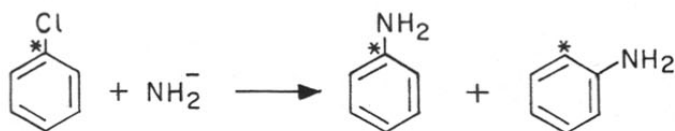
#### (b) SN<sub>1</sub> mechanism

This type of mechanism has not been observed for aromatic halides and is important only to diazonium salts.

The rate is first order with respect to the diazonium salt and independent of the concentration of the attacking nucleophile. The effect of ring substituents is also consistent with unimolecular rate determining cleavage. These reactions are not influenced by the presence of added species for catalytic activity. However, the nature of the leaving group markedly influences the rate of reaction, F<sup>-</sup> being the poorest leaving group. The rate of the reaction with the most labile leaving group is 3300 times higher as compared with the least labile group.

(b) Benzyne mechanism

This mechanism operates in reactions of aryl halides in the absence of activating groups. Generally, strong bases act as catalysts and the incoming group does not always take the place vacated by the leaving group. By labelling techniques it was shown that in the reaction of chlorobenzene<sup>266-67</sup> with sodium amide, the product consisted of equal amounts of aniline with substitution at the position vacated by the chloro group and ortho to it.



Thus ortho substituted aryl halides cannot be substituted and with electron donating groups, the substituting group is directed to the meta position.

In the present investigation, the following reactions were conducted to postulate a possible mechanism for the polycondensation reaction to form PPS.

- (i) Reaction of PDCB with sodium sulfide at a molar ratio of PDCB to  $\text{Na}_2\text{S}$  at 1.0614:1.
- (ii) Use of sodium parachloro thiophenoxide as a possible initiating species to catalyse the reaction.
- (iii) Effect of base catalyst such as sodium hydroxide.
- (iv) Use of excess PDCB at a molar ratio of 2.122:1.
- (v) Reaction of PDBB in place of PDCB with sodium sulfide at identical molar concentration and reaction conditions.

The variation in the concentration of the reactants especially the nucleophile, in this case sodium sulfide, did influence the rate. In reactions where excess PDCB was used, the initial rate was faster while no change should have been observed for  $SN_1$  reaction (Section 3.4). Also, if  $SN_1$  mechanism were to be operative, the reaction should be first order and independent of the nucleophile concentration. A considerable enhancement in the rate should be observable with the use of bromo derivative in place of the chloro derivative. The rate enhancement with PDBB was only an order of magnitude faster as compared to the PDCB reaction (Section 3.4.2.). Also the reactions were second order in nature in all the experimental variations studied. These observations rule out the  $SN_1$  mechanism being operative.

It is highly improbable that the benzyne mechanism operates in the reaction conditions specified for this investigation. The polymer formed has been found to have all para substituted backbone based on IR spectra. If benzyne mechanism were to be the only preferred route, meta linkages and to a small extent, ortho linkages should be observed in addition to the para substitution. These substitutions would lead to a non-linear chain structure adversely affecting the crystallizing ability of the polymer. In the present investigation the polymer formed has been found to crystallize readily. The observed thermal properties also point towards a para configuration.

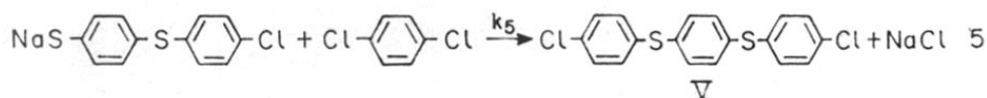
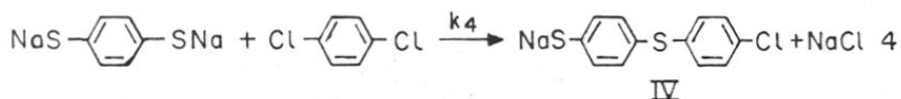
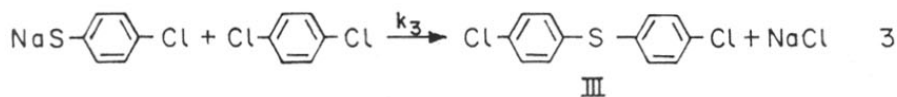
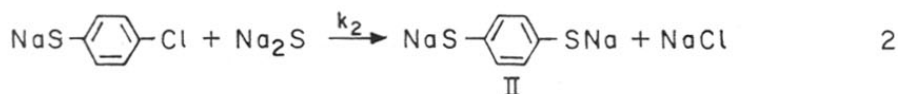
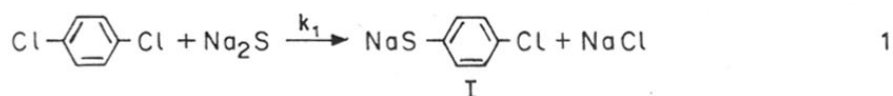
In technical literature, catalysis by added nucleophiles have been reported. Addition of sodium hydroxide to the reference set of PDCB-sodium sulfide system did not show any significant influence on the reaction rate. The concentration of sodium hydroxide used was 1.25 mole. The



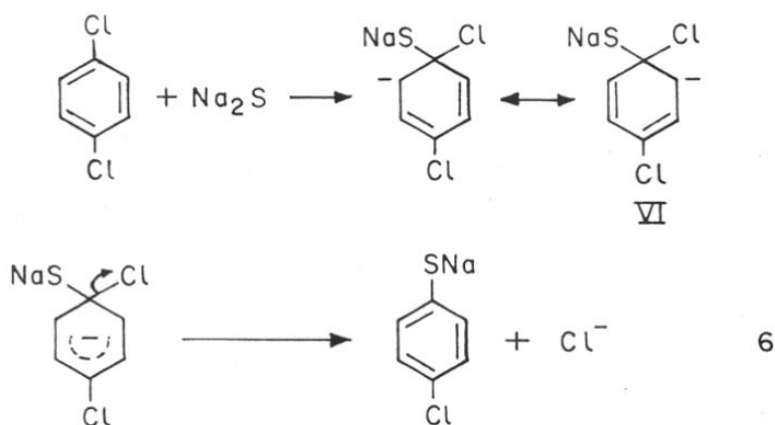
yield and viscosity data were within experimental limitations as compared to the system without the addition of sodium hydroxide. The above observations rule out the possibility of benzyne mechanism being operative.

In the system investigated as the reference set, where the molar concentrations of sodium sulfide and PDCB were 0.1923 and 0.2041 respectively, the concept of equal reactivity (proposed by Flory) is not valid. It is highly probable that the substitution of one functional group alters the reactivity of the second functional group of the same type, as observed in the case of reactions with diisocyanates. Published information on unequal reactivities due to functional variation in the course of reaction are available.<sup>268-69</sup>

It is very plausible that the following reaction sequences postulated to occur in the polycondensation reaction of PDCB and sodium sulfide have differing reactivities/rates. The overall rate is controlled by the slowest step. The reaction scheme could be represented as follows:



After the first step, the subsequent reactions may occur simultaneously. The first step to form sodium 4-chloro thiophenoxide could itself be represented as a combination of two steps. The exact nature of these two steps would be governed by the mechanistic considerations of the reactions. If the reaction occurs by  $S_NAr$  (also called  $S_N2$ ) mechanism, the initial steps could be represented as,



The generation of the transition state complex (VI) will be the rate determining step.

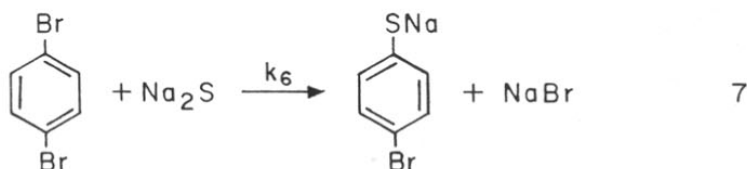
In the system investigated as the reference set, the initial product, sodium 4-chloro thiophenoxide (I) could either react with PDCB or sodium sulfide to generate compounds II and III. Compound (II) could add successively to two moles of PDCB to form compound (IV) and (V) respectively. These steps will have different rates since the end groups of the reacting species are - SNa in the case of step 4, whereas they are - Cl and - SNa in step 5. The reaction sequences to form higher oligomers could be envisaged to be kinetically identical to steps 2 and 5.

The kinetic observations for the system indicate the occurrence of two regions wherein the rate determining steps are different. In the initial region upto 50 percent conversion, the overall rate was slower than that in the second region beyond 50 percent conversion. In the reaction system, PDCB is totally soluble in NMP, while sodium sulfide is only partially soluble at the reaction temperature of 195°C. When observed under an optical microscope at the reaction temperature of 195°C, finely dispersed sodium sulfide particles were found to be floating in NMP. The particles were less than one micron in size. As polycondensation proceeds, the concentration of dissolved sodium sulfide in NMP falls below its saturated limitation allowing solid sodium sulfide to be solvated in NMP to maintain a saturated solution. The solubility constraints limit the possibilities of conclusively elucidating the reaction mechanism. However, logical conclusions can be drawn from the observations of the reactions investigated.

In the reference set of PDCB - sodium sulfide system, the initial slower rate was followed by a faster rate beyond 50 percent conversion. However, in the system where PDCB was replaced by the bromo derivative, PDBB, an initial faster rate was observed. It was followed by a slower rate identical to that observed in the PDCB- sodium sulfide system beyond 50% conversion. Bromine is a better leaving group and a significant increase in the reaction rate could be expected. However, on a comparative evaluation of the two systems, the initial rate in the case of PDBB-sodium sulfide system was only an order of magnitude faster than that observed in the reference set of PDCB-sodium sulfide. The two rates after 50 percent conversion however, were identical. This is an important observation.

In the absence of an exhaustive characterization, the relative amounts of different species present at various conversions cannot be evaluated. However, it can be said that on a statistical average, the predominant species present at 50 percent conversion in the two systems are sodium 4-chloro thiophenoxide and sodium 4-bromo thiophenoxide respectively. The two rate regimes observed for these two systems can be globally related to the generation and the relative rates of consumption of these two species.

The initial reaction in the case of PDBB-sodium sulfide could be represented as,

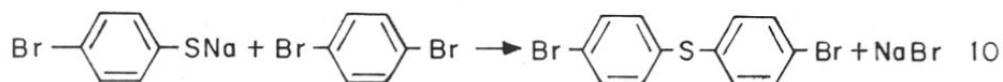
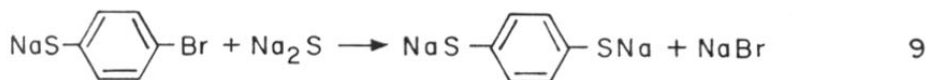


As per earlier discussion, assuming SN mechanism, the rate of formation of the transition complex would be faster with PDBB relative to PDCB. This could explain the faster rate observed with PDBB upto 50 percent conversion. The respective thiophenoxides could react towards product formation. Kinetically, it can be said that  $k_6 > k_2$  and  $k_3 = k_7 > k_1$ , where  $k_7$  represents the product formation from bromothiophenoxide on reaction with PDBB. In essence there is no difference in the rates of substitution involving the species,



The rate determining step in the latter half of the reaction could be the condensation of the halothiophenoxide either with the aromatic

dihalide or with sodium sulfide. The reaction steps for PDBB corresponding to steps 2 and 3 for PDCB may be represented as,



Since the overall reaction rates were comparable for both PDCB and PDBB reactions at conversions beyond 50 percent, it may be concluded that the rate determining step in this region is the reaction of the thiophenoxide with sodium sulfide (steps 2 and 9). The reaction rate in both the regions of conversions exhibited a second order kinetics.

The influence of the addition of sodium 4-chloro thiophenoxide on the reaction rate was investigated under reaction conditions identical to that for the reference set. The objective was to evaluate whether the addition of sodium 4-chloro thiophenoxide, the product of the first step in the reaction scheme, to the reaction mixture enhances the initial rate of reaction in comparison to the reference set. This is highly logical as the growth mechanism observable after 50 percent conversion can be brought into play at the start of the reaction itself. Also, it would have conclusively proved that the first rate determining step was the generation of sodium 4-chloro thiophenoxide. The mole ratio of sodium 4-chloro thiophenoxide used in the investigations, relative to the PDCB concentration was 0.0156. In this concentration range, no perceptible rate enhancement was observed. Rather, the rate enhancement was within experimental errors of observations. In order to be able to investigate this aspect, the homopolymerization behaviour of sodium 4-chloro thiophenoxide with

the same reaction conditions will have to be evaluated.

## 6.2 INFRARED SPECTROSCOPY

General structural features in polymers can be identified by Infrared (IR) spectroscopic studies. The IR absorptions are in the form of sharp, well defined vibrational absorptions in the infrared region and can be related to the various modes of stretching, bending and rotation related to the functional groups present in the polymer. It is expected that the long chain character of polymers will present a very complex absorption spectrum. However, it is observed that the absorptions correspond to only the functional groups as well as the configuration, conformations involved. IR spectra of commercial PPS sample (Ryton) have been catalogued. A comparison of the spectra obtained for the PPS samples investigated (reference set) with that reported for Ryton enables easy relative evaluations as compared to the tedious work of peak identification for new polymers.

(a) The polymer samples investigated in this study are soluble only in 1-chloronaphthalene above 160°C and form a swollen gel at room temperature. Attempts to form films for the IR studies were unsuccessful. The IR spectra were taken of the powder samples in Nujol.

The IR peak locations and intensities for the samples prepared in the investigation were in good agreement with the data reported for linear PPS.<sup>270</sup> The IR spectra are shown in Figure 93.

(b) Extractions with methylene chloride : Methylene chloride extraction of PPS is known to isolate 4 and 5 membered ring compounds.<sup>270</sup> The samples synthesised in the present investigation (reference set) gave buff coloured powder in the range of 3 to 4.5 percent on methylene chloride extraction. In comparison, the commercial sample had over 9 percent

as methylene chloride extractables. The IR spectra of methylene chloride extractables from the present investigation are shown in Figure (84). The spectra compares well with the reported extractions.

In summary, it is postulated that the formation of PPS by polycondensation of PDCB with sodium sulfide in NMP at 195°C operates with  $SN_2$  mechanism.

The experiments in the present investigation were conducted at the temperature of 195°C versus the commercial process at 265°C. A lower percent of 4 and 5 membered cyclic structures are likely to be formed at lower temperatures and is reflected in the results. Therefore, it is concluded that the polymer formed at 195°C has essentially a linear structure with low percentage of cyclic moieties.

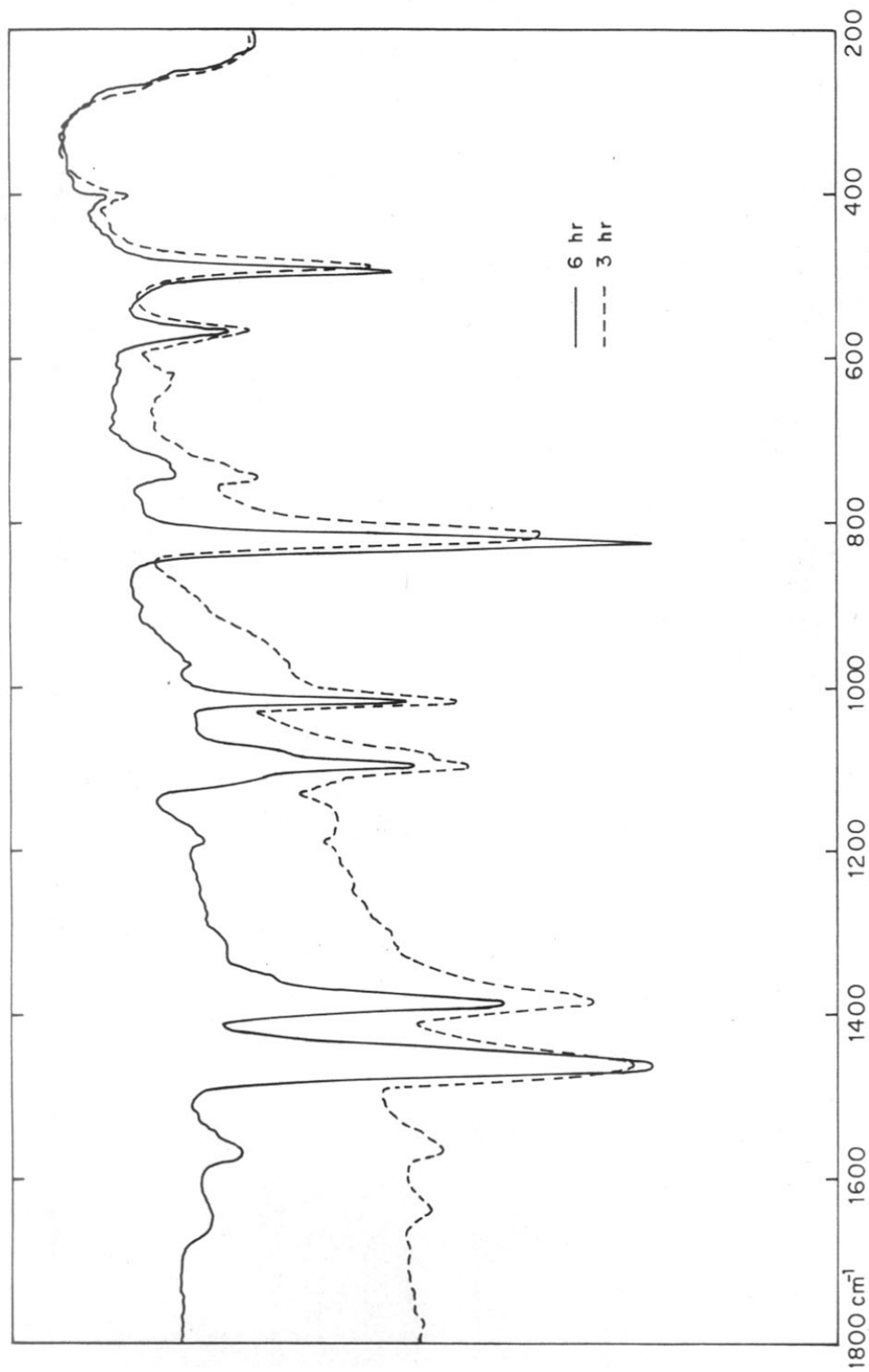


FIG. 83 : IR SPECTRA OF 6 hr AND 3 hr SAMPLE



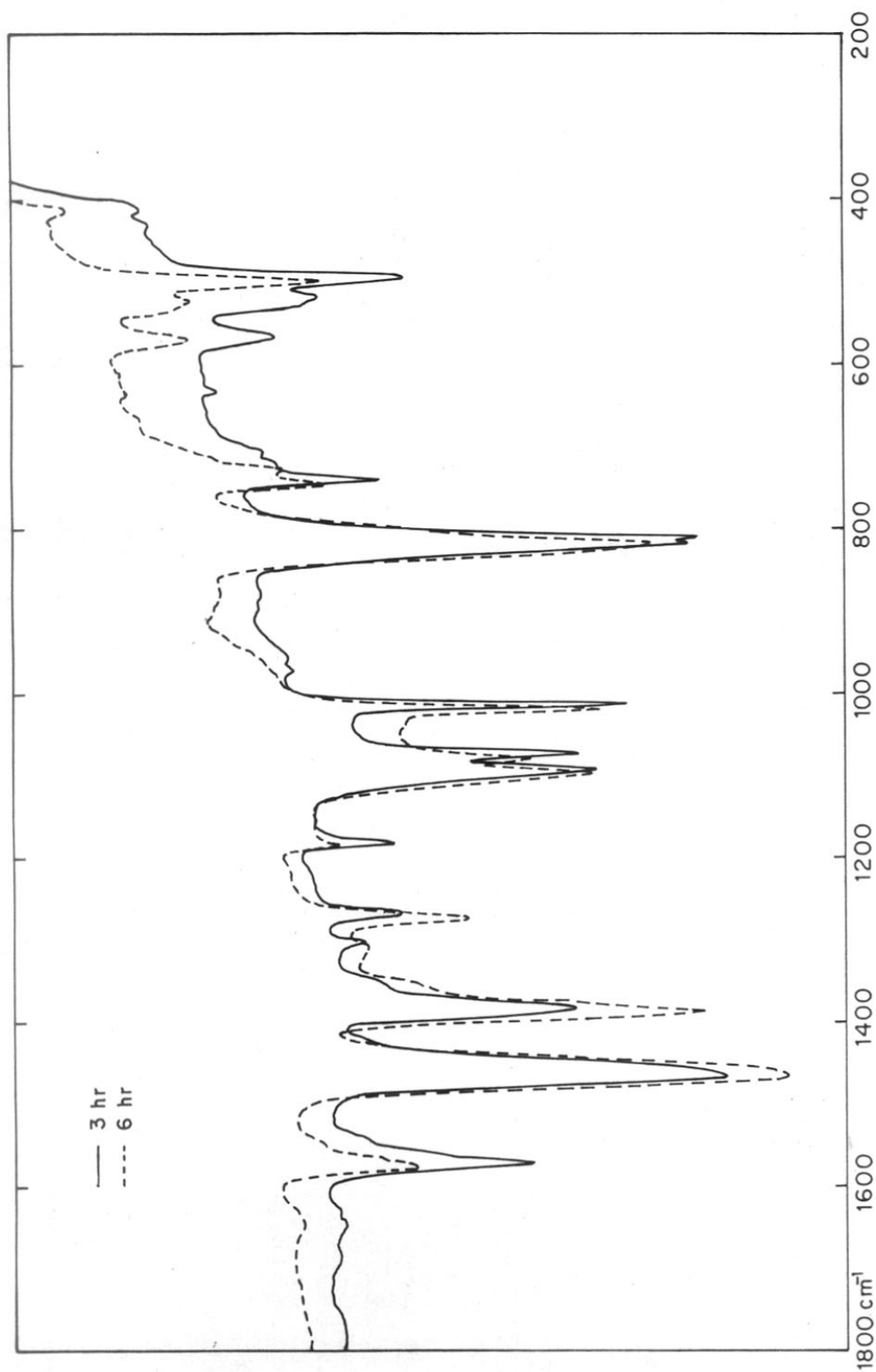
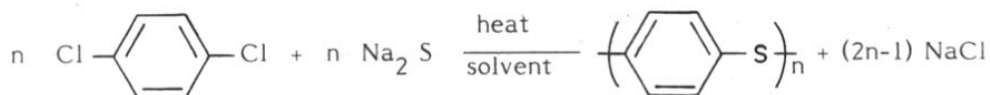


FIG.84: IR SPECTRA METHYLENE CHLORIDE EXTRACT

### SUMMARY AND CONCLUSIONS

The polycondensation reaction to generate PPS involves the reaction of 1,4-dichlorobenzene (PDCB) and sodium sulfide in a highly polar solvent like N-methyl pyrrolidone (NMP). The reaction could be represented as,



In the actual commercial process of Phillips Petroleum, the reaction temperature is set at 265°C which generates a pressure of > 160 psi.

In the present investigation, the reactions were conducted at 195°C and a pressure of about 35 psi. The following aspects concerning the polycondensation reaction were investigated.

(1) Kinetics of polycondensation with concurrent characterization of the degree of polymerization with reaction time by microanalysis and dilute solution viscosity measurements.

(2) The effects of physical reaction parameters such as stirring speed and dilution on the yield and degree of polymerization.

(3) Thermal characterization by differential scanning calorimetry and thermogravimetric analysis to elucidate structure development in polymerization.

(4) Morphological characterization by x-ray diffractometry and scanning electron microscopy to illustrate interaction between kinetics and structure development.

(5) Mechanistic studies involving the variation of reactants to postulate a possible mechanism for the reaction.

The polycondensation kinetics were studied with the reaction of PDCB with sodium sulfide at a molar concentration of 1.0641:1. This was used as the reference set. The synthesis of PPS was found to differ from the conventional polycondensation reactions in the following aspects.

- (i) The polymer yield was significant even at very low conversions.
- (ii) The presence of unreacted monomers was noted even at conversions as high as 97 percent.
- (iii) The polymer precipitated during the course of the reaction. However, the molecular weight of the polymer was found to increase continuously with reaction time indicating that the polymerization continued even after precipitation of the low molecular weight oligomer.
- (iv) The kinetic data showed a second order dependence with two distinct regions of reaction rates. The initial reaction rate was slower upto 50 percent conversion. This was followed by a faster rate from 50 to 97 percent conversion.

The effect of physical and chemical parameters on the kinetics and molecular weight development was studied by conducting the following experiments.

- (a) Variation in reactor geometry . Teflon versus stainless steel reactor.
- (b) Variation in the speed of agitation and extent of dilution under the standard set of conditions.
- (c) Use of sodium parachloro thiophenoxide (SPCTP) as initiating species.
- (d) Use of large excess of PDCB.
- (e) Use of paradibromobenzene (PDBB) in place of PDCB.

The kinetic data obtained in the stainless steel and Teflon reactor were comparable. In experimentations to evaluate the effect of stirring and extent of dilution, the reaction time was fixed at 6 hours while the other parameters were unaltered from those in the reference set. The polycondensation reaction was found to be extremely sensitive to the extent of dilution. Variance in stirring affected the reaction, in comparison, only marginally. The yield and degree of polymerization dropped significantly with increasing dilution.

In the case of the experiments where SPCTP was used, no significant change in the rate was observed. The variation in rate was within experimental limitation. However, the regimes over which two different rates were observed did vary. The initial slow rate was observed upto 36 percent conversion when SPCTP was used versus 50 percent for the reference set.

In reactions wherein a large excess of PDCB was used, the rate was evaluated by using the valid non-stoichiometric equation. The notable feature in this system was the observation that the rate in the later part of the reaction was an order of magnitude slower as compared to the initial rate. The observed trend was thus reversed as compared to the reference set where an initial slower rate was followed by a faster rate in the later stages of the reaction.

In the experiments wherein PDBB replaced PDCB, a conversion of about 50 percent was achieved after a short reaction time of only 10 minutes, whereas in the reference set with PDCB, the half-way point was reached after 2 1/2 hours. The initial reaction rate in this system was an order of magnitude faster as compared to the reference set. The rate in the later part of the reaction was however identical to that observed for the reference set.

The reference set samples were characterized for the number average molecular weight by microanalysis for estimation of chlorine end groups. It was noted that the polymer molecular weight increased with reaction time inspite of polymer precipitation during the reaction once a critical molecular weight was attained. The intrinsic viscosity measurements in 1-chloronaphthalene were made by a single point relative viscosity determination. The intrinsic viscosity levelled off after a reaction time of 6 hours, but the molecular weight as estimated by microanalysis continued to increase further with reaction time. The polymer thus has a wide molecular weight distribution.

The thermal transitions of the reference set were studied using differential scanning calorimetry. The notable feature of the thermograms was the presence of multiple first order transitions in the first heating cycle, which disappeared in the subsequent heating cycle (from the melt crystallized state). The crystallization peaks were however identical. The thermogram from the first heating cycle corresponds to the morphology of the as-precipitated state versus the morphology in the melt crystallized state in the subsequent scans. The differences due to the change in morphology with thermal conditioning were thus brought out in these studies.

The thermogravimetric analysis of the samples were evaluated in air. The polymer samples differed in the concentration of  $-SNa$  end groups. While the polymers formed at low conversions had high concentration of  $-SNa$  end groups, those formed at higher conversions would be relatively richer in  $-Cl$  end groups. This was reflected in the residue formed as a function of reaction time. The polymer samples formed at lower conversions were thermally less stable. A polymer of thermal stability comparable to commercial sample Ryton V-1 was obtained after a reaction time of 6 hours.

The structure, growth and morphology of the polymers synthesized were investigated by x-ray diffractometry and scanning electron microscopy. It was found that the crystal structure was unaffected while the percent crystallinity decreased marginally with increase in reaction time. The growth of the particle size as well as the total polymer mass formed was found to follow a time dependence of the form,

$$X_t = X_o (1 - e^{-\alpha t})$$

where,  $X_t$  represents particle size or mass at time 't', and  $X_o$ , the value of the parameter at large reaction times.

The total number of particles however decreased as the reaction time was increased. The particle size distribution was found to be dependant on the reaction time, stirring speed and also the concentration of the reactants in the feed. The distribution curve was noted to be sharp, containing at small particle size for short reaction time, high speed and low concentration of the reactants.

The particle morphology showed very strong dependence on reaction parameters. The polymer particles obtained initially have sharp, well defined shapes reminiscent of crystalline materials. With increasing reaction time, these develop complex morphologies with sheaf-like structure. This was found to be true for polymer formed at different stirring speeds. Most intricate morphology was noticed in the samples synthesized at very low rpm. The dilution of the reactants in the feed, caused the particles to decrease in size and also to develop an oblong platelet type two dimensional morphology. The results lead to the conclusions that control over reaction time, speed of stirring and concentration of the reactants in the feed are necessary to produce a polymer suitable for specific applications.

### RECOMMENDATIONS FOR FUTURE WORK

(1) The effect of halide substituent on the benzene ring could be studied by reacting sodium sulfide with PDCB, PDBB and para diiodobenzene (PDIB). The trend studied with PDBB and PDCB predict a faster rate at least in the initial stages for the PDIB reaction.

(2) The role of the group at para position to the substitution center could be revealed by the reaction of sodium sulfide with 1-chloro, 4-bromo benzene. The determination of the relative rates of formation of sodium chloride and sodium bromide will be a valuable pointer. Reactions with PDBB indicated a faster rate in the initial stages of the reaction. If this is primarily governed by the bromo group para to the substitution center rather than the leaving group itself, similar trend should be noted for the generation of sodium chloride in this system as well.

(3) Homopolycondensation reactions of sodium parachloro thiophenoxide and sodium para bromothiophenoxide would also help, in deducing the effect of halide centre at the para position. Reactions with PDCB and PDBB indicate that the reaction rates might be comparable. This system would also confirm whether the rate of the reaction is uniform or bimodal.

(4) Molecular weight build up by using a comonomer like dichloro diphenyl sulfone can be studied to prepare copolymers that could be used directly for various end applications. PPS synthesized with PDCB and sodium sulfide requires molecular weight enhancement for molding grade applications.

(5) Addition of reagents like pyridine to the reactants, that would increase the electron density around the halogen atom that is to

be eliminated could be explored. This step would assist the escape of the halogen as an ion from the aromatic nucleus.

(6) ESR studies to evaluate conclusively whether the mechanism is  $S_NAr$  or has free radical characteristics as recently reported.

(7) Systematic evaluation of molecular weight build up and molecular weight distribution as a function of reaction time for the system PDCB-sodium sulfide.





---

REFERENCES

---

REFERENCES

1. Plastics and Rubber International, Vol. 9, No. 4, 22 (1984).
2. Edgar, O.B. and Hill, R., J. Poly. Sci.,8, 1 (1952).
3. Modern Plastics Encyclopaedia, Vol. 58, 10A, (1981-82).
4. Plastics Engineering, 36, No. 6, 18 (1980).
5. Grenvresse, P., Bull. Soc. Chim. Fr.,17, 599 (1897).
6. Plastic Technology, Vol. 31, No. 7, Mid June, p. 564 (1985).
7. Gaylord, N.G., in 'Polyethers', High Polymers, Vol. XIII, Part III, Interscience Publishers, a division of John Wiley & Sons, N.Y. p. 31 (1962).
8. Smith, H.A., Rubber and Plastic Age, 44 (9), 1048 (1963).
9. Mario Russo, Mater. Plast. Elastomeri, 34 (1), 61 (1968).
10. Smith, H.A., Encyclopaedia of Polymer Science and Technology, 10, 659 (1969). Interscience Publishers, N.Y.
11. Hill (Jr), H.W. and Edmonds (Jr), J.T., Amer. Chem. Soc., Div. Org. Coats, Plast. Chem. pap. 30, 199 (1970).
12. 'PPS, a plastic with unique properties,' The Sulfur Institute Journal, 7/3 (1971).
13. Jones, R.V., Hydrocarbon Process, 51 (11), 89 (1972).
14. Hill (Jr), H.W. and Edmonds (Jr), J.T., Polymer preprints Amer. Chem. Soc., Div. Poly. Chem., 13, 603 (1972).
15. Short, J.N. and Hill (Jr), H.W., Chem. Tech., 481 (1972).
16. Bailey, G.C. and Hill (Jr), H.W., New Industrial Resins, R.D.. Deanin ed., ACS Symposium Series 4, 83 (1972).
17. Iwata Shozaburo Purasuchikkusu (Jap), 25, 24 (1973).
18. Hill (Jr), H.W. and Brady, D.G., Adv. Chem. Series, 129, 80, (1973).

19. Baerecke, W., Int. Poly. Sci. and Tech. Vol. 1, 9 (1974), Muamyag Gumi (Hung.), 11 (2), 53 (1974).
20. Jones, R.V., Polymer Age, 5 (6), 166 (1974).
21. Jones, R.V. and Hill (Jr), H.W., Adv. Chem. Series, p. 140 (1975).
22. Hill (Jr), H.W., Werkman, R.T. and Carrow, W.E., Adv. Chem. Series, p. 134 (1974).
23. Hill (Jr), H.W. and Brady, D.G., Adv. Plast. Tech. Annu. Pac. Tech. Conf., Tech. Displ., 1st SPE, 96 (1975).
24. Steele, R., Aust. Plast. Rubber, 26, 15 (1975).
25. Theberge, J., Arkles, B. and Gould, P., Tech. pap. Reg. Tech. Conf., Soc. Plast. Eng. Oct. 7-8, 164 (1975).
26. Callatay, G. and Autin, J., Rev. Plast. Mod. (Spanish), 30, 841 (1975).
27. Craig, R.F., Soc. Plast. Eng. Tech. pap. 22, 141 (1976).
28. Houston, A.M., Mater. Eng., 84, 36 (1976).
29. Murray, J.N., Soc. Plast. Eng. Tech. pap., 22, 259 (1976).
30. Callatay, G. De. and Autin, J., Plast. Mod. Elastomers (Fr), 28, 40 (1976).
31. Penczek Irena Baily Jan, Polimery (Pol), 21, 197 (1976).
32. Callatay, G. De., Munyag Goumi (Hung), 14 (5), 129, (1977).
33. Brady, D.G. and Hill (Jr), H.W., Mod. Plast. 51 (5), 60 (1976), Plastic World 35 (2), 30 (1977).
34. Callatay, G. De., Plast. Electron. Microelectron Plast., p. 21, (1978).
35. Hill (Jr), H.W., Tech. pap. Reg. Tech. Conf., Soc. Plast. Eng., May 5-8, 501 (1980).
36. Kovacs, L., Korroz Figy (Hung), 20 (2), 60 (1980).

37. Dominghaus, H.F., *Feinwer Tech. Mass. Tech. (Ger)*, 88, 310, (1980).
38. Brady, D.G., *J. Appl. Poly. Sci., Appl. Polym. Symp.*, 36, 231 (1981).
39. Jandelli Pierantonid, *Technopolim. Resin (Ital.)*, 6 (5), 37, (1981).
40. Hill (Jr), H.W. and Brady, D.G., in *Kirk-Othmer Encyclo. Chem. Tech.* 3rd edn. 18, 793 (1982).
41. Shue, R.S., in 'Developments in Plastic Technology', Vol. 2, A. Whelam and J.L. Croft ed. Elsevier Applied Science Publishers London and N.Y. p. 259 (1985).
42. Dix, J.S. *Chemical Engineering Progress*, p. 42 (1985).
43. Deuss, J.J.B., *Rec. Trav. Chim. Pays Bas.*, 28, 136 (1909).
44. Tasker, H.S. and Jones, H.O., *Proc. Chem. Soc.*, 25, 24 (1909).
45. Hilditch, T., *J. Chem. Soc.* 97, 2579 (1910).
46. Glass, H.B. and Reid, E.E., *J. Amer. Chem. Soc.*, 51, 3428 (1928).
47. Parekh, V.C. and Guha, P.C., *J. Ind. Chem. Soc.*, 11, 94 (1934).
48. Ellis, C. in 'The Chemistry of Synthetic Resins', Vol. III, Reinhold NY, p. 1183, 1189 (1935).
49. Alexsander, E., Maria, W.J. and Eugeniusz, R., *Polymer*, 19, 438 (1978).
50. Macallum, A.D., *J. Org. Chem.* 13, 154 (1948).
51. Macallum, A.D., US Patent, 2,513,188, June 27 (1950).
52. Macallum, A.D., US Patent, 2,538,941, June 23 (1951).
53. Lenz, R.W. and Carrington, W.K., *J. Poly. Sci.* 41, 333 (1959).
54. Lenz, R.W. and Handlovits, C.E., *J. Poly. Sci.*, 43, 167 (1960).
55. Lenz, R.W., Handlovits, C.E. and Smith, H.A., *J. Poly. Sci.*, 58, 351 (1962).

56. Edmonds (Jr), J.T. and Hill (Jr), H.W., US Patent 3,354, 129 to Phillips Petroleum Co. (Nov. 21,1963).
57. Hill (Jr), H.W. and Edmonds (Jr), J.T., Fr. 1,437,406 (May, 6, 1966).
58. Edmonds (Jr), J.T. and Hill (Jr), H.W., US Patent 3,354,129, to Phillips Petroleum Co. (Nov. 21, 1967).
59. Miles, J.M. and Sherk, F.T., US Patent, 3,783,138 to Phillips Petroleum Co. (Jan. 1, 1974).
60. Edmonds (Jr), J.T., US Patent 3,763,124 to Phillips Petroleum Co. (Oct. 2, 1973).
61. Scoggin, J.S., US Patent 3,786,035 to Phillips Petroleum Co. (Jan. 15, 1974).
62. Vidaurri (Jr), F.C., US Patent 3,790,536 to Phillips Petroleum Co. (Feb. 5, 1974).
63. Hoffman (Jr), A.A., US Patent 3,645,697 to Phillips Petroleum Co. (Feb. 29, 1972).
64. Green, K.J., US Patent 3,756,993 to Phillips Petroleum Co. (Sept. 4, 1973).
65. Edmonds (Jr), J.T. and Campbell, R.W., US Patent 4,089,847, to Phillips Petroleum Co. (May 16, 1978).
66. Campbell, R.W. and Moberly, C.W., US Patent 3,862,095 to Phillips Petroleum Co. (Jan. 21, 1975).
67. Moberly, C.W., US Patent 3,865,795 to Phillips Petroleum Co. (Feb. 11, 1975).
68. Campbell, R.W., US Patent 3,867,356 to Phillips Petroleum Co. (Feb. 18, 1975).
69. Scoggins, L.E., US Patent 3,867,357 to Phillips Petroleum Co. (Feb. 18, 1975).
70. Campbell, R.W., US Patent 3,869,433 to Phillips Petroleum Co. (Mar. 4, 1975).
71. Campbell, R.W., US Patent 3,870,686 to Phillips Petroleum Co. (Mar. 11, 1975).

72. Campbell, R.W., US Patent 3,870,687 to Phillips Petroleum Co. (Mar. 11, 1975).
73. Scoggins, L.E., US Patent 3,876,592 to Phillips Petroleum Co. (Apr. 8, 1975).
74. Campbell, R.W., US Patent 3,876,59 to Phillips Petroleum Co. (Apr. 8, 1975).
75. Moberly, C.W., US Patent 3,878,176 to Phillips Petroleum Co. (Apr. 15, 1975).
76. Campbell, R.W. and Scoggins, L.E., US Patent 3,869,434 to Phillips Petroleum Co. (Mar. 4, 1975).
77. Moberly, C.W., US Patent 3,880,815 to Phillips Petroleum Co. (Apr. 29, 1975).
78. Moberly, C.W., US Patent 3,882,092 to Phillips Petroleum Co. (May 6, 1975).
79. Scoggins, L.E. and Campbell, R.W., US Patent 3,884,884 to Phillips Petroleum Co. (May 20, 1975).
80. Scoggins, L.E. and Edmonds (Jr), J.T., US Patent 3,865,794, to Phillips Petroleum Co. (Feb. 11, 1975).
81. Moberly, C.W., US Patent 3,884,883 to Phillips Petroleum Co. (May 20, 1975).
82. O'Shaughnessy, M.T. and Campbell, R.W., US Patent 3,940,375, to Phillips Petroleum Co. (Feb. 24, 1976).
83. Edmonds (Jr), J.T., Ger. Offen. 2,623,362 (Dec. 9, 1976).
84. Anderson, K.L. and Kuper, D.G., US Patent 4,025,496 to Phillips Petroleum Co. (May 24, 1977).
85. Stapp, P.R. and Brady, D.G., Patent 4,064,115 to Phillips Petroleum Co. (Dec. 20, 1977).
86. Campbell, R.W. and Yelten, H.D., US Patent 4,024,118 to Phillips Petroleum Co. (May 17, 1977).
87. Hawkins, J.T., US Patent 4,046,749 to Phillips Petroleum Co. (Sept. 6, 1977).
88. Tieszen, D.O. and Scoggins, L.E., Ger. Offen. 3,030,488 to Phillips Petroleum Co. (Mar. 26, 1981).

89. Sherk, F.T. and Hammer, H.B., US Patent 4,368,321 to Phillips Petroleum Co. (Jan. 11, 1983).
90. Anderson, K.L., US Patent 4,371,671 to Phillips Petroleum Co. (Feb. 1, 1983).
91. Edmonds (Jr), J.T., US Patent 4,373,090 to Phillips Petroleum Co. (Feb. 8, 1983).
92. Cleary, J.W., Polymer Preparation, Amer. Chem. Soc., Dir. of Poly. Chem., 25 (2), 37 (1984).
93. Vidaurri (Jr), F.C., US Patent 3,607,843 to Phillips Petroleum Co. (May 16, 1969).
94. Vidaurri (Jr), F.C., Ger. Offen. 2,026,665 to Phillips Petroleum Co. (Jan. 5, 1970).
95. Edmonds (Jr), J.T. and Campbell, R.W., US Patent, 4,038,263, to Phillips Petroleum Co. (July 26, 1977).
96. Edmonds (Jr), J.T., Ger. Offen. 2,623,333 to Phillips Petroleum Co. (Dec. 9, 1976).
97. Campbell, R.W., US Patent 4,039,518 to Phillips Petroleum Co. (Aug. 02, 1977).
98. Campbell, R.W. and Edmonds (Jr), J.T., US Patent 4,038,259, to Phillips Petroleum Co. (July 26, 1977).
99. Edmonds (Jr), J.T., US Patent 4,038,262 to Phillips Petroleum Co. (July 26, 1977).
100. Edmonds (Jr), J.T., US Patent 4,096,132 to Phillips Petroleum Co. (June 20, 1978).
101. Campbell, R.W., US Patent 4,038,260 to Phillips Petroleum Co. (July 26, 1977).
102. Campbell, R.W., Ger. Offen. 2,453,749 to Phillips Petroleum Co. (May 26, 1976).
103. Hill (Jr), H.W., Ind. Engg. Chem. Prod. Res. Der. 18, 252 (1979).
104. Phillips Petroleum Co. Neth. Appl. 81,01,243 (Oct. 1, 1982).

105. Crough, W.W. and Edmonds (Jr), J.T., Ger. Offen. 2,623,363, to Phillips Petroleum Co. (Dec. 9, 1976).
106. Edmonds (Jr), J.T., Scoggins, L.E., US Patent 4,116,947 to Phillips Petroleum Co. (Sept. 26, 1978).
107. Campbell, R.W., US Patent 3,966,688 to Phillips Petroleum Co. (Dec. 3, 1974).
108. Campbell, R.W., US Patent 4,016,145 to Phillips Petroleum Co. (Apr. 5, 1977).
109. Campbell, R.W., Ger. Offen. 2,726,861 to Phillips Petroleum Co. (Dec. 29, 1977).
110. Campbell, R.W., US Patent 4,070,349 to Phillips Petroleum Co. (Jan. 24, 1978).
111. Campbell, R.W., US Patent 4,125,525 to Phillips Petroleum Co. (Nov. 14, 1978).
112. Campbell, R.W., US Patent 4,127,713 to Phillips Petroleum Co. (Nov. 28, 1978).
113. Campbell, R.W., Eur. Pat. Appl. 33,906 to Phillips Petroleum Co. (Aug. 19, 1981).
114. Rohling, R.G., US Patent 3,717,620 to Phillips Petroleum Co. (Feb. 20, 1973).
115. Wood, H.V. and Brown, H.V., US Patent 3,699,087 to Phillips Petroleum Co. (Oct. 17, 1972).
116. Walker, J.H., US Patent 3,725,362 to Phillips Petroleum Co. (Apr. 03, 1973).
117. Scoggins, L.E., US Patent 3,737,411 to Phillips Petroleum Co. (Jan. 1, 1973).
118. Scoggins, J.S., US Patent 3,793,256 to Phillips Petroleum Co. (Feb. 19, 1974).
119. Brady, D.G. and Blackwell, J.P., US Patent 3,948,865 to Phillips Petroleum Co. (Apr. 06, 1976).
120. Walton, R.M., US Patent 3,998,767 to Phillips Petroleum Co. (Dec. 21, 1976).



121. Edmonds (Jr), J.T., Belg. BE 891,108 to Phillips Petroleum Co. (May 06, 1982).
122. Sherk, F.T. and Edmonds (Jr), J.T., Belg. BE, 890,647 to Phillips Petroleum Co. (Apr. 06, 1982).
123. Salmon, E.J., Eur. Pat. Appl. EP 64,300 to Phillips Petroleum Co. (Nov. 10, 1982).
124. Anderson, K.L. and Kuper, D.G., US Patent 4,066,632 to Phillips Petroleum Co. (Jan. 03, 1978).
125. Vidaurri (Jr), F.C., US Patent 4,056,515 to Phillips Petroleum Co. (Mar. 30, 1978).
126. Anderson, K.L. and Kuper, D.G., US Patent 4,066,632 to Phillips Petroleum Co. (Jan. 01, 1978).
127. Anderson, K.L. and Vidaurri, F.C., US Patent 3,213,628 to Phillips Petroleum Co. (Dec. 09, 1982).
128. Tsunawaki, S. and Price, C.C., J. Poly. Sci., Part A, 2, 1511, (1964).
129. Handlovits, C.E. in J.A. Moore Ed., 'Macromolecular Syn. Coll. Vol.1' J. Wiley and Sons, N.Y., 1977, p. 345.
130. Montaudo, G., Bruni, G., Maravigna, P. and Bottino, F., J. Poly. Sci., Polym. Chem. Ed. 12(2), 2881 (1974).
131. Sergeev, V.A., Shitikov, V.K., Nederkin, V.I. and Korshak, U.V., Vysokomol. Soedin. Ser., A, 17, 2420 (1975).
132. Horting, B. and Lindberg, J.J., Makromol. Chem., 179, 1707, (1978).
133. Port, A.B. and Still, R.H., J. Appl. Pol. Sci., 24, 1145 (1979).
134. Port, A.B. and Still, R.H., Polym. Degradation Stab., 1, 133, (1979).
135. Sergeev, V.A., Yunnikov, V.V. and Liven, A.V., Vysokomol. Soedin, Ser., A, 23, 682 (1981).
136. Horting, Bo., Soeder, M. and Lindberg, J.J., Agnew. Makromol. Chem., 107, 163 (1982).

137. Thermally Stable Polymers, P.E. Cassidy Ed. Thermally Stable Polymers, Marcel Dekker N.Y. 1980.
138. Neth. Appl. 6,412,884 to Norton Co. (May 10, 1985).
139. Lenz, R.W., Handlovits, C.E. and Carrington, W.K., Belgian 613,003 to DOW Chemical Co. (July 23, 1967).
140. Sagami Chemical Research Center, Fr. 1,589,417 (May, 1970).
141. Kamata, K. and Handa, R., Japan Kokai, 75,123,799 to Mitsubishi Rayon Co. Ltd. (Mar. 19, 1974).
142. Haddad, I., US Patent Appl. 541,489 to US Dept. of Air Force, (Jan. 16, 1975).
143. Liven, A.V., Krutikova, Z.I. and Polyakova, N.N., USSR 525,717 (Aug. 25, 1976).
144. Noto, Y., Yamamoto, H. and Matsumoto, K., Japan Kokai, 76,129,497 to Dainippon Int. and Chemicals Ltd. (May 6, 1975).
145. Takeda, N., Fukaoka, H. and Maki, H., Japan Kokai, 77,102,396 to Mitsui Petrochemical Industries Ltd. (Aug. 27, 1977).
146. Sergeev, V.A., Shitikov, V.K., Nedel'kin, V.I., Kogan, A.S., Tsachenko, H.A., Misyurev, V.I., Yakobson, B.V. and Glebychev, B.S., Otkrytiya Izobrn Prom., Obraztsy, Tovarnye Znaki, 54,93 (1977). CA 88, 51370.
147. Takeda, N., Fukutani, K. and Iwata, T., Japan Kokai, 78,33,297 to Mitsui Petrochemical Ind. Ltd. (Mar. 29, 1978).
148. Sergeev, V.A., Shitikov, V.K., Nedel'kin, V.I., Ust'kachintsev, A.N., Glebychev, B.S., Yakobson, B.V., Kogan, A.S., Lepilin, V.Ya. and Misyurev, V.I., Otkrytiya Izobret, Prom. Obraztsy, Tovarnye Znaki, 55,101 (1978).
149. Vovonkar, M.G., Annekova, V.L., Andreeva, N.I., Annekova, V.M. and Abzaeva, K.A., USSR 698,988 to Irkutsk Inst. of Org. Chem. (Nov. 25, 1979). CA, 92, 59432.
150. Kanda, I. and Kawai, T., Japan Kokai. Tokkyo Koho 80,43,139 to Toray Industries Inc. (Nov. 26, 1980).
151. Smith, H.A., US Patent 4,178,433 to Dow Chemical Co. (Dec. 11, 1979).
152. Asahi-Dow Ltd., Japan Kokai. Tokkyo Koho. 80,54,330 (Apr.21, 1980).

153. Toray Industries, Inc., Japan Kokai, Tokkyo Koho. 80,40,738 (Mar. 22, 1980).
154. Liao Al-De, Li, Shi-Ji. and Shang-Hai, Hua, Kung Hsueh Yuan Hsueh Pao, 1,39,1980.
155. Idel, K. and Merten, J., Eur. Pat. Appl. 23313 to Bayer A.G., (Feb. 4, 1981).
156. Idel, K. and Marten, J., Ger. Offen. 2,930,797 to Bayer A.G., (Feb. 12, 1981).
157. Asahi Dow Ltd., Japan Kokai, Tokkyo Koho., 81,14,531 (Feb. 12, 1981).
158. Idel, K., Reitag, D., Bottenbrush, L., and Marten, J., Ger. Offen. DE, 3,019,732 to Bayer A.G., (Dec. 3, 1981).
159. Idel, K., Freitag, D., Bottenbrush, L. and Neuner, O., Ger. Offen. DE, 3,120,538 to Bayer A.G. (Dec. 9, 1982).
160. Toray Industries Inc., Japan Kokai, Tokkyo Koho., J.P., 57,205,425 (Dec. 16, 1982).
161. Toray Industries Inc., Japan Kokai, Tokkyo Koho. J.P. 59,45,323 (Mar. 14, 1984).
162. Taubitz, C. and Walter, M., Ger. Offen. DE, 3,237,110 to BASF-A.G. (Apr. 14, 1984).
163. Dainippon Ink and Chemicals Inc., Japan Kokai, Tokkyo Koho. JP. 58,206,632 (May 28, 1982).
164. Dainippon Ink and Chemicals Inc., Japan Kokai, Tokkyo Koho. JP, 58,222,113 (June 18, 1982).
165. Dainippon Ink and Chemicals Inc., Japan Kokai, Tokkyo Koho. JP, 59,741,127 (Apr. 26, 1984).
- 166.** Ostlinning, E. and Idel, K., Ger. Offen. DE, 3,243,189 to Bayer, A.G. (May 24, 1984).
167. Asahi Glass Co. Ltd., Japan Kokai, Tokkyo Koho. JP, 59,81,334 (May 11, 1984).
168. Asahi Glass Co. Ltd., Japan Kokai, Tokkyo Koho. JP, 59,81,335 (May 11, 1984).

169. Toray Industries Inc., Japan Kokai, Tokkyo Koho. JP, 59,98,133 (June 6, 1984).
170. Shiiki, Z., Iizuka Yo. and Kawakami, Y., Fr. Demande, Fr. 2,537,589 to Kureha Chem. Ind. Co. Ltd. (Dec. 14, 1982).
171. Toray Industries Inc., Japan Kokai, Tokkyo Koho. JP, 59,115,331 (Jul. 03, 1984).
172. Idel, K., Ostlinning, E., Koch, W., Bottenbrush, L. and Heitz, W., Ger. Offen. DE, 3,312,284 to Bayer A.G. (Oct. 11, 1984).
173. Idel, K., Ostlinning, E., Koch, W. and Heitz, W., Ger. Offen. DE, 3,312,254 to Bayer A.G. (Oct. 11, 1984).
174. Toray Industries Inc., Japan Kokai, Tokkyo Koho. JP, 59,108,032 (Jun. 22, 1984).
175. Toray Industries Inc., Japan Kokai, Tokkyo Koho. JP, 59,115,332 (Dec. 21, 1982).
176. Ebert, W., Meyer, R., Idel, K.J. and Dhein, R., Ger. Offen. DE 3,317,821 to Bayer A.G. (Nov. 22, 1984).
177. Ebert, W., Meyer, R., Idel, K.J. and Schubart, R., Ger. Offen. DE 3,317,820 to Bayer A.G. (Nov. 22, 1984).
178. Sumimoto Chemical Co. Ltd., Japan Kokai, Tokkyo Koho. JP 59,202,222 (Nov. 16, 1984).
179. Sumimoto Chemical Co. Ltd., Japan Kokai, Tokkyo Koho. JP 59,138,229 (Aug. 08, 1984).
180. Nippon Soda Co. Ltd., Japan Kokai, Tokkyo Koho. JP 59,189,124 (Oct. 26, 1984).
181. Dainippon Ink and Chemicals Inc., Japan Kokai, Tokkyo Koho. JP, 59,221,337 (Dec. 12, 1984).
182. Dainippon Ink and Chemicals Inc., Japan Kokai, Tokkyo Koho. JP 59,217,727 (Dec. 7, 1984).
183. Dainippon Ink and Chemicals Inc., Japan Kokai, Tokkyo Koho. JP 59,219,332 (Dec. 10, 1984).
184. Mitsubishi Petrochemical Co. Ltd., Japan Kokai, Tokkyo Koho. JP 60,414,526 (Mar. 9, 1985).

185. Tanbitz, C. and Sterzel, H.J., Ger. Offen. DE 3,339,539 to BASF A.g. (May 9, 1985).
186. Tanbitz, C. and Sterzel, H.J., to BASF A.G., Ger. Offen. DE, 3,339,538 (May 8, 1985).
187. Ostlining, E. and Idel, K., Ger. Offen. DE 3,338,501 (May 2, 1985).
188. Sergeev, V.A., Medel'kin, V.I., Andrinova, O.B., Denisova, M.S., Liven, A.V. and Yunnikov, V.V., USSR SU 816,134 (Jul. 30, 1985).
189. Ostlining, C., Idel, K., Eisermann, W.M. and Freitag, D., Ger. Offen. DE 3,410,642 to Bayer A.G. (Sept. 26, 1985).
190. Kawabata, S., Hasegawa, S., Sugie, T., Furahata, F. and Kodeva, K. Japan Kokai, Tokkyo Koho. JP 60,200,807 to Dainippon Ink and Chemicals Inc. (Oct. 11, 1985).
191. Kawabata, S., Hase Gawa, S., Sugie, T., Furahata, F. and Kodeva, K., Japan Kokai, Tokkyo Koho. JP, 60,200,808 to Dainippon Ink and Chemicals Inc. (Oct. 11, 1985).
192. Principles of Polymer Chemistry, Paul J. Flory, Cornell Univ. Press, London, p.71 (1974).
193. Bhide, B.V. and Sudborough, J.J., J. Ind. Inst. Sci., 8A, 89 (1925).
194. Rabinowitch, E., Trans. Faraday Soc., 33, 1223 (1937).
195. Bailey, M.E., Kriss, V. and Spaunburgh, R.G., J. Amer. Chem. Soc., 80, 1326 (1950).
196. Schulz, S.R. and Baron, A.L., Adv. Chem. Series, 91, 692 (1969).
197. Johnson, R.N., Farnham, A.G., Clenning R.A., Hale W.F. and Kerriam C.N., J. Polym. Sci. pt. A.1, 5, 2325 (1967).
198. Higgins, M.L., J. Amer. Chem. Soc., 64, 2716 (1942).
199. Kramer, E.O., Ind. Engg. Chem., 30, 1200 (1938).
200. Mark, H., 'Des feste Korper', p. 103, HIRZEL LIEPZIG (1938).
200. Houwink R., J. Prakt. Chem. 157, 5 (1940).

201. Schultz, G.V. and Blaschke, F., J. Prakt. Chem., 158, 130, (1941).
202. Solomon, O.F. and Ciuta, I.Z., J. Appl. Poly. Sci., 6, 683 (1962).
203. Naar, R.Z., Zabusky, H.H. and Neitmiller, R.F., J. Appl. Poly. Sci., 7, 530 (1963).
204. Nero, J.R. and Sikdar, S.K., J. Appl. Poly. Sci., 27, 4687 (1982).
205. Palit, S.R. and Kar, I., J. Poly. Sci., A-1, 5, 2629 (1967).
206. Martin, A.F., TAPPI, 34, 363 (1951).
207. Ott, E. and Spurun, H., in Cellulose and Cellulose Derivatives, High Polymers, Vol. 5, Part III, p. 1216, Interscience, New York (1955).
208. Deb, P.C. and Chatterjee, S.R., Ind. J. Appl. Chem., 31, 121 (1968).
209. Khan, H.U. and Bargava, G.S., J. Polym. Sci., Poly. Lett. Ed., 18, 803 (1969).
210. Slade, P.E. and Jenkins, L.T., Thermal Characterization Techniques, Marcel Decker Inc., New York (1966).
211. Slade, P.E. and Jenkins, L.T., Eds., Techniques and Methods of Polymer Education, Vol. I, Marcel Decker Inc., New York (1966).
212. Schwenker, R.F. and Garn, P.D., Thermal Analysis, Vols. I and II, Academic Press, New York (1969).
213. Keattch, C.J., An introduction to thermogravimetry, Heydon, London (1969).
214. Einhorn, I., Thermal analysis - Polymer Conference Series, Univ. of Utah (1970).
215. Mackenzie, R.C., Differential Thermal Analysis, Vols. 1 and 2, Academic Press, London, 1970, 1972, respectively.
216. Daniels, T., Thermal Analysis, Kogan press, London, 1973.

217. Blazek, A., Thermal Analysis, Van Norstand Reinhold, NY, 1974.
218. Wendant, W.W., Thermal Methods of Analysis, 2nd Edn. Wiley, New York, 1974.
219. Ke, B., Ed., Thermal Analysis of High Polymers, Interscience New York (1974).
220. Kamble, H. and Garn, P.D., Thermal Analysis, Wiley, New York, (1974).
221. Loft, B.C. in 'Proceedings of the Australian Polymer Symposium' Bradbury, B.H., Ed. Interscience, New York (1975).
222. Grassile, N., Ed., Developments in Polymer Degradation, Applied Science Publishers, London (1977).
223. Still, R.H., Brit. Polym. J., 11, 101, 1979.
224. Lombardi, G., For better Thermal Analysis, 2nd Edn., International Confederation for Thermal Analysis - Rome, 1980.
225. O'Neill, M.J., Anal. Chem., 38, 1331 (1968).
226. Ennulat, R.D., Mol. Cryst. Liq. Cryst., 3, 405 (1968).
227. Thermal Analysis - Application Study No. 1, Perkin-Elmer Corpn. Norwack (1971).
228. Knox, I.R., Instrument News, 17, No. 4, Perkin-Elmer Corpn. (1967).
229. Fawa, R.S., Polymer, 9, 137, March 1968.
230. Alexander, L.E., X-ray diffraction in polymer science, John Wiley, NY (1969).
231. Bunn, C.W., Chemical crystallography, Oxford University Press, London (1961).
232. Stout, G.H. and Jensen, L.H., X-ray structure determination-A practical guide, MacMillan, NY. (1968).
233. Tanford, C., Physical Chemistry of Macromolecules, John Wiley, N.Y. (1961).

234. Wunderlich, B., *Macromolecular Physics*, Vol.I, Academic Press, New York (1976).
235. Mandelkern, L., *Crystallization of Polymer* McGraw Hill Publishing Co. N.Y. (1964).
236. Kavesh, S. and Schultz, J.M., Meaning and measurement of crystallinity of polymers, *Polymer Engg. Sci.*, 9 (6), 452 (1969).
237. Statton, W.D., *International Symposium on Plastics Testing and Standardization*, ASTM Special Technical Bulletin No. 247, ASTM, Philadelphia, Pennsylvania (1959).
238. Jeffrey, J.W., *Methods in x-ray crystallography*, Academic Press, N.Y. (1971).
239. Posner, A.S., X-ray diffraction, Chap. II, in Gordon M. Kline Ed., *Analytical Chemistry of Polymers - Part II*, Interscience Division, John Wiley & Sons, N.Y. (1962).
240. White, J.R. and Thomas, E.L., *Rubber Chem. and Tech.*, 57, 457 (1984).
241. Baker, F.L. and Princern, L.H., in Mark, H.F., Gaylord, N.G. and Bikales, N.M., Ed., *Encyclopaedia of Poly. Sci. and Tech.*, Vol. 5, Interscience Div., John Wiley & Sons, NY (1971).
242. Kimoto, S. and Russ, J.C., *Am. Scientist*, 57 (1), 112 (1969).
243. Thornton, P.R., *Scanning Electron Microscopy*, Chapman and Hall, London (1968).
244. Odian, G., *Principles of Polymerization*, John Wiley and Sons, N.Y., p. 84 (1981).
245. Radhakrishnan, S., Rajan, C.R. and Nadkarni, V.M., *J. Matl. Sci.*, 21, 597 (1986).
246. Hawkins, R.T., *Macromolecules*, 9, 189 (1976).
247. Rajan, C.R., Ponrathnam, S. and Nadkarni, V.M., *J. Appl. Poly. Sci.* (in press).
248. Sterling, T.C., Smith, C.P. and Kimber, P.J., *Modern Plastics Int.*, March, p. 54 (1982).
249. Hill (Jr), H.W. and Brady, D.G., *Polym. Eng. Sci.* 16, 831 (1976).



250. Tabor B.J., Magre E.P. and Boon J., *Eur. Polym. J.*, 7, 1127, (1971).
251. Radhakrishnan S. and Nadkarni V.M., *Polym. Eng. Sci.* 24, 1383, (1984).
252. Schultz J., *Polymer Material Science*, Princeton Hall, New Jersey, Ch. 9 (1974).
253. Wunderlich B., *Macromolecular Physics*, Vol. 2, Academic Press, New York Ch. 5 (1976).
254. Palma G., Talamini G., Taran M. and Caremza M., *J. Polym. Sci., Polym. Phys. Ed.*, 15, 1537 (1977).
255. Barclay L.M., *Agnew. Makromol. Chem.*, 52, 1 (1976).
256. Wenig W., *J. Polym. Sci., Polym. Phys. Ed.*, 16, 1635 (1978).
257. Butters , "Particulate Nature of PVC", *Applied Science Publ.*, London (1982).
258. Information Bulletin, Ryton grade V, Phillips Petroleum Co., USA.
259. Schacklette L.W., Elsenbaumer R.L. , Chance R.R., Eckhardt H., Frommer J.E. and Baughman R.H., *J. Chem. Phys.* 75, 1919 (1981).
260. Hortling B. and Lindeberg J.J., *Chemica Scripta*, 2, 179 (1972).
261. Zuk A., Maria W.J. and Rogal E., *Polymer*, 19, 438 (1978).
262. Birchall J.M., Green M., Haszeldine R.N. and Pitts A.D., *Chemical Communications*, 10, 338 (1967).
263. Koch W. and Heitz W., *Makromol. Chem.*, 184, 779 (1983).
264. March J., 'Advanced Organic Chemistry', McGraw Hill, International Student edition, Tokyo (1977), p. 595.
265. Bunnet J.F., Garbisch E.W. (Jr) and Pruitt K.M., *J. Am. Chem. Soc.*, 79, 385 (1957).
266. Kirby A.J. and Jencks W.P., *J. Amer. Chem. Soc.* 87, 3217 (1965).
267. Roberts A.D., Semenow D.A., Simmons H.E.(Jr) and Carlsmith, C.A., *J. Am. Chem. Soc.*, 78, 601 (1956).

268. Challa G., Makromol. Chem., 38, 105, 123, 138 (1960).
269. Hodgkin J.H., J. Polym. Sci., Polym. Chem. edn. 14, 409 (1976).
270. Kaplan M.L. and Reents W.D. (Jr), Tetrahedron Letters, 23, 373 (1982).